

ANL-82-59

SNL - X. LINKER  
11/84  
ANL-82-59

**STIRLING ENGINE THERMODYNAMIC ANALYSIS:  
A USERS GUIDE TO SEAM1**

by

**T. J. Heames, D. J. Uherka,  
J. C. Zabel, and J. G. Daley**



---

**ARGONNE NATIONAL LABORATORY, ARGONNE, ILLINOIS**

**Prepared for the U. S. DEPARTMENT OF ENERGY  
under Contract W-31-109-Eng-38**

The facilities of Argonne National Laboratory are owned by the United States Government. Under the terms of a contract (W-31-109-Eng-38) among the U. S. Department of Energy, Argonne Universities Association and The University of Chicago, the University employs the staff and operates the Laboratory in accordance with policies and programs formulated, approved and reviewed by the Association.

#### MEMBERS OF ARGONNE UNIVERSITIES ASSOCIATION

The University of Arizona  
Carnegie-Mellon University  
Case Western Reserve University  
The University of Chicago  
University of Cincinnati  
Illinois Institute of Technology  
University of Illinois  
Indiana University  
The University of Iowa  
Iowa State University

The University of Kansas  
Kansas State University  
Loyola University of Chicago  
Marquette University  
The University of Michigan  
Michigan State University  
University of Minnesota  
University of Missouri  
Northwestern University  
University of Notre Dame

The Ohio State University  
Ohio University  
The Pennsylvania State University  
Purdue University  
Saint Louis University  
Southern Illinois University  
The University of Texas at Austin  
Washington University  
Wayne State University  
The University of Wisconsin-Madison

#### NOTICE

This report was prepared as an account of work sponsored by an agency of the United States Government. Neither the United States Government nor any agency thereof, nor any of their employees, makes any warranty, express or implied, or assumes any legal liability or responsibility for the accuracy, completeness, or usefulness of any information, apparatus, product, or process disclosed, or represents that its use would not infringe privately owned rights. Reference herein to any specific commercial product, process, or service by trade name, trademark, manufacturer, or otherwise, does not necessarily constitute or imply its endorsement, recommendation, or favoring by the United States Government or any agency thereof. The views and opinions of authors expressed herein do not necessarily state or reflect those of the United States Government or any agency thereof.

Printed in the United States of America  
Available from  
National Technical Information Service  
U. S. Department of Commerce  
5285 Port Royal Road  
Springfield, VA 22161

NTIS price codes  
Printed copy: A08  
Microfiche copy: A01

SEAMOPT - STIRLING ENGINE OPTIMIZATION CODE

T. J. Heames and J. G. Daley

Argonne National Laboratory  
Argonne, Illinois 60439

## ABSTRACT

Experience is described with use of a fast-running Stirling engine optimization code developed at Argonne intended for public release. Stirling engine modeling is provided by the SEAM1 thermodynamic code. An interface was written to combine SEAM1 with a general optimization code and assess maximum component stress levels. Thus full engine thermodynamic and structural simulation is done during the optimization process. Several examples of the use of this code to optimize the GPU-3 engine are described. In one case efficiency was improved by over 25%.

## INTRODUCTION

Design optimization is the determination of the "best" relationship among the several variables that describe the physical/economic characteristics of a system. The methodology of optimization has become an area of mathematical specialization that, in general, provides a process for determining the most suitable alternative among many candidates without the designer needing to examine each of the candidates. Optimization theory provides a tool which enables designers to account for nonlinear relationships between the many variables defining a system without tedious calculations, or the need to rely upon intuition as was previously necessary.

Optimization of Stirling engine design involves a complication not encountered in systems typically either at steady state (as in the case of structural design) or at steady flow (as in the case of process plant design). The working fluid of Stirling engines experiences unsteady, reversing flow due to the reciprocating motion of the pistons. Rigorous analytical models of fluid dynamics within Stirling engines require considerable computation time before conditions from cycle-to-cycle are approximately matched (cyclic steady state). Use of such analytical models to provide the system description for an optimization algorithm

where hundreds of executions of the system simulation may be needed to obtain a single solution would require excessive computation time. Therefore, no Stirling engine optimization work has been reported that contains realistic physical models.

This paper describes experience with a Stirling engine optimization code that combines a full Stirling engine simulation with a general-purpose optimization program. This is feasible, in terms of computation time required, because of two features: (1) the Stirling engine simulation is itself fast-running, and (2) the optimization algorithm used makes very efficient use of information from the simulation. The results obtained suggest that it is possible to raise the performance of an existing engine several points, both in power and efficiency, through design changes that simplify and lower the cost of the engine.

The present work described is a part of a program to make available nonproprietary analysis codes and to otherwise broaden the technology base for Stirling engines through experiments and exploratory development of advanced component designs. A previous result was the release of a general-purpose code for analyzing most Stirling engine configurations.

## STIRLING ENGINE ANALYSIS

Argonne's program to release government developed Stirling engine analysis codes has been reported previously (1,2,3). The basic philosophy has been to make use of published analysis methods rather than attempt to develop a "new" Stirling engine analysis code, and also to provide

- (1) A user-oriented menu of Stirling engine design options that permit the user to easily specify the physical characteristics of the engine of interest,
- (2) Library functions of typical properties and correlations, and

(3) Standard input and output processors.

The current analysis capability is summarized in Table 1. A principal feature is that, once data have been provided to describe the physical geometry of the engine, analysis can be performed at any of the levels indicated in the table.

Improvements in Stirling engine analysis capability are needed before the performance of a new design can be confidently predicted. This problem cannot be resolved through numerical procedures such as dividing the engine into a finer computational mesh, or developing new techniques for integrating the relevant equations. A more basic understanding of energy flows during the cycle must be determined from experiments; only when this understanding is used to modify the existing Stirling analysis codes will the predictive capability of the codes be improved. A related area is the experimental

determination of heat transfer and flow friction under reversing flow conditions occurring in Stirling engines. These data would provide a basis for improving the present steady flow correlations. These modifications can be easily incorporated into the Argonne code structure as they become available, improving both the standard library and the various analysis modules.

OPTIMIZATION

Figure 1 illustrates the process for Stirling engine design using an optimization program; the designer is directly involved in making decisions and modifying calculations. Formulating the design objective is the first task faced by the designer. Although the concept may be simple, such as the desire to maximize efficiency or power, it is necessary to mathematically express these concepts in terms of design

Table 1. Summary of Argonne Stirling Engine Analysis Capability  
SEAM (Stirling Engine Analysis Module) Structure

Description	Approaches/Features	Use	Status
SEAM Library	<ul style="list-style-type: none"> <li>• Temperature dependent properties of working fluids and structural materials</li> <li>• Heat transfer and fluid flow correlations</li> <li>• All mechanical drives</li> <li>• Standard Input and Output processors</li> </ul>	<ul style="list-style-type: none"> <li>• Available to all SEAM codes</li> </ul>	
SEAM1	<ul style="list-style-type: none"> <li>• Divides engine into five basic zones (heater, cooler, expansion space, compression space and regenerator) and calculates average temperature in each zone.</li> <li>• Calculates power, efficiency, and cycle average losses (conduction, friction, leakage, etc.)</li> <li>• Theoretical heat input and power corrected by calculated losses until convergence is obtained</li> <li>• Fast convergence (&lt; 0.5 sec/case)</li> <li>• Precise accounting for separate phenomena which affect power and efficiency</li> </ul>	<ul style="list-style-type: none"> <li>• Performance predictions</li> <li>• Parametric study (see SEAMOPT below)</li> <li>• Preliminary engine design</li> </ul>	Code and documentation can be obtained through NESC*
SEAM2	<ul style="list-style-type: none"> <li>• Finite difference analysis—engine divided into as many cells as desired</li> <li>• Simultaneous integration of mass, energy and state equations with small time steps</li> <li>• Calculates detailed physical phenomena within each cell</li> <li>• Very long time to converge (many cycles needed to reach steady state)</li> <li>• No data available to validate predictions during cycle</li> </ul>	<ul style="list-style-type: none"> <li>• Flexibility for geometries to be analyzed—can analyze non-Stirling engine configurations if desired</li> <li>• Detailed engine analysis and design</li> </ul>	Available January 1985
SEAMOPT	<ul style="list-style-type: none"> <li>• Combines SEAM1 (above) with general optimization code</li> <li>• All important influences on engine performance considered simultaneously during design</li> <li>• Maximum stress levels and other structural constraints can be specified</li> <li>• Fast-running-optimizations problems with 15 independent design variables requires approximately two minutes</li> </ul>	<ul style="list-style-type: none"> <li>• Engine design—trade-off studies</li> </ul>	Under development

\* National Energy Software Center, Argonne National Laboratory, Building 203, 9700 South Cass Ave., Argonne, IL 60439

## SEAMOPT: A FAST-RUNNING STIRLING ENGINE DESIGN CODE

variables. The "physical system boundaries" or constraint equations, shown in Figure 1 refer to variables such as the maximum stress in individual components, or the largest allowable dimension of components. Often these boundaries are changed by the designer, as shown in Figure 1, until a feasible solution to the design objectives is found. The designer also must decide whether the design is satisfactory after computations have been completed. There are three circumstances in which the optimization program discontinues computation:

- (1) The original objectives are satisfied,
- (2) An optimum solution was not found but a criterion for maximum number of computations has been exceeded, and
- (3) The system boundaries (constraints) are violated.

In any of these cases, the designer must decide whether to accept the present design as satisfactory, or redefine the design objectives and/or the system boundaries and continue.

Thus, optimization is an important tool that greatly expands a designer's capability, but the value of the final design is still determined by the skill and imagination of the designer.

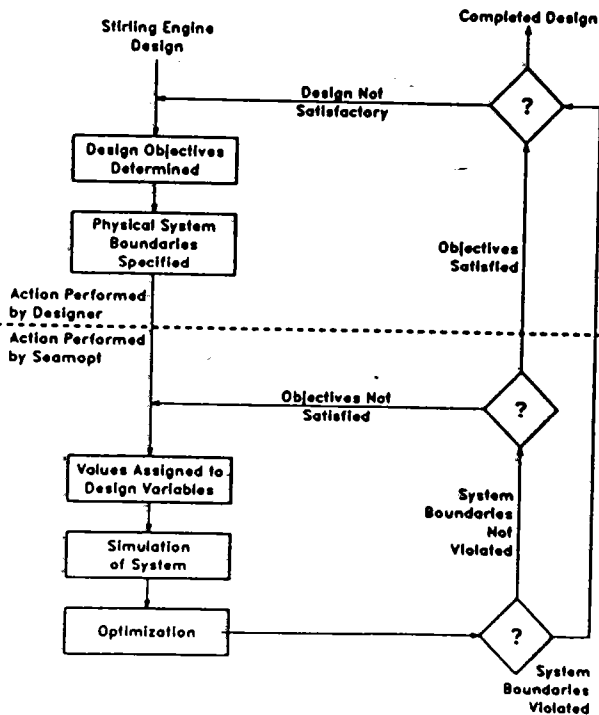


Figure 1. Process of Stirling Design Using Optimization Program

Figure 2 shows the SEAMOPT (Stirling Engine Analysis Module for Optimization) framework. The input, output, and standard functions modules are the same ones used in SEAM1 and SEAM2 (see Table 1). The analysis module currently used is from SEAM1 (2). The engine is modeled as five zones (cooler, heater, regenerator, expansion space, and compression space) of uniform temperature at any instant in time. An inner integration loop integrates the mass, energy, and state equations during the cycle for the ideal case, which does not include losses due to friction, heat leaks, conduction, etc. These energy flows are calculated separately and their effects included in an outer integration loop. Cyclic steady state (when temperature and energy flows are the same at a 0° crank angle as at a 360° crank angle) is normally obtained within four cycles. In Figure 2, dashed lines are used around the analysis module because an alternative method, such as SEAM2, which calculates a more detailed energy balance, could be used at the expense of increased computation time. The solution scheme employed in SEAM2 is similar to that used by Tew (4). Recent improvements to the SEAM structure include:

- Additional material properties,
- Additional friction and heat transfer correlations,
- More accurate volume initialization,
- Isothermal variable volumes and adiabatic connecting ducts (SEAM1),
- Leakage between the buffer and compression zone (SEAM1), and
- More accurate pressure drop, gas temperature, and regenerator reheat calculations (SEAM1).

### OPTIMIZATION MODULE - VMCON

The optimization algorithm currently used was originally suggested by Powell (5), and is the basis of an Argonne developed code, VMCON (6), for general nonlinear systems. VMCON uses gradients generated from the system simulation, but requires very few gradient calculations compared with other optimization methods.

Values of the design parameters as well as the gradients of both the objective function and the constraint equations with respect to these parameters are used. Therefore VMCON either requires a new set of gradients before calculating a new set of design parameters, or estimates a new set using what is called a "line search" technique. In the original VMCON these gradient

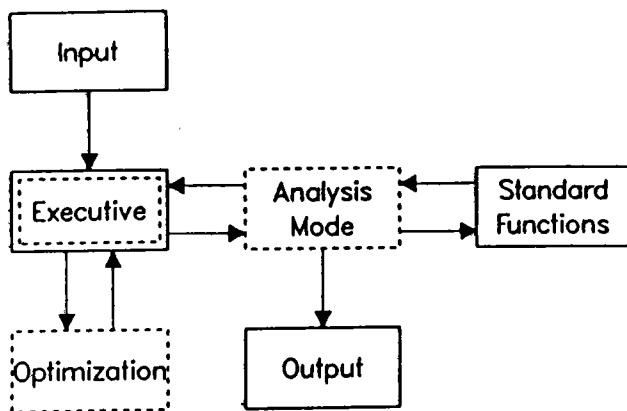


Figure 2. SEAMOPT Framework

calculations were made, but not used during the "line search", so they have been eliminated in SEAMOPT. The current version of VMCON was also modified to include bounds on the design parameters in addition to the constraints. These controls are included in the executive module shown in Figure 2.

VMCON is available through the National Energy Software Center, and has been used successfully in a variety of applications. The present work shows that VMCON is suitable for Stirling engine optimization; convergence has been obtained in the cases tested, and computation time is significantly less than previous algorithms tested. However, other optimization techniques can be implemented; hence, the dashed line around the optimization element in Figure 2.

#### EXECUTIVE MODULE

The executive module shown in Figure 2 controls the flow of calculation. It initially calls the SEAM code to determine a base design and provide default values for the optimization variables. Then it determines which design parameters of the 30 listed in Table 2 will be used, as well as initial minimum or maximum values of design variables based on user supplied specifications. The module initializes the link between the optimization code and the SEAM code and provides for "line search" and "gradient" calculations. After a set of design parameters has been chosen by VMCON and the resulting design point performance has been calculated by SEAM, the executive module calls a limit routine that evaluates the objective function and constraints as listed in Table 3.

After the original set of design variables shown in Table 2 was assembled, it became obvious that some, such as temperature,

Table 2. Engine Design Variables Presently Available to SEAMOPT

1	engine mean pressure (Pa)
2	engine speed or frequency (Hz)
3	compression/expansion crank radius (m)
4	compression/expansion rod length (m)
5	compression/expansion crank eccentricity (m)
6	expansion rod diameter (m)
7	volume phase angle (degree)
8	combustor temperature (K)
9	cooler water temperature (K)
10	expansion cylinder bore (m)
11	cylinder wall thickness (m)
12	displacer length (m)
13	displacer wall thickness (m)
14	heater tube length (m)
15	heater tube diameter (m)
16	heater tube wall thickness (m)
17	number of heater tubes per regenerator
18	regenerator length (m)
19	regenerator diameter (m)
20	regenerator wall thickness (m)
21	ratio of the minimum flow area to the total frontal area in the regenerator
22	regenerator screen wire diameter (m)
23	number of regenerators per cylinder
24	cooler tube length (m)
25	cooler tube diameter (m)
26	cooler tube wall thickness (m)
27	number of cooler tubes per regenerator
28	cold connecting duct diameter (m)
29	number of cold connecting ducts per regenerator
30	compression cylinder bore (m)

would seldom be used. The process of determining meaningful optimization parameters is continuing. Variables (in addition to the design variables from Table 2) are also changed during SEAMOPT computation. For example, if the regenerators increase in number, or diameter, they must be located farther from the expansion-compression zone in the GPU-3 design, and the connecting ducts made longer. Also, if the regenerator becomes longer it will impact the size and shape of the connecting tube between the heater and regenerator as the heater bottom is fixed in the GPU-3 design. These, and other design concerns are included. The current module is specific to the GPU-3 and would have to be modified for other engines, hence the dashed lines in Figure 2.

The constraint equations of Table 3 evolved through experience. For example, component walls may be thinned into non-existence to reduce heat conduction losses unless constrained by consideration of maximum allowable stress. Similarly, unswept

Table 3. Objective Functions and Constraint Equations

Objective Functions

- 1 Maximum indicated efficiency
- 2 Minimum entropy production from heat exchange at heater and cooler
- 3 Maximum power

Constraint Equations

- 1 Power level > input value
- 2 Top of regenerator is kept below expansion piston dome,
- 3 Regenerator axial thermal stress <152 MPa
- 4 Heater wall temperature gradient <20°C
- 5 Heater tube gas Mach number <0.05
- 6 Total frictional pressure drop <10% mean pressure
- 7-10 Hoop stress in the displacer, heater, cooler, and regenerator walls <152 MPa
- 11 Efficiency > input value

volume may be completely eliminated unless constrained by maximum pressure drop and Mach number limitations. Other constraints such as piston rod bearing loads and several temperature and gradient limits have been tried.

The executive module also compares performance against objectives. The designer must analytically represent design goals such as those listed in Table 3.

After attaining a specific objective, the executive module runs a map of RPM vs. performance for the new engine design. This allows the user to examine off design point performance and determine suitability of the new design application.

RESULTS

The code system was used to optimize the GPU-3 engine. This design was chosen because of its familiarity to the Stirling engine community and since adequate geometric information has been published (4,7). Two cases will be discussed here:

- The first case shows the effect of optimizing regenerator design to accomplish three separate objectives—maximum power, minimum entropy, and maximum efficiency, and
- The second case changes the design of the entire engine thermodynamic section to maximize efficiency.

In both cases the GPU-3 engine is optimized at the design point for the operating conditions and constraints shown in Table 4.

Table 4. Operating Conditions and Constraints for GPU-3 Engine Optimization

Working fluid	Hydrogen
Mean pressure	2.74 MPa (27 atm)
Speed	3000 RPM (50 Hz)
Hot outer wall temperature	927 K (1200°F)
Cooling water temperature	287 K (55°F)
Maximum mean pressure	7 MPa (69 atm)
Maximum allowable stress	152 MPa (22 Ksi)

Performance calculations for the various new designs (as shown in Figures 3 and 4) were calculated using the changed engine geometries derived by SEAMOPT. A summary of these design changes is given in Table 5.

Regenerator Porosity

Table 6 illustrates the improvement in performance possible simply by reducing the number of wires in the regenerator matrix. The resulting increase in porosity significantly improves both power and efficiency by reducing frictional flow losses. The performance improvement is greater at higher engine speeds where flow losses predominate. This improvement could be realized at a lower cost and with a simpler design than the original regenerator matrix.

Case 1 - Regenerator Optimization

The first case varies only five regenerator design parameters—height, diameter, wall thickness of the shell, wire diameter, and mesh size of the steel screen matrix. Three different objectives were considered:

- (1) Efficiency is maximized while power is constrained to be no less than in the original design.
- (2) Irreversibilities in terms of entropy change at the heater and cooler are minimized.
- (3) Power is maximized while efficiency is constrained to be no less than in the original design.

These are the design objectives and constraint equations shown in Table 3. Constraints 2 through 10 apply to all three objectives, while 1 and 11 apply to the efficiency objective and power objective, respectively.

Table 5. Change in Regeneration Design Due To Optimization

	<u>Original</u>	<u>Max <math>\eta</math></u>	<u>Min <math>\Delta S</math></u>	<u>Max Power</u>	<u>Case 2</u>
height (mm)	22.6	30.	25	16.7	36.9
diameter (mm)	22.6	30.	29	20.5	31.6
wall thickness (mm)	1.7	0.77	0.75	0.64	0.89
wire size (mm)	0.04	0.039	0.04	0.046	0.04
mesh (wires/mm)	7.8	4.6	5.2	3.8	4.4
porosity	0.7	0.8	0.78	0.81	0.81

Comparison of Figures 3 and 4 shows the trade-off of power versus efficiency. Efficiency is gained at the expense of power and, without the constraint on power a design having lower power and higher efficiency than that shown would have resulted. This was not the case when power was optimized, in that a small gain in efficiency was obtained even though this was not included as a design objective. It did not appear that power could be further increased by reducing efficiency. The variation in regenerator design corresponding to these effects is presented in Table 5, where in general, high efficiency implies larger regenerators while high power requires less volume. Thinner walls, reduced wire size, reduced mesh (number of wires/mm) and increased porosity benefit both power and efficiency.

Minimizing entropy production proved to provide a favorable objective function as shown in Figures 3 and 4. Efficiency was improved while an increase in power was also obtained.

Case 2 - Maximum Efficiency of Entire Engine Thermodynamic Section

Fifteen design parameters were allowed to vary in this study. These are, from Table 2, Numbers 14 through 22, and 24 through 29 (heater, regenerator, cooler, and cold connecting duct dimensions). Power was held constant at 3.25 kW and efficiency was maximized.

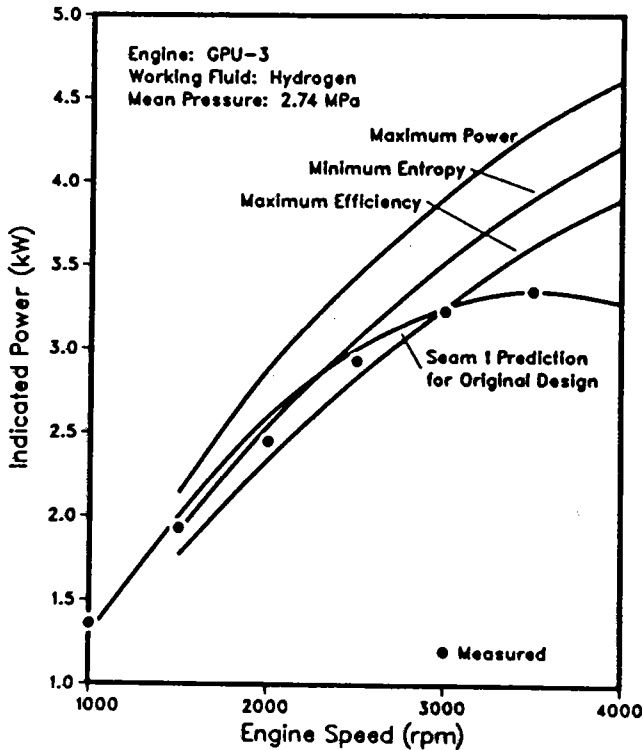


Figure 3. Effect of Different Optimization Objectives on Power

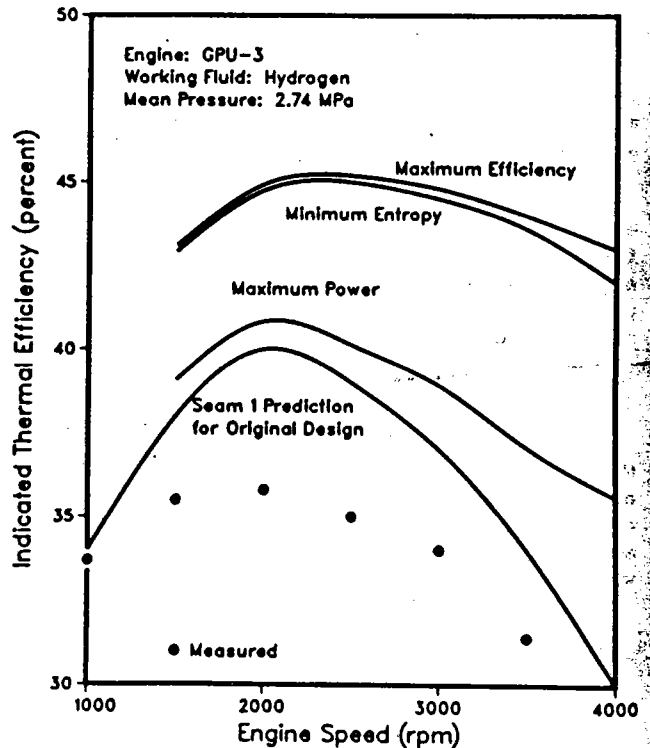


Figure 4. Effect of Different Optimization Objectives on Efficiency



A measure of the effectiveness of an optimization code is the rate at which convergence is obtained; Figure 5 shows that the major improvements were achieved in under 10 iterations and convergence essentially obtained in 20 to 25 iterations. This consumed less than 2 minutes of computation time.

As indicated in Figure 5, efficiency is first increased by reducing flow friction (increasing the flow area of components). Conduction losses were then reduced by reducing wall thickness and lowering thermal gradients. Finally, heater and cooler performance is improved and the volume of the heater and cold connecting duct reduced. Table 6 compares design point performance for all the cases discussed.

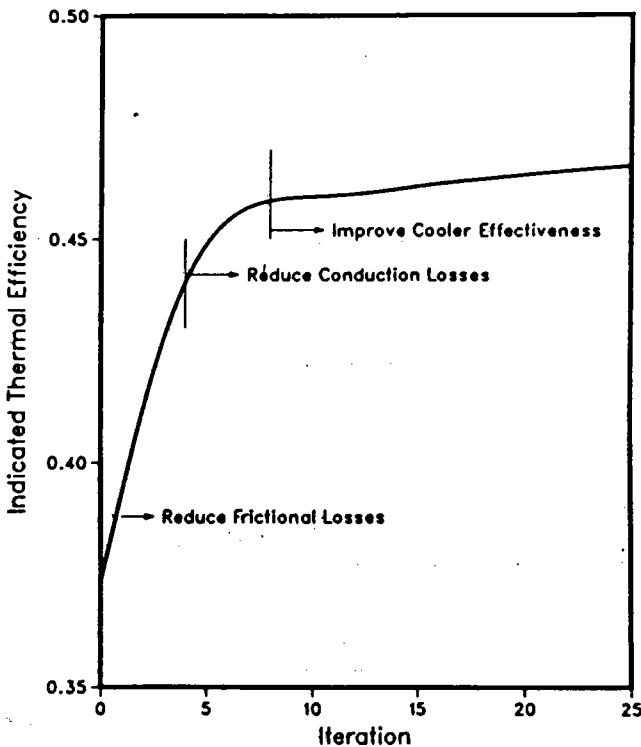


Figure 5. Heat Exchanger Optimization

#### CONCLUSIONS

The SEAMOPT code system has been shown to be an efficient technique for optimizing Stirling engine design. Furthermore, it has been shown that with variations in objective, significantly different design requirements can be met. Finally, the code system produced results that are consistent and, in retrospect, understandable.

This code offers an important new tool to Stirling engine researchers and designers, whose creativity in formulating objective functions and constraints remains the deter-

Table 6. Effect of Design Change on GPU-3 Performance at Design Point (Original design is calculated to develop 3.25 kW with 37% efficiency.)

Description of Design Change	Predicted Performance Change (%)	
	Indicated Power	Indicated Thermal Efficiency
40% fewer wires in regenerator	+16	+9.7
Regenerator Design Optimized (5 design variables considered)		
Efficiency	0	+21.1
Minimum Entropy	+8.3	+20.3
Maximum Power	+21.2	+5.4
Thermodynamic Section Optimized (15 design variables considered)		
Efficiency	0	+25.9

mining factor in the usefulness of the code. While not treated in this paper, SEAMOPT can be used to design an engine to a power level specified by the user. Improvements in performance prediction are still required and can easily be incorporated as necessary experimental data is generated and/or published.

#### ACKNOWLEDGEMENTS

The analysis development effort described in this paper is supported by the Energy Conversion and Utilization Technology Division of the U.S. Department of Energy, Office of Energy Systems Research. The encouragement of Mr. Marvin Gunn, program manager for energy conversion technology projects, is appreciated. The authors take pleasure in expressing our appreciation to Eric Richardson of the University of Iowa for his assistance in the development of the executive module and to Dr. Michael Minkoff of Argonne for his assistance with this implementation of VMCON.

#### REFERENCES

1. T.J. Heames et al., "A User Oriented Design System for Stirling Cycle Codes," Proceedings of 17th IECEC, Paper No. 828278, August 1982.

2. T.J. Heames et al., "Stirling Engine Thermodynamic Analysis: A Users Guide to SEAM1," ANL-82-59, September 1982.
3. G.A. McLennan et al., "Stirling Analysis Code Validation Using Free-Piston Engine Base Line Data," Proceedings of 18th IECEC, PAPER NO. 839362, August 1983.
4. R. Tew et al., "A Stirling Engine Computer Model for Performance Calculations," NASA-TM-78884, May, 1978.
5. M.J.D. Powell, "A Fast Algorithm for Nonlinearly Constrained Optimization Calculations," Proceedings 17th Power Conference on Numerical Analysis, Lecture Notes in Mathematics, Vol. 630, 1978.
6. R.L. Crane et al., "Solution of the General Nonlinear Programming Problem with Subroutine VMCON," ANL-80-64, July, 1980.
7. L.G. Thieme, "Low Power Baseline Test Results for the GPU-3 Stirling Engine," NASA-TM-79103, April, 1979.

---

ANL-82-59

---

ARGONNE NATIONAL LABORATORY  
9700 South Cass Avenue  
Argonne, Illinois 60439

STIRLING ENGINE THERMODYNAMIC ANALYSIS:  
A USERS GUIDE TO SEAM1

by

T. J. Heames, D. J. Uherka,\*  
J. C. Zabel,\*\* and J. G. Daley

Components Technology Division

September 1982

\*Faculty Research Leave Participant from University of North Dakota.  
\*\*Resident Student Associate.

## TABLE OF CONTENTS

	<u>Page</u>
NOMENCLATURE	viii
ABSTRACT	ix
1. INTRODUCTION.....	1
2. DESCRIPTION OF THE CODE SYSTEM.....	3
2.1 DESCRIPTION OF GENERAL MODULES.....	3
2.2 INPUT MODULE.....	4
2.2.1 The Tasks of the Input Module.....	4
2.2.2 Driver Module.....	4
2.2.3 Input Data.....	4
2.2.4 Input Initialization.....	7
2.2.5 Input Edit.....	7
2.3 STANDARD FUNCTIONS MODULE.....	7
2.3.1 Gas and Metal Properties.....	7
2.3.1.1 Description of Property Subroutines.....	8
2.3.1.2 Implementation of the Property Subroutines.....	9
2.3.1.3 Values in Property Subroutines.....	10
2.3.2 Heat Transfer and Friction Factor Subroutine.....	10
2.3.2.1 Friction Factors.....	11
2.3.2.1.1 Friction Factor for Round Tubes.....	13
2.3.2.1.2 Friction Factor for Rectangular Tubes.....	14
2.3.2.1.3 Friction Factor for Screen Matrix.....	14
2.3.2.1.4 Friction Factor for Packed Sphere Matrix.....	15
2.3.2.1.5 Friction Factor for Metnet Matrix.....	15
2.3.2.1.6 Friction Factor for SLRE Matrix.....	16
2.3.2.1.7 Loss Factor for Orifice.....	16
2.3.2.1.8 Loss Factor for Area Contraction and Expansion.....	16
2.3.2.2 Heat Transfer Coefficients.....	17
2.3.2.2.1 Heat Transfer Coefficient for Round Tubes.....	18
2.3.2.2.2 Heat Transfer Coefficient for Rectangular Tubes.....	18
2.3.2.2.3 Heat Transfer Coefficient for Screen Matrix.....	19
2.3.2.2.4 Heat Transfer Coefficient for Packed Sphere Matrix.....	19
2.3.2.2.5 Heat Transfer Coefficient for Metnet Matrix.....	19
2.3.2.2.6 Heat Transfer Coefficient for SLRE Matrix.....	20
2.3.2.3 Implementation of Subroutine HTF.....	20
2.3.3 Volume Subroutine.....	22
2.3.3.1 Initial Calculations.....	25
2.3.3.2 Implementation of Subroutine VOLUME.....	26
2.3.3.3 Free-Piston Volume Variation.....	28

## TABLE OF CONTENTS

	<u>Page</u>
2.3.4 Additional Losses Subroutine.....	28
2.3.4.1 Dynamic Piston Motion Losses - QDYNAMIC.....	28
2.3.4.1.1 Shuttle Conduction Loss.....	29
2.3.4.1.2 Gap Loss.....	29
2.3.4.1.3 Total Dynamic Piston Motion Losses.....	30
2.3.4.2 Axial Conduction Losses.....	30
2.3.4.3 Implementation of the Losses Subroutine.....	30
2.3.4.4 Future Additions to the Losses Subroutine.....	31
2.3.5 Engine Constraints and Optimization.....	31
2.4 ANALYSIS MODULE (GENERIC).....	32
2.4.1 Tasks of the Analysis Module.....	32
2.5 OUTPUT MODULE.....	32
2.5.1 Tasks of the Output Module.....	32
2.5.2 Controlling Output with Input.....	33
2.5.3 Filling the Output Arrays.....	33
2.5.4 Calling the Output Subroutine.....	35
3. SEAM1 (STIRLING ENGINE ANALYSIS MODULE 1).....	36
3.1 BACKGROUND.....	36
3.1.1 Rios Analysis.....	36
3.2 DESCRIPTION OF SEAM1 COMPUTATIONAL PROCEDURES.....	36
3.2.1 What the Code Calculates and Predicts.....	36
3.2.2 General Scheme for Solution of Governing Equations.....	36
3.2.3 Calculation of Expansion and Compression Work During Cycle.....	38
3.2.4 Analysis of Losses.....	42
3.2.4.1 Pressure Drop Losses Due to Fluid Frictional Effects.....	42
3.2.4.2 Imperfect Heat Exchanger Loss.....	46
3.2.4.3 Regenerator Ineffectiveness ( $Q_{\text{REGEN}}$ ).....	48
3.2.4.3.1 Correction to Regenerator Ineffectiveness.....	49
3.3 DESCRIPTION OF SUBPROGRAM ELEMENTS OF SEAM1.....	49
3.3.1 RIOSIN Subroutine.....	49
3.3.2 ANALIS Subroutine.....	50
3.3.3 CYCLER Subroutine.....	50
3.3.4 HTFLOW Subroutine.....	51
3.3.5 RIOSPR Subroutine.....	52

## TABLE OF CONTENTS

	<u>Page</u>
4. TEST RESULTS AND CONCLUSIONS.....	53
4.1 GPU-3 PERFORMANCE PREDICTIONS USING SEAM1.....	53
4.2 CONCLUSIONS.....	57
APPENDICES	
A. DIRECTIONS FOR USING THE CODE.....	59
A.1 GENERAL INPUT DATA GROUPS.....	59
A.2 TITLE AND GENERAL INPUT.....	61
A.2.1 COMMON IGEN.....	61
A.2.2 COMMON FLTGEN.....	69
A.3 INPUT FOR THE WORKING FLUID VOLUMES.....	73
A.3.1 COMMON INCELL.....	73
A.3.2 COMMON FLCCELL.....	75
A.4 INPUT FOR THE ADDED VOLUMES.....	81
A.4.1 COMMON IADD.....	81
A.4.2 COMMON FADD.....	83
A.5 PERTURBATION INPUT.....	85
A.5.1 Additional Input Options.....	86
A.5.2 Interactive Perturbations.....	87
A.6 SAMPLE INPUT DECK.....	87
A.7 SAMPLE OUTPUT.....	95
A.8 GRAPHICS CAPABILITY.....	95
A.8.1 IGRAPH=1.....	95
A.8.2 IGRAPH=2.....	98
A.9 OBTAINING THE CODE FROM NESL.....	98
B. GPU-3 SAMPLE PROBLEM OUTPUT.....	100
C. DEFINITIONS.....	123
D. GRAF LISTING.....	133
E. GRAF OUTPUT/TELLAGRAF INPUT.....	139
REFERENCES.....	145
ACKNOWLEDGEMENT.....	148

## LIST OF FIGURES

<u>No.</u>	<u>Title</u>	<u>Page</u>
1	Framework of Stirling Engine Analysis System.....	3
2	INPDRV Subprogram.....	6
3	The Three Flow Regions.....	12
4	Contraction and Expansion.....	17
5	Drive Type 0 Connecting Rod Drive.....	23
6	Drive Type 1 Rhombic Drive.....	23
7	Equivalent to Rhombic Drive.....	24
8	Crank Phase Angle, $\phi_{\text{crank}}$ .....	27
9	Volume Phase Angle, $\phi_{\text{vol}}$ .....	27
10	Main Program.....	37
11	ANALIS Subprogram.....	50
12	Power Comparison.....	55
13	Efficiency Comparison.....	56
14	Engine Map.....	58
A-1	GPU-3 SEAM1 Cell Location.....	60
A-2	Design Type 1 In-Line Design.....	62
A-3	Design Type 2 Double Acting Design.....	63
A-4	Design Type 3 Displacer Design.....	64
A-5	Diagram of Rhombic Drive.....	65
A-6	GPU-3 Dimensions for Heat Conduction.....	77
A-7	GPU-3 Power Flow Comparisons.....	96
A-8	GPU-3 Power Loss Comparisons.....	97

## LIST OF TABLES

<u>No.</u>	<u>Title</u>	<u>Page</u>
I.	Requirements Considered in Development of Argonne Stirling Engine Analysis Code.....	2
II.	Design Options Available.....	5
III.	Fluid and Metal Properties Available.....	8
IV.	Types of Flow Passages Modeled.....	12
V.	Engine Loss Mechanisms Modeled.....	28
VI.	Assumptions Used in Computing SEAM1 Expansion and Compression Work Terms.....	39
VII.	Comparison of SEAM1 Calculations with GPU-3 Experimental Data and NASA Code Predictions.....	54
A-1	Sample Input Deck for GPU-3 Example.....	88
A-2	Worksheet for Namelist CELL.....	91
A-3	Sample Interactive Session.....	93





NomenclatureMajor SymbolsDefinitionGreek Symbols

AF	Free-flow area
AW	Wetted surface area
AX	Cross-sectional area
C	Specific heat
D	Diameter
d	Derivative of a variable
E	Energy
e	Eccentricity
f	Fanning friction factor
H	Enthalpy
h	Heat-transfer coefficient
j	Colburn factor
k	Conductivity
L	Length
m	Mass
$\dot{m}$	Mass flow rate
M	Dimensionless mass
P	Pressure
P	Dimensionless pressure
Q	Heat flow rate
R	Gas constant, effective thermal resistance
Re	Reynolds Number = $\rho u D_h / \mu$
r	Radius
$^{1/2}v_T$	Dimensionless volume to temperature ratio
$S_T$	Stanton number = $h/C_p \rho u$
T	Gas temperature
T	Dimensionless temperature
T*	Gas temperature of adjacent heat exchanger
TE	Outside environment temperature
TW	Inner wall temperature
t	Time
u	Gas velocity
V	Volume
V	Dimensionless volume
W	Work
W	Dimensionless work
X	Volume fraction

$\alpha$	Crank angle
$\gamma$	Specific heat ratio
$\delta$	Differentials of variables
$\mu$	Viscosity
$\pi$	Pi = 3.14159...
$\rho$	Density
$\sigma$	Ratio of minimum free flow area to frontal area
$\omega$	Crank angular speed
$\phi$	Phase angle

Subscripts

AC	Half the maximum compression space
AE	Half the maximum expansion space
C	Compression space
D	Dead space
DC <sub>x</sub>	Dead space on compression side of x
DE <sub>x</sub>	Dead space on expansion side of x
E	Expansion space
f	Friction
g	Gas
H	Heater
h	Hydraulic
i	Inner wall
K	Cooler
o	Outer wall
P	Pressure
R	Regenerator
T	Total
V	Volume
w	Wall
x	Variable component or position notation
$\alpha$	Crank angle

STIRLING ENGINE THERMODYNAMIC ANALYSIS:  
A USERS GUIDE TO SEAM1

by

T. J. Heames, D. J. Uherka, J. C. Zabel, and J. G. Daley

ABSTRACT

This report provides background and procedural information for the use of a general-purpose Stirling-engine analysis code developed at Argonne National Laboratory and available through the National Energy Software Center. Different engine configurations are easily specified, or the user may make use of provided data for existing engines, both kinematic and free piston. The code models heat transfer and fluid mechanics throughout the engine and accounts for system energy flows and losses. Good agreement is shown between code predictions and experimental measurements. The present analysis method was chosen for fast execution and useful information on energy flows in the system. A description is provided of the code structure that is intended to accept different analysis modules that can provide improved system modeling or optimization capability.

## 1. INTRODUCTION

In the last 15 years various techniques and codes for analyzing Stirling engines have emerged. See, for example, Rios [1], Urieli [2], Tew [3], Martini [4], Schock [5], Gedeon [6], Kirkley [7], Glassford [8], Rauch [9], Organ [10], and Beans [11]. These, as well as earlier techniques and codes, may be separated into the following categories for purposes of comparison.

### Category 1: Engine Performance Predictions Made

These codes calculate overall performance parameters such as engine power and efficiency, but provide no information on component performance or transient conditions during the cycle. They use closed-form solutions to simplified dynamic equations. Typical assumptions are that piston motion is sinusoidal and that temperatures within the engine do not vary with time.

### Category 2: Limited Transient Information Calculated

These codes account for actual piston movement, compute changing conditions within the engine during the cycle, and calculate engine performance. Typical assumptions are that the working fluid is an ideal gas, momentum effects are ignored, and pressure is uniform within the engine at any time.

### Category 3: Detailed Transient Information Calculated

In these codes the entire set of field equations is solved in terms of position and time; i.e., conditions are determined in each engine cell at each time step. Typical assumptions are that one-dimensional analysis is sufficient and that steady flow correlations may be used to predict heat-transfer and fluid-friction coefficients.

Examples of analysis models in the above three categories are Schmidt [12], Martini [4], and Urieli [2], respectively. The analysis codes outlined in the latter two categories attempt to realistically model heat transfer and fluid flows in the system. However, a comparative code study [13] found the available codes were too constrained to permit a comparison on the basis of the same set of experimental data. Existing codes:

- Were generally calibrated for a particular engine or type of engine,
- Had differing gas and metal properties,
- Had differing heat transfer and friction correlations,
- Were unable to achieve stable cyclic steady state, or
- Were classified as proprietary and accessible only under license.

Each category of codes was intended for a particular need; however, the relative merits of codes within each class or between classes could not be assessed. Nor was there the capability of analyzing different Stirling engines over a range of operating conditions with any of the existing codes, much less the capability of comparing such calculations between codes. The requirements considered in the development of the Argonne Stirling engine analysis code are listed in Table I.

---

TABLE I. Requirements Considered in Development of  
Argonne Stirling Engine Analysis Code

Available for wide distribution

Well documented

Validated against real engines

User oriented

Compatible with both mini and large computers

Able to evaluate a wide range of volume-variation techniques

Able to compute answers using different components, materials, and working fluids easily

Able to achieve cyclic steady state

Able to compute answers using a stable numerical-integration scheme

Able to determine mass and energy flows

Able to be used with different solution techniques for the governing equations describing Stirling engine fluid dynamics

---

The approach selected to meeting these requirements was to separate the analysis method from the more general requirements of providing standardized input and output capabilities and libraries of standard functions. The code is thus structured to have the generalized modules described in Chapter 2 and the replaceable analysis modules, in this case SEAM1 (Stirling Engine Analysis Module 1), which is described in Chapter 3. SEAM1 is based upon the D.Sc. Thesis of Rios [1] and falls into the second category of code types described in the introduction. That is, performance and transient information are provided, but computation time is short. Thus, the needs of most Stirling-cycle researchers are accommodated. Future code releases will provide improved analysis capability. The details of how to use the code, including input, perturbation, and graphics are in Chapter 4. Finally, Chapter 5 compares code predictions with experimental data.

The code and sample input and output are available from the National Energy Software Center.

## 2. DESCRIPTION OF THE CODE SYSTEM

### 2.1 DESCRIPTION OF GENERAL MODULES

The Stirling engine analysis system consists of the four modules as shown in Fig. 1.

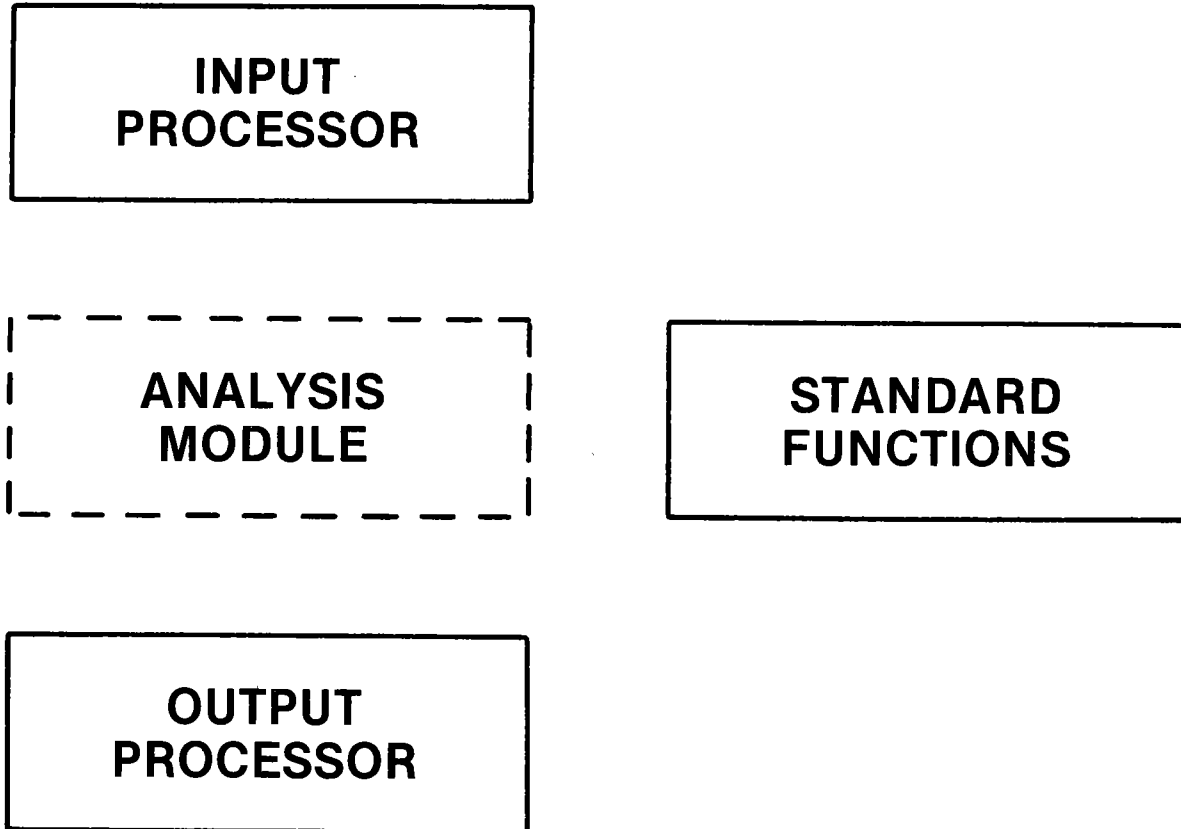


Fig. 1. Framework of Stirling Engine Analysis System

The analysis module provides a specific analysis capability and is discussed in detail in Chapter 3. The more general system modules are now discussed as well as the general function of the analysis module.

Briefly stated, the Input module reads the engine specifications and operating data, provides default values, estimates initial conditions, and edits the results to verify the starting point. The Output module writes out transient and summary results as specified by the Input data. The Standard Functions module contains standard calculation subroutines that any Stirling-engine code might need, such as gas and metal properties, heat-transfer and friction coefficients, variable volume calculations, and additional heat losses that are not integrated into the analysis module.

## 2.2 INPUT MODULE

This section contains a general description of how the Input Module works and how the data are input. The meanings of the individual input variables are given in Appendix A.

2.2.1 The Tasks of the Input Module. The Input Module does the following tasks for the ANL Stirling Engine Analysis Model through the use of four subprograms:

Reads the optional perturbation data to control the number of cases, and calls the other subroutines (INPDRV).

Reads the data describing the engine type, dimensions, and operating conditions, as well as calculation parameters such as time step, number of cycles, etc. (INPUT).

Computes omitted input variables (if possible), default options, and other initializing values from the input data (INITAL).

Organizes and prints the input data in an easy-to-read format for editing by the user (EDTINP).

The design options available are shown in Table II.

2.2.2 Driver Module. The INPDRV Subroutine is called from the Main program for each case. As is shown in Fig. 2 this routine determines where the input is to be read from and whether the data needs to be reinitialized or edited.

2.2.3 Input Data. The INPUT Subroutine is called from INPDRV one time and reads three types of data:

- (1) The title, and general scalar values describing the engine and operating conditions as a whole.
- (2) An array of values for each of 30 or less contiguous engine cells through which the working gas flows.
- (3) An array of values for each of four or less other types of engine components such as a buffer space.

Each of the above types of input can be seen in the sample input deck, Table A-1 of Appendix 4.

All input is read from logical unit 5. The three input blocks are briefly described below.

- (1) The title is read as an 80-character alphanumeric array and occupies one card (or record). The title should be used as a general input deck identifier. The general scalar variables, such as gas type, frequency, engine design, etc. are listed in Namelist GINPT. This Namelist is read only once.
- (2) The basic cell information arrays, II (dimension 8) and AA (dimension 18), are in Namelist CELL, which is read once for each of the adjacent cells. Array II contains integer values,

---

 TABLE II. Design Options Available

 1. Mechanical Configurations

In line design or alpha engine; two pistons, two cylinders (Fig. A-2).

Double acting piston design (Fig. A-3).

Displacer design (Fig. A-4).

GPU-3: IDESGN = 3

 2. Type Drive Mechanisms

Connecting rod mechanism.

Rhombic drive.

Dynamic analysis (not yet available) for free piston.

GPU-3: IDRIVE = 1 (Fig. A-5).

 3. Working Fluids

Hydrogen	Air
----------	-----

Helium	Carbon dioxide
--------	----------------

Nitrogen	Methane
----------	---------

 4. Structural Materials

Aluminum T4-2024	Stainless steels 304, 310, 316
------------------	--------------------------------

Copper	Titanium nickel
--------	-----------------

Inconel X-750	Nickel
---------------	--------

K Monel	
---------	--

---

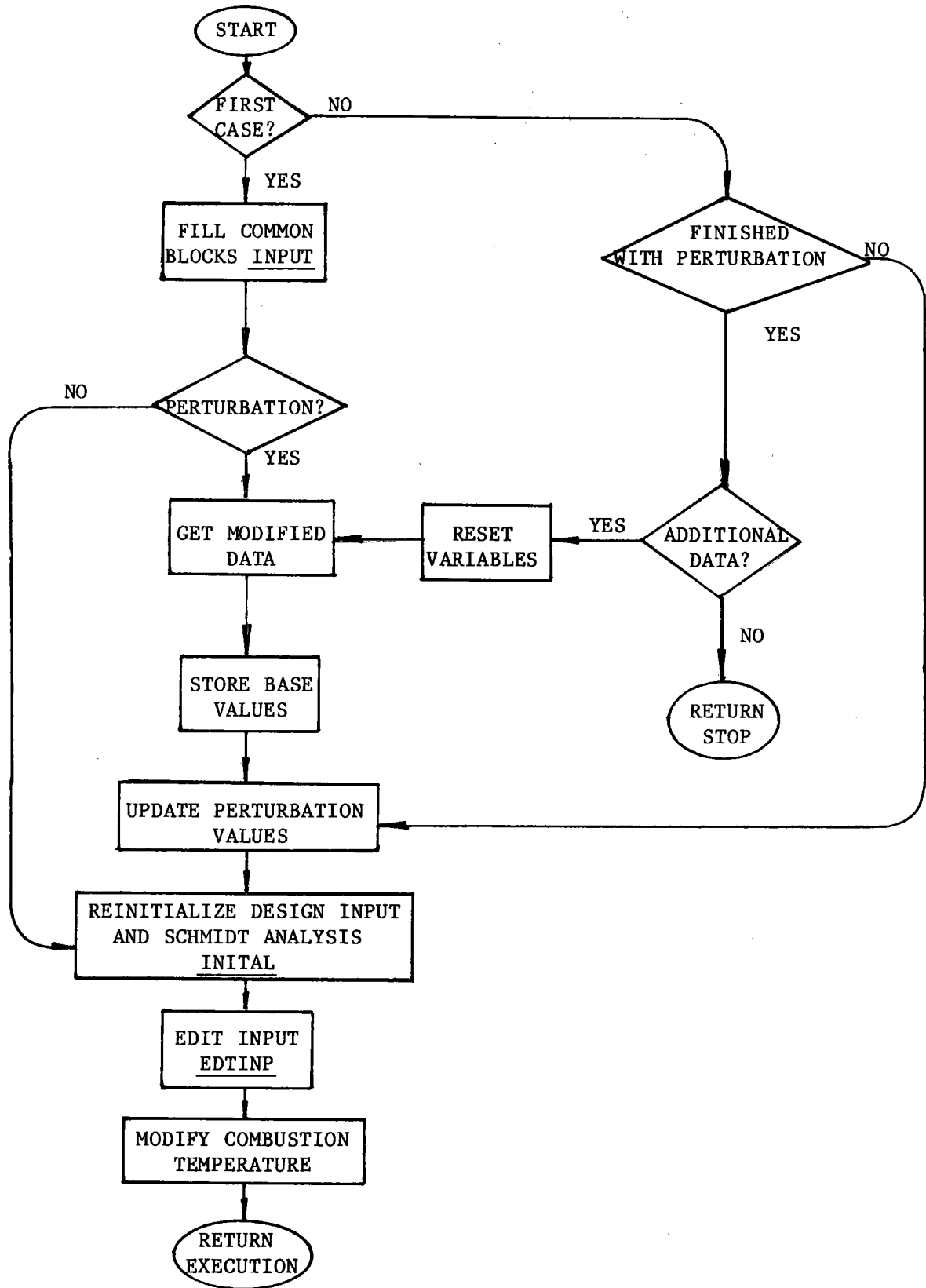


Fig. 2. INPDRV Subprogram



and AA contains floating-point values for the cell. After Namelist CELL is read, the temporary values in II and AA are assigned to the appropriate location in the permanent storage (see Appendix A).

- (3) Namelist ADDED is read once for each "other" type of cell. The cell information arrays in Namelist ADDED are JJ (dimension 6) and BB (dimension 13). As above, these values are stored each time they are read. These array names are described in Appendix A.

2.2.4 Input Initialization. The Initial Subprogram is called from INPDRV as a function of the value in variable ICHNG. The program is broken into two segments, the first of which initializes variables for every case such as temperature convergence and time-step related variables. The second segment is called whenever a significant data change is input. This section:

- Initializes piston areas and cylinder bores.
- Determines which cells are associated with the various heat exchangers,
- Initializes the variable volume routine discussed in Sec. 2.3.3 and determines the crank angle for minimum total compression volume.
- Initializes gas reference conditions.
- Sets up "Schmidt Analysis" constants.
- Resets gas mass and pressure to be consistent.

2.2.5 Input Edit. The EDTINP Subprogram is called from INPDRV as a function of the value in variable ICHNG. The program edits the input for the convenience of the user.

### 2.3 STANDARD FUNCTIONS MODULE

This module consists of separate subroutines used to calculate values that are needed by most Stirling-engine codes. The calculation of gas and metal properties, heat-transfer and friction coefficients, volumes, and conduction losses are put in separate subroutines, which will be used by the various analysis modules. Hence, the analysis modules may be compared without being influenced by these standard calculations. The various subroutines in this module are described below.

2.3.1 Gas and Metal Properties. The following routines are used by the various modules to determine the thermophysical properties of gas and metal.

- XGAS: a function subprogram to return gas values
- XMETAL: a function subprogram to return metal values
- VALUE: a subroutine used to evaluate the polynomial approximation of the experimental data
- BLOCK DATA: a tabulation of the coefficients needed by the polynomial fit

The gas and metal properties returned to the calling program are shown in Table III.

---

TABLE III. Fluid and Metal Properties Available

<u>Fluid Properties</u>	<u>Gases Included</u>	
Specific Heat, $C_p$	H <sub>2</sub> , He, N <sub>2</sub> , Air, CO <sub>2</sub> , CH <sub>4</sub>	
Thermal Conductivity, k		
Viscosity, $\mu$		
Gas Constant, R		
<u>Metal Properties</u>	<u>Metals Included</u>	
Specific Heat, $C_p$	Aluminum T4-2024	K Monel
Thermal Conductivity, k	Copper	Titanium
Density, $\rho$	Inconel X-750	Nickel
	Stainless Steel 304, 310, 316	

---

Each of the above properties, except for the gas constant, is dependent upon the gas or metal temperature. Therefore, to obtain property values, the temperature and property identifying number must be supplied as arguments. A metal property also requires that the engine cell number be supplied as an argument, since different components of the engine may have different wall metals.

2.3.1.1 Description of Property Subroutines. Each gas and metal property is approximated as a function of temperature T by cubic splines using a library program contained in the International Mathematical and Statistical Library (IMSL) package.

The temperature range for each approximated set of property data is taken to be  $300 \text{ K} < T < T_{\text{max}}$ , where  $T_{\text{max}}$  is determined by the availability of reliable data for the given gas or metal. For consistency, this temperature range is transformed to the interval [0,1]. The interval is then divided into four subintervals with "nodes" at 0, 0.25, 0.5, 0.75, and 1. The data on the four subintervals are approximated with four cubic polynomials that meet smoothly at the interior nodes.

The Property Subroutine then evaluates a function  $f(T)$  of a gas or metal property for T between 300 K and  $T_{\text{max}}$ :

$$f(T) = \sum_{i=0}^3 C_i (TR - n)^i = \text{property value}, \quad (1)$$

where,

$TR = (T - 300)/(T_{\max} - 300) = \text{temperature ratio,}$

$n = \text{the "node" just to the left of TR. (} n = 0, 0.25, 0.5, 0.75, \text{ or } 1),$

and

$C_0, C_1, C_2, C_3 = \text{the appropriate set of cubic coefficients for the given property, material, and sub-interval.}$

If  $T < 300 \text{ K}$  or  $T > T_{\max}$ , the property value is calculated at  $T = 300 \text{ K}$  or  $T = T_{\max}$ , respectively. The user should, however, be aware that for metals,  $T_{\max} \cong \text{melting point.}$

2.3.1.2 Implementation of the Property Subroutines. To calculate one of the four gas properties and store its value in location X, the following Fortran statement is used in the Analysis Module:

$X = \text{XGAS}(\text{IPROP}, T),$

where

$T = \text{temperature (K)}$

and

IPROP = an integer variable, initialized in INITIAL and stored in common, that identifies the gas property desired, as shown below:

<u>IPROP</u>	<u>Gas Property Value Returned</u>	<u>Units</u>
IRGAS	Gas constant, R	J/(kg-K)
IMUGAS	Viscosity, $\mu$	N-S/m <sup>2</sup>
ICPGAS	Specific heat, $C_p$	J/(kg-K)
IKGAS	Thermal conductivity, k	W/(m-K)

Note that other gas properties, such as  $C_v$  and  $\gamma = C_p/C_v$ , can be obtained from the above properties. The type of gas is identified by the input variable IGAS, which is in common block IGEN and has a value from 1 to 6 as listed in Sec. 4.2.1.

To obtain one of the three metal properties and store the value in location X, the following Fortran statement is used:

$X = \text{XMETAL}(\text{IPROP}, \text{ICELL}, T)$

where

$T = \text{temperature (K)}$

ICELL = the engine cell number. The property value returned is for the wall metal, MTLWAL (ICELL) (see App. A.3.1),

and

IPROP = an integer variable, initialized in INITIAL and stored in common, that identified the metal property, as shown below:

<u>IPROP</u>	<u>Metal Property Value Returned</u>	<u>Units</u>
IKM	Conductivity, k	W/(m-K)
ICPM	Specific heat, C <sub>p</sub>	J/(kg-K)
IRHOM	Density, ρ	kg/m <sup>3</sup>

In two cases we use properties of metal from places other than an ordinary engine cell wall: (a) the filler metal in the regenerator, or (b) the wall metal in one of the four additional types of engine components: displacer dome, cold piston buffer space, hot piston buffer space, and crankcase.

To obtain a property of the filler metal in a regenerator cell with cell number ICELL, the following Fortran statement is used:

$$X = \text{XMETAL}(\text{IPROP}, \text{ICELL} + 1000, T),$$

where

IPROP, ICELL, and T are as above.

Finally, to obtain a property of the wall metal of one of the four additional components in case (b) above, we use the statement:

$$X = \text{XMETAL}(\text{IPROP}, \text{ICELL} + 2000, T),$$

where

IPROP and T are as above, and ICELL is the appropriate subscript for IAMTL.

In each of the above cases, the metal properties subroutine determines the metal type from the value of ICELL and from the values of the arrays MTLWAL, MTLWIR, and IAMTL (see the input description in Appendix A).

**2.3.1.3 Values in Property Subroutines.** The data values for the gas and metal properties were obtained from Refs. [15]-[17]. When computed and tabulated values were compared, the accuracy of the Properties Subroutine was found to be within 2% for gases and 8% for metals. The 816 cubic coefficients for the spline approximation (51 approximations x four intervals for each approximation x four coefficients for each interval = 816 coefficients) are stored in a BLOCK DATA subroutine.

**2.3.2 Heat-Transfer and Friction-Factor Subroutine.** When supplied with an engine cell number as well as the Reynolds and Prandtl numbers, Re and Pr, for the gas flowing through a passage, this subroutine, HTF, returns the Stanton number and "Fanning" friction factor, for a variety of flow passages. The convective heat-transfer coefficient, h, can easily be obtained from the Stanton number, St, since

$$\text{St} = h/C_p G, \quad (2)$$

where

C<sub>p</sub> = specific heat at constant pressure

and

G = mass flux of the gas.

The correlation formulas for friction and heat-transfer coefficients were taken from a variety of standard sources and were derived from experimental steady flow data, even though they are being used for reversing flow. Some results are available for nonsteady and reversing flow, such as [18]-[24], and limited formulas are available. However, most of these studies have not settled the pertinent question of how reversing-flow correlations compare with steady-flow correlations. Kim [25], for example, reports that heat-transfer and friction factors in reversing-flow experiments with randomly packed sphere regenerators were about 20% higher than the steady-flow correlations. The "uncertainty" in these results was estimated to be within 20%. On the other hand, Murray and Martin [26] indicate that in wire-mesh-screen regenerators, sinusoidal flow conditions give heat-transfer factors that are lower than under steady flow. Finally, the more recent paper by Baibikov et al. [21], indicates that for accelerated flow in a rectangular tube, the instantaneous laminar friction factor is initially above and later below the steady-state correlation, but the instantaneous turbulent friction factor is always below the steady-flow value. Presently, steady-flow correlations are used.

The formulas giving friction factors and Stanton numbers have different forms, depending on whether the flow is laminar ( $Re < 2100$ ), turbulent ( $Re > 4000$ ), or in the transition region ( $2100 < Re < 4000$ ). Authors seem to disagree as to the Reynolds number range constituting the transition region. The lower limit is well established around  $Re = 2000$  or  $2100$ , but the upper limit varies, depending on the author. Some authors, for example, Tew ([3], p. 42), use a Reynolds number as high as 10,000 for the beginning of the turbulent region. Others do not have a transition region and make an abrupt jump from laminar to turbulent flow, for example, Martini ([27], p. 120). However, many authors agree that friction factors and heat transfer coefficients are quite unpredictable in the transition region.

For the ANL code, the transition region,  $2100 < Re < 4000$ , has been chosen because the upper limit 4000 is recommended by some of the more recent texts, such as Benedict ([28], pp. 231-133) and Ward-Smith ([29], p. 21). In this region a linear approximation is used resulting in curves of the form shown in Fig. 3, for both  $f$  and  $St$ .

Due to the small hydraulic diameter in the regenerator matrix of the Stirling engine, the average Reynolds number is always less than 2100 and is therefore in the "laminar" region. Thus, only the laminar portion of the formulas is needed. By comparing the empirical formulas with the experimental data published by various authors, the accuracy of the formulas is estimated to be within 20% for steady flow. However, because of the limited available data, it is difficult to estimate their accuracy for reversing flow. These empirical formulas are believed to provide the correct order of magnitude for friction factors and Stanton numbers.

The subroutine does not correct for the temperature gradient from the fluid to the wall, as discussed in Kays and London ([30], [31]). The Analysis Module makes these corrections as necessary.

2.3.2.1 Friction Factors. The friction factor,  $f$ , computed by the subroutine, HTF, is the "Fanning" friction factor defined by the equation

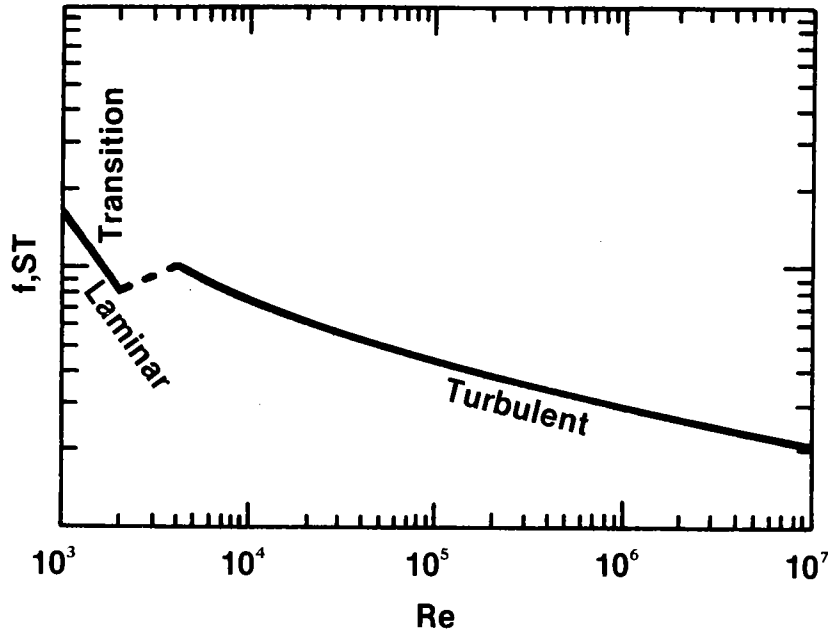


Fig. 3. The Three Flow Regions

$$\Delta P = 4f \frac{L}{D_H} \frac{1}{2} \rho U^2, \quad (3)$$

where

$\Delta P$  = pressure drop due to friction in a flow passage of length L

and

U = velocity of flow.

The "Fanning" friction factor is a dimensionless quantity and generally is a function of the Reynolds number and  $L/D_H$ . If the factor  $4f$  in Eq. 3 is replaced by  $\lambda$ , then  $\lambda$  is called the "Darcy" friction factor. Since the ANL subroutine HTF computes the "Fanning" friction factor, any added correlation that calculates the larger "Darcy" factor must be divided by four.

Flow losses due to friction or area changes within the element are calculated for each type of flow passage shown in Table IV.

TABLE IV. Types of Flow Passages Modeled

Round tubes	Parallel plane + spheres, SLRE matrix
Rectangular tube	Orifice
Screen regenerator matrix	Area contraction coefficient
Packed sphere matrix	

The friction-factor formulas used and references for each of the cases are described below.

### 2.3.2.1.1 Friction Factor for Round Tubes

Laminar ( $Re < 2100$ ).

$$f = \begin{cases} 16/Re & \text{if } Re < 10L/D_H \\ 6.137 \left(\frac{D_H}{L}\right)^{0.416} Re^{-0.584} & \text{if } Re > 10L/D_H \end{cases} \quad (4)$$

Turbulent ( $Re > 4000$ ).

$$f = \left[ 1 + \left(\frac{D_H}{L}\right)^{0.5} \right] (0.0014 + 0.125Re^{-0.32}) \quad (5)$$

Transition ( $2100 < Re < 4000$ )

$$f = f_1 + (f_2 - f_1)(Re - 2100)/(4000 - 2100), \quad (6)$$

where  $f_1$  and  $f_2$  are the friction factors at  $Re = 2100$  and  $Re = 4000$ , respectively, from Eqs. 4 and 5, giving a linear variation between the values of  $f$  with  $Re$ .

References. laminar: Benedict ([28], p. 256).

turbulent: Benedict ([28], p. 250-251), Kays and London ([30], p. 56), Kreith ([32], p. 433), and Ward-Smith ([29], p. 233).

Remarks. The laminar equation has two parts. The first part of the laminar solution is the classical Hagen-Poiseuille formula. The second part is an approximation to the Langhaar equation for  $Re > 10L/D_H$ . A third part would have been added, valid for  $Re > 1000L/D_H$ , except that  $Re$  is not expected to be in this region since the tubes where most of the frictional loss occurs generally satisfy  $L/D_H > 2$ , which implies that  $1000L/D_H > 2000$  or a Reynolds number in the transition region. In this third part Benedict [28] recommends using the Kline-Shapiro equation:

$$f = 3.435 (Re L/D_H)^{-0.5}.$$

The turbulent equation (Eq. 5) has two factors. The first factor of Eq. 5 accounts for entrance effects. It was obtained as an approximation of the entrance effects shown on the curves in Kays and London ([30], p. 56) and was found to be in good agreement with entrance-effect factors in the other references. The second factor is the Drew et al. formula, which, according to Benedict ([28], pp. 250-251), is in excellent agreement with Prandtl's equation for  $4000 < Re < 3 \times 10^6$  and is easier to use.

Finally, the transition equation (Eq. 6) is simply the equation of a straight line in the  $(f, Re)$  plane. It gives practically the same results as

a straight line in the  $(\log_{10}f, \log_{10}Re)$  plane and is more efficient to calculate. Since usually  $L/D_H < 200$  in the Stirling engine tubes, the value  $Re = 2100$  will occur in the Langhaar portion (i.e., the second part) of the laminar formula, Eq. 4, so only that part of the laminar equation is used to compute  $f_1$ .

### 2.3.2.1.2 Friction Factor for Rectangular Tubes

Laminar ( $Re \leq 2100$ ).

$$f = [1.47 - 1.48(a/b) + 0.92(a/b)^2]f_{\text{round}}, \quad (7)$$

where

$a/b$  = ratio of small side to large side of the rectangular cross section of the tube or aspect ratio

and

$f_{\text{round}}$  = the friction factor for round tubes of the same hydraulic diameter.

Turbulent ( $Re > 4000$ ).

$$f = 1 f_{\text{round}} \quad (8)$$

Transition ( $2100 < Re < 4000$ ).

$$f = f_1 + (f_2 - f_1) + (Re - 2100)/(4000 - 2100),$$

where  $f_1$  and  $f_2$  are calculated at  $Re = 2100$  and  $Re = 4000$ .

References. Laminar and turbulent--Ward-Smith ([29], pp. 180-184), Kays and London ([30], pp. 56-59).

Remarks: The first factor in the laminar formula (Eq. 7) is a quadratic least-squares fit of data in Table C3 of Ward-Smith ([29], p. 180), with an approximation error less than 3%. This multiplier is for fully developed flow, but it is also being used for short tubes due to a lack of data for short tubes.

The multiplier 1 in the turbulent formula (Eq. 8) is from Table C5 of Ward-Smith ([29], p. 184). The above remark about fully developed flow holds here also.

### 2.3.2.1.3 Friction Factor for Screen Matrix. For any Reynolds number in the regenerator,

$$f = 10^{(A \cdot Re^{-0.33})} \cdot B, \quad (9)$$

where

$$A = \frac{1.33}{p^2} \left( \frac{1-p}{\sigma} \right)^{-0.33},$$

$$B = 10^{-0.54/P} \cdot P^3/[8(1-p)\sigma^2],$$

$P$  = porosity, void fraction, of the regenerator matrix.

$\sigma$  = ratio of minimum free flow area over frontal area for the matrix.



References. Tong ([33], pp. 32, 64, 80)

Remarks. The ratio  $\sigma$  in Eq. 9 can be computed for a square weave mesh from the formula

$$\sigma = (1 - Md)^2,$$

where

$$M = \text{mesh number (number of wires per unit length)}$$

and

$$d = \text{wire diameter.}$$

Finally, note that data from which Eq. 9 is derived were taken at  $Re < 1000$  and the relation is not valid for  $Re > 1000$ . However, due to the small hydraulic diameter, Reynolds numbers in the regenerator are not likely to exceed this range.

#### 2.3.2.1.4 Friction Factor for Packed Sphere Matrix

$$f = \begin{cases} 24.92Re^{-0.698} & \text{if } Re < 100 \\ 5.12Re^{-0.347} & \text{if } Re > 100. \end{cases} \quad (10)$$

References. Kays and London ([30], pp. 86,123).

Remarks. This formula was obtained by forming linear least-square fits to the data in the above reference.

#### 2.3.2.1.5 Friction Factor for Metnet Matrix

$$4f = A(y)[1 + 10.38/Re(d)](D_H/d) \quad (11)$$

where

$$A(y) = 583.3y^3 - 107.72y^2 + 12.032y - 0.0336,$$

$y$  = "filler factor" for the Metnet,

$d = 0.432 \times 10^{-4}$  m, fiber diameter in the Metnet  
for the GM tests resulting in the above correlation  
formula,

$$Re(d) = Re \, d/D_H, \quad 10 < Re(d) < 650,$$

= Reynolds number based on fiber diameter instead of  
hydraulic diameter,

and

$$D_H/d = \text{ratio of } D_H \text{ to } d; \text{ Ref. Eq. 9}$$

References. General Motors [34, Sec. 6.006]

Remarks. This correlation formula (Eq. 11) was obtained from GM for the low-cost nickel base regenerator material, Metnet. The GM formula used the "Darcy" friction factor, and so the formula was divided by 4 to obtain the "Fanning" factor. Also, the GM formula used a Reynolds number based on their unique fiber diameter,  $d$ . If a Metnet with a different fiber diameter is used, then the value of  $d$  (DIAM in the code) should be changed in subroutine HTF, provided one agrees that the GM correlation is still valid for a range of fiber sizes. The "filler factor," denoted by  $y$  in Eq. 11, is defined to be

the fraction of the Metnet matrix volume that is filled with metal. The fibers are hollow, so that the porosity  $p$ , which is the fraction of the volume that the working gas can fill, is not quite equal to  $1 - y$ , but instead  $P < 1 - y$ . However, the friction routine assumes that in the case of Metnet, the user has input  $1 - y$  for the porosity.

#### 2.3.2.1.6 Friction Factor for SLRE Matrix

$$f = \text{friction factor for rectangular tubes.} \quad (12)$$

References. Hoehn et al. [35]

Remarks. This type of regenerator matrix was used by Jet Propulsion Labs (JPL), for the tests described in the above reference. The matrix is a corrugated sheet rolled into a spiral in which the flow passages approximate parallel infinite planes. On both ends of the spiral device an array of small balls were placed. This entire matrix was then tested at JPL. The results correlated well with rectangular tube data with a constant multiplier. In this case the subroutine simply uses the rectangular tube formulas (Eqs. 7 and 8) with aspect ratio  $a/b = 0$ .

#### 2.3.2.1.7 Loss Factor for Orifice

$$f = \text{ORIFCE(ICELL)} \quad (13)$$

References. Ward-Smith ([29], pp. 306-434)

Remarks. In case the engine cell numbered ICELL has an orifice, it is assumed that the user has supplied the orifice coefficient with the input data, and that the coefficient is stored in the array ORIFCE.

The orifice coefficient,  $f$ , gives the pressure loss  $\Delta P$  through the orifice, by means of the equation

$$\Delta P = f \cdot \frac{1}{2} \rho U^2,$$

where

$$\rho = \text{gas density}$$

and

$$U = \text{velocity of the gas entering the orifice.}$$

2.3.2.1.8 Loss Factor for Area Contraction and Expansion. The area contraction and expansion coefficients are for calculated nonrecoverable pressure loss due to the flow from a larger flow area into a smaller flow area or vice versa, as in Fig. 4.

Both the contraction and expansion formulas above were taken from the "NASA" code by Tew et al. [3]. These formulas, in turn, agree with intermediate curves shown in Kays and London ([30], Fig. 18, p. 45). Note that the cutoff Reynolds number 3000 in the above contraction and expansion correlations is roughly the midpoint of the transition range  $2100 < Re < 4000$ .

The nonrecoverable pressure loss  $\Delta P$  due to flow-area contraction or expansion is obtained from

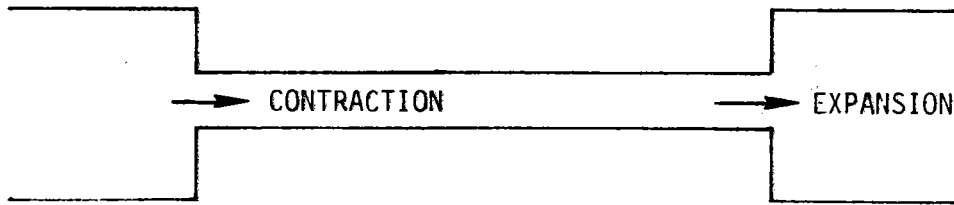


Fig. 4. Contraction and Expansion

$$\Delta P = f \cdot \frac{1}{2} \rho U^2,$$

where

$\rho$  = gas density

and

$U$  = velocity of the gas in the smaller of the two flow areas.

#### Contraction

$$f = K_C = \begin{cases} 1 - 0.4A & \text{if } Re \leq 3000 \\ 0.5 - 0.4A & \text{if } Re > 3000. \end{cases} \quad (14)$$

#### Expansion

$$f = K_E = \begin{cases} 1 - 2.6A + 1.005A^2 & \text{if } Re \leq 3000 \\ 1 - 2.0928A + 0.996A^2 & \text{if } Re > 3000, \end{cases} \quad (15)$$

where

$A$  = quotient of flow areas, smaller over larger.

References. Tew et al. [3]; Kays and London [30].

2.3.2.2 Heat-transfer Coefficients. The Stanton number,  $St$ , is calculated for each of the following types of flow passage:

- Round tubes
- Rectangular tubes
- Screen regenerator matrix
- Packed sphere matrix
- Metnet matrix
- Corrugated spiral, SLRE-type, matrix

In most cases, correlation formulas from the literature were used to obtain the "Colburn factor"  $j = St \cdot Pr^{2/3}$ , from which  $St$  is easily found. The subroutine includes an Input Option defining  $j = f/2$ , the Colburn Analogy, to provide correspondence with other analysis techniques (e.g., Urieli [2]).

The correlations, references, and remarks for each flow passage are given below.

### 2.3.2.2.1 Heat-transfer Coefficient for Round Tubes

Laminar (Re < 2100).

$$St = 1.86Re^{-2/3}(D_H/L)^{1/3}Pr^{-2/3}. \quad (16)$$

Turbulent (Re > 4000).

$$St = 0.036Re^{-0.2}(D_H/L)^{1/18}Pr^{-2/3}. \quad (17)$$

Transition (2100 < Re < 4000).

St is linearly interpolated between Re = 2100 and 4000.

References. Chapman ([36], p. 338); Jacob ([37], pp. 544-547).

Remarks. Among several correlations discussed by Chapman, these were recommended as being the best.

### 2.3.2.2.2 Heat-transfer Coefficient for Rectangular Tubes

Laminar (Re < 2100).

$$St = j \cdot Pr^{-2/3},$$

where

$$j = C \cdot f_{\text{rect}},$$

$f_{\text{rect}}$  = the friction factor for rectangular tubes

$$C = 0.25 + 0.09 \left(1 - \frac{a}{b}\right)^2 + 3.2 \left(\frac{D_H/L}{1 + 0.8D_H/L}\right) \frac{a}{b} \quad (18)$$

a/b = "aspect" ratio.

Turbulent (Re  $\geq$  4000).

$$St = j \cdot Pr^{2/3}, \quad (19)$$

where

$$j = 0.44f_{\text{rect}}$$

and

$f_{\text{rect}}$  = the friction factor for rectangular tubes.

Transition (2100 < Re < 4000).

St is linearly interpolated between Re = 2100 and 4000.

References. Kays and London ([30], pp. 56-59).

Remarks. Both the laminar and turbulent correlations were obtained by trial and error from the curves in Figs. 30-32 of the above reference. In the

laminar case, the multiplier C calculated in Eq. 18 agrees with the corresponding values taken from the Kays-London curves to within about 5%. In the turbulent case, the multiplier 0.44 in Eq. 19 compares with the values 0.41-0.47 taken from the Kays-London curves. The Kays-London curves have a wider transition region than is being used here, and so in the transition region, these correlations may not agree as well.

2.3.2.2.3 Heat-transfer Coefficient for Screen Matrix. For all Re,

$$St = \phi(P) \cdot Re^{-m(P)} \cdot (Pr)^{-1}, \quad (20)$$

where

$$P = \text{porosity},$$

$$m(P) = 0.43P + 0.15,$$

and

$$\phi(P) = \begin{cases} P/2 & \text{if } P < 0.39 \\ 1.54 - 6.36P + 7.56P^2 & \text{if } 0.39 < P < 1. \end{cases}$$

References. Coppage and London [38].

Remarks. The equations for  $m(P)$  and  $\phi(P)$  were obtained from curves given in the above reference.

2.3.2.2.4 Heat-transfer Coefficient for Packed Sphere Matrix. For all Re,

$$St = 0.21Re^{-0.31}(Pr)^{-1} \quad (21)$$

References. Kays and London ([30], p. 123); Coppage and London [38].

Remarks. This correlation is for random packed spheres with a porosity of .39.

2.3.2.2.5 Heat-transfer Coefficient for Metnet Matrix

$$St = C_{\Lambda} \cdot D_H/(4d), \quad (22)$$

where

$$d = 0.432 \times 10^{-4} \text{ m (see the remarks for the Metnet friction factor),}$$

$$C_{\Lambda} = \begin{cases} P_0 - P_1 \cdot Re(d) + [Re(d) + 15]^{-1.185} & \text{if } Re(d) < 30 \\ C_{\Lambda}(30) \left(\frac{Re(d)}{30}\right)^{-0.279} & \text{if } Re(d) > 30, \end{cases}$$

$$Re(d) = Re \cdot d/D_H,$$

$$P_0 = -0.0153 + 1.5745y - 2.865y^2,$$

$$P_1 = 0.000292 + 0.003945y + 0.00835y^2,$$

$$y = \text{"filler factor,"}$$

$$C_{\Lambda}(30) = P_0 - 0.30 P_1 + 0.011$$

References. General Motors [34].

Remarks. See also the remarks for the Metnet friction factor in Sec. 2.3.2.1.5. The GM correlation was based on wire diameter and has been converted here to hydraulic diameter. GM called the variable  $C_\Lambda$  the "heat-transfer factor," and according to [34], Sec. 6.006, pp. 9 and 44,

$$C_\Lambda = \frac{d}{L} \left[ \frac{h A_s}{\dot{m} C_p} \right],$$

where

$h$  = average convective heat-transfer coefficient for surface of regenerator material

and

$A_s$  = wetted surface area of regenerator material.

To convert  $C_\Lambda$  to Stanton number  $St$ , the definition of Stanton number is used:

$$St = h / (C_p \rho U) = h A_F / (C_p \dot{m}),$$

where

$A_F$  = free-flow area.

After rearranging, one has

$$\begin{aligned} St &= \frac{h A_s}{C_p \dot{m}} \frac{d}{L} \frac{A_F}{A_s} \frac{L}{d} \\ &= C_\Lambda \frac{D_H}{4L} \frac{L}{d}, \text{ which is Eq. 22.} \end{aligned}$$

It should also be remarked that the formula for  $C_\Lambda$  in Eq. 22, as was given in the GM report, had only the first part, namely,  $C_\Lambda = P_0 - P_1 \cdot \text{Re}(d) + [\text{Re}(d) + 15]^{-1.185}$ , which was used for all Reynolds numbers. However, this formula gives negative heat-transfer factors for some Reynolds numbers that might occur in the regenerator. For example, when the filler factor is  $y = 0.3$ , then  $C_\Lambda$  is negative when  $\text{Re} > 163$  [or  $\text{Re}(d) > 92$ ], using the original GM correlation. For this reason, in the range  $\text{Re}(d) > 30$ , the GM correlation was replaced by a straight line in the log-log plane.

#### 2.3.2.2.6 Heat-transfer Coefficient for SLRE Matrix

$$St = \text{Stanton number for rectangular tubes with the aspect ratio input by user} \quad (23)$$

References. Hoehn et al. [35].

Remarks. See the remarks for the friction factor for this type of matrix in Sec. 2.3.2.1.6.

2.3.2.3 Implementation of Subroutine HTF. Many of the factors and terms in the preceding correlations are constant throughout the cycle of the engine

for a given cell. For example,  $D_H/L$ , A, and B in Eq. 9, the polynomials in y for the Metnet correlations, and several others need be computed only once for a given cell. Therefore, subroutine HTF has two entry points: an initialization entry and a main entry.

The first call to the subroutine is from subroutine RIOSIN and is of the form

```
CALL HTF(ICELL,DUMMY,DUMMY,DUMMY,DUMMY)
```

where

ICELL is any value less than 1

and

DUMMY is a dummy variable.

At this time, the subroutine calculates constant information for each cell, such as the length L of the passage containing the cell,  $D_H/L$  for the cell, and others. This information is initialized and stored in a container array.

Subsequently, when the Analysis Module needs the value of a heat-transfer coefficient or a friction factor other than a contraction or expansion coefficient, the following call is made:

```
CALL HTF(ICELL,RE,PR,F,ST),
```

where

ICELL = the cell number, from 1 to 30, for which  
the friction and heat-transfer coefficient  
are needed,

RE = Reynolds number based on hydraulic diameter,

and

PR = Prandtl number.

The subroutine then returns the friction factor (or orifice coefficient) F and Stanton number ST for cell number ICELL.

To obtain an area contraction coefficient, a statement of the form

```
CALL HTF(108,RE,AR,F,ST)
```

is used where,

AR = flow-area ratio, smallest over largest.

The subroutine then returns the contraction coefficient as F and also returns  $St = 0$ .

An area expansion coefficient is obtained in the same way except that 109 is the first argument:

```
CALL HTF(109,RE,AR,F,ST).
```

The subroutine then returns similar values.

When  $1 < ICELL < 30$ , the subroutine determines the type of flow passage from the common array value  $MTYPE(ICELL)$ , which is an input value described in Appendix A. To introduce a new type of flow passage into this subroutine, the

user must: (a) input a different value for MTYPE, (b) change the array IT in the DATA statement of subroutine HTF to transfer logical control, and (c) introduce coding for the additional correlation formulas in subroutine HTF.

2.3.3 Volume Subroutine. Subroutine VOLUME performs two major tasks for a variety of engine designs and drives:

- (1) It provides minimum and maximum piston positions, strokes, phase angle, and the crank angle at which the compression volume is minimum. It also calculates the compression displacement when the design is a displacer type.
- (2) It calculates the volumes in the expansion and compression spaces and their rates of change with respect to time for a given crank angle.

The subroutine performs these calculations for three different designs: in-line, double-acting, and displacer, which are shown in Appendix A, Figs. A-2, A-3, and A-4, respectively. Two drive types may be specified: connecting-rod drive and rhombic drive, which are illustrated schematically in Figs. 5 and 6.

In these figures, the following notation is used:

- r = crank radius,
- L = connecting-rod length,
- e = eccentricity,

and

- $\alpha$  = variable crank angle, measured from a line parallel to the piston axis (radians) with piston at T.D.C.

A double-acting design is treated as a variation of an in-line design. It is assumed, in the double-acting case, that the user has input an appropriate value of the volume phase angle or an equivalent crank phase angle. The motion can then be considered equivalent to that of an in-line design with the compression space in back of the compression piston. In some double-acting cases this equivalence is not exact, but a reasonable approximation of the actual motion is obtained if the correct volume phase angle is input.

For a rhombic drive, the two connecting rods are of the same length as shown in Fig. 6. This is equivalent to the drive in Fig. 7 where the two crank angles in the latter figure are constrained to be the same. The desired volumes and derivatives can be calculated from these figures.

The piston position  $x$  is given by

$$x = r \cos \alpha + g(\alpha), \quad (24)$$

where

$$g(\alpha) = (L^2 - (e - r \sin \alpha)^2)^{1/2}$$

= the projection of the connecting rod on the cylinder axis.



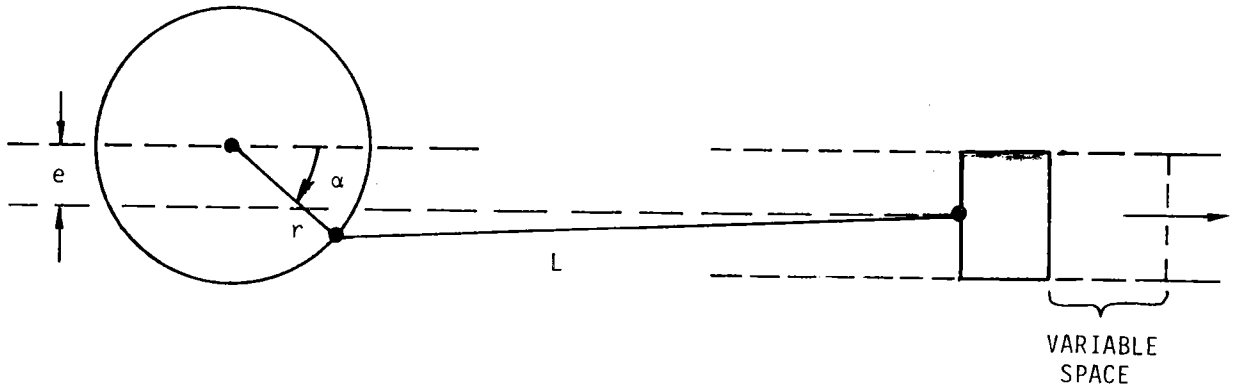


Fig. 5. Drive Type 0 Connecting-Rod Drive

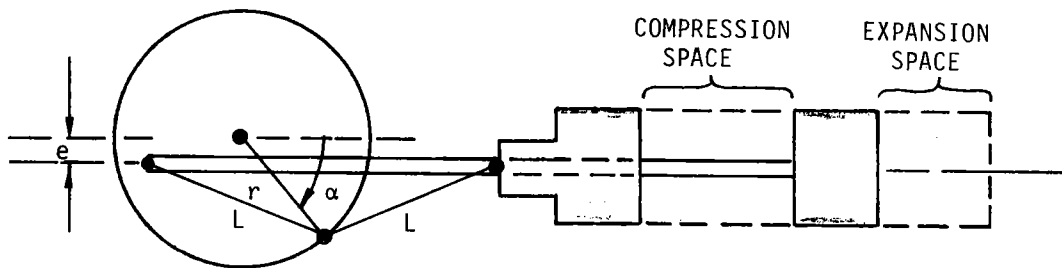


Fig. 6. Drive Type 1 Rhombic Drive

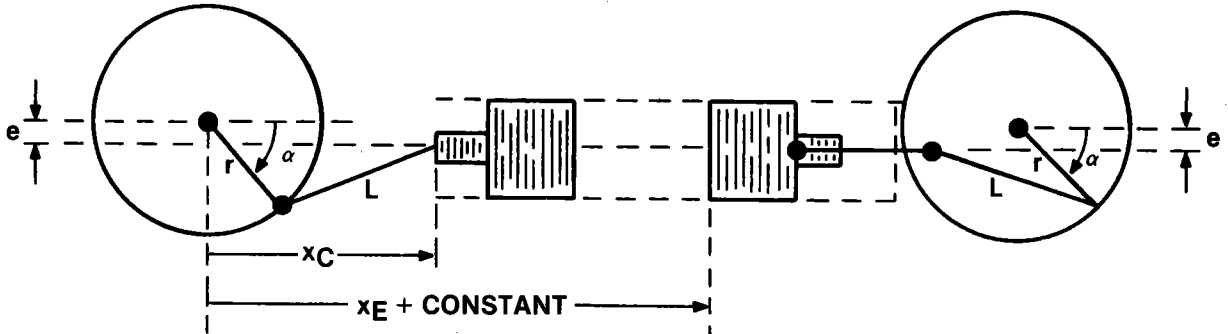


Fig. 7. Equivalent to Rhombic Drive

For the rhombic drive in Figs. 6 or 7, the position of the expansion piston is given by

$$x_{E,\text{rhombic}} = r \cos \alpha - g(\alpha). \quad (25)$$

The function  $g$  is evaluated by means of an arithmetic statement function in subroutine VOLUME.

In the nonrhombic drive cases, the Subroutine VOLUME does not require identical  $r$ ,  $L$ , and  $e$  for the compression and expansion pistons. The expansion and compression crank angles,  $\alpha_E$  and  $\alpha_C$ , are constrained to differ by a constant,  $\phi_{\text{crank}}$ , so that

$$\alpha_E = \alpha_C + \phi_{\text{crank}}, \quad (26)$$

where

$$\phi_{\text{crank}} = \text{crank phase angle.}$$

The piston velocities (except for the expansion piston of the rhombic drive) can be obtained by differentiating Eq. 24 with respect to time  $t$ :

$$dx/dt = [-r \sin \alpha + g'(\alpha)](d\alpha/dt) \quad (27)$$

where

$$g'(\alpha) = r(\cos \alpha)(e - r \sin \alpha)/g(\alpha).$$

In Eq. 27 the sign in front of  $g'(\alpha)$  must be reversed for the expansion piston of the rhombic drive.

Given the parameters  $r$ ,  $L$ , and  $e$  for both the compression and expansion pistons, as well as  $\phi_{\text{crank}}$ ,  $\alpha$ , and  $d\alpha/dt$ , the compression and expansion space volumes, and their derivatives are calculated using the preceding equations.

2.3.3.1 Initial Calculations. Since most Stirling engine codes begin the computation cycle at the point where the compression space volume is minimum, subroutine VOLUME calculates the compression crank angle at which this minimum occurs. If the engine design is "in-line," this minimum occurs when the compression piston position is maximum, i.e., at a compression crank angle  $\alpha_C = \psi$  such that

$$\sin \psi = e_C / (r_C + L_C). \quad (28)$$

However, when the engine design is a "displacer type," the compression space is between the two pistons. The change in compression-space displacement is then a function of the motion of both pistons, which are in turn separated by a phase angle. In this case, an iterative scheme is required to find the minimizing angle  $\alpha_C = \psi$ . The expression to be minimized is the volume of the compression space.

For a "connecting-rod-type" drive, this volume is

$$\begin{aligned} S(\alpha) &= AF_E \cdot x_E - AF_C \cdot x_C + \text{constant} \\ &= AF_E [r_E \cos(\alpha + \phi_{\text{crank}}) + g_E(\alpha + \phi_{\text{crank}})] \\ &\quad - AF_C [r_C \cos \alpha + g_C(\alpha)] + \text{constant}, \end{aligned} \quad (29)$$

where  $A$  is the cross-sectional area of the cylinders, and the constant term accounts for unswept volume and where the subscripts  $E$  and  $C$  mean that expansion and compression values for  $e$ ,  $r$ ,  $L$  are to be used, respectively. The variable angle,  $\alpha$ , is found by solving  $S'(\alpha) = 0$ , numerically using a "bisection" method, i.e., the root  $\alpha = \psi$  is bracketed into successively smaller intervals.

From Eqs. 24 and 25, the distance between the piston positions for the rhombic drive case is

$$S_{\text{rhombic}}(\alpha) = \text{constant} - 2g(\alpha). \quad (30)$$

In this case, the minimizing angle,  $\alpha = \psi$ , is easily found to be

$$\psi = \begin{cases} \pi/2 & \text{if } e > r \\ \arcsin(e/r) & \text{if } e < r. \end{cases}$$

Note that Eq. 30 also implies that  $S_{\text{rhombic}}$  is maximum when  $g(\alpha)$  is minimum, i.e., when  $\alpha = 1.5\pi$ . The compression displacement volume, therefore, is given by

$$\text{compression displacement} = 2[g(\psi) - g(1.5\pi)](\text{piston area}).$$

The input subroutine allows the user to specify either the crank phase angle,  $\phi_{\text{crank}}$ , or the volume phase angle,  $\phi_{\text{vol}}$ . The crank phase angle is the difference between the crank angles at which the expansion and compression pistons are at top dead center, as shown in Fig. 8:

$$\phi_{\text{crank}} = \alpha_E - \alpha_C.$$

The volume phase angle,  $\phi_{\text{vol}}$ , is the angle at which the expansion volume minimum precedes the compression volume minimum at top dead center, as shown in Fig. 9. These phase angles are related by the equation

$$\phi_{\text{crank}} = \phi_{\text{vol}} - \psi + \alpha_{E,\text{min}}, \quad (31)$$

where

$\psi$  = the compression crank angle  $\alpha_C$  at which  $V_C$  is minimum

and

$$\begin{aligned} \alpha_{E,\text{min}} &= \text{the expansion crank angle } \alpha_E \text{ at which } V_E \text{ is minimum} \\ &= \arcsin (e_E / (L_E + r_E)). \end{aligned}$$

If the user specifies  $\phi_{\text{vol}}$  but not  $\phi_{\text{crank}}$ , then the volumes subroutine calculates  $\phi_{\text{crank}}$ . However, in an engine with a displacer design and a connecting-rod drive, inspection of Eqs. 29 and 31 reveals that  $\phi_{\text{crank}}$  and  $\psi$  are both unknowns. Thus, in this situation the subroutine numerically solves Eqs. 31 and  $S'(\alpha) = 0$  simultaneously to find  $\phi_{\text{crank}}$  and  $\psi$ .

2.3.3.2 Implementation of Subroutine VOLUME. The first call to subroutine VOLUME is from subroutine INITIAL and is of the form

```
CALL VOLUME(2,DUMMY).
```

The subroutine then calculates various values needed for later calls, such as maximum and minimum piston positions, strokes,  $\psi$ ,  $\phi_{\text{crank}}$ , or  $\phi_{\text{vol}}$ . See Appendix C for definitions of the corresponding Fortran variable names. These variables are in common block VARVOL.

If the engine design is a displacer-type, a second call to the volumes subroutine is made by EDINPT and by RIOSIN and is of the form

```
CALL VOLUME(3,DUMMY).
```

The subroutine then computes the compression volume displacement for the convenience of the user, i.e., the portion of the compression volume swept by the pistons. This calculation is used to provide a normalizing volume for the Analysis Module.

All subsequent calls are of the form

```
CALL VOLUME(1,DUMMY).
```

The subroutine then calculates the following values, which are variables in common block VARVOL:

VOLS(1) = expansion volume, including dead volume  
in the expansion zone,

VOLS(2) = the portion of the swept compression volume  
behind the expansion piston in the case of an  
engine with a displacer design, otherwise

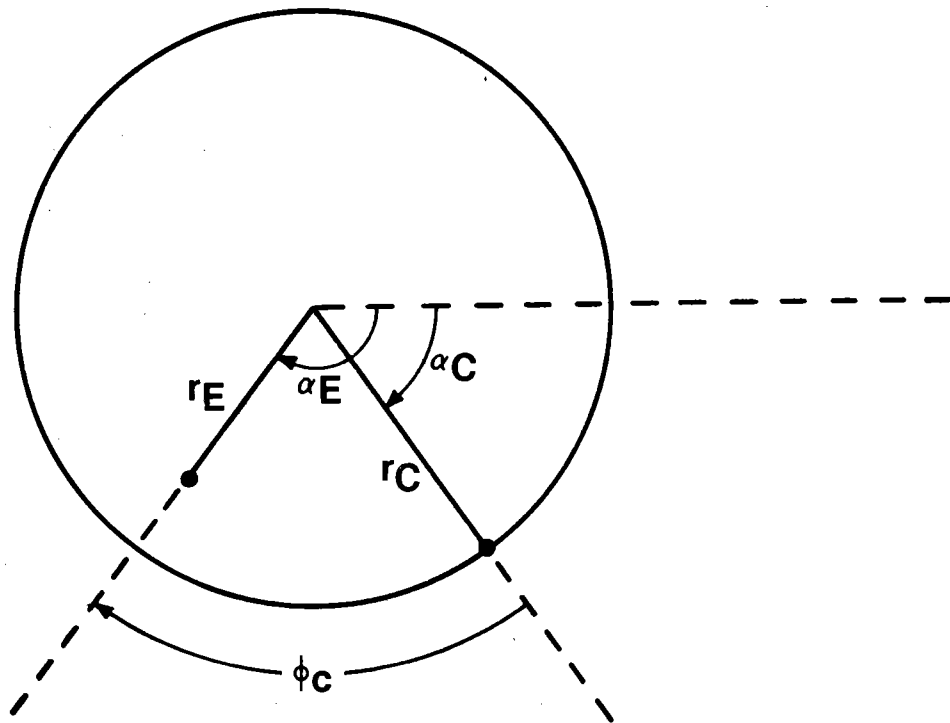


Fig. 8. Crank Phase Angle,  $\phi_{\text{crank}}$

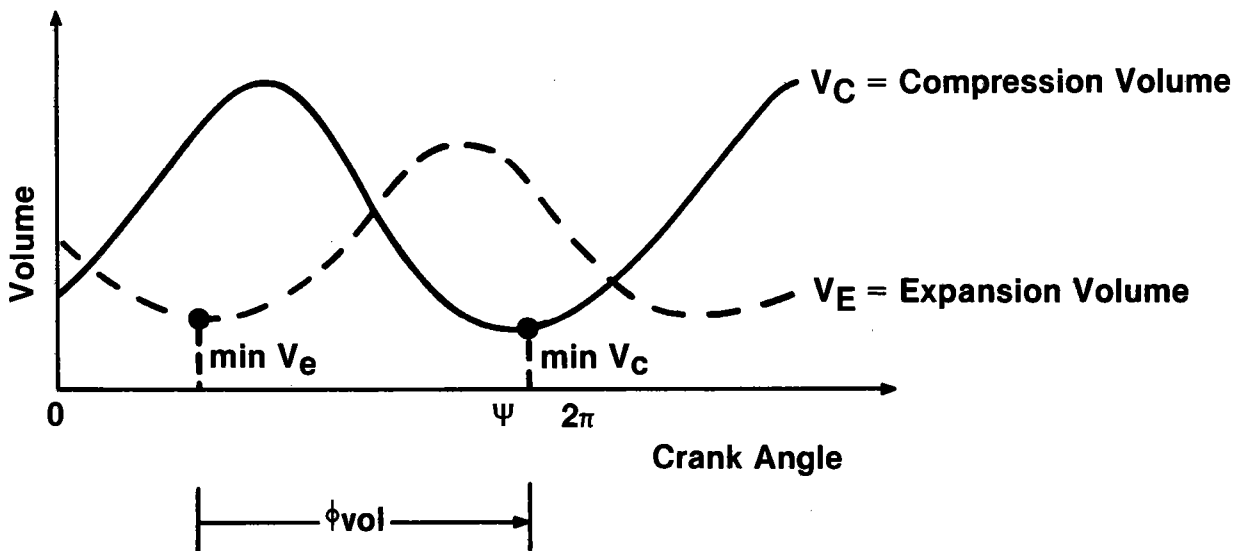


Fig. 9. Volume Phase Angle,  $\phi_{\text{vol}}$

VOLS(3) = the remainder of the compression volume,  
including the dead compression volume;

VOLS(4), VOLS(5) = buffer space live volumes, i.e.,  
volume swept by rear of expansion  
and compression pistons, respectively;

DVOLDT(I), (I = 1,2,3,4,5) = the rate of change of each of  
the above five volumes with  
respect to time.

Thus, after the above CALL statement, the active expansion volume is VOLS(1) and the active compression volume is VOLS(2) + VOLS(3).

2.3.3.3 Free-Piston Volume Variation. In order that a thermodynamic analysis of free-piston Stirling engines be performed, the motion of the pistons must be specified. Harmonic motion of fixed frequency and phase can easily be specified by requiring the pistons to behave as though they are connected by any of the mechanical drive systems described in Sec. 2.3.3. An alternative is that the user provide his own volume-variation routine that either prescribes piston motion or calculates piston motion from the dynamics of the system.

2.3.4 Additional Losses Subroutine. This subroutine calculates several energy losses that need to be calculated at the end of a cycle. In the present version of the code, SEAM1, these extra losses are regarded as additional heat loads that must enter into the heater and, in some cases, must exit through the cooler.

The following loss calculations presently included are shown in Table V.

---

TABLE V. Engine Loss Mechanisms Modeled

Dynamic Piston Motion  
Axial Conduction along:  
Piston walls  
Cylinder walls  
Regenerator walls  
Regenerator filler.

---

Each of the above losses is discussed below.

2.3.4.1 Dynamic Piston Motion Losses - QDYNAMIC. These losses are related to the dynamic motion of the displacer piston in the expansion zone. The loss is considered to flow from the expansion to the cylinder walls and then to the cooling water. In an in-line design this loss does not exist. The code breaks the loss into two components: shuttle and gap.

2.3.4.1.1 Shuttle Conduction Loss. Shuttle conduction takes place when the expansion piston absorbs heat at the hot end of a stroke and releases it at the cold end of the stroke. The present formula used by the Losses Subroutine for the shuttle loss assumes sinusoidal piston motion, a linear and constant longitudinal temperature distribution, and no axial piston conduction. It was derived by Rios ([1], pp. 129-135), and is

$$Q_{\text{shuttle}} = \frac{\pi}{8} \frac{D}{g} \frac{S}{L} \left[ \frac{2\lambda_1^2 - \lambda_1}{2\lambda_1^2 - 1} \right] (k_g \Delta T), \quad (32)$$

where

$$\lambda_1 = (k_p/k_g) \sqrt{\omega g^2 / (2\alpha_p)},$$

D = piston diameter,

S = piston stroke,

$\Delta T$  = temperature change from hot to cold end of piston,

L = "shuttle length," usually the distance from piston face to seal or the displacer stroke; see Rios ([1], p. 135);

g = width of "gap" between piston and cylinder,

$k_p, k_g$  = piston and gas conductivities,

$\alpha_p$  = diffusivity of piston wall metal,

$\omega$  = frequency,

and

$Q_{\text{shuttle}}$  has units of watts.

2.3.4.1.2 Gap Loss. This loss, also known as the "appendix" or "pumping" loss, occurs in displacer piston engines. The radial gap between the displacer piston and the cylinder is assumed to be sealed at the cold end. Pressurization and depressurization of the gas cause the gas to flow into and out of the gap. The gas loses heat while it is at the cold end of the gap and must be reheated once it leaves the gap at the warm end. To estimate this loss, the Losses Subroutine uses a formula originally developed by Rios ([1], pp. 136-138) for a refrigerator and later modified by Martini ([27], Appendix D) to apply to a heat engine. The modification was necessary because, in a refrigerator the maximum gap pressure and minimum gap temperature occur simultaneously, while in a heat engine both gap pressure and gap temperature reach a maximum simultaneously. With Martini's modification, the Rios formula for gap loss in watts is

$$Q_{\text{gap}} = \left| \frac{\gamma}{\gamma - 1} \frac{y}{2} V_{\text{gap}} \sin \phi \cdot [P_{\text{min}} / (x - y) - P_{\text{max}} / (x + y)] \omega \right| \quad (33)$$

where

$\phi$  = pressure-volume phase angle,

$$x = (T_E + T_K) / (T_E - T_K)$$

$$y = S/L,$$

and other notations are as defined in Eq.32 and in the nomenclature.

In developing this formula, sinusoidal volume, pressure, temperature, and mass variations were assumed.

2.3.4.1.3 Total Dynamic Piston Motion Losses. The total dynamic piston motion loss is the sum of the shuttle and gap losses, or

$$Q_{\text{dynamic}} = Q_{\text{shuttle}} + Q_{\text{gap}}. \quad (34)$$

2.3.4.2 Axial Conduction Losses. Each of these conduction losses is computed by means of the simple linear conduction formula,

$$Q = k \cdot AX(\Delta T/L), \quad (35)$$

where

$k$  = thermal conductivity evaluated at  $T_{\text{mean}}$ ,

$AX$  = cross-sectional area,

$L$  = conduction length,

and

$\Delta T$  = temperature difference.

In the case of conduction through the regenerator filler material, allowance is made for the nonsolid conduction path by multiplying the right side of Eq. 35 by a factor named FUDGE, which is defined as

$1 - \sigma$ , for tube matrices

FUDGE =  $0.05(1 - \sigma)$ , for screens or spheres

$0.5(1 - \sigma)$ , for Metnet.

The last two factors were approximated based on the contact between different layers of the matrix.

2.3.4.3 Implementation of the Losses Subroutine. The Losses Subroutine is called by the Analysis Module with the Fortran statement

CALL LOSSES.

All information needed by the subroutine is stored in common blocks. These losses are returned as the following Fortran variables:

QEXPSH = shuttle loss

QEXPGP = gap loss

QDYNAM = shuttle + gap losses

QPISWL = conduction along expansion piston wall

QCYLWL = conduction along expansion cylinder wall

QREGWL = conduction along regenerator wall

QREGFL = conduction along regenerator filler

QSTATC = the sum of the above four conduction losses.



When returned, each of these losses has already been multiplied by the total number of cylinders (NCYL) and has units of watts.

2.3.4.4 Future Additions to the Losses Subroutine. The following changes or additional losses are being considered for future inclusion in this routine:

- (1) Revised shuttle and pumping formulas will be added after investigating the recent literature on the subject.
- (2) Radiation losses through the displacer or hot cap will be added.
- (3) Power losses due to gas leakage will be added. This includes leakage between expansion and compression spaces as well as between these spaces and the appropriate buffer spaces.
- (4) Power losses due to ring friction will be added.
- (5) Hysteresis losses in the expansion, compression, and buffer spaces will be added. This loss, called the "cyclic heat transfer loss" by Toscano et al. ([39], p. 56), is the result of periodic heating and cooling of the gas near the gas-wall interface inside the cylinders and other spaces. The effect is a decrease in the maximum pressure and an increase in the minimum pressure of the working gas, resulting in a loss of power.

2.3.5 Engine Constraints and Optimization. The present code is capable of predicting engine performance over a wide range of temperatures, pressures, and frequencies. Not all of these results are meaningful because the code does not address:

- Mechanical friction
- Alternator inefficiencies
- Combustion inefficiencies
- Auxiliary power needs for cooling, etc.

These losses do not affect the thermodynamic engine performance, but are of major importance in determining the overall performance of the system. Indeed, high thermodynamic efficiency can be calculated for conditions in which the mechanical losses are so large that the engine cannot operate. The above effects must be included so that overall performance be calculated and should be included as engine constraints.

When engines are subjected to the pressures and temperatures predicted by a Stirling engine code, stresses occur that may be near or beyond the limits of the engine materials. Whether these material limits are approached or exceeded with the engine and conditions being modeled would establish additional constraints on the engine parameters. These additional constraints could be used along with an optimization routine to give optimal design values.

## 2.4 ANALYSIS MODULE (GENERIC)

The general features of the Analysis Module for the ANL System are discussed in this section. The first such Analysis Module, SEAM1, prepared for the ANL System is described in Chapter 3.

2.4.1 Tasks of the Analysis Module. The following are the major tasks and characteristics of the Analysis Module:

- The Analysis Module solves the field equations describing the mass and energy flows in the engine. It predicts temperatures, pressures, and other parameters that determine the state of the engine during each cycle. These calculations are continued for successive cycles until steady-state (periodic) conditions are reached (defined as conditions being repeated from one cycle to the next within a specified convergence criterion).
- The Analysis Module calls the Losses Subroutine for additional losses due to conduction, radiation, leakage, etc., and obtains net performance characteristics such as power and efficiency.
- The Analysis Module uses the three other modules of the ANL Stirling Engine Analysis System: Input, Special Functions, and Output. It must therefore be applicable to a large variety of engines and operating conditions.
- The Analysis Module must use a solution method that converges quickly and provides meaningful results.

## 2.5 OUTPUT MODULE

2.5.1 Tasks of the Output Module. The Output Module writes in an easy-to-read format the answers to various questions that Stirling engine designers may have regarding a specific engine or type of engine. It also answers questions about the analysis code itself. Some specific answers are:

- The values of certain performance characteristics, such as power, efficiency, energy losses, energy flows, etc., for an engine under specified operating conditions.
- How these performance characteristics vary when the operating conditions are varied.
- How engine conditions, such as pressures, temperatures, and velocities, vary throughout a complete cycle (crankshaft revolution) of the engine.
- How the conditions vary from one end of the engine to the other end.
- The speed of the code's iterative technique used to find a cyclic steady-state solution.
- How accurate the code's solution is after it converges.

The Output Subroutine OUT1, has been designed to work with any analysis module and writes the results of the computation in several ways to answer the above questions. The arrangement of the output data is controlled by several input parameters which are outlined below.

2.5.2 Controlling Output with Input. The form of the output is controlled by the three input variables NPRT1, NPRT2, and IGRAPH, which control the writing of:

Engine zone-by-zone information (NPRT1)

Cycle-to-cycle or case-to-case comparison information (NPRT2)

Graphics data (IGRAPH).

The uses of these three parameters are described as follows:

(1) NPRT1 = the number of computational time steps between prints of engine zone-by-zone information. The current Analysis Module, SEAM1, requires NPRT1 to be a multiple of the number of steps in a cycle, NSTEP.

(2) NPRT2 = 1 directs the Output Subroutine to write cycle-to-cycle convergence information.

NPRT2 > 1 directs the Output Subroutine to write case-to-case comparison information for NPRT2 cases at a time. The term case refers to a running of the code for a specific engine and specific operating conditions. For example, if a perturbation study is run having two pressures each with five frequencies, the case results may be separated into two pressure groups by setting NPRT2 = 5.

(3) IGRAPH = 0 results in no graphics data being written.

IGRAPH = 1 is a directive to write curve data (such as P-V data) at 5° intervals. This data is saved for the last cycle of each case.

IGRAPH = 2 signals that graphics data are to be saved for case-to-case comparisons. This option is designed for perturbation runs in which the user wants curves that show the variations in performance parameters.

The Output Subroutine writes all output on unit 6, except for graphics output, which is written on unit 8.

2.5.3 Filling the Output Arrays. The information in this section is for use by those wishing to replace the current analysis module, SEAM1, with another analysis module.

The Output subroutine, OUT1, writes values from the three arrays given below. (Dimensions are included in parentheses.)

```
SCALR(50,10)
VECTR(15,30)
GRAFIC(10,75).
```

These arrays are in a COMMON block and must be filled by the analysis module of the code before OUT1 is called. The arrays have indices (I and K). The second index, K, indicates variation in time for GRAFIC, cycle number for SCALR when NPRT2 = 1, or case number when NPRT2 > 1, and engine zone for VECTR (see Appendix A). The first index, I, identifies the type of information that is being stored. For example,

```

SCALR(1,K) = average engine pressure (MPa)
SCALR(2,K) = engine speed (RPM)
  etc.      :
            :

VECTR(1,K) = maximum gas temperature in zone K (K)
VECTR(2,K) = average gas temperature in zone K (K)
  etc.      :
            :

GRAFIC(1,K) = Kth compression crank angle (rad.) at
              5° increments
GRAFIC(2,K) = live expansion volume at Kth angle (cm3)
  etc.      :
            :

```

For definitions of the other information identifiers for each array, see code variable definitions (Appendix C), the actual code listing comments, and the output edit (Appendix B).

The Analysis Module fills each of the above three arrays during or after the appropriate computational cycles, as directed by the input parameters, NPRT1, NPRT2, and IGRAPH.

For the array SCALR(I,K), if NPRT2 = 1, then K represents the cycle number. But if NPRT2 > 1, then K represents the case number. The Analysis Module distinguishes between these two situations as follows:

- If NPRT2 = 1, fill array SCALR(I,K) (for I = 1,...,50) at the end of each cycle, where K = the cycle number, NCYCLE; however, when NCYCLE passes 10, K will start over at 1 after editing the last 10 cycles. For example, if NCYCLE = 13 then K = 3, and if NCYCLE = 30 then K = 10. (A Fortran statement for this is  $K = \text{MOD}(\text{NCYCLE} - 1, 10) + 1$ .)
- If NPRT2 > 1, do as above except let K = 10 each time. In this situation, the Output routine will properly rearrange the information in the array SCALR for successive cases.

The zone-by-zone array, VECTR(I,K), and the graphics array, GRAFIC(I,K), can be filled at the end of each Analysis Module cycle, and results edited as specified by the user.

The subroutine of SEAM1 that fills the arrays SCALR and VECTR is called RIOSPR. For SEAM1, the number of engine zones for which information is stored in array VECTR is set to 5 in RIOSPR.

2.5.4 Calling the Output Subroutine. Assuming that the three output arrays SCALR, VECTR, and GRAFIC have been filled, the computations have been completed, and the convergence criterion has been checked, the Output Subroutine is called after each cycle, as follows:

```
CALL OUT1(NCASE,IGONOW)
```

where

```
NCASE = the case number
```

and

```
IGONOW = 0 if convergence has occurred  
        1, if convergence has not occurred.
```

The subroutine OUT1 will then use NPRT2, IGRAPH, and the other variables stored in COMMON blocks to automatically:

- Write zone-by-zone information every NPRT1 cycles.
- Save cycle-to-cycle or case-to-case comparison information in array SCALR if IGONOW = 1.
- Write or save array SCALR in the appropriate way if IGONOW = 0.
- Write or save graphics data, if requested, and IGONOW = 0. The graphics data are written from the array GRAFIC if IGRAPH = 1, or from part of the array SCALR if IGRAPH = 2.

Basically, IGONOW = 1 directs OUT1 to write transient engine data, and IGONOW = 0 directs OUT1 to write summary information for the case or perturbation study.

### 3. SEAM1 (STIRLING ENGINE ANALYSIS MODULE 1)

#### 3.1 BACKGROUND

3.1.1 Rios Analysis. The original code, which provides the basis for the Analysis Module, was developed in 1969 by Rios [1] as part of his D.Sc. thesis at Massachusetts Institute of Technology. His work was a continuation of previous work by Rea and Smith [40] and Qvale and Smith [41], [42], [43] on Stirling-cycle analysis. The original code was designed for a refrigerator of the two-piston, two-cylinder configuration, but has since been modified for a heat engine.

Rios' objective for his code was that it be more generally applicable than previously developed codes. Rios' model is one in which the power output and heat input of the basic cycle are calculated first without losses. These total cycle results are then modified with energy losses typical of a real engine. Numerous other codes have been written since his, some of which give more detailed evaluation of newer, more complex Stirling engine designs. Examples are Urieli [2], Tew et al. [3], and Schock [4]. Such codes divide the engine into many small control volumes, and the basic governing differential equations of fluid mechanics applied to each volume are solved. Although these methods provide detailed information on engine performance, interrelate the losses with each other, and also solve the basic power output, the resulting system of equations is large and requires extensive computer time to reach a stable solution. Therefore, a simpler model such as Rios', is better suited for a first analysis of Stirling engine designs.

#### 3.2 DESCRIPTION OF SEAM1 COMPUTATIONAL PROCEDURES

3.2.1 What the Code Calculates and Predicts. The code calculates the efficiency of the engine based on net power and net heat input. The net heat input is the work performed during a cycle in the expansion space plus heat-loss terms. The net power is defined as the P-V power (the difference between the expansion and compression work done during a cycle calculated by integrating  $\oint p dV$ ) minus the power loss terms. Section 3.2.3 gives the derivation of the analysis used for calculation of expansion and compression work.

Losses that reduce net power are due to two effects. The first is frictional losses of the working fluid as it passes through system components. The second is due to a lowering of the gas temperature in the expansion space and a raising of the temperature in the compression space due to the thermal resistances encountered in the heater and cooler. The analysis for calculating these two effects is derived in Sec. 3.2.4.

The heat-loss terms that must be added to expansion power in order to determine net heat input are described in Sec. 3.2.4.

3.2.2 General Scheme for Solution of Governing Equations. Section 2 described the general Stirling engine code system which is intended to provide a framework for a series of analysis modules which will meet the differing needs of Stirling engine designers. A flow chart of the entire code is shown in Fig. 10. The case to be run is defined by the input data as described in Sec. 2. Because the input routines are general a call is made to the ANALIS

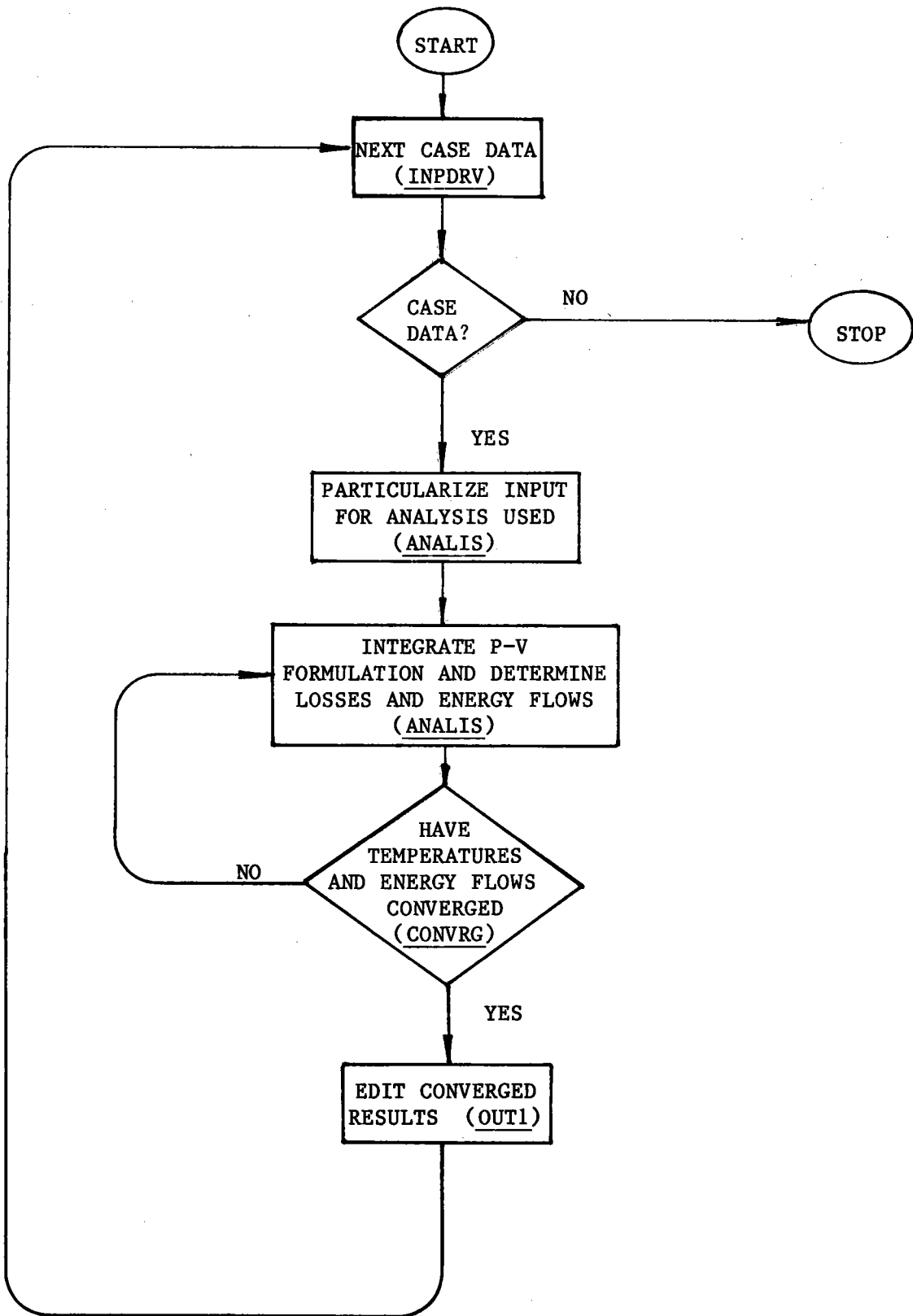


Fig. 10. Main Program

subroutine to particularize the input for the assumptions to be used in the analysis. Then the outer-loop iteration on temperature and energy flows is started.

Successive calls to the ANALIS module will compute these temperatures and energy flows until the values at 0° crank angle match those after 360° of integration. In the case of the Rios' type analysis this usually takes about four cycles. The CONVRG subroutine determines the level of accuracy, currently at 0.1 percent change, and what the next estimate of the conditions at 0° will be, currently the last value is used. As additional analysis modules are written CONVRG will be modified to retain this low number of outer loop cycles per case.

As was mentioned, the first call to the ANALIS subroutine particularizes the input for the analysis to follow. In the case of the Rios' analysis a routine called RIOSIN, described in Sec. 3.3.1 was included to fulfill this need.

All subsequent calls to the ANALIS routine, described in Sec. 3.3.2, result in the calculation of power, efficiency, and the distribution of energy through the cycle. The description of the cycle integration of pressure and mass flow is given in Sec. 3.3.3. Once the mass flows and pressures through the cycle have been determined the energy flows through the heat exchangers as detailed in Sec. 3.3.4, are computed. The losses due to conduction are calculated, as shown in Sec. 2.3.4, and added to the energy flow terms resulting in a change in the temperatures in the engine. The calculations are displayed as determined by the various output options available and logic control is returned to the Main Program to determine convergence.

3.2.3 Calculation of Expansion and Compression Work During Cycle. The assumptions necessary for the following derivations are shown in Table VI. The equations for the conservation of energy, the conservation of mass, and the equation of state are used. The momentum equation does not apply due to the assumption of uniform pressure distribution at any instant.

The derivation of the differential equations for pressure and mass are included in Rios' thesis [1], but they will be repeated here in condensed form for completeness and continuity of this report. This is also the case with some of the loss calculations later in this section. Rios' analysis obtains expressions similar to earlier work by Kirkley [7] and Qvale and Smith [43].

The energy equation for a variable cylinder volume may be written

$$dE = dQ - P dV + H dm \quad (36)$$

The  $dQ$  term is zero for an adiabatic cylinder. The internal energy change and enthalpy flux are written as

$$dE = C_v T dm + mC_v dT \quad \text{and} \quad H dm = C_p T dm.$$

Equation 36 then reduces to



---

TABLE VI. Assumptions Used in Computing SEAM1 Expansion and Compression Work Terms

1. Pressure throughout the engine is uniform at any instant.
  2. Perfect heat transfer in the heater, regenerator, and cooler.
  3. Temperature in the heat exchange components is constant with time at any point.
  4. Uniform cross-sectional temperatures and velocities.
  5. Hot and cold cylinders are adiabatic.
  6. Perfectly mixed gases in the cylinders.
  7. Ideal Gas Law applies.
- 

$$C_v T dm + mC_v dT = -P dV + C_p T dm. \quad (37)$$

When gas is moving into the cylinder ( $dm > 0$ ),  $T$  is the adjacent heat-exchanger gas temperature  $T^*$ . Thus, Eq. 37 may be written for both inflow and outflow:

$$C_v T dm + mC_v dT = -P dV + C_p T^* dm \quad (\text{inflow: } dm > 0); \quad (38)$$

$$C_v T dm + mC_v dT = -P dV + C_p T dm \quad (\text{outflow: } dm < 0). \quad (39)$$

The equation of state for the system

$$PV = mRT \quad (40)$$

yields the following formula when differentiated:

$$RT dm + mR dT = PdV + VdP. \quad (41)$$

Substituting Eq. 41 into Eq. 38, reducing, and rearranging yields

$$dm = \frac{PdV}{RT^*} + \frac{VdP}{\gamma RT^*} \quad (\text{inflow}), \quad (42)$$

where  $\gamma$  is the specific heat ratio.

Equation 39 can be manipulated to yield a similar equation,

$$dm = \frac{PdV}{RT} + \frac{VdP}{\gamma RT} \quad (\text{outflow}). \quad (43)$$

The cylinder gas temperature can be eliminated from Eq. 43 by substituting Eq. 46 to yield

$$dm = m \left[ \frac{dV}{V} + \frac{dP}{\gamma P} \right]. \quad (44)$$

Equations 42 and 44 are valid for both expansion and compression cylinders.

The conservation of mass, when written for the closed system of the expansion, compression, and dead volumes is

$$m_T = m_C + m_D + m_E = \text{constant}.$$

Differentiating the above equation yields

$$dm_C + dm_D + dm_E = 0. \quad (45)$$

The constant reduced isothermal dead volume is defined as the ratio of mass in the dead space to mass in one-half the maximum expansion volume at  $T_E^*$  and the same pressure

$$V_D = \frac{m_D}{\left( \frac{PV_{AE}}{RT_E^*} \right)}, \quad (46)$$

where

$$V_{AE} \equiv (V_{E_{MAX}})/2.$$

Note that script is used for nondimensionlized quantities. Since mass in the dead space is proportional to pressure, rearranging and differentiating Eq. 46 gives

$$dm_D = V_D \frac{V_{AE} dP}{RT_E^*}. \quad (47)$$

Four mass flows are possible between the variable cylinder volumes and the dead volume:

$$dm_C < 0, \quad dm_E > 0, \quad (48)$$

$$dm_C < 0, \quad dm_E < 0, \quad (49)$$

$$dm_C > 0, \quad dm_E > 0, \quad (50)$$

and

$$dm_C > 0, \quad dm_E < 0. \quad (51)$$

Substituting the mass derivatives of Eqs. 42 and 47 into Eq. 45, and using situation 50 yields

$$\frac{P}{RT_C^*} \frac{dV_C}{V_C} + \frac{V_C}{\gamma RT_C^*} \frac{dP}{P} + V_D \frac{V_{AE}}{RT_E^*} \frac{dP}{P} + \frac{P}{RT_E^*} \frac{dV_E}{V_E} + \frac{V_E}{\gamma RT_E^*} \frac{dP}{P} = 0. \quad (52)$$

With the following variables to nondimensionalize Eq. 52

$$P \equiv \frac{P}{P_{MAX}}, \quad V_C \equiv \frac{V_C}{V_{AC}}, \quad V_E \equiv \frac{V_E}{V_{AE}}, \quad \nu_{VT} \equiv \frac{V_{AC} T_E^*}{V_{AE} T_C^*} \quad (53)$$

the result is

$$P(\nu_{VT} dV_C + dV_E) + \left( \frac{1}{\gamma} \nu_{VT} V_C + \frac{1}{\gamma} V_E + V_D \right) dP = 0.$$

The differential pressure may then be expressed as

$$dP = -\gamma P \frac{\nu_{VT} dV_C + dV_E}{\nu_{VT} V_C + V_E + \gamma V_D} \quad \text{for } dm_C > 0, dm_E > 0. \quad (54)$$

As with Eq. 52, the mass derivatives of Eqs. 42 and 44 can be nondimensionalized to yield

$$dM = P dV + \frac{V dP}{\gamma} \quad (\text{inflow}) \quad (55)$$

and

$$dM = M \frac{dV}{V} + \frac{dP}{\gamma P} \quad (\text{outflow}), \quad (56)$$

where

$$M_X = \frac{RT_X^*}{V_{AX} P_{max}} m_X$$

and X refers to the volume used: E, C, or D.

In a manner similar to that used to find Eq. 54, the following differential pressures can be found:

$$dP = -\gamma \frac{\nu_{VT} M_C \frac{dV_C}{V_C} + M_E \frac{dV_E}{V_E}}{\frac{\nu_{VT} M_C}{P} + \frac{M_E}{P} + \gamma V_D} \quad \begin{array}{l} (dm_C < 0) \\ (dm_E < 0), \end{array} \quad (57)$$

$$dP = -\gamma \frac{PdV_E + \kappa_{VT} M_C \frac{dV_C}{C}}{V_E + \kappa_{VT} \frac{M_C}{P} + \gamma V_D} \quad \begin{array}{l} (dm_C < 0) \\ (dm_E > 0), \end{array} \quad (58)$$

and

$$dP = -\gamma \frac{\kappa_{VT} PdV_C + M_E \frac{dV_E}{V_E}}{\kappa_{VT} V_C + \frac{M_E}{P} + \gamma V_D} \quad \begin{array}{l} (dm_C > 0) \\ (dm_E < 0). \end{array} \quad (59)$$

The dimensionless work for both expansion and compression cylinders is found using

$$W = \frac{\oint p \, dV}{P_{MAX} V_A} = \oint P \, dV. \quad (60)$$

The integration implied in Eq. 60 is performed numerically as described in Sec. 3.3.3.

**3.2.4 Analysis of Losses.** The losses found in a typical Stirling engine can be divided into two categories: those affecting basic power (the P-V diagram) and those that appear as a heat load on the heat exchangers. Five heat losses are evaluated: (1) regenerator ineffectiveness or reheat loss; (2) a correction to regenerator ineffectiveness due to the oscillating temperature of the regenerator matrix; (3) dynamic power loss, found in engines where a piston displacer separates the hot and cold spaces and "shuttles" heat between them; (4) a correction to the dynamic power loss due to the temperature change of the gas flowing in and out of the gap between the displacer piston and cylinder; and (5) static conduction losses. The first two are calculated in the Analysis Module; the last three are calculated in the Standard Functions Module.

**3.2.4.1 Pressure Drop Losses Due to Fluid Frictional Effects.** Equation 60 was derived assuming uniform pressure; however, friction pressure loss occurs in all the heat-exchanger components, with the primary loss incurred in the regenerator. To account for these losses, Rios ([1], p. 106) begins by defining the system reference pressure as the expansion cylinder pressure

$$P_E \equiv P.$$

There is no reason given for choosing the expansion space as the reference. In some codes, for example Tew [2], the reference pressure is at the midpoint of the regenerator. We have retained the Rios assumption for consistency. He then states that the pressure difference between the expansion and compression spaces can be represented as

$$\delta P_f \equiv P_C - P_E. \quad (61)$$

If the expansion work is represented as

$$W_E = \oint P_E dV_E$$

an approximation to the compression work is

$$\begin{aligned} W_C &= \oint P_C dV_C = \oint (P_E + \delta P_f) dV_C \\ &= \oint P_E dV_C + \oint \delta P_f dV_C. \end{aligned}$$

The correction to the compression work due to pressure drop is then defined as

$$\delta W_C = \oint \delta P_f dV_C. \quad (62)$$

Two problems arise with this method of maintaining the expansion space variables the same while varying the compression space variables due to pressure drop. The first problem relates to the net work done by the engine. The net work is the sum of the expansion and compression works. The work correction due to friction loss should be applied to either the changing compression volume,  $\delta V_C$ , as is done in Eq. 62, or to the changing expansion volume,  $\delta V_E$ , if the system reference pressure is assumed in the compression zone. In the Tew code the pressure loss term would be split between  $\delta V_C$  and  $\delta V_E$  as the reference pressure is in the regenerator. Therefore, the work correction due to friction is a function of the reference pressure assumption. We have run a few cases changing the reference pressure from the expansion zone to the compression zone and have noted that although the net power does change about 5% in some hydrogen cases, and even more in helium cases, the code consistently predicts a higher work correction term and a lower efficiency for the Rios assumption of expansion space reference pressure. As was indicated we have retained this assumption. The second problem with this simplified model is that conservation of mass is no longer satisfied in the compression zone. To examine this problem, Rios introduces an artificial compression zone volume variation

$$V_C \text{ with } \delta P_f \equiv V_C \text{ w/o } \delta P_f + \delta V_C.$$

The compression work then becomes

$$W_C = \oint (P_E + \delta P_f) d(V_C + \delta V_C). \quad (63)$$

A more accurate estimate of work lost due to pressure drop than Eq. 62 would be

$$\delta W_C \equiv \underset{\substack{\text{with} \\ \delta P}}{W_C} - \underset{\substack{\text{w/o} \\ \delta P}}{W_C} = \oint (P_E + \delta P_f) d(V_C + \delta V_C) - \oint P_E dV_C$$

or

$$\partial W_C = \oint \delta P_f dV_C + \oint P_E d(\delta V_C) + \oint \delta P_f d(\delta V_C). \quad (64)$$

The last integral in Eq. 64 containing the two differential terms is negligible for the pressure and volume differences of a practical Stirling engine. The nondimensionalized pressure-drop work loss then becomes

$$\delta W_C = \oint \delta P_f dW_C + \oint P_E d(\delta V_C) \quad (65)$$

Rios derives a discrete form of  $\oint P_E d(\delta V_C)$  in Appendix B of his thesis, but does not include it in his code because it is negligible when  $\delta P_f$  is small relative to  $P_{MAX} - P_{MIN}$ , as is typical of a real engine. He therefore uses the nondimensional form of Eq. 62 in his model.

Rios begins his evaluation of  $\oint \delta P_f dV_C$  ([1], pp. 107-114) by stating that the total pressure drop is the sum of the pressure drops of each component

$$\delta P_f = \delta P_K + \delta P_R + \delta P_H.$$

Since the evaluation of all three pressure drops is essentially the same, only that of one component will be described here.

To facilitate the evaluation of the pressure drop along the length of the component, a dimensionless length ( $x/L$ ) is defined as the distance from the end of the component nearest the cold cylinder ( $x$ ) divided by the component length ( $L$ ). Appropriate subscripts for  $x$  and  $L$  are K (cooler), R (regenerator), and H (heater). The pressure drop at a point in the component may then be expressed as the product of a friction factor and a kinetic-energy term ([24], p. 21). For any of the three components

$$d(\delta P_f) = f_x \frac{L}{D_h} \rho_x \frac{u_x^2}{2} d\left(\frac{x}{L}\right). \quad (66)$$

The friction factor  $f_x$ , density  $\rho_x$ , and velocity  $u_x$  are functions of position  $x$  and time. It is assumed that the hydraulic diameter  $D_h$  does not vary with position. The velocity at  $x$  can be expressed as

$$u_x = \frac{1}{\rho_x AF} \frac{\partial \dot{m}_x}{\partial t} = \frac{\dot{\hat{m}}_x}{\rho_x AF}, \quad (67)$$

where  $AF$  is the free-flow area within the component, and  $\dot{\hat{m}}_x$  is defined as the mass flow rate on the warm (expansion) side of position  $x$  at time  $t$ ; the dimensionless equivalent of  $\dot{\hat{m}}_x$  is

$$\hat{M}_x = \frac{\dot{\hat{m}}_x R T_x^*}{P_{MAX} V_{AX}}. \quad (68)$$

In Eq. 61,  $\partial P_f$  was defined as positive when the pressure decreases toward the warm end. Thus,  $d(\delta P_f)$  is positive when  $\dot{m}_x$  is positive. Using this fact, along with Eq. 67 and the ideal gas expression

$$\rho_x = \frac{P_x}{RT_x},$$

Eq. 67 can be rewritten and integrated over the length to yield the following equation for each component:

$$\delta P_f = \frac{1}{2} \frac{L}{D_h} \frac{R}{AF^2} \int_{\frac{x}{L}=0}^{\frac{x}{L}=1} \left[ \frac{1}{P_x} f_x \left| \dot{m}_x \right| \dot{m}_x T_x \right] d\left(\frac{x}{L}\right) \quad (69)$$

$P_x$  can be taken out of the integral if it is replaced with the reference pressure  $P_E$ ; this will cause negligible error for  $\delta P_f \ll P_E$ .

Using Eq. 69, the work-loss integral becomes

$$\oint \delta P_f dV_c = \frac{1}{2} \frac{L}{D_h} \frac{R}{AF^2} \oint \left[ \frac{1}{P_x} \int_{\frac{x}{L}=0}^{\frac{x}{L}=1} \left[ f_x \left| \dot{m}_x \right| \dot{m}_x T_x \right] d\left(\frac{x}{L}\right) \right] dV_c.$$

Reversing the order of integration yields

$$\oint \delta P_f dV_c = \frac{1}{2} \frac{L}{D_h} \frac{R}{AF^2} \int_{\frac{x}{L}=0}^{\frac{x}{L}=1} \left[ T_x \oint \frac{f_x \left| \dot{m}_x \right| \dot{m}_x dV_c}{P_x} \right] d\left(\frac{x}{L}\right). \quad (70)$$

By defining the variable

$$\alpha \equiv \omega t,$$

which leads to

$$\dot{m}_x = \omega \frac{dm_x}{d\alpha},$$

Eq. 70 may be nondimensionalized using Eqs. 53 and 68:

$$\oint \delta P_f dV_c = \frac{1}{2} \left(\frac{L}{D_h}\right) \frac{\omega^2 V_{AC}^2}{AF^2 RT_c^*} \int_{\frac{x}{L}=0}^{\frac{x}{L}=1} \frac{T_x}{T_c^*} \oint f_x \left[ \frac{\left| \frac{\delta M_x}{\partial \alpha} \right| \frac{\delta M_x}{\partial \alpha} \frac{dV_c}{\partial \alpha}}{P_x} d\alpha \right] d\left(\frac{x}{L}\right). \quad (71)$$

Equation 71 is integrated for each component by determining the values for the constants, the positional gas temperature,  $T_x$ , the average friction factor,

$f_x$ , and the integral of the bracketed angular dependent values. The positional gas temperature  $T_x$  can be approximated as  $T_c$  for the cooler,  $T_e$  for the heater, and the following linear relationship for the regenerator:

$$T_R = T_c^* + (T_e^* - T_c^*) \left(\frac{x}{L}\right)_R \quad (72)$$

To determine the variation  $\partial M_x / \partial \alpha$  in Eq. 71, Rios approximates the pressure in the dead space as uniform. Therefore, with  $X$  as the fraction of reduced dead volume on the compression side of  $x$

$$m_{DC_x} = X m_D \text{ and } m_{DE_x} = (1 - X)m_D.$$

Using the conservation of mass for the total system, the time derivative causes

$$dm_C + dm_D + dm_E = 0 = dm_C + \frac{dm_{DE_x}}{1 - X} + dm_E. \quad (73)$$

With  $m_x$  as the mass of the system on the expansion side of  $x$

$$dm_x = dm_{DE_x} + dm_E. \quad (74)$$

Combining Eqs. 73 and 74 yields

$$dm_C + \frac{dm_x - dm_E}{1 - X} + dm_E = 0.$$

Nondimensionalizing as in Eq. 71 and solving for  $\partial M_x / \partial \alpha$ ,

$$\frac{\partial M_x}{\partial \alpha} = X \frac{\partial M_C}{\partial \alpha} + \frac{1}{\mu_{VT}} \frac{\partial M_E}{\partial \alpha} - \frac{\partial M_C}{\partial \alpha}. \quad (75)$$

By determining the average value of  $\partial M_x / \partial \alpha$  for the various components, the Reynolds number and hence the average friction factor,  $f_x$  can be determined. The bracketed term in Eq. 71

$$\phi \frac{\left| \frac{\partial M_x}{\partial \alpha} \right|}{\frac{\partial M_x}{\partial \alpha} \frac{dV_c}{\partial \alpha}} \frac{1}{P_x} \partial \alpha$$

can then be integrated separately for each component, thereby providing the  $\phi \partial P_f \partial V_c$  needed to determine the work loss in Eq. 65.

3.2.4.2 Imperfect Heat-Exchanger Loss. Imperfect heat-exchanger heat transfer is the second type of loss affecting the basic power. Since a



temperature gradient exists between the heat-exchanger walls and the gas due to thermal resistance of the fluid film, gas entering the cylinder and regenerator will not be at the heat-exchanger wall temperature. However, if the temperature difference between the gas and the heat-exchanger wall is small, the effect on the cycle will be negligible.

SEAMI's approach for evaluating this loss begins by first calculating actual heat flows into and out of the engine. Actual heat in per cycle is computed by adding the heat converted to useful work in the expansion cylinder and those heat flows that increase the load on the heater; these include dynamic shuttle and piston-gap losses, regenerator ineffectiveness and its correction, and conduction down the cylinder wall, piston wall, regenerator wall, and regenerator filler material. Subtracted from this total is the friction loss for the hot end of the engine that lessens the heat load. Mathematically this can be expressed as

$$Q_H = W_E + Q_{DYNAMIC} + Q_{REGEN} + Q_{CYLWL} + Q_{PISWL} \\ + Q_{REGWL} + Q_{REGFIL} - Q_{HTRFRIC} - Z1 \cdot Q_{REGFRIC}, \quad (76)$$

where  $Z1$  is the input fraction of regenerator frictional heat generation in the heater space.

Actual heat out of the engine per cycle is the sum of the cold cylinder work and those heat flows that increase the cooler load. (Since the cold work is a negative value, the heat flows are subtracted from it to increase the magnitude of actual heat out.) The heat flows that increase the cooler load are the regenerator ineffectiveness and its correction, and the friction loss on the cold end of the engine, plus some conduction losses that find their way into the cooler. Because not all engine designs are alike, some of the conduction losses can go directly to the cooling water. These options are explained in Appendix A. When all these losses went through the cooler, the heat flow out of the cooler would be

$$Q_C = W_C - Q_{REGEN} - Q_{COOLFRIC} - (1-Z1) Q_{REGFRIC} \\ - Q_{PISWL} - Q_{REGFIL} - Q_{DYNAMIC} - Q_{CYWLW}, \quad (77)$$

where the second line represents the optional heat loads.

In both Eqs. 76 and 77

$W_x$	is from the integration of Eq. 65,
$Q_{XXFRIC}$	is from the appropriate form of Eq. 71,
$Q_{DYNAMIC}$	is from Eq. 34,
$Q_{REGEN}$	is from the evaluation of Eq. 84

and the remaining  $Q$ 's due to conduction are from Eq. 35.

With these actual heat flows in the heater and cooler, the effective inner-wall temperatures of these exchangers can be computed using the heat-transfer formula,

$$Q_x = \frac{TE_x - TW_x}{R_x}, \quad (78)$$

where  $Q_x$  = actual heat flow,  $TE_x$  = the temperature of the medium outside the heater or cooler tubes (combustor or water temperature, respectively),  $TW_x$  = inner-wall temperature, and  $R_x$  = the sum of the thermal resistances between TE and TW. These resistances include the convective resistance between the outer and inner walls, and assuming circular tubes in the heater and cooler have the form

$$R_x = \left( \frac{1}{h_o AW_o N} \right)_x + \left( \frac{\ln(D_o/D_i)}{2\pi k_w L N} \right)_x, \quad (79)$$

where  $h_o$  = convective coefficient for the tube exterior,  $AW_o$  = outside-tube surface area,  $N$  = number of tubes,  $k_w$  = wall thermal conductivity, and  $L$  = tube length.

The effective gas temperatures can be found from the inner-wall temperatures by using

$$T_x = TW_x - Q_x / (h AW)_x. \quad (80)$$

Of course, the user also has other options, such as specifying constant gas temperature in a heat exchanger. These options are explained in Appendix A.

3.2.4.3 Regenerator Ineffectiveness ( $Q_{REGEN}$ ). Regenerator ineffectiveness also known as reheat loss, represents the ratio of the net enthalpy flow per cycle through the regenerator to the heat transfer necessary to heat the gas from the cold-end temperature to the hot-end temperature. To examine regenerator ineffectiveness, Rios used the derivations of Qvale and Smith [42]. However, since their solution was derived for sinusoidal pressure and flow variations, Rios rederived their equations for general flow and pressure variations. The entire derivation is included in Rios' thesis ([1], pp. 121-127); for brevity, only the assumptions and the final result will be given here.

The assumptions are:

- (1) The regenerator gas state is unaffected by fluid friction.
- (2) The matrix temperature at any point in the regenerator is constant with time.
- (3) The regenerator is efficient; therefore, the gas to matrix temperature difference is small relative to the longitudinal temperature change.

(4) There is no axial conduction.

The reheat loss is given by the dimensionless formula

$$\lambda_R = \left[ \frac{1}{\frac{NTU_{CR}}{I_{2CR}} + \frac{NTU_{ER}}{I_{2ER}} \frac{M_{ACR}}{M_{AER}}} \right] \left[ 1 + N_{PH} \frac{I_{1CR}}{I_{2CR}} + \frac{I_{1ER}}{I_{2ER}} \frac{M_{ACR}}{M_{AER}} \right]. \quad (81)$$

The notation is that of Rios [1].

The terms in the first pair of brackets of the above equation represent the regenerator's transfer qualities. The second pairs of brackets represent the effect of heat transfer due to compression and expansion of the gas in the regenerator dead space.

This yields the actual reheat loss as

$$Q_{REHEAT} = N \dot{m}_R C_P \pi \lambda_R (T_H - T_K). \quad (82)$$

3.2.4.3.1 Correction to Regenerator Ineffectiveness. This correction results from an oscillation of the regenerator-matrix temperature during the cycle. In calculating the reheat loss, this oscillation was assumed negligible; however, this assumption is not always valid. The temperature swing loss is the additional heat load resulting from a finite regenerator heat capacity. Martini ([27], p. 139) gives the regenerator-matrix temperature change as

$$\Delta T_{MATRIX} = \frac{\dot{m}_H C_v (T_{WH} - T_{WC})}{3 \text{FREQ} (M C_P)_{MATRIX}}$$

and gives the actual correction to the reheat loss as

$$Q_{TSWING} = \left[ \frac{\dot{m}_R C_v}{3} \right] \frac{\Delta T_{MATRIX}}{2} \quad (83)$$

and the total regenerator ineffectiveness is the sum of Eqs. 82 and 83).

$$Q_{REGEN} = Q_{REHEAT} + Q_{TSWING} \quad (84)$$

### 3.3 DESCRIPTION OF SUBPROGRAM ELEMENTS OF SEAMI

The analysis module consists of five major routines: RIOSIN, ANALIS CYCLER, HTFLOW, and RIOSPR.

3.3.1 RIOSIN Subroutine. As was indicated in Sec. 3.2.2 the general input is particularized for the analysis to be used. The RIOSIN routine collapses the cell input into the five volumes monitored by the analysis. It

computes and stores the volumes and their derivatives for every step to be calculated. Although this requires several large arrays, it was felt the calculational time saved was worthwhile. In addition, the routine initializes the masses, temperatures, and pressures to be used.

3.3.2 ANALIS Subroutine. The ANALIS subroutine (Fig. 11) provides the framework for execution of the Rios technique. Few calculations are performed by it, its primary purpose being to direct the execution by calling the appropriate routines. Note that ANALIS calls the LOSSES routine described in Chapter 2 to compute the standard loss mechanisms. ANALIS is called from the MAIN program at the start of each cycle.

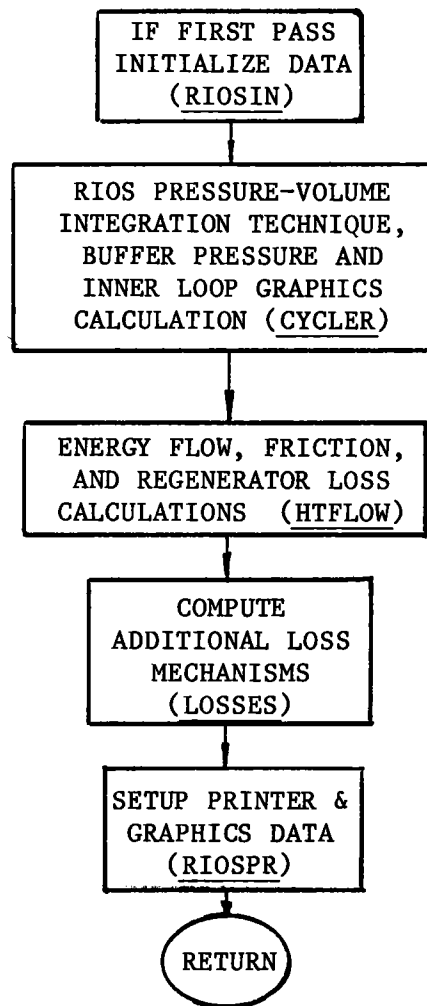


Fig. 11. ANALIS Subprogram

3.3.3 CYCLER Subroutine. The main purpose of CYCLER is to compute the pressure variations during a cycle, and the net work per cycle by evaluating the pressure-volume integral. The routine follows these basic steps:

(1) Initialization. Initialize the cycle by calculating values for the hot and cold space masses based upon the current gas temperature and pressure. Initialize the dimensionless works, negative mass accumulators, and minimum/maximum gas temperatures.

(2) Define Decision Matrix. Determine which of the four options for work integration is appropriate by evaluating the direction of mass flows (Eqs. 48-51). For the first step, mass is assumed to be increasing in the cold space and decreasing in the hot space (Eq. 51).

(3) Main Loop for Work Integration. The pressure, mass, and work Eqs. 54-60 are written in discrete form and are represented by DP, DMW, DMC, WC, and WW. A numerical integration of the Runge-Kutta second-order type ([45] pp. 52-54) is then performed. The volume, mass, and pressure at the start of a step are used to calculate the same variable at the midpoint of the step. Both values are averaged to calculate the complete step. After each integration step, the signs of the mass derivative terms are checked to determine which of the four mass-flow possibilities is appropriate. The entire cycle is integrated in this way for NSTEP steps.

(4) Record Results. The pressure and the differentials of pressure, compression-zone mass, and expansion-zone mass are saved for each step. The variable volume gas temperature are calculated, and the maximum/minimum values are updated if necessary.

(5) Buffer Zone Calculation. The variation in volume of the buffer zone was saved previously so an isothermal relationship is assumed when a buffer (added volume) calculation is desired.

(6) Graphics. If desired, the code will save

- |                               |                                 |
|-------------------------------|---------------------------------|
| 1. Crank angle                | 2. Expansion-zone volume        |
| 3. Pressure                   | 4. Compression-zone volume      |
| 5. Compression-zone mass      | 6. Expansion-zone mass          |
| 7. Cold piston torque         | 8. Compression zone temperature |
| 9. Expansion zone temperature |                                 |

These data are used for an additional print option as well as various crank angle curves.

(7) Convergence. The last part of the inner loop checks the agreement of the final cycle values of dimensionless pressure,  $P$ , and hot space mass,  $XMW$ , with the values from the beginning of the cycle. If  $\Delta P > 0.5\%$  or  $\Delta XMW > 0.1\%$ , the cycle is iterated with the final dimensionless pressure and hot space mass of the previous cycle as starting values. The NITE counter allows a maximum of 15 cycles before exiting the loop and printing.

3.3.4 HTFLOW Subroutine. This routine calculates the flow of energy from the heater to the cooler water. Because this calculation resides outside of the cycle loop it requires the inclusion of a calculation for: regenerator ineffectiveness; cooler, regenerator, and heater frictional losses; and

average values of heat-transfer coefficients. The routine follows these basic steps:

(1) Calculate Dimensionless Pressure. The average cycle pressure PNAVG is found by summing the pressures of each increment and then dividing by NSTEP. The maximum pressure is found and the dimensionless quantities are adjusted to the new maximum pressure. The phase angle between the pressure and volume variations, FIPV, is calculated for use in the piston gap loss, Eq. 33.

(2) Compute Values Used in Loss Calculations. Subroutine PDINT integrates Eq. 75 to determine the mass-flow-rate terms needed to evaluate the loss  $\oint \partial P_f \partial V_C$ , Eq. 71. It additionally evaluates the integrals used in the reheat loss, Eq. 81, such that  $XI1 = I_{1x}$ ,  $XI2 = I_{2x}$ ,  $XI3 = I_{1x}/I_{2x}$ . where x refers to either the compression or the expansion side of the regenerator.

The flow integrals UIN and UDM (equivalent to XINT and DMRE), are linearly interpolated in routine XNTERP for five volume locations in the heat exchangers to determine appropriate Reynolds numbers and kinetic energies.

(3) Pressure-Drop Losses. The pressure drop is expressed as the kinetic energy multiplied by a friction factor as shown in Eq. 66. It is represented in the code by GLS (cooler) and GLH (heater). The QP factor found in the code contains the engine parameters necessary to convert the pressure drops GLS and GLH to power losses QKOLFR and QHTRFR. The HTF routine in the Standard Functions module is called to compute contraction and expansion losses in the heater (ALOSSH) and cooler (ALOSSC); these are added to QHTRFR and QKOLFR, respectively, to obtain total friction losses.

The regenerator pressure-drop loss is similar to the heater and cooler losses in that it is expressed in the same form with the kinetic energy term multiplied by a friction factor. However, it differs by splitting the regenerator into three sections: cool, middle, and warm. The Reynolds number and friction factor are evaluated at each section. A weighted average of these individually calculated pressure drops is taken by using Simpson's Rule.

(4) Calculate Wall and Gas Temperature for the Heater and Cooler. Actual heat flows are computed for the heater (QACTH) and cooler (QACTC). Unless some other option has been chosen by the user, the inner-wall temperatures TWALLD(JHOT) and TWALLD(JCOOL) are then found using Eq. 78; effective gas temperatures TGASD (JHOT) and TGASD (JCOOL) are then found with a form of Eq. 80.

(5) Regenerator Ineffectiveness Loss and its Correction. The regenerator ineffectiveness loss QREGRH is found from Eq. 84 as was discussed earlier.

3.3.5 RIOSPR Subroutine. This routine provides a method of cataloguing the results of a cycle using the Rios technique so that they may be edited by the output processor. The routine saves about 50 variables on a cycle-by-cycle or case-by-case system as a function of the output-edit control variable NPRT2. In addition, the routine saves an array of variables for each zone used in the calculation, including heat flows, temperatures, mass flows and effective Nusselt numbers.

#### 4. TEST RESULTS AND CONCLUSIONS

This chapter describes the results of using SEAM1 to analyze the GPU-3 engine. A comparison is made between SEAM1 calculations, calculations reported from the Tew/NASA code [47], and experimental measurements made at NASA/LeRC on the GPU-3 engine [46].

##### 4.1 GPU-3 PERFORMANCE PREDICTIONS USING SEAM1

GPU-3 engine and component measurements [46] were used to prepare data for the input processor. Power and efficiency were determined as follows from the measured alternator output and cold-side heat flows:

$$P = P_a + P_L,$$

where

$P$  = "indicated" engine power (gross output with no mechanical losses),

$P_a$  = measured alternator power/alternator efficiency,

$P_L$  = measured mechanical losses (sum of heat to engine oil plus buffer water);

$$Q_H = Q_C + P,$$

where

$Q_H$  = heat into heater head

and

$Q_C$  = measured cooling-water reject heat (sum of heat from crankcase and cooler tubes)

Therefore the efficiency  $\eta$  is obtained from

$$\eta = P/Q_H.$$

These definitions are the basis for the values of power and efficiency given in Table VII and used in Figs. 12-14.

A sample map run requires that pressure, gas type, frequency, and heater wall temperature be supplied in addition to other fixed engine specifications. In the experimental runs, the cooling-water flows and inlet temperatures were reasonably constant, which implied that the heat-transfer film coefficient between the water and tube wall was also constant. Data given for temperature probes on the outer heater wall were used to provide heater temperature.

Since the GPU-3 crankcase is water cooled, conduction and other heat losses between the hot and cold ends of the engine combine to raise the temperature of the cooling water. The remaining energy losses and compression work are associated with the working fluid and combine as the heat transferred from the working fluid to the cooler tubes. The gas temperature is then predicted according to the Rios assumption that "Work in the movable spaces is provided from energy transferred by the adjacent heat exchanger." This model is not exact, but produced calculated values of cooling-water heat flow close to that measured.

TABLE VII. Comparison of SEAM1 Calculations with GPU-3 Experimental Data and NASA Code Predictions [47]

Operating Conditions				Indicated Power (kW)			Indicated Efficiency (%)		
Gas	Temperature (K)	Mean Pressure (MPa)	Engine Speed	NASA Code	SEAM1 Code	Experimental Data	NASA Code	SEAM1 Code	Experimental Data
H <sub>2</sub>	Heater Reference: 922	2.7	1500	1.94	1.91	1.95		36.8	35.5
			2500	2.93	2.91	2.93		37.1	35.0
	Water Inlet: 289	3500	3.35	3.34	3.37		32.9	31.4	
He	Heater Reference: 922	2.7	3000	2.2	1.91	2.06	24.7	22.4	23.1
				3.64	3.41	3.43	27.6	27.3	26.4
	Water Inlet: 289	5.5	5.12	4.48	4.64	30.4	27.6	27.1	
		6.9	6.18	5.29	5.48	30.2	26.9	26.5	

Table VII compares performance predictions from SEAM1 with experimental data and with a more sophisticated analysis code developed at NASA [3]. SEAM1 is seen to provide good predictions for engine power, but somewhat overestimates efficiency. Optimistic predictions of efficiency from approximate models are common since all engine losses are not included in simplified analyses. Computations from SEAM1 indicate that frictional losses and losses due to imperfect regeneration are the dominating influence on efficiency. Table VII shows that the agreement between measured and calculated values is maintained whether engine speed, system pressure, or working fluid is varied.

Figure 12 shows predictions of indicated power as a function of engine speed and mean cycle pressure. A good match is shown with experimental data. However, the engine was unable to overcome losses and develop power above 3 kW at engine speeds below 1500 rpm, so a comparison could not be made in this region.

Figure 13 shows the prediction of efficiency as a function of engine speed and mean cycle pressure. A large increase in efficiency is seen when the pressurization is increased from 2.76 to 4.1 MPa, but negligible improvement occurs for further increases in pressurization except at speeds below 1500 rpm. These effects can be explained in terms of the relative magnitudes of the conduction, friction losses, and regenerator losses. Conduction losses are determined almost entirely by the temperature difference between the hot and cold sides of the engine, thus only changing slightly with pressurization and speed. When pressurization is increased, gross power



## GPU-3 HELIUM 927K/339K

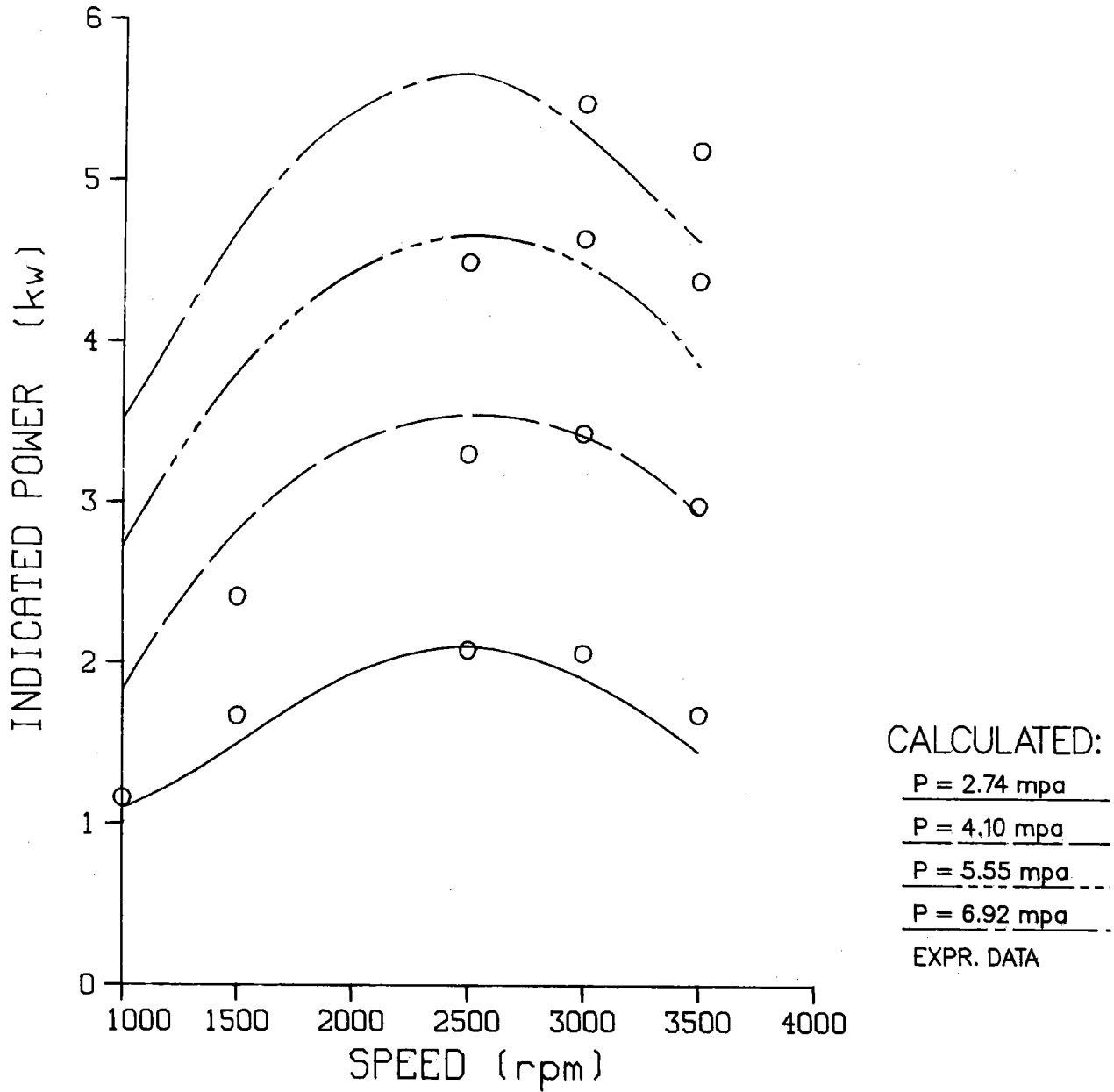


Fig. 12. Power Comparison

## GPU-3 HELIUM 927K/339K

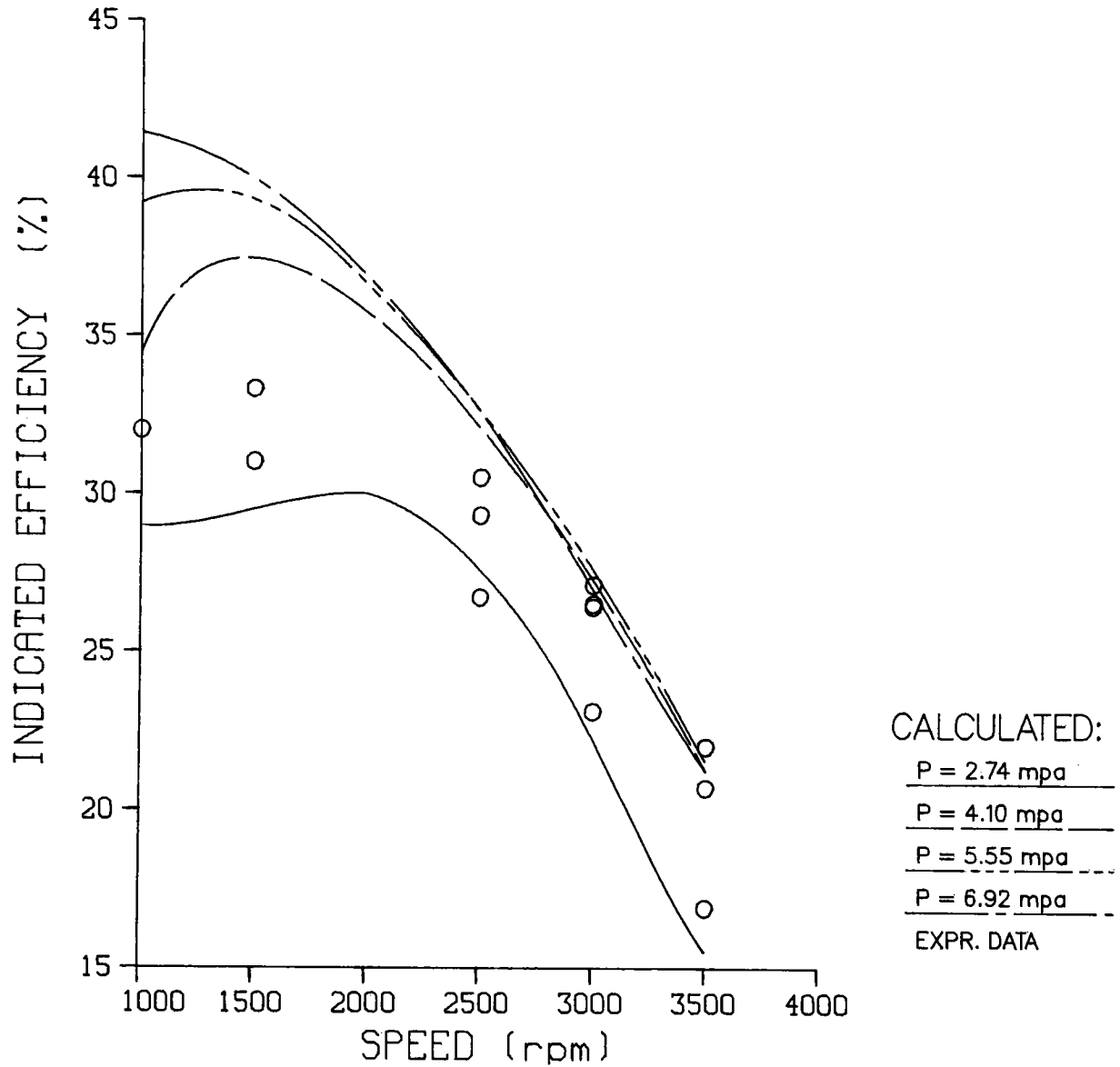


Fig. 13. Efficiency Comparison

increases faster than losses, and efficiency improves. At 4.1 MPa, flow losses dominate conduction losses, and further pressurization does not significantly improve efficiency since flow losses also increase with pressurization. At low speed, flow losses are reduced and efficiency improvements can be obtained by increased pressurization as is shown by Fig. 13. No measurements of efficiency above 33% were made, although the code predicts 40% should have been possible at the lower speeds.

Figure 14 presents the same data as an engine map of power versus efficiency at different pressurization levels. In this figure the combined deviations from measured values of power and efficiency are most noticeable. The significant result is that the trends are correct and only the magnitude needs more work.

Heat transfer between the gaseous working fluid and the heater and cooler walls was found to occur in the transition region between laminar and turbulent effects. A linear variation is assumed for the correlations in the transition region. We assumed a transition to turbulence at a Reynolds number of 4000, as was discussed in Chapter 2. These assumptions significantly affect the computed gas temperature and therefore the magnitude of power and efficiency.

#### 4.2 CONCLUSIONS

The GPU-3 example above shows that SEAM1 makes reasonably accurate predictions of Stirling-engine performance characteristics. This capability is a result of appropriately accounting for energy losses as well as heat flows into, out of, and through the engine. In addition to providing useful design information, SEAM1 required very little computer computation time since convergence to a solution usually occurred within three iterations. SEAM1 thus provides Stirling-engine analysis capability that should meet the needs of a wide spectrum of researchers in this field.

## GPU-3 HELIUM 927K/339K

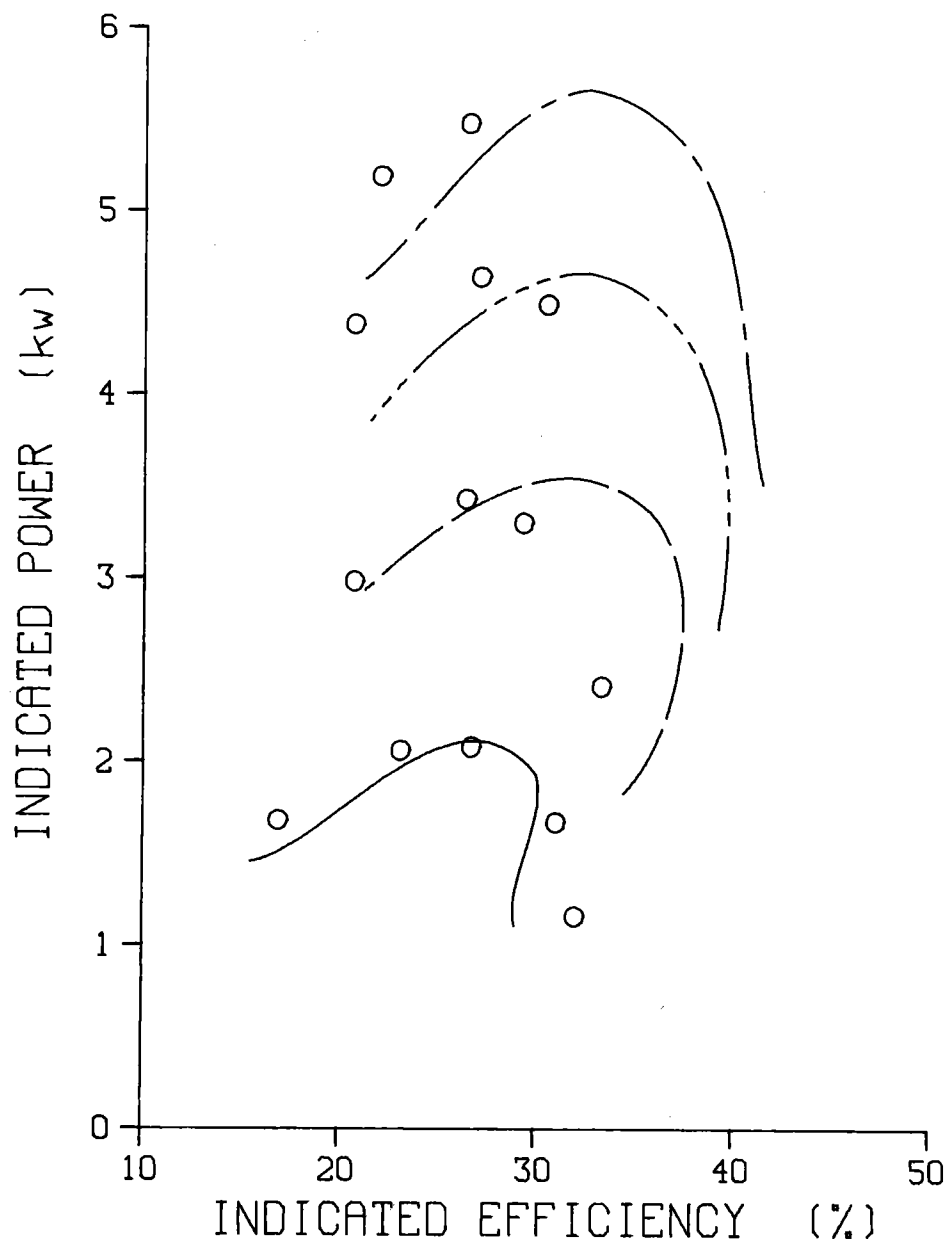


Fig. 14. Engine Map

APPENDIX A  
DIRECTIONS FOR USING THE CODE

This appendix contains directions for specifying input for the current version of the ANL Stirling Engine Analysis Code.

A.1 GENERAL INPUT DATA GROUPS

The input information is broken into three groups.

The first group provides general information to the code, such as title, frequency, gas type, and number of components in the other groups.

The second group provides information for the basic Stirling-cycle calculation. These data are put in by component, and an option is given to subdivide the component into cells for greater accuracy. For example, for the cooler (a relatively constant parameter component), data could be input once and then subdivided into constant volume cells to modify the cell-to-cell volume ratio and decrease numerical diffusion. It is important to remember that all codes treat a 200-tube heat exchanger as 200 identical tubes and therefore simulate only the average tube. The input emphasizes this by expecting the data on a per-tube basis. In those cases in which one expansion space feeds several heat exchangers, the number of tubes is the number per exchanger times the number of exchangers per expansion-compression unit.

The third group provides information for those volumes not directly connected to the working space. These added volumes include the various buffer spaces, crankcase, and hot piston dome. In Fig. A-1 they are the alphabetic labeled volumes. The information provided includes the data necessary to calculate the mass, pressure, and heat flow in these spaces.

All data are input according to Namelist conventions. The general data are entered by name into Namelist name GINPT. The second group is entered through the dummy variables II and AA using Namelist name CELL for each component. The third group of data is entered through the dummy variables JJ and BB using the Namelist name ADDED. These added volume values are only input if the option NADD has been previously input in the general data group.

See Table A-1 of Section A.6 for the actual input deck used for the GPU-3 example discussed below. It is suggested that before attempting to put together an input deck, the user should make up some input data worksheets as in Table A-2. On these worksheets the data are organized for easy reading when writing the Namelist statements that appear in the input deck, Table A-1.

All input variables are zeroed out initially, so if any input values are omitted from a Namelist, they will remain equal to zero. All data values are input using the International System of Units (SI).

The following description of the input variables used by the input processor module has two parts: the general description and the GPU-3 example (Fig. A-1). Each input variable is described and assigned values that model the GPU-3 (ground power unit) engine built by General Motors for the U.S. Army in 1965 and recently tested extensively at NASA/LeRC ([46],[47]).

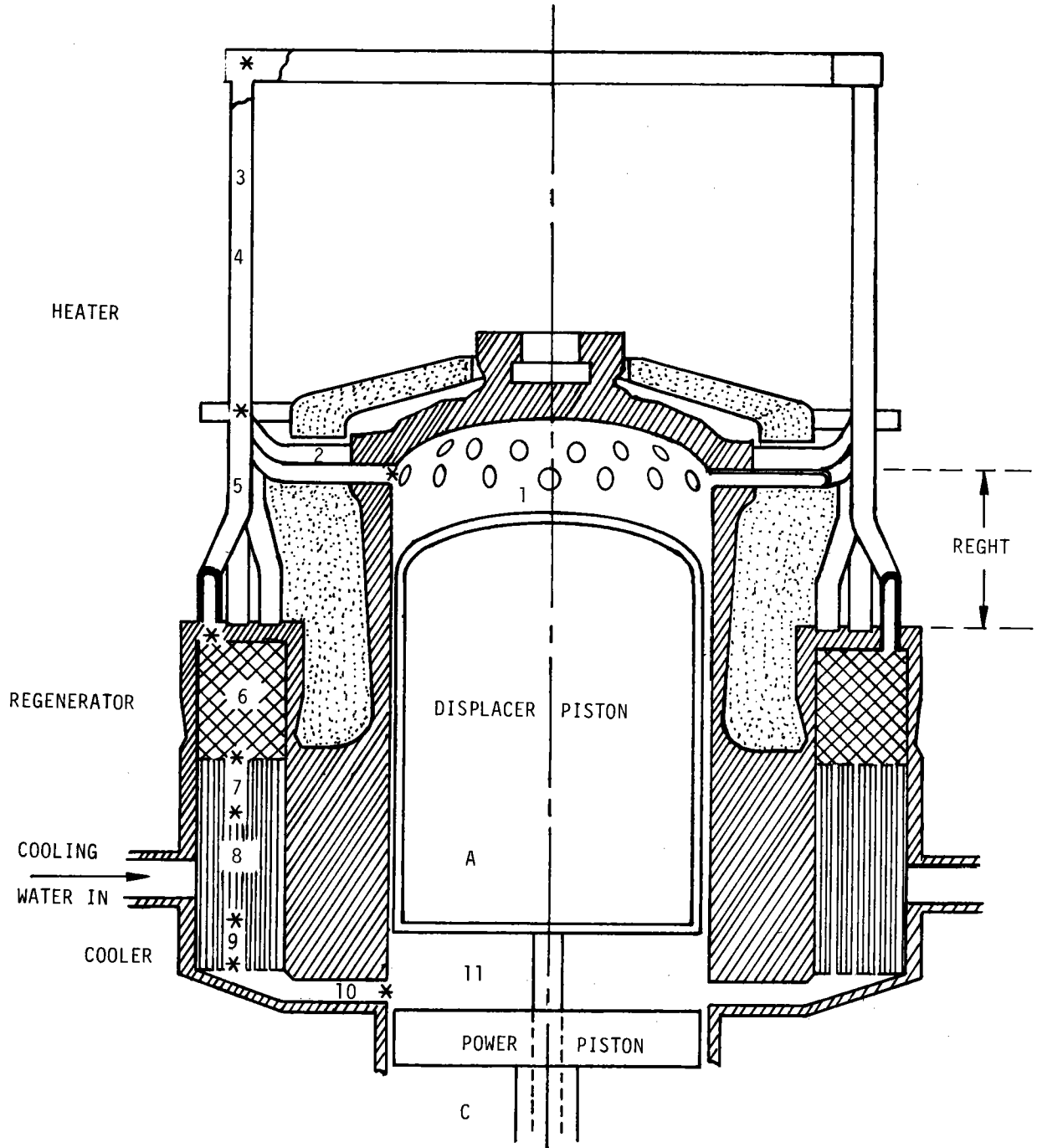


Fig. A-1. GPU-3 SEAM1 Cell Location

## A.2 TITLE AND GENERAL INPUT

### First Input. Title

The first card image is used to head each page of printout, up to 80 columns. In the graphics routine the first 24 columns are used as a general plot title.

### General Input. Namelist Name GINPT

The GINPT namelist block can be divided into two categories:

- (1) Integer values - saved by the input processor as common IGEN.
- (2) Floating-point values - saved in common FLTGEN.

#### A.2.1 COMMON IGEN

##### ICHNG

Determines if changes will be made to the initial input

0 - No additional changes.

Non 0 - Used to signal perturbation option (see Sec. A.5).

GPU-3: ICHNG = 1 so that frequency could be varied.

##### IDESGN

Type of engine design: three options

- 1 - In-line design, also known as an alpha engine; two pistons, two cylinders (Fig. A-2).
- 2 - Double-acting piston design; repetitive arrangement of two or more basic configurations (Fig. A-3)
- 3 - Displacer design; one cylinder contains both a displacer and a piston (Fig. A-4).

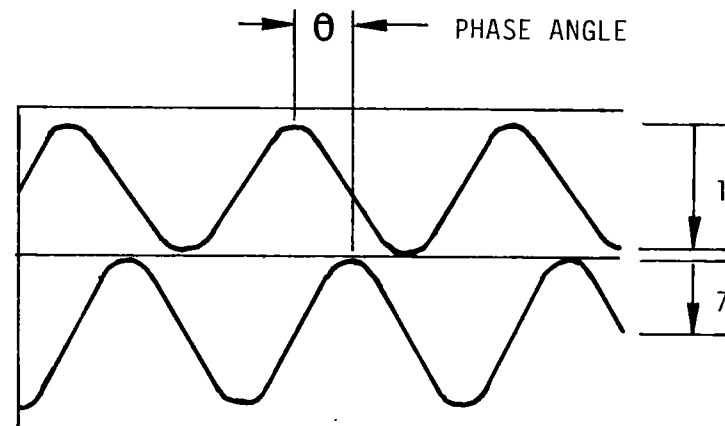
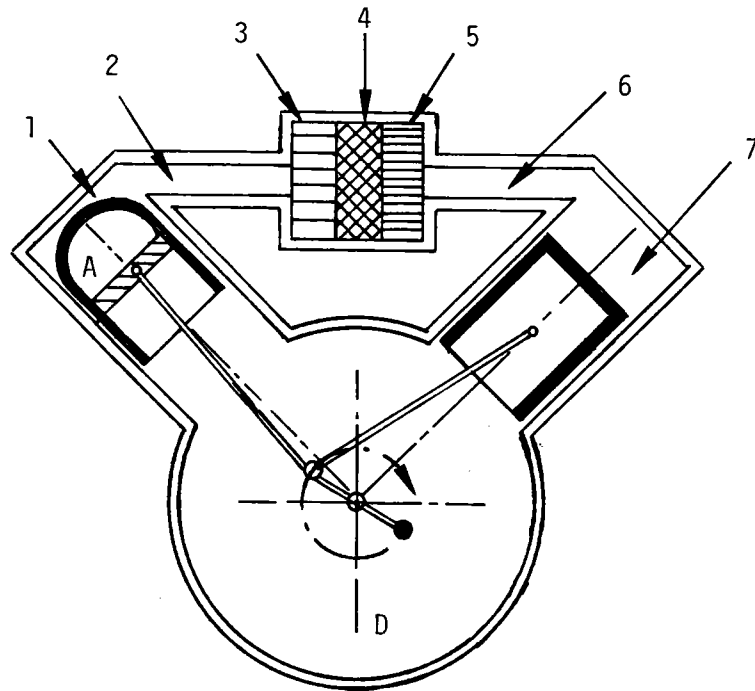
GPU-3: IDESGN = 3

##### IDRIVE

Drive mechanism used: three options

- 0 - Connecting-rod mechanism
- 1 - Rhombic drive
- 2 - Dynamic analysis (not yet available)

GPU-3: IDRIVE = 1 (Fig. A-5).

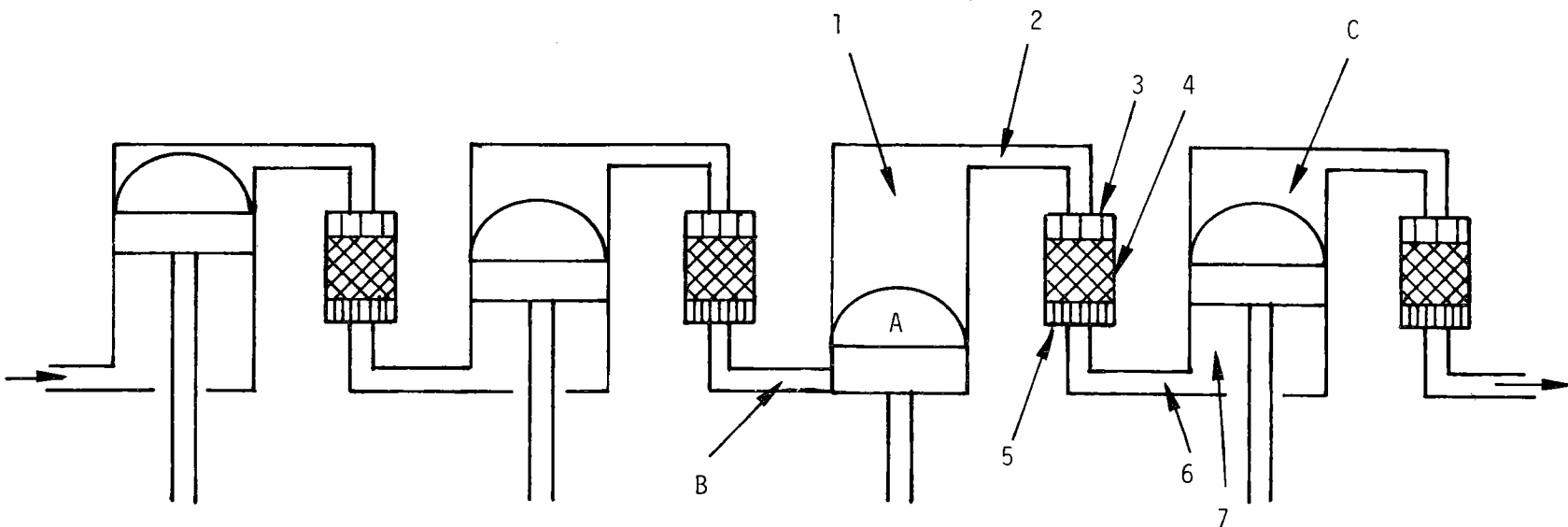


- 1 EXPANSION SPACE
- 2 HOT CONNECTING DUCT
- 3 HEATER
- 4 REGENERATOR
- 5 COOLER
- 6 COLD CONNECTING DUCT
- 7 COMPRESSION SPACE

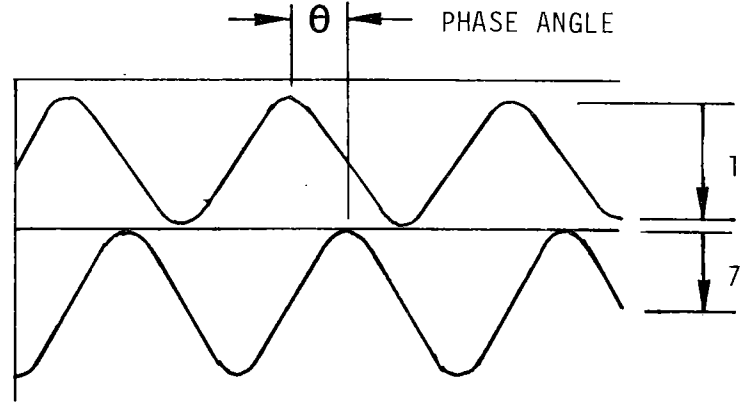
- A DISPLACER
- B DISPLACER BUFFER
- C COLD PISTON BUFFER
- D CRANKCASE

Fig. A-2. Design Type 1 In-Line Design





- 1 EXPANSION SPACE
- 2 HOT CONNECTING DUCT
- 3 HEATER
- 4 REGENERATOR
- 5 COOLER
- 6 COLD CONNECTING DUCT
- 7 COMPRESSION SPACE



- A DISPLACER
- B DISPLACER BUFFER
- C COLD PISTON BUFFER
- D CRANKCASE

Fig. A-3. Design Type 2 Double Acting Design

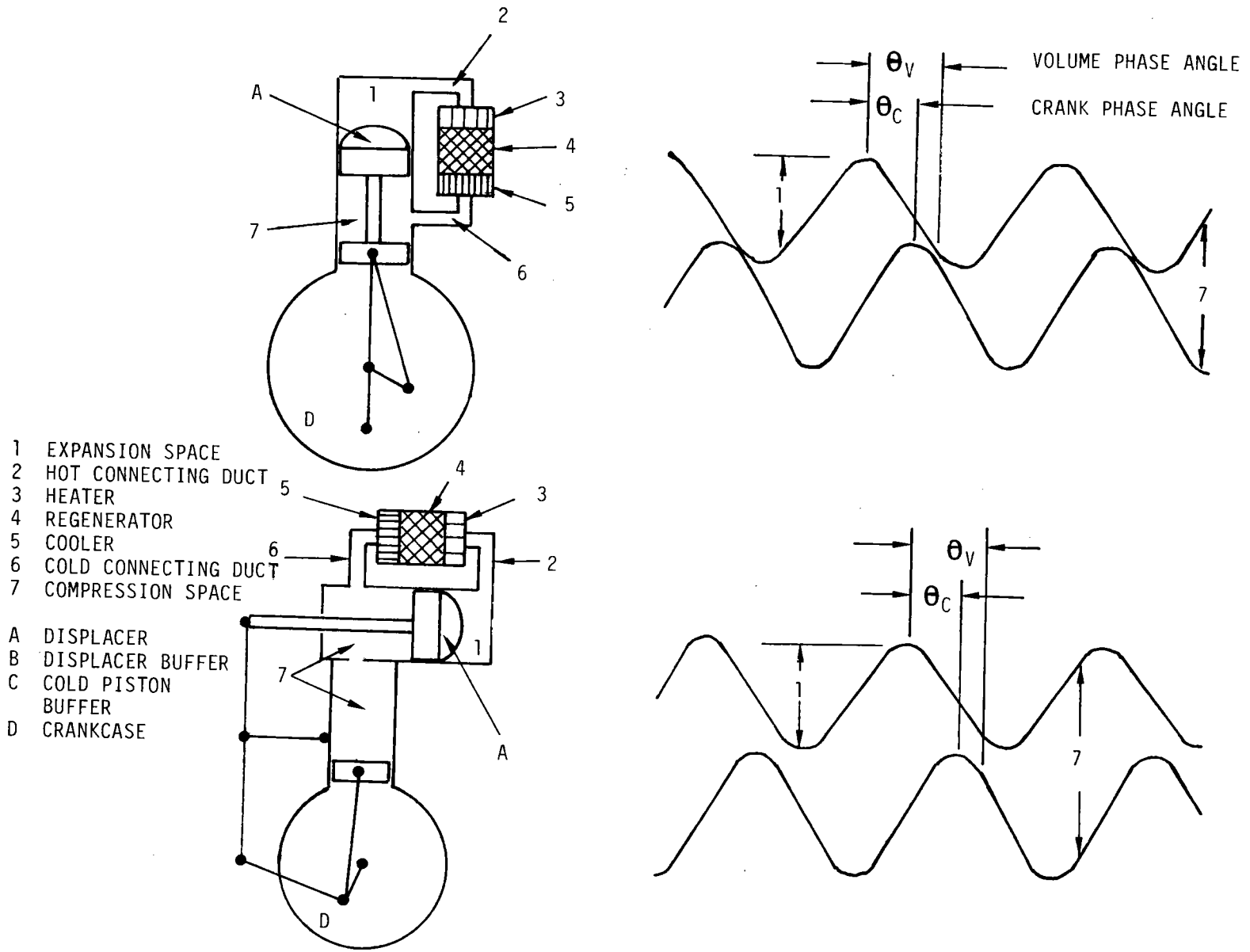


Fig. A-4. Design Type 3 Displacer Design

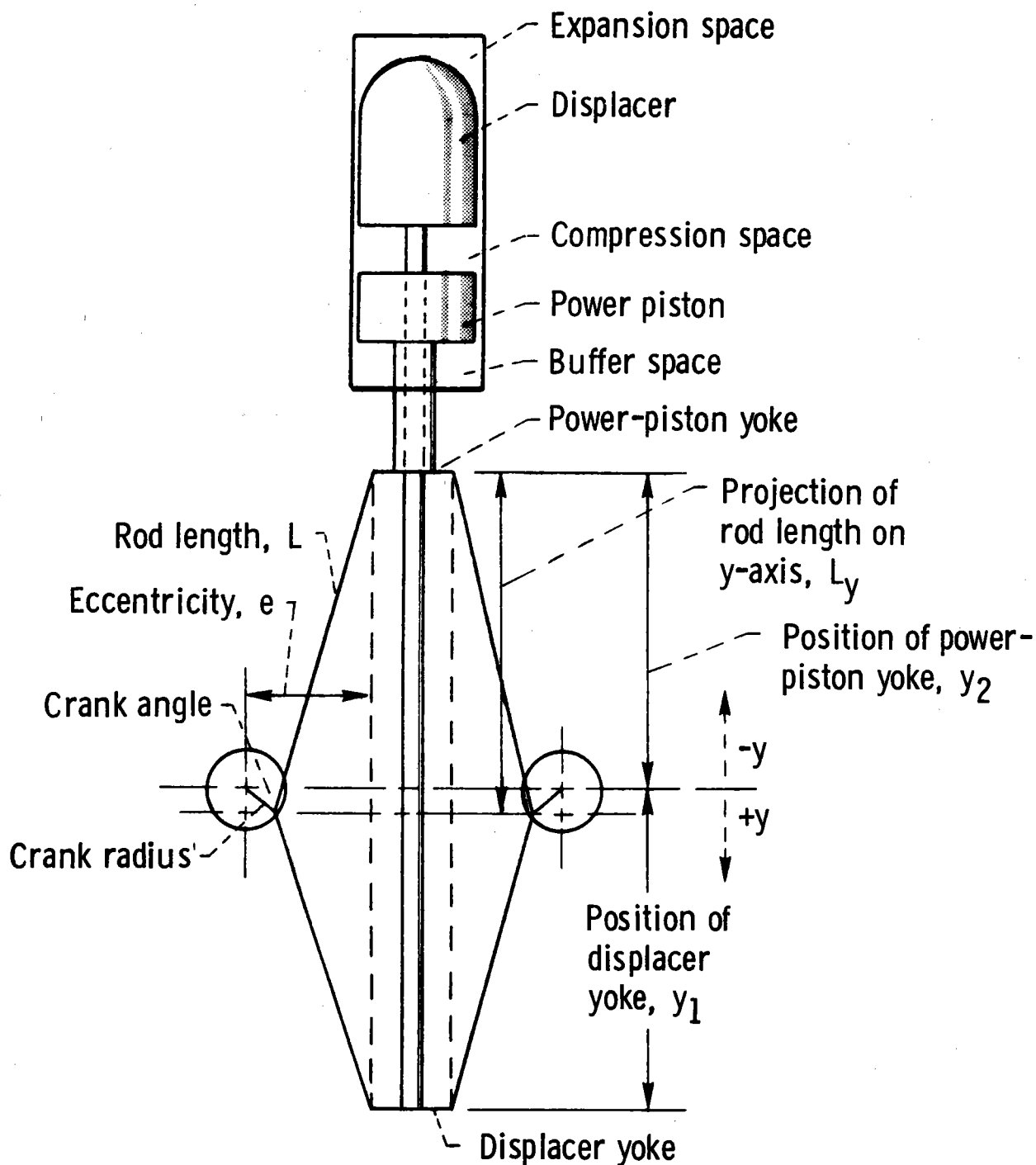


Fig. A-5. Diagram of Rhombic Drive

IGAS

Working fluid: six options

- |              |                    |
|--------------|--------------------|
| 1 - hydrogen | 4 - air            |
| 2 - helium   | 5 - carbon dioxide |
| 3 - nitrogen | 6 - methane        |

GPU-3: IGAS = 1, hydrogen is used in this sample run; other gases have been used experimentally and by other codes for the GPU-3.

IMASS

This is used to select which of the following two parameters is to be held fixed while the other is to be allowed to vary as the program iterates to convergence on the effective gas temperatures: PMEAN (mean gas pressure for one cycle) or TMASS (total gas mass in the engine). With this option the code will model engines that can be characterized as either operating at a specified mean pressure, or sharing a fixed mass in the system, in which case then, mean pressure will be computed.

- 0 - PMEAN fixed, TMASS calculated.
- 1 - TMASS fixed, PMEAN calculated.

GPU-3: IMASS = 0; not input, selected to match method used by NASA-Lewis code.

IMOM

Consideration of working fluid momentum effects: two options

- 0 - Momentum equation used in calculating friction only (no gas inertial effects are considered).
- 1 - Momentum equation is used as an integral part of the basic analysis (e.g., Urieli-type code).

GPU-3: IMOM = 0; not input, approach originally designed by RIOS and used by SEAM1.

IPRT1

Debugging variable if > 0, more output will be printed to observe internal calculations: four options

- 1 - Initialization output increased.
- 2 - Energy-flow output increased.
- 3 - Entire-convergence output increased.
- 4 - Final cycle parameters output increased.

GPU-3: IPRT1 = 0.

IGRAPH

Determines if results are saved to be graphed by the computer: three options

- 0 - No graph.
- 1 - Save graphics info for each case.
- 2 - Save graphics info for case to case comparison. Current version of SEAM1 uses a proprietary graphics package, TELLAGRAF by ISSCO to graph P-V diagrams and engine maps (see Sec. A.8).

GPU-3: IGRAPH = 1.

NADD

Number of alphabetic added volumes; integer value from 0 to 4, depends on engine design, analysis used, and user discretion (Figs. A-2, A-3, and A-4 for possible added volumes).

GPU-3: NADD = 2 (Fig. A-1). Displacer space (A) used for heat-transfer calculations; conduction down its walls to cold space and internal radiation from the hot end to the cold end. Buffer space (C), for use in torque calculations.

NCODE

Used to select analysis module:

- 0 - SEAM1 (Rios based) (Ref. [1])
- 1 - SEAM2 (Tew based) (Ref. [3])
- 2 - SEAM3 (Urieli based) (Ref. [2])

GPU-3: NCODE = 0; not input.

NCOMP

Number of components the engine is divided into by the user. The value chosen for NCOMP depends upon engine complexity and user discretion; it is suggested that the components be chosen to geometrically separate different gas-flow areas. These components can be partitioned into smaller, identically sized cells using input NCEL to give them cell-to-cell volumetric consistency. The minimum value of NCOMP for a typical Stirling engine would be 5: expansion space, heater, regenerator, cooler, and compression space. The maximum value is 30.

GPU-3: NCOMP = 11 (Fig. A-1). This value is greater than the minimum value because the heater was divided into two cells and the connecting ducts between the five components mentioned above were designated as individual cells.

NCYL

Number of cylinders in the engine; one expansion compression unit per cylinder.

GPU-3: NCYL = 1.

NOPT

Indicates additional losses to be included in heat flow from the gas through the cooler walls to the cooling fluid. Four options:

- 0 - No additional losses (friction, reheat, and compression work only).
- 1 - Conduction along piston walls + axially through the regenerator mesh added to NOPT = 0.
- 2 - Dynamic losses (shuttle + gap) added to NOPT = 1.
- 3 - Axial conduction along cylinder walls added to NOPT = 2.

GPU-3: NOPT = 1.

NPRT1

Number of time steps/printouts of general zone information. In the SEAM1 analysis, general zone information is not available within the cycle, so this option is less relevant.

GPU-3: NPRT1 = 720; two full cycles/printout.

NPRT2

Number of cases/full printout of power and energy flows. If only one case is being run this value should be 1.

GPU-3: NPRT2 = 6; six cases compared together.

NREVL

Maximum number of iterations the analysis portion of the program goes through to evaluate the effective gas temperatures; generally, gas temperatures converge sufficiently by the fourth iteration.

GPU-3: NREVL = 12; Convergence is satisfactory with SEAM1 when hot and cold gas temperatures are within 2 K of previous values, and the energy flow has been resolved to less than 2%.

NSTEP

Number of time steps in one revolution. Maximum present value is 720 (dimensioned array limitation).

GPU-3: NSTEP = 360, one time step per one degree of revolution.

A.2.2 COMMON FLTGENCMPCR

Compression piston crank radius; used by the volume subroutine.

Note: The stroke can be calculated from the geometry, for example,  $Stroke = ((CMPCRL + CMPCR)^2 - CMPECC^2)^{1/2} - ((CMPCRL - CMPCR)^2 - CMPECC^2)^{1/2}$ .

GPU-3: CMPCR = 1.38E-2 m, Table 1, Ref. [46]; see Fig. A-5. Same as EXPCR for rhombic drive. If the eccentricity is zero, then CMPCR = STROKE/2.

CMPCRL

Compression piston connecting rod length; used by the volume subroutine.

Note: Sinusoidal motion will be approximated if CMPECC = 0 and CMPCR << CMPCRL. It is recommended that the user set CMPCRL = 100 \* CMPCR if sinusoidal motion is desired. Similar comments hold for the expansion piston parameters.

GPU-3: CMPCRL = 4.60E-2 m, Table 1, Ref. [46]; and Fig. A-5. Same as EXPCRL for rhombic drive.

CMPDV

Compression zone dead volume; sum of all volumes in compression cylinder not swept by compression piston, such as the piston-cylinder clearance volumes. In a displacer design (Fig. A-4) this volume can be substantial, especially with variable stroke piston drives. There must always be at least a small amount of dead volume.

GPU-3: CMPDV = 1.09E-5 m<sup>3</sup>; Table 2 of Ref. [47]; sum of last 5 volumes in Section 5.

CMPECC

Compression piston crank radius eccentricity.

GPU-3: CMPECC = 2.08E-2 m; Table 1 of Ref. [46] and Fig. A-5. Same as EXPECC for rhombic drive. See note after CMPCRL.

CMPGAP

Compression piston-cylinder wall gap. Used for computing dead volume around compression piston; not presently used.

GPU-3: CMPGAP = 1.5E-4 m; Table 1 of Ref. [46] (cylinder bore at liner - piston diameter)/2).

CMPRD

Compression piston rod diameter; used in volume calculations to determine the area behind the compression piston.

GPU-3: CMPRD = 2.22E-2 m; Table 1 of Ref. [46].

CRANKD

Crank angle between top dead center for expansion and compression pistons in degrees. If input as 0, will be calculated from PHASED.

GPU-3: CRANKD = 0.0°; not input, for a rhombic drive, CRANKD is calculated by the code.

EXPCR

Expansion piston or displacer crank radius.

GPU-3: EXPCR = 1.38E-2 m; Table 1 of Ref. [46] and Fig. A-5, same as CMPCR for rhombic drive.

EXPCRL

Expansion piston or displacer connecting rod length.

GPU-3: EXPCRL = 4.60E-2 m; Table 1 of Ref. [46]; see Fig. A-5, same as CMPCRL for rhombic drive.

EXPDV

Expansion zone dead volume; sum of all volumes in expansion zone not swept by the expansion piston or displacer, such as the manifold and clearance gaps. There must always be at least a small amount of dead volume.

GPU-3: EXPDV = 1.25E-5 m<sup>3</sup>; Table 2 of Ref. [46], sum of all dead volumes in Section 1.

EXPECC

Expansion piston or displacer crank radius eccentricity.

GPU-3: EXPECC = 2.08E-2 m; same as CMPECC for rhombic drive.

EXPGAP

Gap between cylinder wall and expansion piston or displacer. Used to compute the dead volume around the displacer for the dynamic gap loss calculation in SEAM.

GPU-3: EXPGAP = 2.5E-4 m; Table 1 of Ref. [46] (cylinder bore above liner - displacer diameter)/2.

EXPRD

Rod diameter for the expansion piston or displacer; used in volume calculations to determine the area behind the expansion piston.

GPU-3: EXPRD = 9.52E-3 m; Table 1 of Ref. [46].



FREQ

Frequency of the system (Hz).

GPU-3: FREQ = 16.67, 25., 33.33, 41.67, 50., 58.33; varied to match cases run by experiment and NASA-Lewis code. Only the first of these frequencies is included in namelist GINPT. The others are input by means of Namelist PERTIN (see Sec. A.5).

HYSTF

Thermal hysteresis factor. Not used by SEAM1.

GPU-3: HYSTF = 0; not input.

PHASED

Crank angle (degrees) between minimum volumes of the expansion and compression zones; if input as 0, computed from CRANKD.

GPU-3: PHASED = 0.0°; not input, for a rhombic drive, PHASED is calculated by code.

PMEAN

System gas pressure averaged over the cycle. Either PMEAN or TMASS is held fixed while the other is allowed to vary (see TMASS and IMASS). If 0, it will be either computed from ideal gas formula or averaged from the sum of the cell pressures.

GPU-3: PMEAN = 2.74E+6 Pa; Case H141B, Ref. [46].

REGHT

Distance from the top of the regenerator to the bottom of the curved portion of the cylinder dome, measured parallel to the cylinder axis. Its primary use is in steady-state heat conduction; the sum of this length and XLNGTH for the regenerator is the conduction path distance from the expansion space to the cooler.

GPU-3: REGHT = 2.86E-2 m; approximation from available data (see Fig. A-1.).

STARTD

Crank angle (degrees) at time = 0.0; compression volume will start at a minimum if STARTD = 0.0.

GPU-3. STARTD = 0.0°.

TCMBST

Either combustor or external heater tube wall temperature. The code decides which of the two has been input by using the input value of HCEXT for the

heater cell. If HCEXT is greater than 0.0, TCMBST is assumed to be the combustor temperature. If HCEXT is equal to 0.0, TCMBST is assumed to be the external heater wall temperature. Note: When HCEXT is very large, combustor and external heater wall temperature become nearly equal.

GPU-3: TCMBST = 0.0 K; set equal to TWALL of the heater by the input processor. Heater TWALL was perturbed along with the frequency to better match the results of the NASA-Lewis experiments, Ref. [46]. See perturbation section on how TWALL of the heater was varied.

#### TWATER

Similar to TCMBST but for cooler; either mean coolant temperature or external cooler tube wall temperature. As with TCMBST, the code decides which of the above temperatures has been input by using the input value of HCEXT for the cooler. If TWATER = 0.0, it will be set equal to the cooler wall temperature.

GPU-3: TWATER = 287.0 K; inlet cooler water temperature was used as an approximation for the mean coolant temperature; the outlet temperature varied from the inlet by only a few degrees K (Ref. [46]).

#### TMASS

Total mass in the contiguous system. If not input, or input as 0.0, it will be computed provided that the other three parameters needed by the ideal gas equation have been input.

Pressure -- PMEAN for the system or PGAS for each cell.

Volume -- VOL for each cell or inputs to compute VOL.

Temperature -- TGAS or TWALL for each cell. (If TGAS is not input, it is initially assigned the value of TWALL for that cell.)

Depending on the value of IMASS, TMASS will be either held fixed or allowed to vary as the program iterates to convergence on the effective gas temperatures.

GPU-3: TMASS = 0.0 kg; not input.

#### TWENVR

External temperature; either room temperature or engine surface temperature. If TWENVR = 0.0, then it will be assigned 300 K as a default.

GPU-3: TWENVR = 0.0 K; not input.

#### ZOPT1

Code dependent option.

SEAM1: ZOPT1 is the fraction of the regenerator friction energy that is added to the heater; the remainder is added to the cooler.

GPU-3 ZOPT1 = 0.5. Half the energy to both the heater and cooler.

### A.3 INPUT FOR THE WORKING FLUID VOLUMES

Data for each of the component cells are input using Namelist name CELL. As with the general input, the individual cell values can be split into two categories:

- (1) Integer values - input in array II - stored in COMMON INCELL.
- (2) Floating-point value - input in array AA - stored in COMMON FLCELL.

The input format for the GPU-3 sample run is shown in Table A-1. The input module reads the numerical data assigned to the elements of arrays II and AA for each component. It then assigns each element to a particular COMMON BLOCK array whose subscript represents the cell number. The first component is assumed to be the expansion cylinder and the last is the compression cylinder.

The analysis module only uses three of the dead volume cells when determining temperatures, heat flow options, etc. As other modules are developed, more dead volume cells will be used. Therefore, this option is included for all cells, even though not currently used.

The variables and their location in array II are described below.

#### A.3.1 COMMON INCELL

$$\underline{\text{MHTRF}} = \text{II}(1)$$

Heat-transfer correlation system; allows the user to specify the formula for computing gas-wall heat transfer. Three options:

- 0 - Reference formula; the (St,Re) correlation currently available in the heat-transfer subprogram will be used.
- 1 - Colburn analogy. Sets Colburn number,  $j = \text{Fanning friction factor}/2$ .
- 2 - Constant value - allows the user the option of entering his own value for heat transfer (not currently available).

GPU-3: MHTRF = 0 for all cells.

$$\underline{\text{MQFLOW}} = \text{II}(2)$$

Component gas-wall-external environment heat flow; four options

- 0 - Wall temperature is constant over all cycles.
- 1 - Wall temperature changes with heat flow (typical heater or cooler options).
- 2 - Constant gas temperature.
- 3 - No net heat flow wall-gas (typically used for adiabatic components).

GPU-3: MQFLOW = 3 for components 2, 5, 7, 9 and 10. These components are adiabatic (relative to the environment) connecting ducts. Their walls absorb and emit heat, but the sum of such energy transfers is zero for a cycle.

MQFLOW = 1 for components 1, 3, 4, 6, 8, and 11. The SEAM1 sample run allowed the cooler wall temperature to vary from cycle to cycle. This in turn caused the regenerator wall temperature to vary, since SEAM1 computes it using the heater and cooler wall temperatures.

$$\underline{MTLWAL} = \text{II}(3)$$

Metal type of wall materials; nine options:

- |                      |                       |
|----------------------|-----------------------|
| 7 - Aluminum 2024-T4 | 12 - Stainless 310    |
| 8 - Copper           | 13 - Stainless 316    |
| 9 - Inconel X-750    | 14 - Titanium 120-VCA |
| 10 - K MONEL         | 15 - Nickel           |
| 11 - Stainless 304   |                       |

GPU-3: MTLWAL = 12 for all cells. The power piston was actually SAE 4340 steel, but this was not available as an option.

$$\underline{MTLWIR} = \text{II}(4)$$

Metal type for regenerator filler. Same options as MTLWAL.

GPU-3: MTLWIR = 11 for cell 6, MTLWIR = 0 for all others.

$$\underline{MTYPE} = \text{II}(5)$$

Component description; all cells fall into one of four categories:

Heat Exchanger

- 10 - Heater or cooler cylinder or tube
- 11 - Heater or cooler rectangular duct

Connecting Duct

- 15 - Cylindrical
- 16 - Rectangular
- 17 - Orifice

Variable Volume (21 and 22 are typically used in gamma and free piston designs)

- 20 - Cold
- 21 - Displacer side cold

22 - Piston side cold

25 - Hot

#### Regenerator

30 - Screen

31 - Sphere

32 - MET NET

33 - Corrugated metal (rectangular tubes)

34 - Round tube matrix

GPU-3: MTYPE = 25 for cell 1 (expansion space)

MTYPE = 15 for cells 2, 5, 7, 9, 10 (connecting ducts)

MTYPE = 10 for cells 3, 4, 8 (heater and cooler)

MTYPE = 30 for cell 6 (regenerator)

MTYPE = 20 for cell 11 (compression space)

$$\underline{NIHX = II(6)}$$

Number of units of this type per expansion-compression unit. Each tube or duct in a heater or cooler is considered 1 NIHX.

GPU-3: NIHX = 1 for cells 1 and 11; expansion and compression spaces will always have this value by definition.

NIHX = 40 for cells 2, 3, 4, and 5 (heater tubes)

NIHX = 8 for cells 6 and 10; regenerators and cooler-to-compression space ducts.

NIHX = 312 for cells 7, 8, and 9 (cooler tubes).

$$\underline{NOPT1 = II(7)}$$

Optional input variable; meaning depends on analysis module used. Not used by SEAM1.

GPU-3: NOPT1 = 0 for all cells; need not be input.

$$\underline{NCEL = II(8)}$$

Number of computational cells that this component is divided equally into; this value is not saved in common.

GPU-3: NCEL(6) = 5 (regenerator); NCEL = 1 for all other cells.

Currently the expansion and compression spaces can only be one cell in length.

#### A.3.2 COMMON FLCELL

Common FLCELL contains the mnemonics for array AA. For brevity,

actual values from the GPU-3 sample for each variable and each cell have been left out of the descriptions below; they are included in the input-data printout (Table A-1) in SI units.

$$\underline{\text{AFLOW}} = \text{AA}(1)$$

Gas flow area with its normal parallel to the axis of the component. In a regenerator,  $\text{AFLOW} = \text{SIGMA} * \text{Duct Frontal Area}$ ; this gives the minimum flow area that is used in the heat-transfer and friction correlations. If AFLOW is not input, it will be computed, provided either the hydraulic diameter (DH) or the combination of the volume (VOL) and length (XLNGTH) is input. In the variable volumes, the flow area must be input. The AFLOW value is per NIHX.

GPU-3 The area of the displacer rod was subtracted from the total cross-sectional area for the compression space AFLOW. All other AFLOW values were direct area calculations as described above and are explicitly input.

$$\underline{\text{ASPECT}} = \text{AA}(2)$$

Ratio of the short side to the long side of a rectangular duct; used in heat-transfer and friction calculations.

GPU-3: Not input; no rectangular ducts.

$$\underline{\text{AXWALL}} = \text{AA}(3)$$

Cross-sectional area of the wall, used for axial heat conduction calculations. Values are not needed from the cooler cell to the compression cell as these walls are approximately at the cooler temperature. In the regenerator, AXWALL corresponds to the casing, not the filler. All AXWALL values are per NIHX. The code assumes that the temperature varies linearly in space and that the conductivity varies linearly with temperature. An appropriate cross-sectional area for heat flow is needed for variable area walls.

GPU-3: Inner and outer wall diameters were available for all cells (Fig. A-6 and Ref. [47]).

$$\underline{\text{AWET}} = \text{AA}(4)$$

Wetted area used for wall to gas flow; if not input, computed from VOL and DH. For expansion and compression zones, AWET is determined at maximum volume, not including the wetted area within the piston-cylinder wall gap. AWET is per NIHX.

GPU-3: Expansion space:  $\text{AWET}(1) = \text{stroke} * \text{perimeter} + \text{displacer head area} + \text{cylinder dome area} - \text{heater tube inlet area}$ .  
Compression space (at full stroke):  $\text{AWET}(11) = \text{cylinder wall area} + \text{connecting rod area} + \text{piston head area} + \text{displacer bottom area} - \text{cooler tube inlet area}$ .  
Regenerator:  $\text{AWET}(6) = 0.0$ , left to be calculated. All other cells were tubes or ducts:  $\text{AWET} = \text{perimeter} * \text{length} = 4 \text{ Vol} / D_h$ .

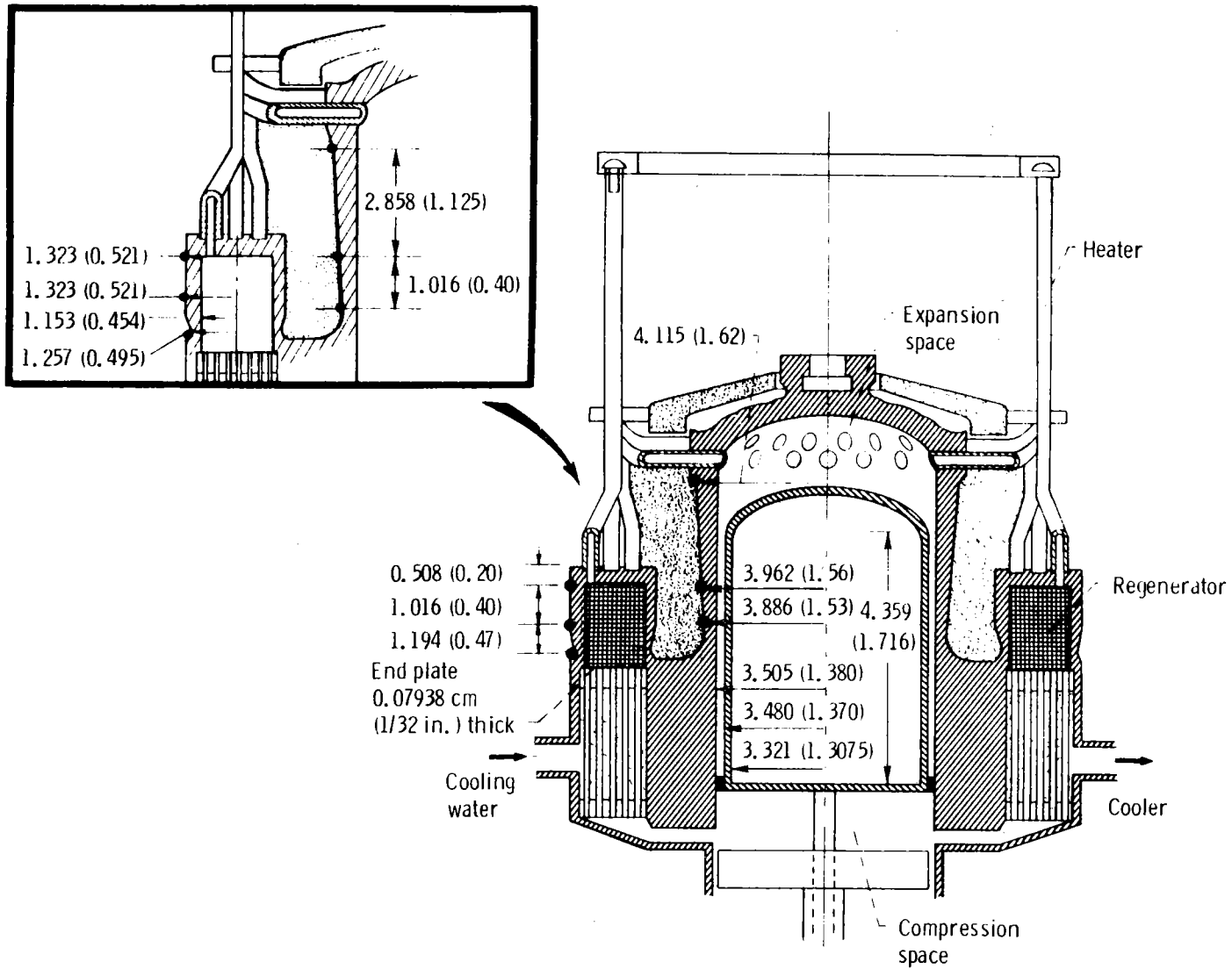


Fig. A-6. GPU-3 Dimensions for Heat Conduction

$$\underline{DH = AA(5)}$$

Mean hydraulic diameter. If not input, calculated from VOL and AWET. For screen regenerators,  $DH = (\text{porosity} \times \text{wire diameter}) / (1 - \text{porosity})$ ; (Ref. [33] pp. 8 and 25). (For METNET regenerators, Ref. [34], Section 6.004, p. 26).

GPU-3: A piston rod passed through the compression space, and a screened regenerator was used; DH for these two cells was computed as mentioned above. For all other cells, DH = actual diameter.

$$\underline{FRICML = AA(6)}$$

Friction multiplier, used to account for differences between the available friction correlations and actual conditions (i.e, reversing flow modeled as steady flow). If FRICML = 1.0, the correlations in the friction subprogram (HTS) are not altered. If FRICML = 0.0, there will be no flow friction in that component. The default value is 1.0.

GPU-3: In the regenerator, FRICML(6) = 2.0 to attempt to model the friction loss of the GPU-3 regenerator. FRICML = 1.0 for all other cells.

$$\underline{HCEXT = AA(7)}$$

External film heat-transfer coefficient. Used with TCMBST, TWATER, TWENVR, and QFLOW (if MQFLOW < 2); for determining outer-wall temperature or environment-to-wall heat flux. If HCEXT = 0. for a cell, either TCMBST (if heater cell), TWATER (if cooler cell), or TWENVR (if any other cell) is assumed to be the cell's outer-wall temperature. The same result is obtained if HCEXT is very large.

GPU-3: HCEXT = 3000.0 W/(m<sup>2</sup>·K) for cooler cell 8; used with TWATER and the calculated heat flow to find TWALL(8). HCEXT = 0.0 for all other cells. TCMBST was the heater outer-wall temperature from test results (Ref. [46]). For all other cells, no heat flux to the environment is calculated by SEAM1.

$$\underline{ORIFICE = AA(8)}$$

Orifice coefficient (see MTYPE = 17); used to account for pressure-drop losses caused by orifices commonly found in test engines. It is not to be used for expansion and contraction losses between components; those are accounted for in the friction-factor portion of the heat-transfer subprogram.

GPU-3: ORIFICE = 0.0 for all cells; no orifices.

$$\underline{PGAS = AA(9)}$$

Initial gas pressure. If not input, computed either from total mass and the sum of the volumes or from PMEAN; in such a situation, all cell pressure will be equal.

GPU-3: PGAS = 0.0 Pa, for all cells.



$$\underline{\text{POROS}} = \text{AA}(10)$$

Porosity = (void volume)/(total volume); for regenerator filler material or MTLWIR. If MET NET, use POROS = 1.0 - filler factor. Not the same as SIGMA, POROS gives average flow area and should be used with average flow velocity in friction and heat-transfer calculations.

GPU-3: POROS = 0.697

$$\underline{\text{QFLOW}} = \text{AA}(11)$$

External wall surface to environment heat flux; used with TCMBST, TWATER, and TWENVR when MQFLOW = 1. This allows a constant heat flux to be input. If 0.0, then heat flow will be computed.

GPU-3: QFLOW = 0.0 W, for all cells.

$$\underline{\text{SIGMA}} = \text{AA}(12)$$

Minimum flow area/frontal area for regenerator. Less than or equal to porosity; used with maximum velocity in heat-transfer and friction correlations. For screen regenerators, SIGMA = (1-mesh\*wire dia.)\*\*2; (Ref. [33]).

GPU-3: SIGMA = 0.468 using the screen formula above.

$$\underline{\text{TGAS}} = \text{AA}(13)$$

Design-point initial gas temperature; if not input, TGAS = TWALL. Either TGAS or TWALL must be input.

GPU-3: TGAS = 0.0 K for all cells; set equal TWALL.

$$\underline{\text{TWALL}} = \text{AA}(14)$$

Design-point inner-wall temperature; constant within any one cycle for SEAM1. TWALL = TGAS if set to 0 or not input. Only TWALL in the heater and cooler is used by the SEAM1 analysis module. However, approximate values for the other cells are needed because the input processor computes the initial system mass (TMASS) with them if it was not input. Regenerator filler is initialized to regenerator wall temperature.

GPU-3: Cells 1-5 were assigned the experimental heater temperature (TCMBST) and cells 7-11 were assigned the cooler temperature. Regenerator cell 6 was set at the average of the two. In the test engine, heater temperature changed as the frequency was varied (Ref. [46]). To match this situation in the sample run, TCMBST was varied with frequency (Table A-1).

$$\underline{\text{VOL}} = \text{AA}(15)$$

Gas volume or total displacement. The expansion and compression volumes need not be input here; they are variable and either their time-dependent values are computed by the volume subprogram or the user can replace this subprogram

with a different method. If other cells are not input, they will be calculated from AFLOW\*XLNGTH. If known, VOL values should be input since AFLOW\*XLNGTH may not include all the dead volume for that cell.

GPU-3: All values were taken from Table 2 of Ref. [46] and are listed below:

<u>Component Cell</u>	<u>Volume (m<sup>3</sup>)</u>
1	0
2	$(9.68E-6)/40 = 2.42E-7$
3	$\frac{(47.46 + 7.67)(E-6)}{2(40)} = 6.891E-7$
4	6.891E-7
5	$\frac{(13.29 + 2.74 + 7.36)(E-6)}{40} = 5.848E-7$
6	$\frac{5.3E-5}{8} = 6.68E-6$
7	$\frac{(2.59 + 2.18)(E-6) + (4.838E-9)}{312}$
8	$\frac{1.313E-5}{312} \frac{3.55}{4.61} = 3.241E-8$
9	$\frac{1.313E-5}{312} \frac{(4.61 - 3.55)}{2(4.61)} = 4.838E-9$
10	$\frac{(3.92 + 2.77 + 3.56)(E-6)}{8} = 1.281E-6$
11	0

$$\underline{VOLWL = AA(16)}$$

Volume of wall material used in wall-temperature calculations; if not input, computed from AXWALL\*XLNGTH. Not presently used.

GPU-3: Both XLNGTH and AXWALL were approximated to compute VOLWL (10) for the irregularly shaped connecting duct. Compression space VOLWL(11) was assumed to equal expansion space VOLWL(1). All other cells were computed from AXWALL\*XLNGTH. These values were input for future use; they are not presently used.

$$\underline{WALLTH = AA(17)}$$

Wall thickness; used primarily for calculating the heat flow through and temperature gradient across the heater and cooler tube walls. It will be used with the other cells in future applications for heat-flow calculations with the environment. If not input, it is calculated from AXWALL and the wall diameter.

GPU-3: Taken from Table 1 of Ref. [46] for the cooler tubes; not input for the others.

$$\underline{XLNGTH = AA(18)}$$

Component length; used for heat-conduction calculations and computing VOL, VOLWL, and AFLOW if they are not input. If XLNGTH is 0.0 or not input, it is computed from VOL/AFLOW.

GPU-3: For expansion and compression spaces, XLNGTH = stroke + clearance. XLNGTH for all other cells came from Table 1 of Ref. [46].

#### A.4 INPUT FOR THE ADDED VOLUMES

Information for the added alphabetic cells is input in a manner similar to that for the cells described above. A separate Namelist entry, ADDED, is used for the added cells. Numerical data are entered in arrays JJ (integer) and BB (floating point). The input processor assigns variables to the elements of both arrays and places the JJ values in common IADD, while BB values are put in common FADD.

In engines similar to the GPU-3, which is a displacer design, three added cells are common: A, C, and D (Fig. A-4). However, for this sample run, only cells A and C were input; cell D, the crankcase space, was unspecified in the available data and is not used in the present code. For this run cell 1 is type A and cell 2 is type C.

##### A.4.1 COMMON IADD

$$\underline{IACOND = JJ(1)}$$

Heat-transfer mechanism(s) present between the added cell and the adjacent variable volume. Three options:

- 0 - no heat transfer
- 1 - only conduction
- 2 - conduction and radiation (e.g., hollow displacer)

Only options 0 and 1 are presently used. No radiation transfer is calculated.

GPU-3: IACOND(1) = 2; heat transfer in the hollow displacer is both by conduction down the wall and radiation to the compression space. The conduction only is presently calculated.

IACOND(2) = 1; conduction paths exist from the compression zone to the buffer space via the compression piston and cylinder walls. Heat flow along these paths is generally negligible due to the small temperature gradient and hence is not included.

$$\underline{\text{IALEAK}} = \text{JJ}(2)$$

Leak condition between added and variable volumes; four options:

- 0 - no leaks
- 1 - gas leakage in both directions
- 2 - gas leakage into the added volume only (unidirectional)
- 3 - gas leakage out of the added volume only

Gas leakage is not presently computed. This option is intended for later code versions.

GPU-3: IALEAK = 1 for both added cells; input for future use. Gas leakage between the expansion space and the displacer is the result of a small pressure release hole in the displacer side; this hole allows the pressure inside the displacer to be near equilibrium with the expansion space pressure, thus relieving stress on the displacer wall. Flow through the hole during a cycle is assumed to be insignificant due to its small (unspecified) size. Leakage between the compression space and buffer space C occurs past the piston rings.

$$\underline{\text{IAMTL}} = \text{JJ}(3)$$

Wall material; same nine options as MTLWAL. Used presently for determining conduction properties.

GPU-3: IAMTL(1) = IAMTL(2) = 12; stainless 310.

Note: IAMTL(2) refers to the wall material surrounding buffer space C, not to the material the power piston is made of.

$$\underline{\text{IATYPE}} = \text{JJ}(4)$$

Component description; four options:

- 10 - piston dome or displacer (volume A)
- 20 - cold piston buffer space (volume C)
- 25 - hot piston buffer space (volume B)
- 40 - crankcase (volume D)

Not all added volumes are common to each design (Figs. A-2, A-3, and A-4).

GPU-3: Of the three IATYPES that are common to design 3, 10, 20, and 40, IATYPE = 10 for cell 1 and 20 for cell 2 were used. IATYPE 25 is not used in design 3 engines because the displacer is bounded by the expansion and compression zones.

$$\underline{\text{NRINGS}} = \text{JJ}(5)$$

Number of rings in leakage calculations; not used by SEAM1.

GPU-3: NRINGS(1) = 0; leakage from the expansion space to the compression space past the displacer rings is not evaluated.

For displacer leakage see IALEAK.

NRINGS(2) = 2 for the power piston.

$$\underline{\text{NSHELD}} = \text{JJ}(6)$$

Number of radiation shields in displacer A (IATYPE = 10); primarily for IDESGN = 3. Not presently used.

GPU-3: NSHELD(1) = 2.

#### A.4.2 COMMON FADD

$$\underline{\text{ADPGAS}} = \text{BB}(1)$$

Gas pressure in added cell; buffer space pressure will be used for torque calculations in future versions. ADPGAS for all cells will be used in future leakage calculations. If not input, it is set equal to PMEAN.

GPU-3: ADPGAS(1) = 0.0 Pa. If needed, it would be approximately the same as the expansion space pressure.

ADPGAS(2) = 3.23E6 Pa; Ref. [46].

$$\underline{\text{ADRADA}} = \text{BB}(2)$$

Radiation surface area term for inside the displacer (engines with IDESGN = 3); ADRADA = shape factor\*surface area. Intended use:

$$q = \sigma A_1 F_{12} \left( T_1^4 - T_2^4 \right) = \sigma (\text{ADRADA}) \left( T_1^4 - T_2^4 \right).$$

Not presently used.

GPU-3: ADRADA(1) = 0.0 W/K<sup>4</sup>.

$$\underline{\text{ADTGAS}} = \text{BB}(3)$$

Gas temperature inside added volume at the start of the cycle.

GPU-3: ADTGAS for A and C was set equal to the expansion and compression space temperatures, respectively; for use in later versions.

$$\underline{\text{ADVOL}} = \text{BB}(4)$$

Gas volume; if variable, maximum used. Note: The displacer volume is not considered part of the dead volume.

GPU-3: ADVOL(1) calculated from dimensions (Fig. A-6) (assuming displacer dome was flat).

ADVOL(2) from Table 1 of Ref. [47].

$$\underline{\text{ADWALX}} = \text{BB}(5)$$

Effective length for axial conduction along displacer (IATYPE = 10); generally assumed to be the displacer length. In an in-line design, ADWALX is the length used for axial wall conduction from the expansion zone to the hot buffer space.

GPU-3: Displacer length (Fig. A-6).

$$\underline{\text{ADWLDI}} = \text{BB}(6)$$

Wall inner diameter; for use with ADWLTH in heat-conduction calculations.

GPU-3: Inner displacer diameter and piston cylinder bore (Table 1 of Ref. [41]).

$$\underline{\text{ADWLTH}} = \text{BB}(7)$$

Wall thickness; for heat-conduction calculations.

GPU-3: ADWLTH(1) from Table 1 of Ref. [46].

ADWLTH(2) approximated as minimum expansion cylinder wall thickness (Fig. A-6).

$$\underline{\text{EMIS}} = \text{BB}(8)$$

Emissivity of radiation shields in displacer; not currently used by SEAM1.

GPU-3: 0.3.

$$\underline{\text{RINGCL}} = \text{BB}(9)$$

Clearance between ring and wall; no leakage is possible unless RINGLK > 0.0. Not presently used.

GPU-3: Not input.

RINGFR = BB(10)

Ring friction coefficient. Typical values: 0.15 = plastics, 0.8 = metals. Not presently used.

GPU-3: RINGFR(2) = 0.15.

RINGHT = BB(11)

Ring height; not presently used.

GPU-3: 0.002 m.

RINGLK = BB(12)

Ring-leak coefficient; not presently used. If input as 0.0 in later versions, then it will be calculated from RINGCL, RINGHT, NRING, gas properties, and laminar flow through an annulus.

GPU-3: Not used.

SLNGTH = BB(13)

Effective length for shuttle heat-transfer calculation in IDESGN = 3 engines, usually displacer stroke (Ref. [27], p. 129).

GPU-3: Displacer stroke (Table 1 of Ref. [46]).

#### A.5 PERTURBATION INPUT

All of the previous input information can be thought of as a description of the design point conditions. To allow the user an easy method of seeing the effect of changes, two perturbation options are included: a batch and an interactive technique. The batch technique can be used to generate engine maps where many cases are generated, and the interactive technique to modify geometry. With both systems the user may change any of the previous inputs and execute the new case (see Table A-1).

Two previously described integer variables control the input and output: ICHNG and NPRT2.

ICHNG; Five Options

- 0 - The current case will be the last case to be executed.
- 1 - An additional case will be run, the data changes will follow the base input deck.
- 2 - The added case requires reinitialization of the input, used for changes to variable volume input (see subroutine INITAL).
- 3 - An additional case will be run, the data changes will come from logical unit 10. This allows for interactive input (see Section A.5.2).
- 4 - Interactive added case requires reinitialization.

-N N is 1-4 as above; the negative indicates a full input edit is desired for the added case.

GPU-3: In the base data input, ICHNG is set to 1. It remains 1 until the last case, where it is then set to 0.

#### NPRT2

The number of cases to be compared on the output and graphically displayed as group.

GPU-3: NPRT2 = 6, because six frequencies were run.

#### A.5.1 Additional Input Options

All data modifications are input through the namelist block PERTIN. All cell variables are input by their used name and actual cell location, as displayed by the input editor. For example, AWET(15) is the wetted area in the compression zone in the sample problem. In addition to all the previously mentioned input names related to common blocks IGEN, FLTGEN, INCELL, FLCELL, FADD, and IADD, six additional variables have been added:

#### NMODS

The number of cases in this perturbation group. This allows the variation of frequency, combustion temperature, and stroke ratio to be input easily. It allows the user to run a 24-case engine map as four pressure runs with six frequency changes instead of 24 pressure-frequency combinations.

GPU-3: In the first group it is set to 6 for the six speed settings. In the next three groups, it is set to 1 because neither frequency nor stroke ratio is to be varied.

#### ITWLCH; Two Options:

0 - no modification of combustion temperature

1 - modification of combustion temperature with case

GPU-3: In the first group it is set to 1 and values for TWLHI are input.

#### DFREQ

The incremental change in frequency in a perturbation run (cycles/sec).

GPU-3: It is set to 8.33; therefore the frequency varies from the initial 16.67 to 58.32 Hz in six intervals. In the second perturbation group, it is set to 0.0 as NMODS was set to 1. Note that the base frequency was also input in the second group, the default value is the initial value of 16.67 Hz.



DSTRK

The incremental change in stroke ratio in a perturbation run. In many free piston designs, the frequency is fixed and the displacer to power-piston stroke ratio is varied to change the power. This is not a percentage change, but rather an absolute change in the ratio.

GPU-3 not used

TWLHI

The combustion temperature for each case. Only input if ITWLCH is greater than 0.

GPU-3 Set to outer-wall temperatures given in test results (see Ref. [46]).

A.5.2 Interactive Perturbations

To help the designer perfect his device, the code allows an interactive session. The cases run in this manner will still edit the results as discussed in Sec. 4.6 for the system printer, logical unit 6. In addition, selected variables will be displayed on logical unit 11. We normally assign units 10 (interactive input) and 11 to the terminal. The output is determined in subroutine OUT1 and currently displays:

- Engine Speed
- Total Heat In
- Total Heat Out
- Total Heat Recovered
- Engine Efficiency
- Cooler Gas Temperature
- Heater Gas Temperature

A typical session is shown in Table A-3; this session followed the first seven cases shown in Table A-1 by changing the value of ICHNG to 3 in case 7.

A.6 SAMPLE INPUT DECK

A copy of the sample problem input is shown in Table A-1. The input was prepared from worksheets similar to those shown in Table A-2.

The input is for the GPU-3 engine and corresponds to the hydrogen cases in Table VII. In the sample problem the code predicts power, efficiency, etc. for six speed settings at 2.74 MPa. Case 7 is a duplicate of the 3500 rpm speed setting with some internal prints turned on. Case 8 is a duplicate of Case 7 with the total gas mass fixed instead of the more common mean pressure being held constant. The values for wall and gas temperatures are input to reduce the number of iterations. The final case is a duplicate of Case 8 with added final prints turned on.



TABLE A-1. Sample Problem Input for GPU-3 Example (Contd.)

AA=1.88E-4,	0.0,	1.322E-4,	0.,	9.35E-5
2.,	3*0,	.697,	0.,	.468,
0.,	634.,	6.68E-6,	2.99E-6,	0.,
.0226,	&END			
*				
REGENERATOR TO COOLER TUBES				
&CELL	II=0,	3,	12,	0,
	15,	312,	0,	1,
AA=9.16E-7,	0.0,	1.070E-6,	1.80E-5,	3.08E-3
1.0,	7*0.,	339.,	2.013E-8,	5.67E-9,
2.55E-4,	.0053,	&END		
*				
COOLER				
&CELL	II=0,	1,	12,	0,
	10,	312,	0,	1,
AA=9.16E-7,	0.,	1.070E-6,	1.20E-4,	1.08E-3,
1.0,	3000.,	6*0.,	339.,	3.241E-8,
3.80E-8,	2.55E-4,	.0355,	&END	
*				
COOLER TO CONNECTING DUCT TUBES				
&CELL	II=0,	3,	12,	0,
	15,	312,	0,	1,
AA=9.16E-7,	0.0,	1.07E-6,	1.80E-5,	1.08E-3,
1.0,	7*0.,	339.,	4.838E-9,	5.67E-9,
2.55E-4,	.0053,	&END		
*				
CONNECTING DUCTS				
&CELL	II=0,	3,	12,	0,
	15,	8,	0,	1,
AA=2.80E-5,	0.0,	3.8E-5,	0.0,	5.97E-3,
1.0	7*0.,	339.,	1.281E-6,	1.20E-6,
0.,	3.18E-2,	&END		
*				
COMPRESSION SPACE				
&CELL	II=0,	1,	12,	0,
	20,	1,	0,	1,
AA=3.77E-3,	0.0,	3.8E-5,	1.52E-2,	6.04E-2,
1.0,	7*0.,	339.,	0.0,	3.54E-5,
0.,	3.18E-2,	&END		
*				
DISPLACER DOME				
&ADDED	JJ=2,	1,	12,	10,
	0,	2,		
BB=2*0.,	890.,	1.66E-4,	.04359,	.06642,
.00159,	0.3,	4*0,	.04359,	&END
*				
POWER PISTON BUFFER SPACE				
&ADDED	JJ=2*1,	12,	20,	2,
	0,			
BB=3.23E+6,	0.,	315.,	5.21E-4,	0.,
.0701,	.00381,	2*0.,	.15,	.002,

TABLE A-1. Sample Problem Input for GPU-3 Example (Contd.)

```

&END
*
SINGLE PRESSURE MAP RUN CHANGING TCMBST....CASES 1-6
&PERTIN      DFREQ=8.33,      NMODS=6,      ITWLCH=1,      TWLHI=890.,
              899.0,      909.0,      918.0,      927.0,      937.0,
              4*0.0,      &END
*
LAST RPM WITH ADDED CYCLE PRINTS....CASE 7
&PERTIN      DFREQ=0.0,      NMODS=1,      ITWLCH=0,      TCMBST=937.0,
              FREQ=58.3, IPRT1=2,      ICHNG=2,      &END
*
      NOTE THAT ICHNG IS A 2 TO REINITIALIZE CASES 8 AND 9
*
SAME CASE WITH THE MASS FIXED AND PMEAN VARIABLE....CASE 8
      MASS AND TEMPERATURE VALUES ARE FROM CASE 7 FOR THIS EXAMPLE
&PERTIN      IPRT1=2,      IMASS=1,      TMASS=3.263E-4, PGAS(1)=15*0.0,
TGAS(1)=5*887.77,5*578.45,5*351.28,
TWALL(1)=887.77,4*932.61 5*627.96,4*323.30,351.28,
&END
*
SAME CASE WITH ADDED FINAL PRINTS....CASE 9
&PERTIN      IPRT1=4,      ICHNG=0,      &END
*
      NOTE THAT ICHNG IS 0, FINAL CASE IS CASE 9

```





TABLE A-3. Sample Interactive Session

RUN TERMINAL

FI 6 DISK OUTPUT DATA  
 FI 5 DISK TERMINAL DATA  
 FI 8 DISK PLOT DATA  
 FI 9 DISK DUMMY DATA  
 FI 10 TERMINAL  
 FI 11 TERMINAL  
 LOAD SEAM RIOS  
 START  
 EXECUTION BEGINS...

CASE NUMBER 1

RPM	QIN	POWER	QOUT	EFFIC	TGAS	KOL	TGAS	HOT
1000.2	6745.8	2760.2	-3985.1	0.409	327.297		843.071	

CASE NUMBER 2

RPM	QIN	POWER	QOUT	EFFIC	TGAS	KOL	TGAS	HOT
1500.0	9404.8	3863.4	-5541.1	0.411	340.073		848.927	

CASE NUMBER 3

RPM	QIN	POWER	QOUT	EFFIC	TGAS	KOL	TGAS	HOT
1999.8	11955.5	4769.0	-7186.5	0.399	353.219		856.177	

CASE NUMBER 4

RPM	QIN	POWER	QOUT	EFFIC	TGAS	KOL	TGAS	HOT
2499.6	14371.5	5445.9	-8925.6	0.379	366.870		862.895	

CASE NUMBER 5

RPM	QIN	POWER	QOUT	EFFIC	TGAS	KOL	TGAS	HOT
2999.4	16643.7	5889.8	-10753.9	0.354	381.061		870.017	

CASE NUMBER 6

RPM	QIN	POWER	QOUT	EFFIC	TGAS	KOL	TGAS	HOT
3499.2	18774.5	6100.9	-12673.7	0.325	395.840		878.457	

NEXT DATA CHANGE FOR INTERACTIVE RUNNING?

AWET (12)=2.4E-4

MORE INPUT? Y=YES N=NO

N

CASE NUMBER 7

RPM	QIN	POWER	QOUT	EFFIC	TGAS	KOL	TGAS	HOT
1000.2	6855.6	2877.4	-3978.2	0.420	316.189		842.589	

CASE NUMBER 8

RPM	QIN	POWER	QOUT	EFFIC	TGAS	KOL	TGAS	HOT
1500.0	9584.7	4055.2	-5529.2	0.423	327.486		848.312	

TABLE A-3. Sample Interactive Session (Contd.)

CASE NUMBER 9							
RPM	QIN	POWER	QOUT	EFFIC	TGAS KOL	TGAS HOT	
1999.8	12210.2	5040.0	-7169.9	0.413	339.265	855.444	

CASE NUMBER 10							
RPM	QIN	POWER	QOUT	EFFIC	TGAS KOL	TGAS HOT	
2499.6	14698.1	5801.8	-8896.1	0.395	351.583	862.082	

CASE NUMBER 11							
RPM	QIN	POWER	QOUT	EFFIC	TGAS KOL	TGAS HOT	
2999.4	17049.3	6331.2	-10718.2	0.371	364.467	869.105	

CASE NUMBER 12							
RPM	QIN	POWER	QOUT	EFFIC	TGAS KOL	TGAS HOT	
3499.2	19263.4	6627.2	-12636.2	0.344	377.948	877.440	

NEXT DATA CHANGE FOR INTERACTIVE RUNNING?

ICHNG=0

MORE INPUT? Y=YES N=NO

Y

NEXT DATA CHANGE FOR INTERACTIVE RUNNING?

NMODS=0

MORE INPUT? Y=YES N=NO

N

CASE NUMBER 13							
RPM	QIN	POWER	QOUT	EFFIC	TGAS KOL	TGAS HOT	
1000.2	6855.6	2877.4	-3978.2	0.420	316.189	842.589	

PRINT OUTPUT DATA (CC

PRINT TERMINAL DATA

R: T=21.81/23.08 16:38:21



## A.7 SAMPLE OUTPUT

Appendix B shows the output printout that was generated on unit 6 by running the code with the GPU-3 input deck of Sec. A-6. To avoid further reductions in size we have truncated the output beyond column 90. This should only effect the pages with added prints and little information should be lost. The total execution time for the nine cases was less than 20 sec on an IBM 3033. Less than 200K bytes (50K words) of core storage were required for the object code and common blocks.

## A.8 GRAPHICS CAPABILITY

As mentioned in Sec. 2.5, the Output routine OUT1 writes certain graphics information on output device 8. The nature of the information written depends on the value of IGRAPH. Since graphics systems are installation-dependent, the data are written in "raw" form, and are therefore up to the user to read the data and use them in a way compatible with their own graphics system. Currently, at ANL, a Fortran program GRAF (Appendix D) is being used for the case-to-case results. The program was used to generate the three map displays discussed in Sec. 4. In addition to these displays the code generates two power-versus-RPM curves (Figs. A-7 and A-8). The first graph displays separation of cooler heat flow, power out and losses versus RPM. The second graph displays the major loss mechanisms in a Stirling engine versus RPM. The code uses the SEAM1 graphics output, read in through logical unit 10, and generates a file on logical unit 11 that the proprietary package "TELLAGRAF" uses to generate displays. A listing of the logical unit 11 file is included as Appendix E.

This section describes the graphics information that is written on the output file by OUT1. The appropriate Format statements can be found in the code listing for OUT1. Also, definitions of the variables used below appear in Appendix C.

### A.8.1 IGRAPH = 1

If IGRAPH = 1, the following information is written on unit 8 after the final cycle.

- NTITLE
- NCASE, engine speed, mean pressure (PMEAN), combustion temperature (TCMBST), gas mass (TMASS), Schmidt Analysis ratio (SCHDEL) and phase angle (THETA), and compression zone minimum crank angle (PSIMIN)
- (GRAFIC(L, I), I = 1, 75), L = 1, 9 for I = 1, 2, ..., 73

GRAFIC(1,I) = the Ith angle 5°, 10°, ..., 360°

GRAFIC(2,I) = expansion live volume at angle I

GRAFIC(3,I) = pressure at angle I

GRAFIC(4,I) = compression live volume at angle I

GRAFIC(5,I) = compression live mass at angle I

GPU-3 HELIUM 927K/339K  
POWER FLOWS VS SPEED  
PRESSURE= 6.92 MPA

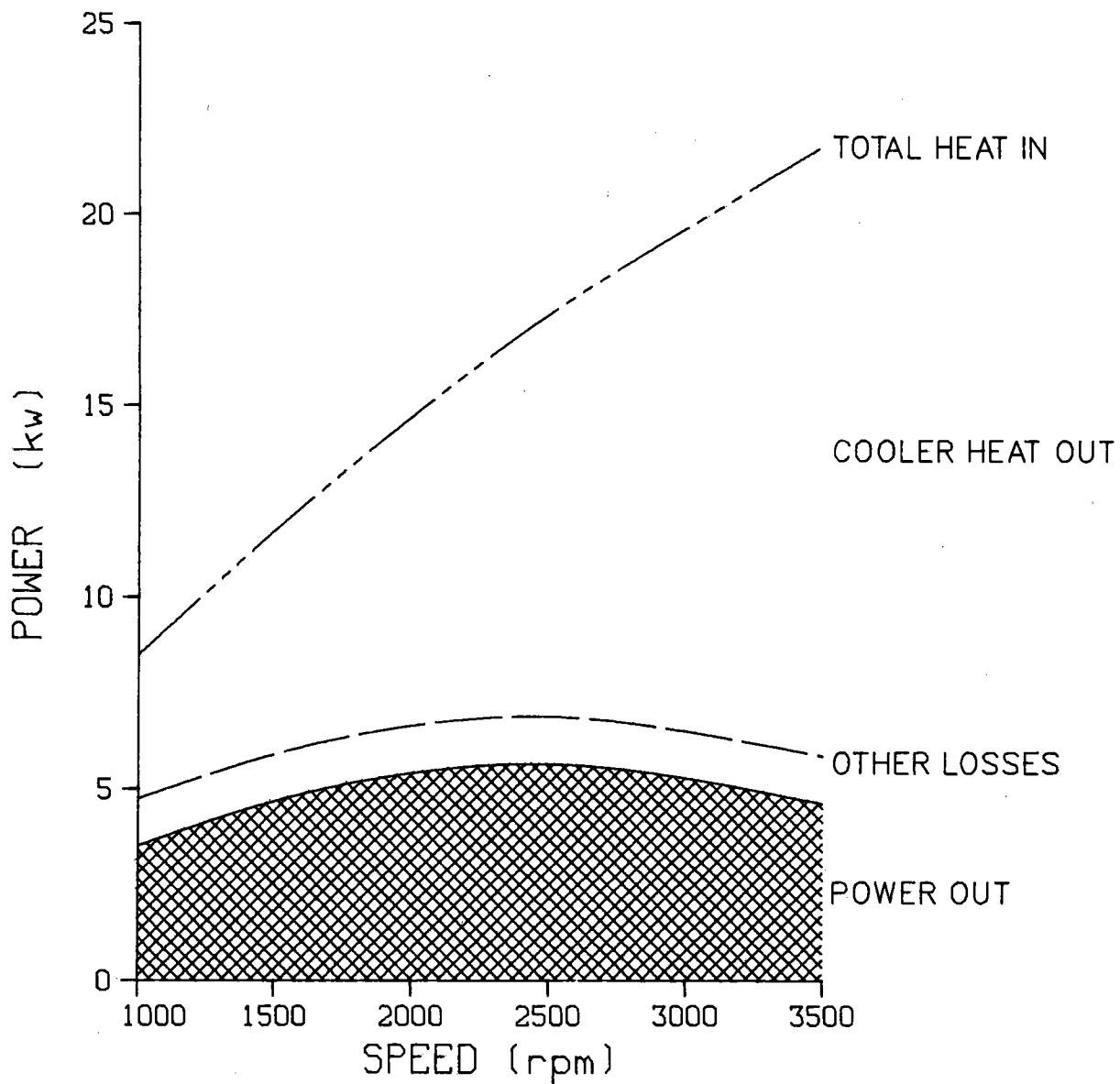


Fig. A-7. GPU-3 Power Flow Comparisons

GPU-3 HELIUM 927K/339K  
POWER LOSSES VS SPEED  
PRESSURE= 6.92 MPA

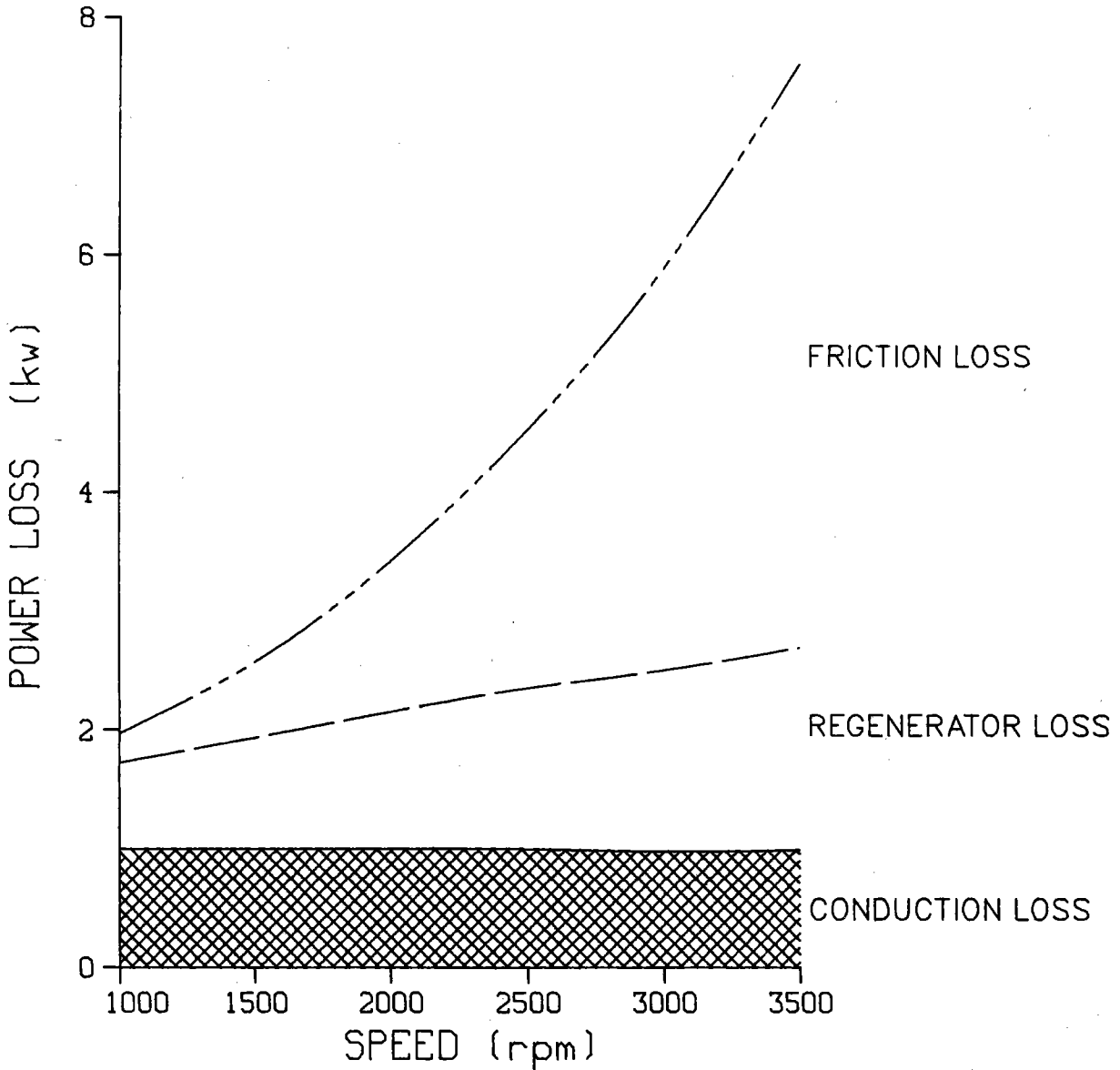


Fig. A-8. GPU-3 Power Loss Comparison

GRAFIC(6,I) = expansion live mass at angle I  
 GRAFIC(7,I) = crankshaft torque at angle I  
 GRAFIC(8,I) = cooler gas temperature at angle I  
 GRAFIC(9,I) = heater gas temperature at angle I

and for I = 74,75

GRAFIC(L,I) is undefined.

#### A.8.2 IGRAPH = 2

If IGRAPH = 2, the following information is written on unit 8. The purpose is to provide graphs that show the case-to-case variation of the SEAM1 code predictions.

Written once for each NPRT2 case:

- NTITLE
- IMASS, engine speed (rpm), PMEAN, TCMBST, TWATER, gas mass (kg) written for each case
- NCASE
- Average pressure (MPa)
- Engine speed (rpm)
- Gas mass (kg)
- Energy flow into heater (kW)
- Net power (kW)
- Efficiency
- Heater gas temp. (K)
- Cooler gas temp. (K)
- Cooler wall to gas heat flow (negative) (kW)
- Conduction losses to cooling water (kW)
- Static conduction losses (kW)
- Dynamic conduction losses (shuttle + gap) (kW)
- Fluid friction losses (kW)
- Regenerator reheat loss (kW)
- Gas leakage loss (= zero for SEAM1) (kW)
- Total heat flow out (kW)

#### A.9 OBTAINING THE CODE FROM NESC

A copy of the ANL Stirling Engine Analysis System Fortran code can be obtained on tape from the National Energy Software Center (NESC) located at

ANL. A nominal service fee may be charged by NESC. This report is part of the user documentation sent by NESC with the code. The address and phone number of NESC are:

National Energy Software Center, Bldg. 221  
Argonne National Laboratory  
9700 South Cass Avenue  
Argonne, Illinois 60439

Telephone: (312) 972-7250

APPENDIX B  
GPU-3 SAMPLE PROBLEM OUTPUT

GPU-3 HYDROGEN 927K/339K STIRLING ENGINE DATA: 1 (UPDATED JAN 83)

THIS RUN STARTED AT TIME 11.33.22

EDIT COMMON IGEN FOR RUN NUMBER 1

0-NO CHANGES TO CELL INFORMATION	1-CHANGES TO BE MADE	1				
1-IN-LINE	2-DOUBLE ACTING	3-DISPLACER	3			
0-CONNECTING ROD	1-RHOMBIC DRIVE	2-DYNA. ANALYSIS(NA)	1			
WORKING FLUID TO BE USED			1			
1-H2	2-HE	3-N2	4-AIR	5-CO2	6-CH4	
0=PMEAN IS CONSTANT,	1=TMASS IS CONSTANT		0			
0-FRICTION ONLY MOMENTUM EQUATION			0			
1-FULL MOMENTUM EQUATION						
0-STANDARD PRINT	>0-CODE DEPENDENT ADDITIONAL PRINTS		0			
0 NO GRAPHICS,	1=SAVE CYCLE FILE,	2=SAVE CASE FILE	1			
NUMBER OF ADDED COMPONENTS (LETTERED VOLUMES IN DESIGN)			2			
0-RIOS	1-UREILI	2-TEW	0			
NUMBER OF COMPONENTS (NUMBERED VOLUMES IN DESIGN)			11			
NUMBER OF CYLINDERS IN ENGINE			1			
COOLER GAS HEAT FLOW OPTION			1			
NUMBER OF STEPS/PRINT OF ZONE INFORMATION			720			
NUMBER OF CASES/PRINT OF ENERGY FLOW INFORMATION			6			
NUMBER OF FULL REVOLUTIONS TO BE CALCULATED(CYCLES)			12			
NUMBER OF TIME STEPS IN 1-REVOLUTION			360			

EDIT COMMON FLTGEN

COMPRESSION PISTON CRANK RADIUS (M)	0.01380
COMPRESSION PISTON CONNECTING ROD LENGTH (M)	0.04600
COMPRESSION ZONE DEAD VOLUME (CU M)	1.093E-05
COMPRESSION PISTON CRANK RADIUS ECCENTRICITY (M)	0.02080
COMPRESSION PISTON-CYLINDER WALL GAP (M)	0.00015
COMPRESSION PISTON ROD DIAMETER (M)	0.02220
EXPANSION PISTON CRANK RADIUS(M)	0.01380
EXPANSION PISTON CONNECTING ROD LENGTH (M)	0.04600
EXPANSION ZONE DEAD VOLUME (CU M)	1.250E-05
EXPANSION PISTON CRANK RADIUS ECCENTRICITY (M)	0.02080
EXPANSION PISTON-CYLINDER WALL GAP (M)	0.00025
EXPANSION PISTON ROD DIAMETER (M)	0.00952
FREQUENCY OF SYSTEM (CYCLES/SEC)	16.67
THERMAL HYSTERISIS FACTOR	0.0
VOLUME PHASE ANGLE (DEGREES)	110.35
PISTON PHASE ANGLE (DEGREES)	0.0
AVERAGE PRESSURE OF SYSTEM IN CYCLE (PA)	2.740E+06
CRANK ANGLE AT TIME = 0.0 (DEGREES)	0.0
DISTANCE BETWEEN TOP OF REG. AND BOTTOM OF CYL. DOME	0.02860
EXTERNAL HEATER TEMPERATURE	890.00
EXTERNAL COOLER TEMPERATURE	287.00
TOTAL MASS IN CONTIGUOUS SYSTEM (KG)	3.886E-04
EXTERNAL ENVIRONMENT TEMPERATURE	300.00
CODE DEPENDENT OPTION ZOPT1	0.50
TIME STEP (SEC)	1.666E-04

## GPU-3 HYDROGEN 927K/339K STIRLING ENGINE DATA: 1 (UPDATED JAN 83)

## EDIT MOST OF COMMON JMISC

FIRST FIXED VOLUME CELL	2
FIRST CELL IN HEATER	3
TYPICAL HEATER VALUES COME FROM CELL	3
LAST CELL IN HEATER	4
FIRST CELL IN REGENERATOR	6
TYPICAL REGENERATOR VALUES COME FROM CELL	8
LAST CELL IN REGENERATOR	10
FIRST CELL IN COOLER	12
TYPICAL COOLER VALUES COME FROM CELL	12
LAST CELL IN COOLER	12
LAST FIXED VOLUME CELL	14
CELL NUMBER OF COMPRESSION ZONE	15
LAST CONTIGUOUS CELL IN SYSTEM	15

## EDIT COMMON VARVOL

CURRENT CRANK ANGLE (RAD)	0.0
COMPRESSION PISTON AREA (SQ M)	3.770E-03
COMPRESSION CYLINDER BORE (M)	0.06993
COMPRESSION ZONE PISTON OVERLAP (M)	0.02120
COMPRESSION PISTON MAXIMUM STROKE POSITION (M)	0.05607
COMPRESSION PISTON MINIMUM STROKE POSITION (M)	0.02458
COMPRESSION PISTON CURRENT STROKE POSITION (M)	0.04546
COMPRESSION PISTON TOTAL STROKE (CMPMAX-CMPMIN) (M)	0.03149
COMPRESSION ZONE MAXIMUM DISPLACEMENT (CU M)	1.142E-04
CRANK ANGLE BETWEEN TDC OF EXP. & COM. PISTONS(RAD)	0.0
VOLUME PHASE ANGLE (RADIAN)	1.92605
ABSOLUTE ANGLE AT MINIMUM VOLUME (RAD)	1.57080
ABSOLUTE EXPANSION CRANK ANGLE AT STARTD=0. (RAD)	1.57080
SCHMIDT ANALYSIS PRESSURE RATIO	3.08777
SCHMIDT ANALYSIS PRESSURE PHASE ANGLE (RAD)	0.96302
INCREMENTAL CRANK ANGLE (RAD/SEC)	0.01745
EXPANSION PISTON AREA (SQ M)	3.860E-03
EXPANSION CYLINDER BORE (M)	0.07010
EXPANSION MAXIMUM STROKE POSITION (M)	0.05607
EXPANSION MINIMUM STROKE POSITION (M)	0.02458
EXPANSION PISTON CURRENT POSITION (M)	0.04546
EXPANSION PISTON TOTAL STROKE (M)	0.03149
EXPANSION ZONE MAXIMUM DISPLACEMENT (CU M)	1.215E-04
ACTIVE VOLUMES: (CU M)	
1.....	9.311E-05
2.....	0.0
3.....	1.093E-05
4.....	1.487E-06
5.....	7.065E-05

## EDIT COMMON GASPRP

GAS SPECIFIC HEAT AT CONSTANT PRESURE (J/KG-K)	1.456E+04
GAS SPECIFIC HEAT AT CONSTANT VOLUME (J/KG-K)	1.043E+04
GAS SPECIFIC HEAT RATIO	1.39529
GAS CONSTANT (J/KG-K)	4124.6





## GPU-3 HYDROGEN 927K/339K STIRLING ENGINE DATA: 1 (UPDATED JAN 83)

CELL	EDIT HEAT EXCHANGER VALUES PER NIHX					- COMMONS INCELL AND FCELL				
	* 11 *	* 12 *	* 13 *	* 14 *	* 15 *	*	*	*	*	*
MHTRF =	0	0	0	0	0					
MQFLOW =	3	1	3	3	1					
MTLWAL =	12	12	12	12	12					
MTLWIR =	0	0	0	0	0					
MTYPE =	15	10	15	15	20					
NIHX =	312	312	312	8	1					
NOPT1 =	0	0	0	0	0					
AFLOW =	9.160E-07	9.160E-07	9.160E-07	2.800E-05	3.770E-03					
ASPECT =	0.0	0.0	0.0	0.0	0.0					
AXWALL =	1.070E-06	1.070E-06	1.070E-06	3.800E-05	3.800E-05					
AMET =	1.800E-05	1.200E-04	1.800E-05	5.966E-04	1.520E-02					
DH =	1.080E-03	1.080E-03	1.080E-03	5.970E-03	6.040E-02					
FRICML =	1.00	1.00	1.00	1.00	1.00					
HCEXT =	0.0	3000.00	0.0	0.0	0.0					
ORIFCE =	0.0	0.0	0.0	0.0	0.0					
PGAS =	4.056E+06	4.056E+06	4.056E+06	4.056E+06	4.056E+06					
POROS =	0.0	0.0	0.0	0.0	0.0					
QFLOW =	0.0	0.0	0.0	0.0	0.0					
SIGMA =	0.0	0.0	0.0	0.0	0.0					
TGAS =	339.00	339.00	339.00	339.00	339.00					
TWALL =	339.00	339.00	339.00	339.00	339.00					
VOL =	2.013E-08	3.241E-08	4.838E-09	1.281E-06	1.093E-05					
VOLWL =	5.670E-09	3.800E-08	5.670E-09	1.200E-06	3.540E-05					
WALLTH =	0.00026	0.00026	0.00026	0.00160	0.00020					
XLNGTH =	0.00530	0.03550	0.00530	0.03180	0.03180					

VOLUME	EDIT ADDED VOLUME VALUES- COMMONS IADD AND FADD		
	* 1 *	* 2 *	*
IACOND =	2	1	
IALEAK =	1	1	
IAMTL =	12	12	
IATYPE =	10	20	
NRINGS =	0	2	
NSHELD =	2		
ADPGAS =	2.740E+06	3.230E+06	
ADRADA =	0.0		
ADTGAS =	890.00	315.00	
ADVOL =	1.660E-04	5.210E-04	
ADWALX =	0.04359		
ADWLDI =	0.06642	0.07010	
ADWLTH =	0.00159	0.00381	
EMIS =	0.30000		
RINGCL =	0.0	0.0	
RINGFR =	0.0	0.15000	
RINGHT =	0.0	0.00200	
RINGLK =	0.0	0.0	
SLNGTH =	0.04359		

## GPU-3 HYDROGEN 927K/339K STIRLING ENGINE DATA: 1 (UPDATED JAN 83)

## RIOS/SEAM1 ANALYSIS CONSOLIDATED INPUT INFORMATION

ZONE	EXPANSION 1	HEATER 2	REGENERATOR 3	COOLER 4	COMPRESSION 5
VOLUME (CU M)	1.2153E-04	8.8200E-05	5.3440E-05	2.8150E-05	1.1425E-04
FLOW AREA (SQ M)	3.8600E-03	2.8640E-04	1.5040E-03	2.8579E-04	3.7700E-03
WETTED AREA (SQ M)		5.8960E-02	1.4541E+00	3.7440E-02	
HYD DIA (M)	0.070100	0.003020	0.000093	0.001080	0.060400
TOT LNTH (M)		0.246300	0.022600	0.046100	
HT EXCH LNTH (M)		0.155400		0.035500	
TEMPERATURE (K)	927.00	927.00	584.52	339.00	339.00
REGENERATOR WALL DIAMETER (M)		0.02262	AVG HT TRANSF REYN EXPONENT		0.5503
MINIMUM TOTAL VOLUME (CU M)	2.3248E-04		MAXIMUM TOTAL VOLUME (CU M)		3.5261E-04
ANGLE AT MIN TOTAL VOLUME (DEG)	290.4998		ANGLE AT MAX TOTAL VOLUME (DEG)		128.5000
AVERAGE PRESSURE (MPA)	2.7400		TOTAL GAS MASS (KGS)		3.9565E-04
NORMALIZED VALUES FOR XMASE, TEMP RATIO, RVT =			0.00002478	2.7345	2.5705

## GPU-3 HYDROGEN 927K/339K STIRLING ENGINE DATA: 1 (UPDATED JAN 83)

ZONE OUTPUT FOR CASE 1 CYCLE NUMBER 1 FLUX ERROR= -534.07

ZONE NUMBER		1	2	3	4	5
TEMP GAS MAX	K	950.30	819.91	584.52	323.17	390.29
TEMP GAS AVG	K	819.91	819.91	584.52	323.17	323.17
WALL-GAS DEL T AVG	K	0.0	68.89	0.0	-28.76	0.0
WALL-GAS DEL T MAX	K	-130.38	68.89	0.0	-28.76	-67.11
WALL-GAS CHNG Q	W	-604.01	2591.75	-176.27	-1154.22	69.94
AVG MASS FLOW	KG/S	0.003343	0.003343	0.004020	0.004833	0.004833
MAX MASS FLOW	KG/S	0.003343	0.003343	0.004020	0.004833	0.004833
REYNOLDS NUMBER		77.34	1796.17	17.56	1878.62	25.53
DEL-P FRICTION	MPA	0.0	0.000842	0.022585	0.000616	0.0
NUSSELT NUMBER		0.0	4.78	3.77	5.84	0.0

ZONE OUTPUT FOR CASE 1 CYCLE NUMBER 3 FLUX ERROR= -6.02

ZONE NUMBER		1	2	3	4	5
TEMP GAS MAX	K	815.26	803.33	531.47	332.73	382.02
TEMP GAS AVG	K	803.33	803.33	531.47	332.73	332.73
WALL-GAS DEL T AVG	K	0.0	85.15	0.0	-36.26	0.0
WALL-GAS DEL T MAX	K	-11.93	85.15	0.0	-36.26	-49.29
WALL-GAS CHNG Q	W	-570.03	3184.77	-189.07	-1472.61	66.01
AVG MASS FLOW	KG/S	0.003744	0.003744	0.004384	0.005133	0.005133
MAX MASS FLOW	KG/S	0.003744	0.003744	0.004384	0.005133	0.005133
REYNOLDS NUMBER		96.30	2236.63	20.47	2020.59	27.46
DEL-P FRICTION	MPA	0.0	0.000842	0.020842	0.000665	0.0
NUSSELT NUMBER		0.0	5.34	4.11	5.98	0.0

ZONE OUTPUT FOR CASE 1 CYCLE NUMBER 5 FLUX ERROR= -0.58

ZONE NUMBER		1	2	3	4	5
TEMP GAS MAX	K	820.16	802.04	533.26	332.78	382.00
TEMP GAS AVG	K	802.04	802.04	533.26	332.78	332.78
WALL-GAS DEL T AVG	K	0.0	86.44	0.0	-36.31	0.0
WALL-GAS DEL T MAX	K	-18.12	86.44	0.0	-36.31	-49.22
WALL-GAS CHNG Q	W	-568.21	3199.26	-187.92	-1473.64	65.77
AVG MASS FLOW	KG/S	0.003729	0.003729	0.004371	0.005125	0.005125
MAX MASS FLOW	KG/S	0.003729	0.003729	0.004371	0.005125	0.005125
REYNOLDS NUMBER		95.50	2218.11	20.37	2017.58	27.42
DEL-P FRICTION	MPA	0.0	0.000841	0.020903	0.000663	0.0
NUSSELT NUMBER		0.0	5.26	4.10	5.98	0.0

ZONE OUTPUT FOR CASE 1 CYCLE NUMBER 6 FLUX ERROR= 0.15

ZONE NUMBER		1	2	3	4	5
TEMP GAS MAX	K	820.62	801.92	533.44	332.77	382.01
TEMP GAS AVG	K	801.92	801.92	533.44	332.77	332.77
WALL-GAS DEL T AVG	K	0.0	86.55	0.0	-36.30	0.0
WALL-GAS DEL T MAX	K	-18.70	86.55	0.0	-36.30	-49.24
WALL-GAS CHNG Q	W	-568.04	3200.09	-187.82	-1473.45	65.75
AVG MASS FLOW	KG/S	0.003727	0.003727	0.004370	0.005125	0.005125
MAX MASS FLOW	KG/S	0.003727	0.003727	0.004370	0.005125	0.005125
REYNOLDS NUMBER		95.42	2216.23	20.36	2017.27	27.41
DEL-P FRICTION	MPA	0.0	0.000840	0.020909	0.000663	0.0
NUSSELT NUMBER		0.0	5.25	4.09	5.98	0.0

## GPU-3 HYDROGEN 927K/339K STIRLING ENGINE DATA: 1 (UPDATED JAN 83)

ZONE OUTPUT FOR CASE 2 CYCLE NUMBER 1 FLUX ERROR= -41.69

ZONE NUMBER		1	2	3	4	5
TEMP GAS MAX	K	950.21	828.47	584.52	328.55	390.36
TEMP GAS AVG	K	828.47	828.47	584.52	328.55	328.55
WALL-GAS DEL T AVG	K	0.0	68.42	0.0	-28.54	0.0
WALL-GAS DEL T MAX	K	-121.74	68.42	0.0	-28.54	-61.81
WALL-GAS CHNG Q	W	-614.89	4600.64	-270.09	-2024.86	70.92
AVG MASS FLOW	KG/S	0.005014	0.005014	0.006029	0.007248	0.007248
MAX MASS FLOW	KG/S	0.005014	0.005014	0.006029	0.007248	0.007248
REYNOLDS NUMBER		115.99	2693.97	26.34	2817.30	38.28
DEL-P FRICTION	MPA	0.0	0.001773	0.035279	0.001261	0.0
NUSSELT NUMBER		0.0	8.54	4.72	10.32	0.0

ZONE OUTPUT FOR CASE 2 CYCLE NUMBER 3 FLUX ERROR= 1.59

ZONE NUMBER		1	2	3	4	5
TEMP GAS MAX	K	861.25	839.24	545.50	328.64	378.02
TEMP GAS AVG	K	839.24	839.24	545.50	328.64	328.64
WALL-GAS DEL T AVG	K	0.0	57.56	0.0	-27.55	0.0
WALL-GAS DEL T MAX	K	-22.02	57.56	0.0	-27.55	-49.39
WALL-GAS CHNG Q	W	-632.93	4657.40	-296.99	-2191.08	72.87
AVG MASS FLOW	KG/S	0.005421	0.005421	0.006435	0.007638	0.007638
MAX MASS FLOW	KG/S	0.005421	0.005421	0.006435	0.007638	0.007638
REYNOLDS NUMBER		134.27	3118.40	29.51	3030.73	41.18
DEL-P FRICTION	MPA	0.0	0.001694	0.033930	0.001162	0.0
NUSSELT NUMBER		0.0	11.08	5.02	11.80	0.0

ZONE OUTPUT FOR CASE 2 CYCLE NUMBER 5 FLUX ERROR= 0.02

ZONE NUMBER		1	2	3	4	5
TEMP GAS MAX	K	859.68	839.47	544.71	328.62	377.79
TEMP GAS AVG	K	839.47	839.47	544.71	328.62	328.62
WALL-GAS DEL T AVG	K	0.0	57.33	0.0	-27.53	0.0
WALL-GAS DEL T MAX	K	-20.21	57.33	0.0	-27.53	-49.17
WALL-GAS CHNG Q	W	-633.19	4657.77	-297.49	-2192.01	72.91
AVG MASS FLOW	KG/S	0.005430	0.005430	0.006442	0.007641	0.007641
MAX MASS FLOW	KG/S	0.005430	0.005430	0.006442	0.007641	0.007641
REYNOLDS NUMBER		134.68	3128.00	29.57	3033.66	41.22
DEL-P FRICTION	MPA	0.0	0.001697	0.033903	0.001161	0.0
NUSSELT NUMBER		0.0	11.15	5.03	11.82	0.0

ZONE OUTPUT FOR CASE 3 CYCLE NUMBER 1 FLUX ERROR= -26.22

ZONE NUMBER		1	2	3	4	5
TEMP GAS MAX	K	950.23	857.38	584.52	328.01	390.36
TEMP GAS AVG	K	857.38	857.38	584.52	328.01	328.01
WALL-GAS DEL T AVG	K	0.0	48.86	0.0	-23.06	0.0
WALL-GAS DEL T MAX	K	-92.85	48.86	0.0	-23.06	-62.36
WALL-GAS CHNG Q	W	-662.77	5992.73	-393.80	-2791.14	76.27
AVG MASS FLOW	KG/S	0.006684	0.006684	0.008037	0.009663	0.009663
MAX MASS FLOW	KG/S	0.006684	0.006684	0.008037	0.009663	0.009663
REYNOLDS NUMBER		154.64	3591.47	35.11	3755.97	51.04
DEL-P FRICTION	MPA	0.0	0.002854	0.049807	0.001794	0.0
NUSSELT NUMBER		0.0	15.57	5.53	17.60	0.0

## GPU-3 HYDROGEN 927K/339K STIRLING ENGINE DATA: 1 (UPDATED JAN 83)

ZONE OUTPUT FOR CASE 3 CYCLE NUMBER 3 FLUX ERROR= -1.46

ZONE NUMBER		1	2	3	4	5
TEMP GAS MAX	K	884.01	862.98	553.19	328.14	377.61
TEMP GAS AVG	K	862.98	862.98	553.19	328.14	328.14
WALL-GAS DEL T AVG	K	0.0	43.18	0.0	-22.13	0.0
WALL-GAS DEL T MAX	K	-21.04	43.18	0.0	-22.13	-49.47
WALL-GAS CHNG Q	W	-674.97	6063.20	-421.82	-2957.86	77.30
AVG MASS FLOW	KG/S	0.007100	0.007100	0.008473	0.010110	0.010110
MAX MASS FLOW	KG/S	0.007100	0.007100	0.008473	0.010110	0.010110
REYNOLDS NUMBER		172.74	4012.02	38.47	4016.54	54.58
DEL-P FRICTION	MPA	0.0	0.002989	0.048740	0.001859	0.0
NUSSELT NUMBER		0.0	18.86	5.81	19.86	0.0

ZONE OUTPUT FOR CASE 3 CYCLE NUMBER 4 FLUX ERROR= 0.24

ZONE NUMBER		1	2	3	4	5
TEMP GAS MAX	K	884.10	862.94	553.12	328.15	377.50
TEMP GAS AVG	K	862.94	862.94	553.12	328.15	328.15
WALL-GAS DEL T AVG	K	0.0	43.21	0.0	-22.13	0.0
WALL-GAS DEL T MAX	K	-21.16	43.21	0.0	-22.13	-49.35
WALL-GAS CHNG Q	W	-674.72	6068.71	-421.72	-2958.10	77.29
AVG MASS FLOW	KG/S	0.007101	0.007101	0.008474	0.010109	0.010109
MAX MASS FLOW	KG/S	0.007101	0.007101	0.008474	0.010109	0.010109
REYNOLDS NUMBER		172.76	4012.53	38.48	4017.24	54.59
DEL-P FRICTION	MPA	0.0	0.002991	0.048740	0.001857	0.0
NUSSELT NUMBER		0.0	18.86	5.81	19.86	0.0

ZONE OUTPUT FOR CASE 4 CYCLE NUMBER 1 FLUX ERROR= -5.08

ZONE NUMBER		1	2	3	4	5
TEMP GAS MAX	K	950.24	870.89	584.52	333.53	390.36
TEMP GAS AVG	K	870.89	870.89	584.52	333.53	333.53
WALL-GAS DEL T AVG	K	0.0	43.74	0.0	-23.32	0.0
WALL-GAS DEL T MAX	K	-79.35	43.74	0.0	-23.32	-56.83
WALL-GAS CHNG Q	W	-680.73	7331.89	-517.65	-3610.33	78.23
AVG MASS FLOW	KG/S	0.008354	0.008354	0.010046	0.012079	0.012079
MAX MASS FLOW	KG/S	0.008354	0.008354	0.010046	0.012079	0.012079
REYNOLDS NUMBER		193.28	4488.99	43.88	4694.65	63.79
DEL-P FRICTION	MPA	0.0	0.004348	0.066046	0.002657	0.0
NUSSELT NUMBER		0.0	21.29	6.25	22.51	0.0

ZONE OUTPUT FOR CASE 4 CYCLE NUMBER 3 FLUX ERROR= -2.10

ZONE NUMBER		1	2	3	4	5
TEMP GAS MAX	K	891.62	870.73	561.04	335.42	385.69
TEMP GAS AVG	K	870.73	870.73	561.04	335.42	335.42
WALL-GAS DEL T AVG	K	0.0	43.87	0.0	-24.02	0.0
WALL-GAS DEL T MAX	K	-20.89	43.87	0.0	-24.02	-50.26
WALL-GAS CHNG Q	W	-681.71	7303.18	-543.17	-3796.10	78.00
AVG MASS FLOW	KG/S	0.008766	0.008766	0.010434	0.012416	0.012416
MAX MASS FLOW	KG/S	0.008766	0.008766	0.010434	0.012416	0.012416
REYNOLDS NUMBER		211.97	4923.20	46.91	4861.40	66.06
DEL-P FRICTION	MPA	0.0	0.004390	0.064999	0.002763	0.0
NUSSELT NUMBER		0.0	22.20	6.48	23.14	0.0

## GPU-3 HYDROGEN 927K/339K STIRLING ENGINE DATA: 1 (UPDATED JAN 83)

ZONE OUTPUT FOR CASE 4 CYCLE NUMBER 4 FLUX ERROR= 0.23

ZONE NUMBER		1	2	3	4	5
TEMP GAS MAX	K	891.87	870.70	561.16	335.46	385.75
TEMP GAS AVG	K	870.70	870.70	561.16	335.46	335.46
WALL-GAS DEL T AVG	K	0.0	43.90	0.0	-24.04	0.0
WALL-GAS DEL T MAX	K	-21.17	43.90	0.0	-24.04	-50.29
WALL-GAS CHNG Q	W	-681.46	7309.28	-542.91	-3798.31	77.99
AVG MASS FLOW	KG/S	0.008764	0.008764	0.010431	0.012412	0.012412
MAX MASS FLOW	KG/S	0.008764	0.008764	0.010431	0.012412	0.012412
REYNOLDS NUMBER		211.90	4921.43	46.89	4859.47	66.03
DEL-P FRICTION	MPA	0.0	0.004390	0.065001	0.002761	0.0
NUSSELT NUMBER		0.0	22.20	6.48	23.14	0.0

ZONE OUTPUT FOR CASE 5 CYCLE NUMBER 1 FLUX ERROR= -3.24

ZONE NUMBER		1	2	3	4	5
TEMP GAS MAX	K	950.24	878.58	584.52	340.67	390.37
TEMP GAS AVG	K	878.58	878.58	584.52	340.67	340.67
WALL-GAS DEL T AVG	K	0.0	44.47	0.0	-24.95	0.0
WALL-GAS DEL T MAX	K	-71.66	44.47	0.0	-24.95	-49.69
WALL-GAS CHNG Q	W	-685.65	8585.25	-642.12	-4468.59	78.94
AVG MASS FLOW	KG/S	0.010025	0.010025	0.012055	0.014494	0.014494
MAX MASS FLOW	KG/S	0.010025	0.010025	0.012055	0.014494	0.014494
REYNOLDS NUMBER		231.93	5386.60	52.66	5633.35	76.55
DEL-P FRICTION	MPA	0.0	0.006015	0.083911	0.003698	0.0
NUSSELT NUMBER		0.0	24.52	6.91	26.05	0.0

ZONE OUTPUT FOR CASE 5 CYCLE NUMBER 3 FLUX ERROR= -1.70

ZONE NUMBER		1	2	3	4	5
TEMP GAS MAX	K	899.65	878.68	569.36	343.12	394.26
TEMP GAS AVG	K	878.68	878.68	569.36	343.12	343.12
WALL-GAS DEL T AVG	K	0.0	44.41	0.0	-25.96	0.0
WALL-GAS DEL T MAX	K	-20.97	44.41	0.0	-25.96	-51.14
WALL-GAS CHNG Q	W	-687.89	8482.44	-667.68	-4691.96	78.70
AVG MASS FLOW	KG/S	0.010383	0.010383	0.012327	0.014632	0.014632
MAX MASS FLOW	KG/S	0.010383	0.010383	0.012327	0.014632	0.014632
REYNOLDS NUMBER		249.49	5794.50	54.85	5642.10	76.67
DEL-P FRICTION	MPA	0.0	0.005995	0.082802	0.003817	0.0
NUSSELT NUMBER		0.0	25.30	7.06	26.09	0.0

ZONE OUTPUT FOR CASE 5 CYCLE NUMBER 4 FLUX ERROR= 0.23

ZONE NUMBER		1	2	3	4	5
TEMP GAS MAX	K	899.82	878.65	569.54	343.17	394.47
TEMP GAS AVG	K	878.65	878.65	569.54	343.17	343.17
WALL-GAS DEL T AVG	K	0.0	44.44	0.0	-25.99	0.0
WALL-GAS DEL T MAX	K	-21.18	44.44	0.0	-25.99	-51.30
WALL-GAS CHNG Q	W	-687.65	8487.48	-667.37	-4694.95	78.69
AVG MASS FLOW	KG/S	0.010381	0.010381	0.012322	0.014623	0.014623
MAX MASS FLOW	KG/S	0.010381	0.010381	0.012322	0.014623	0.014623
REYNOLDS NUMBER		249.40	5792.51	54.82	5636.94	76.60
DEL-P FRICTION	MPA	0.0	0.005995	0.082799	0.003815	0.0
NUSSELT NUMBER		0.0	25.29	7.06	26.07	0.0

## GPU-3 HYDROGEN 927K/339K STIRLING ENGINE DATA: 1 (UPDATED JAN 83)

ZONE OUTPUT FOR CASE 6 CYCLE NUMBER 1 FLUX ERROR= -5.71

ZONE NUMBER		1	2	3	4	5
TEMP GAS MAX	K	950.23	887.46	584.52	348.15	390.36
TEMP GAS AVG	K	887.46	887.46	584.52	348.15	348.15
WALL-GAS DEL T AVG	K	0.0	45.05	0.0	-26.56	0.0
WALL-GAS DEL T MAX	K	-62.78	45.05	0.0	-26.56	-42.22
WALL-GAS CHNG Q	W	-694.52	9787.29	-771.86	-5330.79	79.85
AVG MASS FLOW	KG/S	0.011695	0.011695	0.014064	0.016909	0.016909
MAX MASS FLOW	KG/S	0.011695	0.011695	0.014064	0.016909	0.016909
REYNOLDS NUMBER		270.58	6284.25	61.43	6572.08	89.30
DEL-P FRICTION	MPA	0.0	0.007920	0.103334	0.004894	0.0
NUSSELT NUMBER		0.0	27.59	7.52	29.47	0.0

ZONE OUTPUT FOR CASE 6 CYCLE NUMBER 3 FLUX ERROR= -1.12

ZONE NUMBER		1	2	3	4	5
TEMP GAS MAX	K	908.87	887.79	578.38	351.24	403.29
TEMP GAS AVG	K	887.79	887.79	578.38	351.24	351.24
WALL-GAS DEL T AVG	K	0.0	44.82	0.0	-27.95	0.0
WALL-GAS DEL T MAX	K	-21.08	44.82	0.0	-27.95	-52.05
WALL-GAS CHNG Q	W	-695.23	9599.50	-794.10	-5645.60	79.59
AVG MASS FLOW	KG/S	0.011945	0.011945	0.014146	0.016750	0.016750
MAX MASS FLOW	KG/S	0.011945	0.011945	0.014146	0.016750	0.016750
REYNOLDS NUMBER		284.93	6617.71	62.25	6357.77	86.39
DEL-P FRICTION	MPA	0.0	0.007786	0.102045	0.005009	0.0
NUSSELT NUMBER		0.0	28.13	7.57	28.72	0.0

ZONE OUTPUT FOR CASE 6 CYCLE NUMBER 4 FLUX ERROR= 0.21

ZONE NUMBER		1	2	3	4	5
TEMP GAS MAX	K	908.98	887.77	578.64	351.30	403.67
TEMP GAS AVG	K	887.77	887.77	578.64	351.30	351.30
WALL-GAS DEL T AVG	K	0.0	44.84	0.0	-27.98	0.0
WALL-GAS DEL T MAX	K	-21.21	44.84	0.0	-27.98	-52.37
WALL-GAS CHNG Q	W	-695.01	9602.59	-793.73	-5649.36	79.58
AVG MASS FLOW	KG/S	0.011942	0.011942	0.014138	0.016735	0.016735
MAX MASS FLOW	KG/S	0.011942	0.011942	0.014138	0.016735	0.016735
REYNOLDS NUMBER		284.83	6615.35	62.20	6348.23	86.26
DEL-P FRICTION	MPA	0.0	0.007785	0.102032	0.005006	0.0
NUSSELT NUMBER		0.0	28.13	7.57	28.68	0.0

## GPU-3 HYDROGEN 927K/339K STIRLING ENGINE DATA: 1 (UPDATED JAN 83)

## CASE TO CASE COMPARISON INFORMATION

CASE NUMBER		1	2	3	4	5	6
AVERAGE PRESSURE	MPA	2.7400	2.7400	2.7400	2.7400	2.7400	2.7400
SPEED	RPM	1000.20	1500.00	1999.80	2499.60	2999.40	3499.20
GAS MASS	KG	0.0003526	0.0003470	0.0003426	0.0003373	0.0003319	0.0003263
INDIC HEAT IN	W	3712.12	5176.64	6595.50	7842.74	9027.50	10150.25
INDIC POWER OUT	W	1224.20	1905.46	2512.94	2907.27	3183.35	3337.53
EFFICIENCY		0.3298	0.3681	0.3810	0.3707	0.3526	0.3288
EXPANSION WALL T	K	801.92	839.47	862.94	870.70	878.65	887.77
EXPANSION GAS T	K	801.92	839.47	862.94	870.70	878.65	887.77
WALL TO GAS NET Q	W	-568.04	-633.19	-674.72	-681.46	-687.65	-695.01
P-V WORK	W	2487.09	3833.79	5180.82	6436.45	7674.64	8898.79
HYSTERESIS	W	0.0	0.0	0.0	0.0	0.0	0.0
COMBUSTOR TEMP	K	890.00	899.00	909.00	918.00	927.00	937.00
HEATER WALL T	K	888.47	896.80	906.16	914.60	923.09	932.61
HEATER GAS T	K	801.92	839.47	862.94	870.70	878.65	887.77
WALL TO GAS NET Q	W	3200.09	4657.77	6068.71	7309.28	8487.48	9602.59
WALL CONDUCTION	W	512.03	518.87	526.80	533.46	540.02	547.66
FRICITION P-DROP	MPA	0.0008402	0.0016974	0.0029907	0.0043902	0.0059948	0.0077845
REGENERATOR WALL T	K	592.47	598.94	606.09	613.01	620.13	627.96
REGENERATOR GAS T	K	533.44	544.71	553.12	561.16	569.54	578.64
WALL TO GAS NET Q	W	-187.82	-297.49	-421.72	-542.91	-667.37	-793.73
WALL CONDUCTION	W	512.03	518.87	526.80	533.46	540.02	547.66
FRICITION P-DROP	MPA	0.0209092	0.0339028	0.0487396	0.0650011	0.0827990	0.1020325
WATER TEMPERATURE	K	287.00	287.00	287.00	287.00	287.00	287.00
COOLER WALL T	K	296.47	301.09	306.02	311.42	317.18	323.32
COOLER GAS T	K	332.77	328.62	328.15	335.46	343.17	351.30
WALL TO GAS NET Q	W	-1473.45	-2192.01	-2958.10	-3798.31	-4694.95	-5649.36
WALL CONDUCTION	W	-1014.31	-1079.15	-1124.22	-1136.93	-1148.98	-1163.10
FRICITION P-DROP	MPA	0.0006634	0.0011613	0.0018572	0.0027613	0.0038148	0.0050056
COMPRESSION WALL T	K	332.77	328.62	328.15	335.46	343.17	351.30
COMPRESSION GAS T	K	332.77	328.62	328.15	335.46	343.17	351.30
WALL TO GAS NET Q	W	65.75	72.91	77.29	77.99	78.69	79.58
P-V WORK	W	-1177.30	-1717.81	-2258.75	-2840.63	-3430.81	-4027.26
HYSTERESIS	W	0.0	0.0	0.0	0.0	0.0	0.0
MAX PRESSURE	MPA	3.6098	3.6248	3.6326	3.6291	3.6254	3.6220
MIN PRESSURE	MPA	1.9415	1.9170	1.9047	1.9102	1.9160	1.9215
INITIAL PRESSURE	MPA	3.2892	3.3199	3.3354	3.3284	3.3212	3.3143
P-VE PHASE ANGLE	DEG	-249.5309	-250.1750	-250.4647	-250.3349	-250.1998	-250.0641
STATIC PWR LOSS	W	-798.19	-831.86	-856.46	-866.13	-875.70	-887.10
DYNAMIC PWR LOSS	W	-325.96	-364.76	-390.17	-394.34	-397.95	-402.05
FRICITION PWR LOSS	W	-85.58	-210.52	-409.13	-688.55	-1060.47	-1533.94
REGENATR PWR LOSS	W	-143.73	-252.92	-376.60	-497.36	-621.39	-747.25
LEAKAGE PWR LOSS	W	0.0	0.0	0.0	0.0	0.0	0.0
NET Q TO COLD H2O	W	-2487.76	-3271.16	-4082.32	-4935.23	-5843.92	-6812.45
UNACCT PWR LOSS	W	0.15	0.02	0.24	0.23	0.23	0.21
REGENATR EFFECTVNS		0.8725	0.8643	0.8574	0.8571	0.8579	0.8595



## GPU-3 HYDROGEN 927K/339K STIRLING ENGINE DATA: 1 (UPDATED JAN 83)

## RIOS/SEAM1 ANALYSIS CONSOLIDATED INPUT INFORMATION

ZONE	EXPANSION 1	HEATER 2	REGENERATOR 3	COOLER 4	COMPRESSION 5
VOLUME (CU M)	1.2153E-04	8.8200E-05	5.3440E-05	2.8150E-05	1.1425E-04
FLOW AREA (SQ M)	3.8600E-03	2.8640E-04	1.5040E-03	2.8579E-04	3.7700E-03
WETTED AREA (SQ M)		5.8960E-02	1.4541E+00	3.7440E-02	
HYD DIA (M)	0.070100	0.003020	0.000093	0.001080	0.060400
TOT LNTH (M)		0.246300	0.022600	0.046100	
HT EXCH LNTH (M)		0.155400		0.035500	
TEMPERATURE (K)	927.00	927.00	584.52	339.00	339.00
REGENERATOR WALL DIAMETER (M)		0.02262		AVG HT TRANSF REYN EXPONENT	0.5503
MINIMUM TOTAL VOLUME (CU M)	2.3248E-04			MAXIMUM TOTAL VOLUME (CU M)	3.5261E-04
ANGLE AT MIN TOTAL VOLUME (DEG)	290.4998			ANGLE AT MAX TOTAL VOLUME (DEG)	128.5000
AVERAGE PRESSURE (MPA)	2.7400			TOTAL GAS MASS (KGS)	3.9565E-04
NORMALIZED VALUES FOR XHASE, TEMP RATIO, RVT =				0.00002478	2.7345
					2.5705

## GPU-3 HYDROGEN 927K/339K STIRLING ENGINE DATA: 1 (UPDATED JAN 83)

NITE,TEST,TEST1,DUMC,DUME,COEFM= 2 1.75476E-04 1.43051E-05 0.0 0.0  
 1 1.00375 0.16859 1.55161 2 1.00446 0.16819 1.54934 2 1.00444 0.

(VC/VE)\*(TH/TC) = 2.5705 VDEAD = 4.1129  
 COLD WORK = -0.3196 WARM WORK = 0.7147  
 PRESSURE RATIO = 1.9296 MAXIMUM PRESSURE = 1.0874  
 XME = 1.5491 XMC = 0.1682  
 P-V ANGLE IN RAD = 1.2351 TOTAL GAS MASS = 0.0003255 MEAN PRESSURE = 2740  
 PBUFN = 0.8852 PMAX = 3643316.0 PMIN = 1888

PRESSURE DROP INTEGRAL

X/L	INTEGRAL	DMRE	XI1	XI2
0.0	1.2913	0.3381	-0.6967	3.6494
0.10	1.1441	0.3195	-0.6712	3.6397
0.20	1.0080	0.3019	-0.6428	3.6263
0.30	0.8828	0.2852	-0.6103	3.6099
0.40	0.7686	0.2694	-0.5739	3.5921
0.50	0.6652	0.2545	-0.5326	3.5743
0.60	0.5725	0.2407	-0.4852	3.5590
0.70	0.4902	0.2280	-0.4302	3.5438
0.80	0.4181	0.2167	-0.3653	3.5460
0.90	0.3556	0.2071	-0.2872	3.5517
1.00	0.3015	0.1997	-0.1918	3.5633

## FLOW PRINTS FROM CYCLER

COOLER =	0.003598	21.672623	65.322189	0.006361	0.310025
HEATER =	0.006876	22.282150	105.710526	0.006080	0.214432
REGENERATOR=	0.016730	1339.4702	1379.3625	0.168992	0.257860

HEAT FLOWS =	-0.4538	-0.3196	747.2517	79.5762	-5506.1641
	0.001590	3000.0	202.5498	-27.1842	349.5789
HEAT FLOWS =	0.7684	0.7147	402.0522	213.3857	46.4770
	0.004830	100000000.	217.2213	45.6611	886.7815

REGENERATOR LOSSES =	719.9810	125.5727	594.4084	6.1876	2.7345
	0.010139	0.342775			

PRINTS FROM ROUTINE LOSSES

	3	1	2	
DYNAMIC PISTON LOSSES	400.12939	2.35135	-9214.0	0.22769 152.58554
	94.79234	0.99478	397.77808	
CONDUCTION LOSSES	887.4648	79.5683	213.3644	548.0149 46.5175
	0.026600	0.003214	0.000340	

## ZONE OUTPUT FOR CASE 7 CYCLE NUMBER 1 FLUX ERROR= 1.94

ZONE NUMBER		1	2	3	4	5
TEMP GAS MAX	K	950.23	886.78	584.52	349.58	390.36
TEMP GAS AVG	K	886.78	886.78	584.52	349.58	349.58
WALL-GAS DEL T AVG	K	0.0	45.66	0.0	-27.18	0.0
WALL-GAS DEL T MAX	K	-63.45	45.66	0.0	-27.18	-40.78
WALL-GAS CHNG Q	W	-693.06	9918.57	-766.50	-5506.17	79.57
AVG MASS FLOW	KG/S	0.011691	0.011691	0.014059	0.016903	0.016903
MAX MASS FLOW	KG/S	0.011691	0.011691	0.014059	0.016903	0.016903
REYNOLDS NUMBER		270.49	6282.15	61.41	6569.87	89.27
DEL-P FRICTION	MPA	0.0	0.007916	0.103287	0.004891	0.0
NUSSELT NUMBER		0.0	27.59	7.52	29.46	0.0

## GPU-3 HYDROGEN 927K/339K STIRLING ENGINE DATA: 1 (UPDATED JAN 83)

NITE, TEST, TEST1, DUMC, DUME, COEFM= 2 3.81470E-05 1.22070E-04 0.0 0.0  
 1 1.00444 0.16815 1.54906 2 1.00365 0.16846 1.55108 2 1.00352 0.1

(VC/VE)\*(TW/TC) = 2.3846 VDEAD = 3.9607  
 COLD WORK = -0.3338 WARM WORK = 0.6955  
 PRESSURE RATIO = 1.8901 MAXIMUM PRESSURE = 1.0937  
 XME = 1.5511 XMC = 0.1685  
 P-V ANGLE IN RAD = 1.2233 TOTAL GAS MASS = 0.0003265 MEAN PRESSURE = 2740  
 PBUFN = 0.8893 PMAX = 3625537.0 PMIN = 1912

## PRESSURE DROP INTEGRAL

X/L	INTEGRAL	DMRE	XI1	XI2
0.0	1.3421	0.3452	-0.6618	3.6518
0.10	1.1938	0.3270	-0.6347	3.6413
0.20	1.0566	0.3099	-0.6041	3.6271
0.30	0.9304	0.2937	-0.5704	3.6099
0.40	0.8152	0.2785	-0.5324	3.5913
0.50	0.7103	0.2644	-0.4901	3.5733
0.60	0.6171	0.2513	-0.4419	3.5584
0.70	0.5338	0.2394	-0.3867	3.5485
0.80	0.4606	0.2289	-0.3225	3.5460
0.90	0.3967	0.2202	-0.2464	3.5513
1.00	0.3411	0.2137	-0.1555	3.5618

## FLOW PRINTS FROM CYCLER

	0.003703	22.024902	66.731796	0.006388	0.318746
COOLER =					
HEATER =	0.006797	22.243500	104.310181	0.006016	0.227440
REGENERATOR =	0.016224	1329.5168	1362.1587	0.167754	0.269295

HEAT FLOWS =	-0.4658	-0.3338	719.9810	79.5683	-5623.9570
	0.001590	3000.0	202.1013	-27.8274	350.9792
HEAT FLOWS =	0.7480	0.6955	400.1294	213.3644	46.5175
	0.004830	100000000.	214.3134	44.8289	887.7791

REGENERATOR LOSSES =	748.2026	131.3669	616.8359	6.3254	2.5367
	0.010253	0.373381			

## PRINTS FROM ROUTINE LOSSES

	3	1	2	
DYNAMIC PISTON LOSSES	401.67383	3.64476	13397.0	0.24274 158.23706
	94.77391	0.99478	398.02930	
CONDUCTION LOSSES	887.3374	79.6120	213.4816	547.7573 46.4866
	0.026600	0.003214	0.000340	

## GPU-3 HYDROGEN 927K/339K STIRLING ENGINE DATA: 1 (UPDATED JAN 83)

NITE,TEST,TEST1,DUMC,DUME,COEFM= 2 7.53403E-05 7.34329E-05 0.0 0.0  
 1 1.00352 0.16847 1.55114 2 1.00341 0.16852 1.55104 2 1.00334 0.1

(VC/VE)\*(TH/TC) = 2.3777 VDEAD = 3.9760  
 COLD WORK = -0.3335 WARM WORK = 0.6933  
 PRESSURE RATIO = 1.8849 MAXIMUM PRESSURE = 1.0933  
 XME = 1.5509 XMC = 0.1685  
 P-V ANGLE IN RAD = 1.2230 TOTAL GAS MASS = 0.0003266 MEAN PRESSURE = 2740  
 PBUFN = 0.8899 PMAX = 3621775.0 PMIN = 1921

## PRESSURE DROP INTEGRAL

X/L	INTEGRAL	DMRE	XI1	XI2
0.0	1.3483	0.3461	-0.6594	3.6520
0.10	1.1993	0.3279	-0.6322	3.6415
0.20	1.0614	0.3107	-0.6017	3.6273
0.30	0.9346	0.2945	-0.5680	3.6100
0.40	0.8188	0.2793	-0.5300	3.5913
0.50	0.7140	0.2651	-0.4878	3.5733
0.60	0.6198	0.2520	-0.4395	3.5583
0.70	0.5362	0.2401	-0.3845	3.5484
0.80	0.4627	0.2296	-0.3203	3.5460
0.90	0.3985	0.2209	-0.2444	3.5512
1.00	0.3427	0.2144	-0.1536	3.5617

## FLOW PRINTS FROM CYCLER

	0.003714	22.040649	66.834412	0.006393	0.319780
COOLER =	0.003714	22.040649	66.834412	0.006393	0.319780
HEATER =	0.006780	22.146515	103.921707	0.006020	0.228081
REGENERATOR=	0.016159	1330.1497	1362.1294	0.168031	0.270087

HEAT FLOWS =	-0.4680	-0.3335	748.2026	79.6120	-5645.0273
HEAT FLOWS =	0.001590	3000.0	201.9176	-27.9571	351.2444
HEAT FLOWS =	0.7482	0.6933	401.6738	213.4816	46.4866
	0.004830	10000000.	214.1055	44.8374	887.7749

REGENERATOR LOSSES =	747.1277	130.7624	616.3655	6.3101	2.5294
REGENERATOR LOSSES =	0.010229	0.373719			

## PRINTS FROM ROUTINE LOSSES

	3	1	2
DYNAMIC PISTON LOSSES	402.14990	4.26043	16105.0
	94.77191	0.99478	397.88965
CONDUCTION LOSSES	887.1472	79.5833	213.4046
	0.026600	0.003214	0.000340

## ZONE OUTPUT FOR CASE 7 CYCLE NUMBER 3 FLUX ERROR= -0.40

ZONE NUMBER		1	2	3	4	5
TEMP GAS MAX	K	908.97	887.77	578.45	351.24	403.36
TEMP GAS AVG	K	887.77	887.77	578.45	351.24	351.24
WALL-GAS DEL T AVG	K	0.0	44.84	0.0	-27.96	0.0
WALL-GAS DEL T MAX	K	-21.20	44.84	0.0	-27.96	-52.11
WALL-GAS CHNG Q	W	-695.14	9599.94	-793.61	-5645.03	79.58
AVG MASS FLOW	KG/S	0.011940	0.011940	0.014139	0.016740	0.016740
MAX MASS FLOW	KG/S	0.011940	0.011940	0.014139	0.016740	0.016740
REYNOLDS NUMBER		284.79	6614.33	62.22	6353.54	86.33
DEL-P FRICTION	MPA	0.0	0.007782	0.101996	0.005005	0.0
NUSSSELT NUMBER		0.0	28.12	7.57	28.70	0.0

GPU-3 HYDROGEN 927K/339K STIRLING ENGINE DATA: 1 (UPDATED JAN 83)

NITE, TEST, TEST1, DUMC, DUME, COEFM= 2 6.77109E-05 6.96182E-05 0.0 0.0  
 1 1.00334 0.16852 1.55093 2 1.00326 0.16850 1.55086 2 1.00319 0.1

(VC/VE)\*(TH/TC) = 2.3759 VDEAD = 3.9720  
 COLD WORK = -0.3338 WARM WORK = 0.6933  
 PRESSURE RATIO = 1.8850 MAXIMUM PRESSURE = 1.0933  
 XME = 1.5508 XMC = 0.1685  
 P-V ANGLE IN RAD = 1.2228 TOTAL GAS MASS = 0.0003263 MEAN PRESSURE = 2740  
 PBUFN = 0.8896 PMAX = 3622020.0 PHIN = 1921

PRESSURE DROP INTEGRAL

X/L = 0.0	INTEGRAL = 1.3483	DMRE = 0.3461	XI1 = -0.6592	XI2 = 3.6520
X/L = 0.10	INTEGRAL = 1.1994	DMRE = 0.3279	XI1 = -0.6320	XI2 = 3.6415
X/L = 0.20	INTEGRAL = 1.0615	DMRE = 0.3107	XI1 = -0.6014	XI2 = 3.6273
X/L = 0.30	INTEGRAL = 0.9348	DMRE = 0.2945	XI1 = -0.5677	XI2 = 3.6100
X/L = 0.40	INTEGRAL = 0.8191	DMRE = 0.2793	XI1 = -0.5297	XI2 = 3.5913
X/L = 0.50	INTEGRAL = 0.7143	DMRE = 0.2652	XI1 = -0.4874	XI2 = 3.5733
X/L = 0.60	INTEGRAL = 0.6202	DMRE = 0.2521	XI1 = -0.4391	XI2 = 3.5533
X/L = 0.70	INTEGRAL = 0.5366	DMRE = 0.2402	XI1 = -0.3841	XI2 = 3.5485
X/L = 0.80	INTEGRAL = 0.4631	DMRE = 0.2297	XI1 = -0.3199	XI2 = 3.5460
X/L = 0.90	INTEGRAL = 0.3990	DMRE = 0.2210	XI1 = -0.2440	XI2 = 3.5512
X/L = 1.00	INTEGRAL = 0.3432	DMRE = 0.2146	XI1 = -0.1533	XI2 = 3.5617

FLOW PRINTS FROM CYCLER

COOLER =	0.003712	22.026779	66.806839	0.006394	0.319784
HEATER =	0.006778	22.140762	103.898178	0.006020	0.228201
REGENATOR=	0.016147	1329.9834	1361.9719	0.168078	0.270161

HEAT FLOWS =	-0.4682	-0.3338	747.1277	79.5833	-5647.0820
	0.001590	3000.0	201.8283	-27.9796	351.2800
HEAT FLOWS =	0.7481	0.6933	402.1499	213.4046	46.4788
	0.004830	100000000.	214.0771	44.8424	887.7698

REGENERATOR LOSSES =	746.9780	130.7183	616.2598	6.3090	2.5275
	0.010228	0.374166			

PRINTS FROM ROUTINE LOSSES

DYNAMIC PISTON LOSSES	402.07202	4.20555	15967.0	0.23501	152.58096
	94.77168	0.99478	397.86670		
CONDUCTION LOSSES	887.1206	79.5786	213.3920	547.6724	46.4780
	0.026600	0.003214	0.000340		

ZONE OUTPUT FOR CASE 7 CYCLE NUMBER 4 FLUX ERROR= 0.10

ZONE NUMBER		1	2	3	4	5
TEMP GAS MAX	K	908.96	887.77	578.63	351.28	403.68
TEMP GAS AVG	K	887.77	887.77	578.63	351.28	351.28
WALL-GAS DEL T AVG	K	0.0	44.84	0.0	-27.98	0.0
WALL-GAS DEL T MAX	K	-21.19	44.84	0.0	-27.98	-52.40
WALL-GAS CHNG Q	W	-695.04	9599.73	-793.46	-5647.08	79.58
AVG MASS FLOW	KG/S	0.011938	0.011938	0.014133	0.016729	0.016729
MAX MASS FLOW	KG/S	0.011938	0.011938	0.014133	0.016729	0.016729
REYNOLDS NUMBER		284.74	6613.28	62.18	6345.94	86.23
DEL-P FRICTION	MPA	0.0	0.007780	0.101985	0.005003	0.0
NUSSELT NUMBER		0.0	28.12	7.57	28.68	0.0

## GPU-3 HYDROGEN 927K/339K STIRLING ENGINE DATA: 1 (UPDATED JAN 83)

## RIOS/SEAM1 ANALYSIS CONSOLIDATED INPUT INFORMATION

ZONE	EXPANSION 1	HEATER 2	REGENERATOR 3	COOLER 4	COMPRESSION 5
VOLUME (CU M)	1.2153E-04	8.8200E-05	5.3440E-05	2.8150E-05	1.1425E-04
FLOW AREA (SQ M)	3.8600E-03	2.8640E-04	1.5040E-03	2.8579E-04	3.7700E-03
WETTED AREA (SQ M)		5.8960E-02	1.4541E+00	3.7440E-02	
HYD DIA (M)	0.070100	0.003020	0.000093	0.001080	0.060400
TOT LNTH (M)		0.246300	0.022600	0.046100	
HT EXCH LNTH (M)		0.155400		0.035500	
TEMPERATURE (K)	887.77	887.77	578.66	351.28	351.28
REGENERATOR WALL DIAMETER (M)		0.02262		AVG HT TRANSF REYN EXPONENT	0.5503
MINIMUM TOTAL VOLUME (CU M)	2.3248E-04			MAXIMUM TOTAL VOLUME (CU M)	3.5261E-04
ANGLE AT MIN TOTAL VOLUME (DEG)	290.4998			ANGLE AT MAX TOTAL VOLUME (DEG)	128.5000
AVERAGE PRESSURE (MPA)	2.7402			TOTAL GAS MASS (KGS)	3.2630E-04
NORMALIZED VALUES FOR XMASE, TEMP RATIO, RVT =			0.00002645	2.5272	2.3757

## GPU-3 HYDROGEN 927K/339K STIRLING ENGINE DATA: 1 (UPDATED JAN 83)

NITE,TEST,TEST1,DUMC,DUME,COEFM= 2 6.96182E-05 7.34329E-05 0.0 0.0  
 1 1.00319 0.16849 1.55075 2 1.00313 0.16847 1.55067 2 1.00306 0.1

(VC/VE)\*(TW/TC) = 2.3757 VDEAD = 3.9714  
 COLD WORK = -0.3339 WARM WORK = 0.6933  
 PRESSURE RATIO = 1.8350 MAXIMUM PRESSURE = 1.0932  
 XME = 1.5506 XMC = 0.1685  
 P-V ANGLE IN RAD = 1.2228 TOTAL GAS MASS = 0.0003263 MEAN PRESSURE = 2740  
 PBUFN = 0.8915 PMAX = 3622088.0 PMIN = 1921

## PRESSURE DROP INTEGRAL

X/L	INTEGRAL	DMRE	XI1	XI2
0.0	1.3484	0.3461	-0.6592	3.6521
0.10	1.1994	0.3279	-0.6320	3.6415
0.20	1.0616	0.3107	-0.6014	3.6272
0.30	0.9349	0.2945	-0.5676	3.6100
0.40	0.8191	0.2793	-0.5297	3.5913
0.50	0.7143	0.2652	-0.4874	3.5732
0.60	0.6202	0.2521	-0.4390	3.5583
0.70	0.5366	0.2402	-0.3840	3.5484
0.80	0.4631	0.2297	-0.3199	3.5460
0.90	0.3990	0.2210	-0.2439	3.5512
1.00	0.3432	0.2146	-0.1532	3.5617

## FLOW PRINTS FROM CYCLER

	0.003712	22.025635	66.805237	0.006394	0.319783
COOLER =	0.006778	22.140823	103.898529	0.006020	0.228219
HEATER =	0.016145	1329.9927	1361.9824	0.168083	0.270172
REGENATOR=					

HEAT FLOWS =	-0.4682	-0.3339	746.9780	79.5786	-5647.8750
	0.001590	3000.0	201.8173	-27.9851	351.3379
HEAT FLOWS =	0.7481	0.6933	402.0720	213.3920	46.4780
	0.004830	100000000.	214.0753	44.8438	887.7683

REGENERATOR LOSSES =	746.8032	130.7051	616.0981	6.3083	2.5272
	0.010228	0.374231			

## PRINTS FROM ROUTINE LOSSES

		3	1	2	
DYNAMIC PISTON LOSSES	401.99219	4.15722	15791.0	0.23500	152.58781
	94.77132	0.99478	397.83521		
CONDUCTION LOSSES	887.0625	79.5722	213.3749	547.6409	46.4748
	0.026600	0.003214	0.000340		

## ZONE OUTPUT FOR CASE 8 CYCLE NUMBER 1 FLUX ERROR= 0.10

ZONE NUMBER		1	2	3	4	5
TEMP GAS MAX	K	908.97	887.77	578.66	351.34	403.75
TEMP GAS AVG	K	887.77	887.77	578.66	351.34	351.34
WALL-GAS DEL T AVG	K	0.0	44.84	0.0	-27.98	0.0
WALL-GAS DEL T MAX	K	-21.20	44.84	0.0	-27.98	-52.41
WALL-GAS CHNG Q	W	-694.94	9599.96	-793.28	-5647.87	79.57
AVG MASS FLOW	KG/S	0.011938	0.011938	0.014133	0.016728	0.016728
MAX MASS FLOW	KG/S	0.011938	0.011938	0.014133	0.016728	0.016728
REYNOLDS NUMBER		284.74	6613.27	62.17	6344.96	86.22
DEL-P FRICTION	MPA	0.0	0.007780	0.101986	0.005002	0.0
NUSSELT NUMBER		0.0	28.12	7.57	28.67	0.0

GPU-3 HYDROGEN 927K/339K STIRLING ENGINE DATA: 1 (UPDATED JAN 83)

\*\*\*\* SCHMIDT ANALYSIS VALUES ARE \*\*\*\*

PSIMIN	TC/TH	RESTR	SCHAA	SCHBB	SCHDEL	THETA
1.57080	0.39569	0.00203	-0.00028	0.00057	-0.49451	0.96302
PSTR/PM	PST	VARVOT	SUMVOT	SUMV	SMPVOT	
1.2043E+00	3.2997E+06	9.0802E-08	3.1706E-07	1.9322E-04	1.0462E+00	

RIOS/SEAM1 ANALYSIS CONSOLIDATED INPUT INFORMATION

ZONE	EXPANSION 1	HEATER 2	REGENERATOR 3	COOLER 4	COMPRESSION 5
VOLUME (CU M)	1.2153E-04	8.8200E-05	5.3440E-05	2.8150E-05	1.1425E-04
FLOW AREA (SQ M)	3.8600E-03	2.8640E-04	1.5040E-03	2.8579E-04	3.7700E-03
WETTED AREA (SQ M)		5.8960E-02	1.4541E+00	3.7440E-02	
HYD DIA (M)	0.070100	0.003020	0.000093	0.001080	0.060400
TOT LNGTH (M)		0.246300	0.022600	0.046100	
HT EXCH LNGTH (M)		0.155400		0.035500	
TEMPERATURE (K)	887.77	887.77	578.66	351.28	351.28
REGENERATOR WALL DIAMETER (M)		0.02262		AVG HT TRANSF REYN EXPONENT	0.5503
MINIMUM TOTAL VOLUME (CU M)		2.3248E-04		MAXIMUM TOTAL VOLUME (CU M)	3.5261E-04
ANGLE AT MIN TOTAL VOLUME (DEG)		290.4998		ANGLE AT MAX TOTAL VOLUME (DEG)	128.5000
AVERAGE PRESSURE (MPA)		2.7402		TOTAL GAS MASS (KGS)	3.2630E-04
NORMALIZED VALUES FOR XMASE, TEMP RATIO, RVT =				0.00002645	2.5272
					2.3757



GPU-3 HYDROGEN 927K/339K STIRLING ENGINE DATA: 1 (UPDATED JAN 83)

ZONE OUTPUT FOR CASE 9 CYCLE NUMBER 1 FLUX ERROR= 0.00

ZONE NUMBER		1	2	3	4	5
TEMP GAS MAX	K	908.97	887.77	578.66	351.34	403.74
TEMP GAS AVG	K	887.77	887.77	578.66	351.34	351.34
WALL-GAS DEL T AVG	K	0.0	44.84	0.0	-27.98	0.0
WALL-GAS DEL T MAX	K	-21.20	44.84	0.0	-27.98	-52.41
WALL-GAS CHNG Q	W	-694.95	9599.70	-793.29	-5647.66	79.57
AVG MASS FLOW	KG/S	0.011938	0.011938	0.014132	0.016728	0.016728
MAX MASS FLOW	KG/S	0.011938	0.011938	0.014132	0.016728	0.016728
REYNOLDS NUMBER		284.74	6613.27	62.17	6344.94	86.22
DEL-P FRICTION	MPA	0.0	0.007780	0.101986	0.005002	0.0
NUSSELT NUMBER		0.0	28.12	7.57	28.67	0.0

## GPU-3 HYDROGEN 927K/339K STIRLING ENGINE DATA: 1 (UPDATED JAN 83)

INNER CYCLE DATA FOR CASE 9 SPEED= 3498. NET MASS= 0.000326

ANGLE	HOT VOLUME CU.CM	COLD VOLUME CU.CM	PRESSURE MPA	SCHMIDT PRESSURE MPA	WORK WATTS	COLD MASS GMS	HOT MASS GMS
0.0	93.576	10.931	3.3143	4.0090	0.0	0.010560	0.041327
10.00	102.679	11.203	3.2185	3.6681	1785.34	0.010587	0.044335
20.00	111.214	12.010	3.1204	3.3303	3511.41	0.011151	0.046881
30.00	118.852	13.458	3.0209	3.0160	5138.30	0.012323	0.048360
40.00	125.260	15.708	2.9202	2.7357	6637.62	0.014202	0.050173
50.00	130.111	18.945	2.8178	2.4928	7990.44	0.016887	0.050735
60.00	133.112	23.355	2.7134	2.2865	9185.43	0.020449	0.050481
70.00	134.026	29.092	2.6080	2.1141	10217.06	0.024907	0.049364
80.00	132.686	36.251	2.5024	1.9721	11083.83	0.030215	0.047403
90.00	129.020	44.835	2.3982	1.8571	11786.46	0.036252	0.046668
100.00	123.059	54.741	2.2976	1.7659	12326.41	0.042837	0.041273
110.00	114.952	65.730	2.2029	1.6960	12704.50	0.049740	0.037369
120.00	104.971	77.419	2.1172	1.6452	12919.50	0.056698	0.033128
130.00	93.511	89.271	2.0433	1.6121	12967.11	0.063438	0.028732
140.00	81.085	100.607	1.9842	1.5957	12839.14	0.069681	0.024361
150.00	68.298	110.638	1.9430	1.5954	12523.57	0.075163	0.020183
160.00	55.805	118.537	1.9230	1.6113	12005.88	0.079633	0.016344
170.00	44.246	123.556	1.9270	1.6438	11271.96	0.082894	0.012959
180.00	34.163	125.171	1.9579	1.6939	10312.92	0.084764	0.010109
190.00	25.928	123.201	2.0178	1.7631	9130.43	0.085139	0.007837
200.00	19.712	117.865	2.1082	1.8535	7741.06	0.083955	0.006153
210.00	15.503	109.717	2.2288	1.9676	6178.73	0.081235	0.005050
220.00	13.165	99.518	2.3771	2.1085	4495.51	0.077074	0.004513
230.00	12.504	88.097	2.5483	2.2798	2760.77	0.071632	0.004527
240.00	13.318	76.233	2.7359	2.4848	1053.75	0.065148	0.005063
250.00	15.427	64.593	2.9303	2.7264	-515.62	0.057916	0.006136
260.00	18.680	53.697	3.1196	3.0055	-1863.39	0.050296	0.007757
270.00	22.959	43.915	3.2912	3.3187	-2891.73	0.042693	0.009920
280.00	28.172	35.470	3.4337	3.6559	-3525.27	0.035505	0.012589
290.00	34.245	28.456	3.5385	3.9972	-3716.72	0.029073	0.015700
300.00	41.108	22.857	3.6012	4.3107	-3453.51	0.023624	0.019161
310.00	48.694	18.572	3.6221	4.5559	-2758.54	0.019257	0.022866
320.00	56.919	15.442	3.6056	4.6926	-1685.07	0.015944	0.026702
330.00	65.678	13.280	3.5587	4.6951	-307.33	0.013569	0.030562
340.00	74.832	11.902	3.4896	4.5628	1290.40	0.011975	0.034347
350.00	84.205	11.153	3.4059	4.3208	3023.77	0.011008	0.037964
359.00	92.646	10.931	3.3235	4.0421	4635.91	0.010583	0.041002

## GPU-3 HYDROGEN 927K/339K STIRLING ENGINE DATA: 1 (UPDATED JAN 83)

## CASE TO CASE COMPARISON INFORMATION

CASE NUMBER		7	8	9
AVERAGE PRESSURE	MPA	2.7400	2.7400	2.7400
SPEED	RPM	3498.00	3498.00	3498.00
GAS MASS	KG	0.0003263	0.0003263	0.0003263
INDIC HEAT IN	W	10147.40	10147.60	10147.34
INDIC POWER OUT	W	3337.09	3336.62	3336.67
EFFICIENCY		0.3289	0.3288	0.3288
EXPANSION WALL T	K	887.77	887.77	887.77
EXPANSION GAS T	K	887.77	887.77	887.77
WALL TO GAS NET Q	W	-695.04	-694.94	-694.95
P-V WORK	W	8895.87	8896.36	8896.37
HYSTERESIS	W	0.0	0.0	0.0
COMBUSTOR TEMP	K	937.00	937.00	937.00
HEATER WALL T	K	932.61	932.61	932.61
HEATER GAS T	K	887.77	887.77	887.77
WALL TO GAS NET Q	W	9599.73	9599.96	9599.70
WALL CONDUCTION	W	547.67	547.64	547.64
FRICTION P-DROP	MPA	0.0077799	0.0077799	0.0077799
REGENERATOR WALL T	K	627.96	627.98	627.98
REGENERATOR GAS T	K	578.63	578.66	578.66
WALL TO GAS NET Q	W	-793.46	-793.28	-793.29
WALL CONDUCTION	W	547.67	547.64	547.64
FRICTION P-DROP	MPA	0.1019847	0.1019855	0.1019857
WATER TEMPERATURE	K	287.00	287.00	287.00
COOLER WALL T	K	323.30	323.35	323.35
COOLER GAS T	K	351.28	351.34	351.34
WALL TO GAS NET Q	W	-5647.08	-5647.87	-5647.66
WALL CONDUCTION	W	-1163.14	-1163.01	-1163.01
FRICTION P-DROP	MPA	0.0050025	0.0050024	0.0050024
COMPRESSION WALL T	K	351.28	351.34	351.34
COMPRESSION GAS T	K	351.28	351.34	351.34
WALL TO GAS NET Q	W	79.58	79.57	79.57
P-V WORK	W	-4026.10	-4027.05	-4027.01
HYSTERESIS	W	0.0	0.0	0.0
MAX PRESSURE	MPA	3.6220	3.6221	3.6221
MIN PRESSURE	MPA	1.9215	1.9215	1.9215
INITIAL PRESSURE	MPA	3.3143	3.3143	3.3143
P-VE PHASE ANGLE	DEG	-250.0633	-250.0625	-250.0627
STATIC PWR LOSS	W	-887.12	-887.06	-887.07
DYNAMIC PWR LOSS	W	-402.07	-401.99	-402.00
FRICTION PWR LOSS	W	-1532.68	-1532.69	-1532.69
REGENATR PWR LOSS	W	-746.98	-746.80	-746.81
LEAKAGE PWR LOSS	W	0.0	0.0	0.0
NET Q TO COLD H2O	W	-6810.21	-6810.88	-6810.67
UNACCT PWR LOSS	W	0.10	0.10	0.00
REGENATR EFFECTVNS		0.8595	0.8595	0.8595

GPU-3 HYDROGEN 927K/339K STIRLING ENGINE DATA: 1 (UPDATED JAN 83)

THIS RUN ENDED AT TIME 11.33.38

THE ELAPSED TIME FOR THIS RUN IS 15.86

## APPENDIX C DEFINITIONS

### DEFINITIONS USED IN SEAM

VARIABLE	COMMON BLOCK	CALC. IN ROUTINE	DEFINITION/UNITS
ADPGAS	( FADD)	INPUT	-GAS PRESSURE IN ADDED VOLUME (MPA)
ADRADA	( FADD)	INPUT	-RADIATION SURFACE AREA TERM (SQ M)
ADTGAS	( FADD)	INPUT	-GAS TEMPERATURE IN ADDED VOLUME (K)
ADVOL	( FADD)	INPUT	-GAS VOLUME IN ADDED VOLUMES (CU M)
ADIALX	( FADD)	INPUT	-EFFECTIVE LENGTH FOR AXIAL HEAT CONDUCTION ALONG DISPLACER SHELL (M)
ADWLDI	( FADD)	INPUT	-WALL INNER DIAMETER OF ADDED VOLUME (M)
ADWLTH	( FADD)	INPUT	-WALL THICKNESS OF ADDED VOLUME (M)
AFC	( RIOSF)	RIOSIN	-COOLER TOTAL FLOW AREA (SQ M)
AFH	( RIOSF)	RIOSIN	-HEATER TOTAL FLOW AREA (SQ M)
AFLOW	(FLCELL)	INPUT	-GAS FLOW AREA PER TUBE FOR A CELL (SQ M)
AFR	( RIOSF)	RIOSIN	-REGENERATOR TOTAL GAS FLOW AREA (SQ M)
ALOSSC	( )	HTFLOW	-COOLER EXPANSION/CONTRACTION FRICTION POWER LOSS (W)
ALOSSE	( )	HTFLOW	-HEATER EXPANSION/CONTRACTION FRICTION POWER LOSS (W)
AMETAL	( )	LOSSES	-REGENERATOR METAL DIFFUSIVITY (SQ.M/SEC)
ANGLE	(VARVOL)	INITAL RIOSIN	-CRANK ANGLE (RADIAN)
ARG	( RIOSF)	HTFLOW	-PRESSURE TO VOLUME PHASE ANGLE (RADIAN)
ARODE	( )	INITAL VOLUME	-CROSS SECTIONAL AREA OF EXPANSION PISTON ROD (SQ M)
ASPECT	(FLCELL)	INPUT	-RATIO OF SHORT/LONG SIDES FOR RECTANGULAR DUCT
AWC	( RIOSF)	RIOSIN	-COOLER TOTAL WETTED AREA (SQ M)
AWET	(FLCELL)	INPUT	-WETTED AREA PER TUBE OF A CELL (SQ M) HYD DIA = VOLUME / AWET
AWH	( RIOSF)	RIOSIN	-HEATER TOTAL WETTED AREA (SQ M)
AWR	( RIOSF)	RIOSIN	-REGENERATOR TOTAL WETTED AREA (SQ M)
AXWALL	(FLCELL)	INPUT	-CROSS-SECTIONAL AREA OF WALL FOR HEAT CONDUCTION (SQ M) FOR ONE TUBE
C	( RIOSD)	RIOSIN	-COMPRESSION ZONE TOTAL DIMENSIONLESS VOLUME AT THE MID TIME STEP
CBUF	( RIOSD)	RIOSIN	-COMPRESSION BUFFER ZONE TOTAL DIMENSIONLESS VOLUME AT THE MID TIME STEP
CI	( RIOSD)	RIOSIN	-COMPRESSION ZONE TOTAL DIMENSIONLESS VOLUME AT THE BEGINNING OF THE STEP
CMPAP	(VARVOL)	INITAL	-COMPRESSION PISTON AREA (SQ M)
CMPBOR	(VARVOL)	INITAL	-COMPRESSION CYLINDER BORE (M)
CMPCR	(FLTGEN)	INPUT	-COMPRESSION PISTON CRANK RADIUS (M)
CMPCRL	(FLTGEN)	INPUT	-COMPRESSION PISTON CONNECTING ROD LENGTH (M) SHOULD BE LESS THAN 1000*CMPCR
CMPDEL	(VARVOL)	VOLUME	-OVERLAP IN COMPRESSION ZONE PISTON MOTION TYPICAL OF DISPLACER MACHINES (M)
CMPDV	(FLTGEN)	INPUT INITAL	-COMPRESSION ZONE DEAD VOLUME (CU M) WILL BE TREATED THE SAME AS ACTIVE VOLUME IE WILL BE ADIABATIC IN SEAM 1
CMPECC	(FLTGEN)	INPUT	-COMPRESSION PISTON CRANK RADIUS ECCENTRICITY (M)
CMPGAP	(FLTGEN)	INPUT	-COMPRESSION PISTON CYLINDER WALL GAP (M)
CMPMAX	(VARVOL)	VOLUME	-COMPRESSION PISTON MAXIMUM STROKE POSITION (M)

## DEFINITIONS USED IN SEAM

VARIABLE	COMMON BLOCK	CALC. IN ROUTINE	DEFINITION/UNITS
CMFMIN	(VARVOL)	VOLUME	-COMPRESSION PISTON MINIMUM STROKE POSITION
CMPPPOS	(VARVOL)	VOLUME	-COMPRESSION PISTON CURRENT STROKE POSITION (M)
CMPRD	(FLTGEN)	INPUT	-COMPRESSION PISTON ROD DIAMETER (M)
CMPSRK	(VARVOL)	VOLUME	-COMPRESSION PISTON NET STROKE (M)
CONVER	( )	HTFLOW	-CONVERSION FACTOR TO CHANGE WORK TERMS TO POWER TERMS FOR A DESIGN
CPGAS	(GASFRP)	INITAL HTFLOW	-REFERENCE VALUE OF GAS SPECIFIC HEAT AT CONSTANT PRESSURE (J/KG-K)
CRANK	(VARVOL)	VOLUME	-CRANK ANGLE BETWEEN TDC OF EXPANSION AND COMPRESSION PISTONS (RAD)
CRANKD	(FLTGEN)	INITAL INPUT INPDRV	-SAME AS CRANK (DEGREES)
CTLL	( RIOSF)	RIOSIN	-COOLER TOTAL LENGTH (M)
CTLS	( RIOSF)	RIOSIN	-COOLED LENGTH OF COOLER (M)
CVGAS	(GASFRP)	INITAL HTFLOW	-REFERENCE VALUE OF GAS SPECIFIC HEAT AT CONSTANT VOLUME (J/KG-K)
DARFRD	( PDROP)	HTFLOW	-DARCY FRICTION FACTOR IN THE COOLER
DARFRH	( PDROP)	HTFLOW	-DARCY FRICTION FACTOR IN THE HEATER
DARFRR	( PDROP)	HTFLOW	-DARCY FRICTION FACTOR IN THE REGENERATOR
DC	( RIOSD)	RIOSIN	-COMPRESSION ZONE VOLUMETRIC TIME DERIV AT MID STEP (DIMENSIONLESS/RAD)
DCI	( RIOSD)	RIOSIN	-COMPRESSION ZONE VOLUMETRIC TIME DERIV AT BEGINING OF STEP (DIMENSIONLESS/RAD)
DE	( RIOSD)	RIOSIN	-EXPANSION ZONE VOLUMETRIC TIME DERIV AT MID STEP (DIMENSIONLESS/RAD)
DEI	( RIOSD)	RIOSIN	-EXPANSION ZONE VOLUMETRIC TIME DERIV AT BEGINNING OF STEP (DIMENSIONLESS/RAD)
DELANG	(VARVOL)	INITAL	-CRANK RADIANS PER TIME STEP (RAD)
DFREQ	( )	INPDRV	-CHANGE IN FREQUENCY IN EACH PERTURBATION (HZ)
DH	(FLCELL)	INPUT	-HYDRAULIC DIAMETER OF A CELL (M)
DPR	( RIOSD)	HTFLOW CYCLER	-ARRAY CONTAINING THE DIMENSIONLESS PRESSURE CHANGE OVER A STEP
DSTRK	( )	INPDRV	-CHANGE IN STROKE RATIO IN EACH PERTURBATION
DTIME	( AMISC)	INITAL	-TIME STEP (SEC)
DVOLDT	(VARVOL)	VOLUME	-VOLUMETRIC TIME DERIVATIVE (CU M/SEC) SAME NUMBERING SCHEME AS VOL
E	( RIOSD)	RIOSIN	-EXPANSION ZONE TOTAL DIMENSIONLESS VOLUME AT THE MID TIME STEP
EBUF	( RIOSD)	RIOSIN	-EXPANSION BUFFER ZONE TOTAL DIMENSIONLESS VOLUME AT THE MID TIME STEP
EI	( RIOSD)	RIOSIN	-EXPANSION ZONE TOTAL DIMENSIONLESS VOLUME AT THE BEGINING OF THE STEP
EMIS	( FADD)	INPUT	-EMISSIVITY OF THE DISPLACER RADIATION SHIELDS
ERR	( )	CONVRG	-MAXIMUM FRACTIONAL CHANGE IN COOLER HEAT FLOW TERMS
EXPAP	(VARVOL)	INITAL	-EXPANSION PISTON AREA (SQ M)
EXPBOR	(VARVOL)	INITAL	-EXPANSION CYLINDER BORE (M)

## DEFINITIONS USED IN SEAM

VARIABLE	COMMON BLOCK	CALC. IN ROUTINE	DEFINITION/UNITS
EXPCR	(FLTGEN)	INPUT INPDRV	-EXPANSION PISTON CRANK RADIUS (M)
EXPCRL	(FLTGEN)	INPUT	-EXPANSION PISTON CONNECTING ROD LENGTH (M) SHOULD BE LESS THAN 1000*EXPCR
EXPDV	(FLTGEN)	INPUT INPDRV	-EXPANSION ZONE DEAD VOLUME (CU M) WILL BE TREATED THE SAME AS ACTIVE VOLUME IE WILL BE ADIABATIC IN SEAM 1
EXPECC	(FLTGEN)	INPUT	-EXPANSION PISTON CRANK RADIUS ECCENTRICITY (M)
EXPGAP	(FLTGEN)	INPUT	-EXPANSION PISTON CYLINDER WALL GAP (M)
EXP:MAX	(VARVOL)	VOLUME	-EXPANSION PISTON MAXIMUM STROKE POSITION (M)
EXP:MIN	(VARVOL)	VOLUME	-EXPANSION PISTON MINIMUM STROKE POSITION (M)
EXP:POS	(VARVOL)	VOLUME	-EXPANSION PISTON CURRENT STROKE POSITION (M)
EXPRD	(FLTGEN)	INPUT	-EXPANSION PISTON ROD DIAMETER (M)
EXPSRK	(VARVOL)	VOLUME	-EXPANSION PISTON NET STROKE (M)
FREQ	(FLTGEN)	INPUT INPDRV	-FREQUENCY (HZ)
FRICML	(FLCELL)	INPUT	-FRICTION MULTIPLIER FOR A CELL
FUNCC		VOLUME	-STATEMENT FUNCTION USED TO COMPUTE THE ABSOLUTE AXIAL POSITION OF THE COMPRESSION PISTON (M)
GAMMA	(GASPRP)	INITAL	-REFERENCE SPECIFIC HEAT RATIO
GRAFIC	( OUTPT)	CYCLER	-ARRAY CONTAINING CYCLIC DATA AT 5 DEGREE INTERVALS-- CURRENTLY CONTAINS: 1-ANGLE, 2-EXP VOL, 3-PRESS, 4-CMP VOL, 5-CMP MASS, 6-EXP MASS, 7-CMP PIS TORQ, 8-CMP TEMP, 9-EXP TEMP, 10-EMPTY
HAF	( AMISC)	INPUT	-0.5
HASC	( )	HTFLOW	-HEAT TRANSFER CONDUCTANCE FROM THE GAS TO THE COOLER WALL (W/K)
HASH	( )	HTFLOW	-HEAT TRANSFER CONDUCTANCE FROM THE GAS TO THE HEATER WALL (W/K)
HCEXT	(FLCELL)	INPUT	-WALL TO ENVIRONS HEAT TRANSFER COEFFICIENT (W/SQ.M-K)
HCMBST	( )	HTFLOW	-HEAT TRANSFER COEFFICIENT BETWEEN THE HEATER WALL AND THE COMBUSTION GAS (W/SQ.M-K)
HCV	( RIOSF)	CYCLER	-DIMENSIONLESS COOLER DEAD VOLUME
HHV	( RIOSF)	RIOSIN	-DIMENSIONLESS HEATER DEAD VOLUME
HRV	( RIOSF)	CYCLER	-DIMENSIONLESS REGENERATOR DEAD VOLUME
HTLL	( RIOSF)	RIOSIN	-HEATER TOTAL LENGTH (M)
HTLS	( RIOSF)	RIOSIN	-HEATER TOTAL HEATED LENGTH (M)
HYSTF	(FLTGEN)	INPUT	-THERMAL HYSTERSIS FACTOR
IACOND	( IADD)	INPUT	-KEY FOR CONDUCTION BETWEEN VARIABLE AND ADDED VOLUMES
IALEAK	( IADD)	INPUT	-KEY FOR GAS LEAKAGE BETWEEN VARIABLE AND ADDED VOLUMES
IAMTL	( IADD)	INPUT	-KEY FOR WALL MATERIAL IN ADDED VOLUMES

## DEFINITIONS USED IN SEAM

VARIABLE	COMMON BLOCK	CALC. IN ROUTINE	DEFINITION/UNITS
IATYPE	( IADD)	INPUT	-KEY FOR ADDED VOLUME DESCRIPTION CURRENTLY USES: 10-PSITON DOME OR DISPLACER (VOL A) 20-COLD PISTON BUFFER SPACE (VOL C) 25-HOT PISTON BUFFER SPACE (VOL B) 40-CRANKCASE (VOL D)
ICHNG	( IGEN)	INPUT	-KEY TO USE PERTURBATION SYSTEM
ICPGAS	( JMISC)	INITAL	-GAS HEAT CAPACITY IDENTIFIER SET TO 12, COEFFICIENTS IN NEXT BLOCK DATA
ICPM	( JMISC)	INITAL	-METAL HEAT CAPACITY IDENTIFIER SET TO 27, COEFFICIENTS IN NEXT BLOCK DATA
IDESGN	( IGEN)	INPUT	-KEY TO DETERMINE ENGINE TYPE 1-IN LINE, 2-DBLE ACTING, 3-DISPLACER
IDRIVE	( IGEN)	INPUT	-KEY TO DETERMINE DRIVE MECHANISM 0-CONNECTING ROD, 1-RHOMBIC DRIVE
IERROR	( JMISC)	MAIN CONVRG INPDRV INPUT INITAL VOLUME ANALIS CYCLER	-GENERAL ERROR KEY IF 0, NO ERROR
IGAS	( IGEN)	INPUT	-WORKING FLUID BEING USED 1-HYDROGEN 2-HELIUM 3-NITROGEN 4-AIR 5-CO2 6-METHANE
IGRAPH	( IGEN)	INPUT	-KEY FOR GRAPHICAL OUTPUT 0-NO OUTPUT 1-CYCLE OUTPUT 2-CASE OUTPUT
IKGAS	( JMISC)	INITAL	-GAS THERMAL CONDUCTIVITY IDENTIFIER SET TO 18, COEFFICIENTS IN NEXT BLOCK DATA
IKM	( JMISC)	INITAL	-METAL THERMAL CONDUCTIVITY IDENTIFIER SET TO 18, COEFFICIENTS IN NEXT BLOCK DATA
IMASS	( IGEN)	INPUT	-KEY TO DETERMINE CONSTANT MASS OR MEAN PRESSURE 0-P FIXED, 1-M FIXED
IMOD	( JMISC)	INPDRV	-CURRENT STEP IN PERTURBATION (0-NMODS) IF LT 0, THEN ON LAST CASE.
IMOM	( IGEN)	INPUT	-KEY FOR INERTIAL EFFECTS CALC
IMUGAS	( JMISC)	INITAL	-GAS DYNAMIC VISCOSITY IDENTIFIER SET TO 6, COEFFICIENTS IN NEXT BLOCK DATA
IND	( )	CYCLER	-KEY FOR INTEGRATION BOUNDARY CONDITIONS 1-MASS INCREASE BOTH VOLUMES 2-MASS INCREASE HOT VOLUME 3-MASS INCREASE COLD VOLUME 4-MASS DECREASE BOTH VOLUMES
IPRT1	( IGEN)	INPUT	-KEY TO PRODUCE ADDED PRINTS 0-NO ADDITIONAL PRINTS 1-ADDED INITIALIZATION PRINTS 2-CYCLE BY CYCLE PRINTS 3-DETAILED WITHIN CYCLE PRINTS 4-CYCLE WRAPUP PRINTS
IRGAS	( JMISC)	INITAL	-GAS CONSTANT IDENTIFIER SET TO 0, COEFFICIENTS IN NEXT BLOCK DATA



## DEFINITIONS USED IN SEAM

VARIABLE	COMMON BLOCK	CALC. IN ROUTINE	DEFINITION/UNITS
IRHON	( JMISC )	INITAL	-METAL DENSITY IDENTIFIER SET TO 36, COEFFICIENTS IN NEXT BLOCK DATA
IRUN	( )	MAIN	-CURRENT CASE NUMBER
ITWLCH	( )	INPDRV	-KEY FOR COMBUSTION TEMPERATURE CHANGE WITH PERTURBATION STEP, INOD
JCELL	( JMISC )	INPUT OUT1	-CELL NUMBER BEING INPUT, AFTER INPUT COMPLETED JCELL=TOTAL NUMBER OF CELLS IN THE ENGINE. ON LAST STEP JCELL IS SET TO 0 TO KEY TIMERS.
JCOLN	( JMISC )	INITAL	-LAST COOLER CELL
JCOL1	( JMISC )	INITAL	-FIRST COOLER CELL
JCOOL	( JMISC )	INITAL	-MIDDLE COOLER CELL
JFIXN	( JMISC )	INITAL	-LAST CONSTANT VOLUME CELL
JFIX1	( JMISC )	INITAL	-FIRST CONSTANT VOLUME CELL
JHOT	( JMISC )	INITAL	-MIDDLE HEATER CELL
JHTRN	( JMISC )	INITAL	-LAST HEATER CELL
JHTR1	( JMISC )	INITAL	-FIRST HEATER CELL
JREG	( JMISC )	INITAL	-MIDDLE REGENERATOR CELL
JREGN	( JMISC )	INITAL	-LAST REGENERATOR CELL
JREG1	( JMISC )	INITAL	-FIRST REGENERATOR CELL
MHTRF	( INCELL )	INPUT	-FRICTION TO NUSSELT NUMBER CORRELATION USED, 0-SEPARATE FORMULA, 1-COLBURN=F/2
MQFLOW	( INCELL )	INPUT	-CELL GAS TO WALL TO EXTERNAL ENVIRONS HEAT FLOW CALCULATION, 0-CONSTANT T WALL, 1-CONSTANT Q WALL 2-CONSTANT T GAS, 3-NO NET Q WALL
MTLWAL	( INCELL )	INPUT	-METAL USED IN WALL 7-AL 2024 T4                    8-COPPER 9-INCONEL X750                10-K MONEL 11-304 SS                        12-310 SS 13-316 SS                        14-TI 120VCA 15-NI
MTLWIR	( INCELL )	INPUT	-METAL USED IN FILLER MATERIAL USED IN REGENERATORS, NUMBER AS MTLWAL
MTYPE	( INCELL )	INPUT	-COMPONENT DESCRIPTION OF CELL: 10-TUBE OR CYLINDER    11-RECT DUCT 15-TUBE CONNECTIR     16-RECT CONNECTOR 17-ORIFICE CONNECTOR 20-VARIABLE COLD VOL    21-DISPLACER SIDE 20 22-PISTON SIDE 20        25-VARIABLE HOT VOL 30-SCREEN REGEN         31-SPHERE REGEN 32-MET NET REGEN        33-SLRE SHEET REGEN 34-TUBE REGENERATOR
NADD	( IGEN )	INPUT	-NUMBER OF ADDED COMPONENTS
NCASE	( )	MAIN	-CURRENT OUTPUT CASE NUMBER, SEE IRUM
NCMPRS	( JMISC )	INPUT	-FIRST, KEY, CELL IN COMPRESSION ZONE
NCODE	( IGEN )	INPUT	-KEY FOR ANALYSIS MODULE 0-RIOS, 1-URIELI, 2-TEW IF GT 9, OPTIMIZATION ALSO IN EFFECT.
NCOMP	( IGEN )	INPUT	-NUMBER OF COMPONENTS INPUT, <=JCELL
NCYCLE	( JMISC )	ANALIS	-CURRENT CYCLE NUMBER, <=NREVL

## DEFINITIONS USED IN SEAM

VARIABLE	COMMON BLOCK	CALC. IN ROUTINE	DEFINITION/UNITS
NCYL	( IGEN)	INPUT	-NUMBER OF CYLINDERS IN ENGINE CYLINDER=EXPAN-HTR-REGEN-COOL-CMPRS ZONES
NDIV	( )	CYCLER	-NUMBER OF STEPS IN CYCLE BEFORE SAVING CYCLE INFORMATION. SET TO NSTEP/72
NDS	( )	HTFLOW	-NUMBER OF AXIAL DIVISIONS USED BY PDINT TO SUBDIVIDE INTEGRAL FOR MASS FLUX TERMS SET TO 10
NIHX	(INCELL)	INPUT	-NUMBER OF HEAT EXCHANGERS REPRESENTED BY THIS CELL, IE NUMBER OF HTR TUBES ETC
NMODS	( )	INPDRV	-NUMBER OF PERTURBATIONS TO BE RUN, USED TO VARY FREQUENCY OR STROKE RATIO
NOPT	( IGEN)	INPUT	-HEAT FLOW OPTION USED IN COOLING WATER 0-QDYNAM+QSTATC DIRECT TO WATER 1-QDYNAM+QREGWL+QCYLWL TO WATER 2-QREGWL+QCYLWL DIRECT TO WATER 3-ONLY QREGWL DIRECT TO WATER (ALL OTHER HEAT FLOWS TO THE GAS THRU THE COOLER INTO THE WATER)
NOPT1	(INCELL)	INPUT	-NOT USED, CELL DEPENDENT INTEGER
NPRT1	( IGEN)	INPUT	-PRINT FREQUENCY WITHIN THE CYCLE I SET THIS TO 2*NSTEP TO EDIT EVERY OTHER CASE, CONTROLS OUTPUT OF VECTR IT WILL BE MORE RELEVANT IN SEAM 2 OR SEAM 3
NPRT2	( IGEN)	INPUT	-NUMBER OF CASES TO BE EDITED TOGETHER
NREVL	( IGEN)	INPUT	-MAXIMUM NUMBER OF CYCLES TO BE COMPUTED IN A CASE
NRINGS	( IADD)	INPUT	-NUMBER OF RINGS FOR LEAKAGE CALC
NSHLD	( IADD)	INPUT	-NUMBER OF SHIELDS IN DISPLACER
NSTEP	( IGEN)	INPUT	-NUMBER OF STEPS IN A REVOLUTION
NSTRK	( JMISC)	INPDRV	-KEY FOR STROKE (1) OR FREQUENCY (0) VARIATION WITH CASE
NTITLE	( JMISC)	INPUT	-CARD IMAGE OF FIRST INPUT CARD THIS APPEARS ON TOP OF EACH PAGE AND IS OUTPUT WITH GRAPHICS, I USE THE FIRST 24 CHARACTERS AS THE TITLE ON PLOTS
NVOLA	( JMISC)	INPUT	-ADDED VOLUME COMPONENT REPRESENTING VOLUME A, DISPLACER OR HOT PISTON DOME
NVOLB	( JMISC)	INPUT	-ADDED VOLUME COMPONENT REPRESENTING VOLUME B, HOT PISTON BUFFER SPACE
NVOLC	( JMISC)	INPUT	-ADDED VOLUME COMPONENT REPRESENTING VOLUME C, COLD PISTON BUFFER SPACE
NVOLD	( JMISC)	INPUT	-ADDED VOLUME COMPONENT REPRESENTING VOLUME D, CRANKCASE
NZONES	( JMISC)	RIOSPR	-NUMBER OF COMPUTATIONAL ZONES TO BE USED IN CALCULATION, SEAM 1 USES 5
OMEGA	( AMISC)	INITAL	-FREQUENCY (RAD)
ONE	( AMISC)	INPUT	-1.000
ORIFCE	(FLCELL)	INPUT	-CELL ORIFICE PRESSURE DROP COEFFICIENT EQUIVALENT TO CONSTANT FANNING FRICTION
PDRGPC	( PDROP)	HTFLOW	-FRICTION PRESSURE DROP IN COOLER (PA)
PDROPH	( PDROP)	HTFLOW	-FRICTION PRESSURE DROP IN HEATER (PA)
PDROPR	( PDROP)	HTFLOW	-FRICTION PRESSURE DROP IN REGENERATOR (PA)

## DEFINITIONS USED IN SEAM

VARIABLE	COMMON BLOCK	CALC. IN ROUTINE	DEFINITION/UNITS
PGAS	(FLCELL)	INPUT INITAL	-GAS PRESSURE IN CELL (PA)
PGASAD	(DYNPRP)	INITAL CYCLER	-CURRENT VALUE OF GAS PRESSURE IN ADDED VOLUMES (PA)
PGASD	(DYNPRP)	INITAL	-CURRENT VALUE OF GAS PRESSURE IN CELLS (PA)
PHASED	(FLTGEN)	INPUT INITAL INPDRV	-CRANK ANGLE BETWEEN EXPANSION VOLUME MINIMUM AND COMPRESSION VOLUME MINIMUM (DEG)
PHASER	(VARVOL)	VOLUME INITAL	-SAME AS PHASED (RAD)
PI	( AMISC)	INPUT	-3.14159...
PIOV4	( AMISC)	INPUT	-PI / 4
PITER	( )	CYCLER	-INNER ITERATION INITIAL DIMENSIONLESS PRESSURE VALUES
PMAX	(ENFLOW)	HTFLOW RIOSIN	-CURRENT MAXIMUM PRESSURE IN CYCLE (PA)
PMEAN	(FLTGEN)	INPUT INITAL	-MEAN PRESSURE IN CYCLE (PA)
PMEAND	(DYNPRP)	INITAL RIOSIN HTFLOW	-CURRENT MEAN PRESSURE IN CYCLE (PA)
PMIN	(ENFLOW)	HTFLOW	-CURRENT MINIMUM PRESSURE IN CYCLE (PA)
PMXANG	(ENFLOW)	HTFLOW	-CRANK ANGLE AT WHICH PRESSURE REACHES A MAXIMUM (DEG)
PNAVG	( )	HTFLOW	-DIMENSIONLESS AVERAGE PRESSURE IN CYCLE
PNMAX	( RIOSF)	HTFLOW	-DIMENSIONLESS MAXIMUM PRESSURE IN CYCLE
POROS	(FLCELL)	INPUT	-POROSITY, VOID FRACTION, OF FILLER MATERIAL
POWER	(ENFLOW)	ANALIS	-NET POWER IN ENGINE (WATTS)
PR	( RIOSD)	CYCLER HTFLOW	-DIMENSIONLESS PRESSURE AT EACH STEP IN CYCLE
PSIMIN	(VARVOL)	VOLUME	-ABSOLUTE ANGLE AT WHICH THE COMPRESSION ZONE VOLUME IS A MINIMUM (RAD)
PSISTR	(VARVOL)	VOLUME	-ABSOLUTE ANGLE AT WHICH THE EXPANSION ZONE VOLUME IS A MINIMUM (RAD)
PST	( )	INITAL	-SCHMIDT ANALYSIS DETERMINED INITIAL PRESSURE (PA)
PSTOPM	( )	INITAL RIOSIN	-RATIO OF STARTING PRESSURE TO AVERAGE PRESSURE, BASED ON SCHMIDT ANALYSIS
QACTC	(ENFLOW)	HTFLOW	-GAS TO COOLER WALL HEAT FLOW (W)
QACTH	(ENFLOW)	HTFLOW	-GAS TO HEATER WALL HEAT FLOW (W)
QCYLWL	(ENFLOW)	LOSSES	-HEAT FLOW ALONG CYLINDER WALL (W)
QDYHAM	(ENFLOW)	LOSSES	-SUM OF HEAT FLOW DUE TO QEXPGRP+QEXPSH (W)
QEXPGRP	( )	LOSSES	-HEAT FLOW DUE TO PISTON GAP PRESSURIZATION (W)
QEXPSH	( )	LOSSES	-HEAT FLOW BETWEEN PISTON AND CYLINDER WALL DUE TO THE RELATIVE MOTION (W)
QFLOW	(FLCELL)	INPUT	-HEAT FLOW FROM CELL WALL TO EXTERNAL ENVIRONMENT (W)
QFRIC	(ENFLOW)	HTFLOW	-TOTAL FRICTIONAL HEAT FLOW (W)

## DEFINITIONS USED IN SEAM

VARIABLE	COMMON BLOCK	CALC. IN ROUTINE	DEFINITION/UNITS
QHTRFR	( )	HTFLOW	-HEAT FLOW DUE TO HEATER FRICTION (W)
QHYSTC	(ENFLOW)		-HYSTERESIS HEAT FLOW IN COMPRESSION ZONE (W)
QHYTE	(ENFLOW)		-HYSTERESIS HEAT FLOW IN EXPANSION ZONE (W)
QKOLFR	( )	HTFLOW	-HEAT FLOW DUE TO COOLER FRICTION (W)
QLEAK	(ENFLOW)	LOSSES	-HEAT FLOW DUE TO GAS LEAKAGE (W)
QPISHL	(ENFLOW)	LOSSES	-HEAT FLOW ALONG PISTON WALL (W)
QREGER	(ENFLOW)	HTFLOW	-TOTAL REGENERATOR REHEAT LOSS (W)
QREGFL	(ENFLOW)	LOSSES	-CONDUCTION HEAT FLOW THRU FILLER MATERIAL (W)
QREGFR	( )	HTFLOW	-HEAT FLOW DUE TO REGENERATOR FRICTION (W)
QREGWL	(ENFLOW)	LOSSES	-CONDUCTION HEAT FLOW ALONG THE REGENERATOR WALL (W)
QSTATC	(ENFLOW)	LOSSES	-SUM OF ALL CONDUCTION HEAT FLOWS (W) QPISHL+QCYLWL+QREGWL+QREGFL
RDIA	(RIOSF)	RIOSIN	-REGENERATOR INNER WALL DIAMETER (M)
REGHT	(FLTGEN)	INPUT	-CONDUCTION HEIGHT FROM THE TOP OF THE REGENERATOR TO THE TOP OF THE EXPANSION CYLINDER (M)
REYC	(PDROP)	HTFLOW	-REYNOLDS NUMBER BASED ON DH AND XMDOT- FOR THE COOLER
REYH	(PDROP)	HTFLOW	-REYNOLDS NUMBER BASED ON DH AND XMDOT- FOR THE HEATER
REYR	(PDROP)	HTFLOW	-REYNOLDS NUMBER BASED ON DH AND XMDOT- FOR THE REGENERATOR
RGAS	(GASPRP)	INITAL	-REFERENCE GAS CONSTANT (J/KG-K)
RGL	(RIOSF)	RIOSIN	-TOTAL LENGTH OF REGENERATOR (M)
RINGCL	( FADD)	INPUT	-GAP BETWEEN RING AND WALL (M)
RINGFR	( FADD)	INPUT	-RING FRICTION COEFFICIENT
RINGHT	( FADD)	INPUT	-RING HEIGHT (M)
RINGLK	( FADD)	INPUT	-RING LEAK COEFFICIENT (KG/PA-SEC)
RP	( )	HTFLOW	-PRESSURE RATIO P <sub>MAX</sub> /P <sub>MIN</sub>
RVT	(RIOSF)	CYCLER	-DISPLACED MASS RATIO COLD (VOL/TEMP) * HOT (TEMP/VOL)
SCALR	( OUTPT)	RIOSPR	-ARRAY CONTAINING 50 VARIABLES FOR OUTPUT A FULL LIST OF THIS CONTAINER ARRAY IS GIVEN IN ROUTINES OUT1 AND RIOSPR
SCHDEL	(VARVOL)	INITAL	-SCHMIDT ANALYSIS CONSTANT, RELATES PRESSURE RATIO, SCHDEL = SCHAA/SCHBB
SIGMA	(FLCELL)	INPUT	-RATIO OF MINIMUM FLOW AREA TO FRONTAL AREA IN A CELL. SIGMA<=POROS
SLNGTH	( FADD)	INPUT	-LENGTH USED FOR SHUTTLE HEAT FLOW (M)
STARTD	(FLTGEN)	INPUT	-CRANK ANGLE AT TIME=0.0 (DEGREE)
STARTR	(VARVOL)	INITAL	-SAME AS STARTD (RAD)
STC	( )	HTFLOW	-COOLER TUBE AVERAGE STANTON NUMBER
SUMDC	(RIOSF)	RIOSIN	-SUM OF THE ABS(DC). (CU M/SEC)

## DEFINITIONS USED IN SEAM

VARIABLE	COMMON BLOCK	CALC. IN ROUTINE	DEFINITION/UNITS
TMBST	(FLTGEN)	INPUT INPDRV INITAL	-EXTERNAL HEATER TEMPERATURE (K)
TEST	( )	CYCLER	-NET CHANGE IN EXPANSION SPACE DIMENSIONLESS MASS OVER THE CYCLE
TEST1	( )	CYCLER	-NET CHANGE IN DIMENSIONLESS ENGINE PRESSURE OVER THE CYCLE
TGAS	(FLCELL)	INPUT	-GAS TEMPERATURE IN A CELL (K)
TGASAD	(DYNPRP)	INITAL	-CURRECNT GAS TEMPERATURE IN A ADDED VOLUME (K)
TGASD	(DYNPRP)	INITAL HTFLOW	-CURRENT GAS TEMPERATURE IN A CELL (K)
TGASO	(DYNPRP)	INITAL CONVRG	-LAST VALUE OF TGASD (K) USED FOR CONVERGENCE
THETA	(VARVOL)	INITAL	-SCHMIDT ANALYSIS PRESSURE VOLUME PHASE ANGLE (RAD)
TIME	( AMISC)	INITAL	-CURRENT TIME (SEC)
TMASS	(FLTGEN)	INPUT	-INITIAL TOTAL MASS OF GAS IN ENGINE (KG)
TMASSD	(DYNPRP)	INITAL RIOSIN HTFLOW	-CURRENT MASS OF GAS IN ENGINE (KG)
TMAXC	( PDROP)	CYCLER	-MAXIMUM GAS TEMPERATURE DURING CYCLE IN COMPRESSION ZONE (K)
TMAXE	( PDROP)	CYCLER	-MAXIMUM GAS TEMPERATURE DURING CYCLE IN EXPANSION ZONE (K)
TMINC	( PDROP)	CYCLER	-MINIMUM GAS TEMPERATURE DURING CYCLE IN COMPRESSION ZONE (K)
TMINE	( PDROP)	CYCLER	-MINIMUM GAS TEMPERATURE DURING CYCLE IN EXPANSION ZONE (K)
TORQC	(ENFLOW)	RIOSIN ANALIS	-TORQUE IN COMPRESSION ZONE
TORQE	(ENFLOW)	RIOSIN ANALIS	-TORQUE IN EXPANSION ZONE
TREGWD	(DYNPRP)	INITAL	-CURRENT REGENERATOR WALL TEMPERATURE (K)
TREGWO	(DYNPRP)	CONVRG INITAL	-LAST REGENERATOR WALL TEMPERATURE (K) USED IN CONVERGENCE SCHEME
TRSHLD	(DYNPRP)		-CURRENT VALUE OF RADIATION SHIELD TEMPERATURE (K)
TRTO	( RIOSF)	HTFLOW RIOSIN CYCLER	-CURRENT GAS TEMPERATURE RATIO THOT/TCOOL
THALL	(FLCELL)	INPUT	-WALL TEMPERATURE OF CELL (K)
THALLO	(DYNPRP)	INITAL HTFLOW	-CURRENT WALL TEMPERATURE OF CELL (K)
THATER	(FLTGEN)	INPUT INITAL	-COOLING WATER AVERAGE TEMPERATURE (K)
THENVR	(FLTGEN)	INPUT INITAL	-AVERAGE ENVIRONMENT TEMPERATURE (K) INITIALIZED TO 300. K
THLHI	( )	INPDRV	-PERTURBATION DEPENDENT TMBST (K)/
TWO	( AMISC)	INPUT	-2.00
VAC	( RIOSF)	RIOSIN	-HALF THE MAXIMUM COMPRESSION DISPLACEMENT (CU M)

## DEFINITIONS USED IN SEAM

VARIABLE	COMMON BLOCK	CALC. IN ROUTINE	DEFINITION/UNITS
VAE	( RIOSF )	RIOSIN	-HALF THE MAXIMUM EXPANSION DISPLACEMENT (CU M)
VCD	( RIOSF )	RIOSIN	-TOTAL COOLER RELATED DEAD VOLUME (CU M)
VD	( RIOSF )	RIOSIN	-TOTAL ENGINE RELATED DIMENSIONLESS DEAD VOLUME
VECTR	( OUTPT )	RIOSPR	-ARRAY CONTAINING 15 VARIABLES BY ZONE FOR OUTPUT 1 TG MAX(K) 2 TG AVG(K) 3 TW-TG AVG(K) 4 TH-TG MAX(K) 5 Q NET (W) 6 M FLUX(KG/S) 7 M FLUX MAX 8 REY NUMBR 9 D-P FRIC(MPA) 10 NUSSELT NUMBR 11-15 NOT USED
VOL	( FLCELL )	INITAL	-CELL VOLUME (CU M)
VOLAD	( DYNPRP )		-ADDED VOLUME CELL CURRENT TOTAL VOLUME (CU.M)
VOLS	( VARVOL )	VOLUME	-VARIABLE VOLUME ARRAY (CU M) 1-EXPANSION 2-HOT SIDE COMPRESSION 3-COLD SIDE COMPRESSION 4-HOT SIDE BUFFER 5-COLD SIDE BUFFER
VOLHL	( FLCELL )	INPUT	-WALL VOLUME BY CELL (CU M)
VRD	( RIOSF )	RIOSIN	-TOTAL REGENERATOR RELATED DEAD VOLUME (CU M)
WALLTH	( FLCELL )	INPUT	-WALL THICKNESS OF A CELL (M)
WC	( RIOSF )	CYCLER	-DIMENSIONLESS COMPRESSION SPACE WORK
WE	( RIOSF )	CYCLER	-DIMENSIONLESS EXPANSION SPACE WORK
WORKC	( ENFLOW )	ANALIS	-COMPRESSION SPACE WORK (J)
WORKE	( ENFLOW )	ANALIS	-EXPANSION SPACE WORK (J)
XLNGTH	( FLCELL )	INPUT	-CELL LENGTH (M)
XDMC	( RIOSD )	CYCLER	-ARRAY OF CHANGES IN DIMENSIONLESS MASS IN THE COMPRESSION SPACE
XDME	( RIOSD )	CYCLER	-ARRAY OF CHANGES IN DIMENSIONLESS MASS IN THE EXPANSION SPACE
XMC	( RIOSF )	CYCLER	-CURRENT DIMENSIONLESS MASS IN COMPRESSION ZONE
XMDOTC	( PDROP )	HTFLOW	-AVERAGE CYCLE MASS FLUX IN COOLER (KG/SEC)
XMDOTH	( PDROP )	HTFLOW	-AVERAGE CYCLE MASS FLUX IN HEATER (KG/SEC)
XMDOTR	( PDROP )	HTFLOW	-AVERAGE CYCLE MASS FLUX IN REGENERATOR (KG/SEC)
XME	( RIOSF )	CYCLER	-DIMENSIONLESS MASS IN EXPANSION ZONE
XNHT	( RIOSF )	RIOSIN	-AVERAGE EXPONENT IN NUSSELT CORRELATION
XNUSC	( PDROP )	HTFLOW	-NUSSELT NUMBER IN COOLER
XNUSH	( PDROP )	HTFLOW	-NUSSELT NUMBER IN HEATER
XNUSR	( PDROP )	HTFLOW	-NUSSELT NUMBER IN REGENERATOR
XPSTRT	( RIOSF )	RIOSIN	-INITIAL DIMENSIONLESS PRESSURE ESTIMATE
ZERO	( AMISC )	INPUT	-0.0

APPENDIX D  
GRAF LISTING

SUBPROGRAM GRAF

C-		GRA00010
C-	SETS UP TELLAGRAF FILE FOR POWER AND POWER LOSS PLOTS	GRA00020
C-	VS RPM IE THESE ARE THE CASE BY CASE PLOT	GRA00030
C-		GRA00040
	DIMENSION PMEAN(50), SPEED(50), XMASS(50), QIN(50),	GRA00050
X	POWER(50), EFFIC(50), THOTG(50), TKOLG(50), QNGKOL(50),	GRA00060
X	QWKKOL(50), QSTDY(50), QDYNAM(50), QFRIC(50), QREGEF(50),	GRA00070
X	QLEAK(50), QOUT(50), DUM(8,50)	GRA00080
	DIMENSION IA(20), PROUT(5), NC10(5), NC20(5)	GRA00090
C-		GRA00100
C-	NEED TO KNOW THAT 4 PRESSURE CASES ARE COMING IN	GRA00110
C-	AND THAT NRPM = NPRT2 IN SEAM IS 6	GRA00120
C-		GRA00130
	NPRES=4	GRA00140
	NRPM=6	GRA00150
	IOUT=3	GRA00160
	IOUT=0	GRA00170
C-		GRA00180
	DO 600 NPR=1, NPRES	GRA00190
C-	IOUT = 0 ONE OF EACH PLOT	GRA00200
C-	IOUT = 1 POWER LOSSES VS RPM IOUT= 2 HEAT LOSSES VS RPM	GRA00210
C-	IOUT = 3 BOTH 1 AND 2	GRA00220
C-	IOUT = 4 POWER VS RPM AND EFFIC VS RPM	GRA00230
C-	IOUT = 5 POWER VS EFFICIENCY	GRA00240
C-	IOUT = 6 BOTH 4 AND 5	GRA00250
C-		GRA00260
	100 CONTINUE	GRA00270
C-		GRA00280
C-	READ UNIT 5, IE TERMINAL FOR WHATEVER	GRA00290
	READ (10,2000) IA	GRA00300
	2000 FORMAT(20A4)	GRA00310
	READ (10,2005) IMASS,RPM,P,TCMB,TWATER,THASS	GRA00320
	2005 FORMAT(I3,F9.2,F9.4,2F9.2,F9.6)	GRA00330
C-		GRA00340
	18 CONTINUE	GRA00350
C-		GRA00360
	DO 200 L=1,NRPM	GRA00370
	READ(10,1000) NCASE, PMEAN(NCASE), SPEED(NCASE), XMASS(NCASE),	GRA00380
X	QIN(NCASE), POWER(NCASE), EFFIC(NCASE), THOTG(NCASE),	GRA00390
X	TKOLG(NCASE)	GRA00400
	READ(10,1001) QNGKOL(NCASE), QWKKOL(NCASE), QSTDY(NCASE),	GRA00410
X	QDYNAM(NCASE), QFRIC(NCASE), QREGEF(NCASE), QLEAK(NCASE),	GRA00420
X	QOUT(NCASE)	GRA00430
C-		GRA00440
	1000 FORMAT(I4,2F9.2,F10.6,2F10.2,F8.4,2F9.2)	GRA00450
	1001 FORMAT(1X,8F9.2)	GRA00460
C-		GRA00470
	1005 FORMAT(1H ,I4,2F9.2,F10.6,2F10.2,F8.4,2F9.2)	GRA00480
	WRITE(6,1005) NCASE, PMEAN(NCASE), SPEED(NCASE), XMASS(NCASE),	GRA00490
X	QIN(NCASE), POWER(NCASE), EFFIC(NCASE), THOTG(NCASE),	GRA00500
X	TKOLG(NCASE)	GRA00510
C-		GRA00520
	DUM(1,L)=POWER(NCASE)-QDYNAM(NCASE)	GRA00530
	DUM(2,L)=QIN(NCASE)+QNGKOL(NCASE)	GRA00540
	DUM(3,L)=-QSTDY(NCASE)	GRA00550

## SUBPROGRAM GRAF

```

DUM(4,L)=DUM(3,L)-QDYNAM(NCASE)
DUM(5,L)=DUM(4,L)-QREGEF(NCASE)
DUM(6,L)=DUM(5,L)-QFRIC(NCASE)
DUM(7,L)=THOTG(NCASE)-TKOLG(NCASE)
IF(L.EQ.1) NC10(NPR)=NCASE
IF(L.EQ.NRPM) NC20(NPR)=NCASE
IF(L.EQ.1) PROUT(NPR)=P
C-
200 CONTINUE
C-
C- BASIC DATA READ IN AND STORED
C-
300 FORMAT(' GENERATE A SIMPLE PLOT .',/' NO BORDER. ',
1 'WINDOW 1.0 8.0 1.0 10.0 . WINDOW FILL. ' )
309 FORMAT(' TITLE HEIGHT=0.5,0.4,0.3, ''',6A4,' '' ' )
310 FORMAT(' ''POWER LOSSES VS SPEED'' ' )
311 FORMAT(' ''POWER FLOWS VS SPEED'' ' )
312 FORMAT(' TITLE HEIGHT=1.0, ''',6A4,' '' .')
313 FORMAT(' ''PRESSURE=',F5.2,' MPA'' .')
314 FORMAT(' ''GAS MASS=',F6.5,' KG'' .')
C-
320 FORMAT(' X AXIS LABEL '' SPEED ((RPM))'' .')
321 FORMAT(' X AXIS LABEL '' INDICATED EFFICIENCY ((%))'' .')
330 FORMAT(' Y AXIS LABEL ''POWER ((KW))'', MIN=0.0 .')
331 FORMAT(' Y AXIS LABEL ''POWER LOSS ((KW))'', MIN=0.0 .')
332 FORMAT(' Y AXIS LABEL '' INDICATED EFFICIENCY ((%))'' .')
333 FORMAT(' Y AXIS LABEL '' INDICATED POWER ((KW))'', MIN=0.0 .')
C-
340 FORMAT(' CURVE 1 SHADE BELOW .')
341 FORMAT(' Y AXIS TRANSFORM 0. 1000000. 0. 1000. ')
342 FORMAT(' Y AXIS TRANSFORM 0. 1. 0. 100. ')
343 FORMAT(' X AXIS TRANSFORM 0. 1. 0. 100. ')
350 FORMAT(' EVERY MESSAGE SIMPLEX, COORDINATE UNITS,X=',F8.2,' .')
C-
360 FORMAT(' MESSAGE 1 ''POWER OUT'', Y=',F8.2,' .')
361 FORMAT(' MESSAGE 2 ''DYNAMIC LOSSES'' , Y=',F8.2,' .')
362 FORMAT(' MESSAGE 3 ''OTHER LOSSES '' , Y=',F8.2,' .')
363 FORMAT(' MESSAGE 4 ''COOLER HEAT OUT '' , Y=',F8.2,' .')
364 FORMAT(' MESSAGE 5 ''TOTAL HEAT IN '' , Y=',F8.2,' .')
365 FORMAT(' MESSAGE=1 ''CONDUCTION LOSS '' ,Y=',F8.2,' .')
366 FORMAT(' MESSAGE=3 ''REGENERATOR LOSS '' ,Y=',F8.2,' .')
367 FORMAT(' MESSAGE=4 ''FRICTION LOSS '' ,Y=',F8.2,' .')
370 FORMAT(' EVERY CURVE SYMBOL COUNT 0,SPLINE .')
371 FORMAT(' EVERY CURVE SYMBOL COUNT 0, PARA3 .')
372 FORMAT(' CURVE 5 SCATTERED, SYMBOL TYPE RING .')
C-
380 FORMAT(' NO LEGEND .')
381 FORMAT(' LEGEND STYLE SIMPLEX, ',1X,
A ' TEXT ''CALCULATED:'' .')
394 FORMAT(' PAGE LAYOUT IS LRV. ')
400 FORMAT(' INPUT DATA. ')
410 FORMAT(' ''CURVE',I2,'''',6(/1X,3(F10.4,F9.1,3X)) )
420 FORMAT(' END OF DATA. ')
422 FORMAT(' SUBPLOT ',I2,' .')
423 FORMAT(' SEND ',I2,' .')

```

```

GRA00560
GRA00570
GRA00580
GRA00590
GRA00600
GRA00610
GRA00620
GRA00630
GRA00640
GRA00650
GRA00660
GRA00670
GRA00680
GRA00690
GRA00700
GRA00710
GRA00720
GRA00730
GRA00740
GRA00750
GRA00760
GRA00770
GRA00780
GRA00790
GRA00800
GRA00810
GRA00820
GRA00830
GRA00840
GRA00850
GRA00860
GRA00870
GRA00880
GRA00890
GRA00900
GRA00910
GRA00920
GRA00930
GRA00940
GRA00950
GRA00960
GRA00970
GRA00980
GRA00990
GRA01000
GRA01010
GRA01020
GRA01030
GRA01040
GRA01050
GRA01060
GRA01070
GRA01080
GRA01090
GRA01100

```



## SUBPROGRAM GRAF

```

424 FORMAT(' ROTATION=MOVIE. ')
C- NLST=NRPM
   NST=NC10(NPR)
   IF(QIN(NCASE).LT.QIN(NST)) NCASE=NST
   IF(NCASE.EQ.NST) NLST=1
C- ISKIP=0
   IF(QDYHAM(NCASE).LT.0.03*QIN(NCASE)) ISKIP=1
   IF(QDYHAM(NCASE).LT.0.03*DUM(6,NCASE)) ISKIP=ISKIP+2
C- IF(IOUT.GT.3) GO TO 600
   IF(IOUT.EQ.0 .AND. NPR.LT.0) GO TO 600
C- WRITE(11,394)
   NC9=NC10(NPR)-1
   IF(IOUT.EQ.2) GO TO 500
C- IOUT = 0, 1, 3
C- GRAPHICS FOR POWER LOSSES VS RPM FOR A MEAN PRESSURE
C-
   WRITE(11,300)
   WRITE(11,309) (IA(I),I=1,6)
   WRITE(11,311)
   IF(IMASS.EQ.0) WRITE(11,313) P
   IF(IMASS.EQ.1) WRITE(11,314) TMASS
   WRITE(11,320)
   WRITE(11,330)
   WRITE(11,340)
   DUM1=SPEED(NLST)
   WRITE(11,350) DUM1
   DUM1=0.001*POWER(NCASE)*0.5
   WRITE(11,360) DUM1
   DUM1=0.001*0.5*(POWER(NCASE)+DUM(1,NLST))
   IF(ISKIP.EQ.0) WRITE(11,361) DUM1
   DUM1=0.001*(DUM(2,NLST)*0.8+0.2*DUM(1,NLST))
   WRITE(11,362) DUM1
   DUM1=0.001*0.5*(DUM(2,NLST)+QIN(NCASE))
   WRITE(11,363) DUM1
CC  DUM1=SPEED(NCASE)*0.5
CC  WRITE(11,364) QIN(NCASE),DUM1
   DUM1=0.001*QIN(NCASE)
   WRITE(11,364) DUM1
   WRITE(11,341)
   WRITE(11,370)
   WRITE(11,380)
   WRITE(11,400)
   II=1
   WRITE(11,410) II,(SPEED(L+NC9),POWER(L+NC9),L=1,NLST)
   IF(ISKIP.GT.0) GO TO 480
   II=II+1
   WRITE(11,410) II,(SPEED(L+NC9),DUM(1,L),L=1,NLST)
480 II=II+1
   WRITE(11,410) II,(SPEED(L+NC9),DUM(2,L),L=1,NLST)
   II=II+1

```

```

GRA01110
GRA01120
GRA01130
GRA01140
GRA01150
GRA01160
GRA01170
GRA01180
GRA01190
GRA01200
GRA01210
GRA01220
GRA01230
GRA01240
GRA01250
GRA01260
GRA01270
GRA01280
GRA01290
GRA01300
GRA01310
GRA01320
GRA01330
GRA01340
GRA01350
GRA01360
GRA01370
GRA01380
GRA01390
GRA01400
GRA01410
GRA01420
GRA01430
GRA01440
GRA01450
GRA01460
GRA01470
GRA01480
GRA01490
GRA01500
GRA01510
GRA01520
GRA01530
GRA01540
GRA01550
GRA01560
GRA01570
GRA01580
GRA01590
GRA01600
GRA01610
GRA01620
GRA01630
GRA01640
GRA01650

```

## SUBPROGRAM GRAF

```

WRITE(11,410) II,(SPEED(L+NC9),QIN(L+NC9),L=1,NLST)
WRITE(11,420)
II=2*NPR-1
WRITE(11,422) II
IF(IOUT.EQ.1) GO TO 600
C-
500 CONTINUE
C-          IOUT=0, 2, 3
C- GRAPHICS FOR HEAT LOSSES VS RPM FOR A MEAN PRESSURE
C-
WRITE(11,300)
WRITE(11,309) (IA(I),I=1,6)
WRITE(11,310)
IF(IMASS.EQ.0) WRITE(11,313) P
IF(IMASS.EQ.1) WRITE(11,314) TMASS
WRITE(11,320)
WRITE(11,331)
WRITE(11,340)
DUM1=SPEED(NLST)
WRITE(11,350) DUM1
DUM1=0.001*DUM(3,NLST)*0.5
WRITE(11,365) DUM1
DUM1=0.001*0.5*(DUM(3,NLST)+DUM(4,NLST))
IF(ISKIP.LE.1) WRITE(11,361) DUM1
DUM1=0.001*0.5*(DUM(5,NLST)+DUM(4,NLST))
WRITE(11,366) DUM1
DUM1=0.001*0.5*(DUM(5,NLST)+DUM(6,NLST))
WRITE(11,367) DUM1
WRITE(11,341)
WRITE(11,370)
WRITE(11,330)
WRITE(11,400)
II=1
WRITE(11,410) II,(SPEED(L+NC9),DUM(3,L),L=1,NLST)
IF(ISKIP.GT.1) GO TO 485
II=II+1
WRITE(11,410) II,(SPEED(L+NC9),DUM(4,L),L=1,NLST)
485 II=II+1
WRITE(11,410) II,(SPEED(L+NC9),DUM(5,L),L=1,NLST)
II=II+1
WRITE(11,410) II,(SPEED(L+NC9),DUM(6,L),L=1,NLST)
WRITE(11,420)
II=2*NPR
WRITE(11,422) II
C-
600 CONTINUE
C-
C- ALL DATA NOW IN POWER, PMEAN, SPEED, AND EFFIC TO DO OTHER PLOTS
C-
IF(IOUT.GT.0.AND. IOUT.LT.4) GO TO 750
C-
WRITE(11,394)
IF(IOUT.EQ.5) GO TO 700
C-          IOUT=0, 4, 6
C- GRAPHICS FOR POWER VS RPM FOR ALL MEAN PRESSURES

```

```

GRA01660
GRA01670
GRA01680
GRA01690
GRA01700
GRA01710
GRA01720
GRA01730
GRA01740
GRA01750
GRA01760
GRA01770
GRA01780
GRA01790
GRA01800
GRA01810
GRA01820
GRA01830
GRA01840
GRA01850
GRA01860
GRA01870
GRA01830
GRA01890
GRA01900
GRA01910
GRA01920
GRA01930
GRA01940
GRA01950
GRA01960
GRA01970
GRA01980
GRA01990
GRA02000
GRA02010
GRA02020
GRA02030
GRA02040
GRA02050
GRA02060
GRA02070
GRA02080
GRA02090
GRA02100
GRA02110
GRA02120
GRA02130
GRA02140
GRA02150
GRA02160
GRA02170
GRA02180
GRA02190
GRA02200

```

## SUBPROGRAM GRAF

C-	AND EFFICIENCY VS RPM FOR ALL MEAN PRESSURES	GRA02210
C-		GRA02220
	WRITE(11,300)	GRA02230
	WRITE(11,312) (IA(I),I=1,6)	GRA02240
	WRITE(11,333)	GRA02250
	WRITE(11,341)	GRA02260
	WRITE(11,320)	GRA02270
	WRITE(11,371)	GRA02280
	WRITE(11,381)	GRA02290
	WRITE(11,400)	GRA02300
	DO 650 NPR=1,NPRES	GRA02310
	NC1=NC10(NPR)	GRA02320
	NC2=NC20(NPR)	GRA02330
	P=PROUT(NPR)	GRA02340
	WRITE(11,1210) P	GRA02350
	WRITE(11,1211) (SPEED(L),POWER(L),L=NC1,NC2)	GRA02360
650	CONTINUE	GRA02370
	WRITE(11,1214)	GRA02380
	WRITE(11,420)	GRA02390
	WRITE(11,372)	GRA02400
	II=25	GRA02410
	WRITE(11,422) II	GRA02420
C-		GRA02430
	WRITE(11,394)	GRA02440
	WRITE(11,300)	GRA02450
	WRITE(11,312) (IA(I),I=1,6)	GRA02460
	WRITE(11,332)	GRA02470
	WRITE(11,342)	GRA02480
	WRITE(11,320)	GRA02490
	WRITE(11,371)	GRA02500
	WRITE(11,381)	GRA02510
	WRITE(11,400)	GRA02520
	DO 675 NPR=1,NPRES	GRA02530
	NC1=NC10(NPR)	GRA02540
	NC2=NC20(NPR)	GRA02550
	P=PROUT(NPR)	GRA02560
	WRITE(11,1210) P	GRA02570
	WRITE(11,1212) (SPEED(L),EFFIC(L),L=NC1,NC2)	GRA02580
675	CONTINUE	GRA02590
	WRITE(11,1214)	GRA02600
	WRITE(11,420)	GRA02610
	WRITE(11,372)	GRA02620
	II=26	GRA02630
	WRITE(11,422) II	GRA02640
C-		GRA02650
	IF(IOUT.EQ.4) GO TO 750	GRA02660
C-		GRA02670
C-	IOUT = 0, 5, 6,	GRA02680
C-	GRAPHICS FOR POWER VS EFFICIENCY FOR ALL MEAN PRESSURES	GRA02690
C-		GRA02700
700	CONTINUE	GRA02710
	WRITE(11,394)	GRA02720
	WRITE(11,300)	GRA02730
	WRITE(11,312) (IA(I),I=1,6)	GRA02740
	WRITE(11,333)	GRA02750

## SUBPROGRAM GRAF

WRITE(11,321)	GRA02760
WRITE(11,371)	GRA02770
WRITE(11,341)	GRA02780
WRITE(11,343)	GRA02790
WRITE(11,381)	GRA02800
WRITE(11,400)	GRA02810
DO 725 NPR=1,NPRES	GRA02820
NC1=NC10(NPR)	GRA02830
NC2=NC20(NPR)	GRA02840
P=PROUT(NPR)	GRA02850
WRITE(11,1210) P	GRA02860
WRITE(11,1213) (EFFIC(L),POWER(L),L=NC1,NC2)	GRA02870
725 CONTINUE	GRA02880
WRITE(11,1214)	GRA02890
WRITE(11,420)	GRA02900
WRITE(11,372)	GRA02910
II=27	GRA02920
WRITE(11,422) II	GRA02930
C-	GRA02940
1210 FORMAT(' ' P =',F5.2,' (MPA)' ' )	GRA02950
1211 FORMAT(1H ,3(3X,F10.4,F10.0) )	GRA02960
1212 FORMAT(1H ,3(3X,F10.4,F10.5) )	GRA02970
1213 FORMAT(1H ,3(3X,F8.5,F10.0) )	GRA02980
1214 FORMAT(' ' EXPR. DATA ' ' )	GRA02990
C-	GRA03000
750 CONTINUE	GRA03010
C-	GRA03020
WRITE(11,424)	GRA03030
IF(IOUT.GT.3) GO TO 820	GRA03040
DO 800 NPR=1,NPRES	GRA03050
IF(IOUT.EQ.0.AND.NPR.LT.0) GO TO 800	GRA03060
IF(IOUT.EQ.2) GO TO 790	GRA03070
II=NPR*2-1	GRA03080
WRITE(11,423) II	GRA03090
IF(IOUT.EQ.1) GO TO 800	GRA03100
790 II=NPR*2	GRA03110
WRITE(11,423) II	GRA03120
800 CONTINUE	GRA03130
C-	GRA03140
820 IF(IOUT.LT.4.AND.IOUT.GT.0) GO TO 850	GRA03150
IF(IOUT.EQ.5) GO TO 840	GRA03160
II=25	GRA03170
WRITE(11,423) II	GRA03180
II=26	GRA03190
WRITE(11,423) II	GRA03200
IF(IOUT.EQ.4) GO TO 850	GRA03210
840 II=27	GRA03220
WRITE(11,423) II	GRA03230
850 CONTINUE	GRA03240
C-	GRA03250
RETURN	GRA03260
END	GRA03270

APPENDIX E  
GRAF OUTPUT/TELLAGRAF INPUT

GRAF OUTPUT / TELLAGRAF INPUT

```

PAGE LAYOUT IS LRV.
GENERATE A SIMPLE PLOT .
NO BORDER. WINDOW 1.0 8.0 1.0 10.0 . WINDOW FILL.
TITLE HEIGHT=0.5,0.4,0.3, ' GPU-3 HELIUM 927K/339K '
'POWER FLOWS VS SPEED'
'PRESSURE= 2.74 MPA' .
X AXIS LABEL ' SPEED ((RPM))' .
Y AXIS LABEL 'PCNER ((KW)) ', MIN=0.0 .
CURVE 1 SHADE BELOW .
EVERY MESSAGE SIMPLEX, COORDINATE UNITS,X= 3499.20.
MESSAGE 1 'POWER OUT', Y= 0.73.
MESSAGE 3 'OTHER LOSSES ', Y= 2.53.
MESSAGE 4 'COOLER HEAT OUT ', Y= 6.04.
MESSAGE 5 'TOTAL HEAT IN ', Y= 9.37.
Y AXIS TRANSFORM 0. 1000000. 0. 1000.
EVERY CURVE SYMBOL COUNT 0,SPLINE .
NO LEGEND .
INPUT DATA.
'CURVE 1'.
1000.2000 1095.1 1500.0000 1494.1 1999.8000 1929.3
2499.6001 2105.2 2999.3999 1907.8 3499.2000 1453.6
'CURVE 2'.
1000.2000 2182.6 1500.0000 2627.8 1999.8000 3119.2
2499.6001 3331.1 2999.3999 3149.6 3499.2000 2708.0
'CURVE 3'.
1000.2000 3781.6 1500.0000 5065.8 1999.8000 6431.2
2499.6001 7629.1 2999.3999 8573.6 3499.2000 9370.0
END OF DATA.
SUBPLOT 1.
GENERATE A SIMPLE PLOT .
NO BORDER. WINDOW 1.0 8.0 1.0 10.0 . WINDOW FILL.
TITLE HEIGHT=0.5,0.4,0.3, ' GPU-3 HELIUM 927K/339K '
'POWER LOSSES VS SPEED'
'PRESSURE= 2.74 MPA' .
X AXIS LABEL ' SPEED ((RPM))' .
Y AXIS LABEL 'POWER LOSS ((KW)) ', MIN=0.0 .
CURVE 1 SHADE BELOW .
EVERY MESSAGE SIMPLEX, COORDINATE UNITS,X= 3499.20.
MESSAGE=1 'CONDUCTION LOSS ',Y= 0.51.
MESSAGE=3 'REGENERATOR LOSS ',Y= 1.60.
MESSAGE=4 'FRICTION LOSS ',Y= 3.48.
Y AXIS TRANSFORM 0. 1000000. 0. 1000.
EVERY CURVE SYMBOL COUNT 0,SPLINE .
NO LEGEND .
INPUT DATA.
'CURVE 1'.
1000.2000 908.0 1500.0000 935.0 1999.8000 970.0
2499.6001 992.0 2999.3999 1003.0 3499.2000 1012.0
'CURVE 2'.
1000.2000 1287.0 1500.0000 1394.0 1999.8000 1532.0
2499.6001 1648.0 2999.3999 1731.0 3499.2000 1812.0
'CURVE 3'.
1000.2000 1483.0 1500.0000 1869.0 1999.8000 2439.0
2499.6001 3169.0 2999.3999 4054.0 3499.2000 5146.0
END OF DATA.

```

## GRAF OUTPUT / TELLGRAF INPUT

SUBPLOT 2.  
PAGE LAYOUT IS LRV.  
GENERATE A SIMPLE PLOT .  
NO BORDER. WINDOW 1.0 8.0 1.0 10.0 . WINDOW FILL.  
TITLE HEIGHT=0.5,0.4,0.3, ' GPU-3 HELIUM 927K/339K '  
'POWER FLOWS VS SPEED'  
'PRESSURE= 4.10 MPA' .  
X AXIS LABEL ' SPEED ((RPM))' .  
Y AXIS LABEL 'POWER ((KW)) ', MIN=0.0 .  
CURVE 1 SHADE BELOW .  
EVERY MESSAGE SIMPLEX, COORDINATE UNITS,X= 3499.20.  
MESSAGE 1 'POWER OUT', Y= 1.47.  
MESSAGE 3 'OTHER LOSSES ', Y= 4.05.  
MESSAGE 4 'COOLER HEAT OUT ', Y= 9.01.  
MESSAGE 5 'TOTAL HEAT IN ', Y= 13.79.  
Y AXIS TRANSFORM 0. 1000000. 0. 1000.  
EVERY CURVE SYMBOL COUNT 0,SPLINE .  
NO LEGEND .  
INPUT DATA.  
'CURVE 1'.  
1000.2000 1828.0 1500.0000 2815.4 1999.8000 3359.6  
2499.6001 3544.2 2999.3999 3413.9 3499.2000 2930.1  
'CURVE 2'.  
1000.2000 3007.6 1500.0000 4064.6 1999.8000 4629.5  
2499.6001 4822.2 2999.3999 4704.1 3499.2000 4230.8  
'CURVE 3'.  
1000.2000 5308.6 1500.0000 7521.6 1999.8000 9401.5  
2499.6001 11050.2 2999.3999 12524.1 3499.2000 13789.8  
END OF DATA.  
SUBPLOT 3.  
GENERATE A SIMPLE PLOT .  
NO BORDER. WINDOW 1.0 8.0 1.0 10.0 . WINDOW FILL.  
TITLE HEIGHT=0.5,0.4,0.3, ' GPU-3 HELIUM 927K/339K '  
'POWER LOSSES VS SPEED'  
'PRESSURE= 4.10 MPA' .  
X AXIS LABEL ' SPEED ((RPM))' .  
Y AXIS LABEL 'POWER LOSS ((KW)) ', MIN=0.0 .  
CURVE 1 SHADE BELOW .  
EVERY MESSAGE SIMPLEX, COORDINATE UNITS,X= 3499.20.  
MESSAGE=1 'CONDUCTION LOSS ',Y= 0.52.  
MESSAGE=3 'REGENERATOR LOSS ',Y= 1.80.  
MESSAGE=4 'FRICTION LOSS ',Y= 4.12.  
Y AXIS TRANSFORM 0. 1000000. 0. 1000.  
EVERY CURVE SYMBOL COUNT 0,SPLINE .  
NO LEGEND .  
INPUT DATA.  
'CURVE 1'.  
1000.2000 974.0 1500.0000 1014.0 1999.8000 1028.0  
2499.6001 1034.0 2999.3999 1042.0 3499.2000 1047.0  
'CURVE 2'.  
1000.2000 1459.0 1500.0000 1657.0 1999.8000 1799.0  
2499.6001 1921.0 2999.3999 2045.0 3499.2000 2160.0  
'CURVE 3'.  
1000.2000 1671.0 1500.0000 2189.0 1999.8000 2836.0  
2499.6001 3674.0 2999.3999 4750.0 3499.2000 6072.0

## GRAF OUTPUT / TELLAGRAF INPUT

```

END OF DATA.
SUBPLOT 4.
PAGE LAYOUT IS LRV.
GENERATE A SIMPLE PLOT .
NO BORDER. WINDOW 1.0 8.0 1.0 10.0 . WINDOW FILL.
TITLE HEIGHT=0.5,0.4,0.3, ' GPU-3 HELIUM 927K/339K '
'POWER FLOWS VS SPEED'
'PRESSURE= 5.55 MPA' .
X AXIS LABEL ' SPEED ((RPM))' .
Y AXIS LABEL 'POWER ((KW)) ', MIN=0.0 .
CURVE 1 SHADE BELOW .
EVERY MESSAGE SIMPLEX, COORDINATE UNITS,X= 3499.20.
MESSAGE 1 'POWER OUT', Y= 1.93.
MESSAGE 3 'OTHER LOSSES ', Y= 4.93.
MESSAGE 4 'COOLER HEAT OUT ', Y= 11.51.
MESSAGE 5 'TOTAL HEAT IN ', Y= 17.92.
Y AXIS TRANSFORM 0. 1000000. 0. 1000.
EVERY CURVE SYMBOL COUNT 0,SPLINE .
NO LEGEND .
INPUT DATA.
'CURVE 1'.
1000.2000 2724.2 1500.0000 3803.5 1999.8000 4429.1
2499.6001 4662.8 2999.3999 4479.6 3499.2000 3854.2
'CURVE 2'.
1000.2000 3921.3 1500.0000 5025.2 1999.8000 5657.9
2499.6001 5897.7 2999.3999 5723.6 3499.2000 5104.4
'CURVE 3'.
1000.2000 6951.3 1500.0000 9680.2 1999.8000 12105.9
2499.6001 14296.7 2999.3999 16244.6 3499.2000 17921.4
END OF DATA.
SUBPLOT 5.
GENERATE A SIMPLE PLOT .
NO BORDER. WINDOW 1.0 8.0 1.0 10.0 . WINDOW FILL.
TITLE HEIGHT=0.5,0.4,0.3, ' GPU-3 HELIUM 927K/339K '
'POWER LOSSES VS SPEED'
'PRESSURE= 5.55 MPA' .
X AXIS LABEL ' SPEED ((RPM))' .
Y AXIS LABEL 'POWER LOSS ((KW)) ', MIN=0.0 .
CURVE 1 SHADE BELOW .
EVERY MESSAGE SIMPLEX, COORDINATE UNITS,X= 3499.20.
MESSAGE=1 'CONDUCTION LOSS ',Y= 0.50.
MESSAGE=3 'REGENERATOR LOSS ',Y= 1.90.
MESSAGE=4 'FRICTION LOSS ',Y= 4.63.
Y AXIS TRANSFORM 0. 1000000. 0. 1000.
EVERY CURVE SYMBOL COUNT 0,SPLINE .
NO LEGEND .
INPUT DATA.
'CURVE 1'.
1000.2000 977.0 1500.0000 991.0 1999.8000 995.0
2499.6001 996.0 2999.3999 999.0 3499.2000 999.0
'CURVE 2'.
1000.2000 1582.0 1500.0000 1775.0 1999.8000 1946.0
2499.6001 2110.0 2999.3999 2267.0 3499.2000 2407.0
'CURVE 3'.
1000.2000 1810.0 1500.0000 2359.0 1999.8000 3101.0

```

## GRAF OUTPUT / TELLAGRAF INPUT

2499.6001 4082.0 2999.3999 5329.0 3499.2000 6855.0  
 END OF DATA.  
 SUBPLOT 6.  
 PAGE LAYOUT IS LRV.  
 GENERATE A SIMPLE PLOT .  
 NO BORDER. WINDOW 1.0 8.0 1.0 10.0 . WINDOW FILL.  
 TITLE HEIGHT=0.5,0.4,0.3, ' GPU-3 HELIUM 927K/339K '  
 'POWER FLOWS VS SPEED'  
 'PRESSURE= 6.92 MPA' .  
 X AXIS LABEL ' SPEED ((RPM))' .  
 Y AXIS LABEL 'POWER ((KW)) ', MIN=0.0 .  
 CURVE 1 SHADE BELOW .  
 EVERY MESSAGE SIMPLEX, COORDINATE UNITS,X= 3499.20.  
 MESSAGE 1 'POWER OUT', Y= 2.31.  
 MESSAGE 3 'OTHER LOSSES ', Y= 5.70.  
 MESSAGE 4 'COOLER HEAT OUT ', Y= 13.84.  
 MESSAGE 5 'TOTAL HEAT IN ', Y= 21.80.  
 Y AXIS TRANSFORM 0. 1000000. 0. 1000.  
 EVERY CURVE SYMBOL COUNT 0,SPLINE .  
 NO LEGEND .  
 INPUT DATA.  
 'CURVE 1'.  

1000.2000	3516.6	1500.0000	4686.2	1999.8000	5424.9
2499.6001	5664.3	2999.3999	5290.7	3499.2000	4627.6

 'CURVE 2'.  

1000.2000	4744.9	1500.0000	5913.6	1999.8000	6656.9
2499.6001	6899.7	2999.3999	6509.2	3499.2000	5872.2

 'CURVE 3'.  

1000.2000	8490.9	1500.0000	11731.6	1999.8000	14713.9
2499.6001	17387.7	2999.3999	19642.2	3499.2000	21799.2

 END OF DATA.  
 SUBPLOT 7.  
 GENERATE A SIMPLE PLOT .  
 NO BORDER. WINDOW 1.0 8.0 1.0 10.0 . WINDOW FILL.  
 TITLE HEIGHT=0.5,0.4,0.3, ' GPU-3 HELIUM 927K/339K '  
 'POWER LOSSES VS SPEED'  
 'PRESSURE= 6.92 MPA' .  
 X AXIS LABEL ' SPEED ((RPM))' .  
 Y AXIS LABEL 'POWER LOSS ((KW)) ', MIN=0.0 .  
 CURVE 1 SHADE BELOW .  
 EVERY MESSAGE SIMPLEX, COORDINATE UNITS,X= 3499.20.  
 MESSAGE=1 'CONDUCTION LOSS ',Y= 0.49.  
 MESSAGE=3 'REGENERATOR LOSS ',Y= 2.04.  
 MESSAGE=4 'FRICTION LOSS ',Y= 5.15.  
 Y AXIS TRANSFORM 0. 1000000. 0. 1000.  
 EVERY CURVE SYMBOL COUNT 0,SPLINE .  
 NO LEGEND .  
 INPUT DATA.  
 'CURVE 1'.  

1000.2000	997.0	1500.0000	995.0	1999.8000	996.0
2499.6001	993.0	2999.3999	973.0	3499.2000	987.0

 'CURVE 2'.  

1000.2000	1722.0	1500.0000	1932.0	1999.8000	2149.0
2499.6001	2348.0	2999.3999	2501.0	3499.2000	2692.0

 'CURVE 3'.



## GRAF OUTPUT / TELLGRAF INPUT

1000.2000 1967.0 1500.0000 2566.0 1999.8000 3412.0  
 2499.6001 4516.0 2999.3999 5876.0 3499.2000 7607.0

END OF DATA.

SUBPLOT 8.

PAGE LAYOUT IS LRV.

GENERATE A SIMPLE PLOT .

NO BORDER. WINDOW 1.0 8.0 1.0 10.0 . WINDOW FILL.

TITLE HEIGHT=1.0, ' GPU-3 HELIUM 927K/339K ' .

Y AXIS LABEL ' INDICATED POWER ((KW))', MIN=0.0 .

Y AXIS TRANSFORM 0. 1000000. 0. 1000.

X AXIS LABEL ' SPEED ((RPM))' .

EVERY CURVE SYMBOL COUNT 0, PARA3 .

LEGEND STYLE SIMPLEX, TEXT 'CALCULATED:' .

INPUT DATA.

' P = 2.74 (MPA)'

1000.2000	1095.	1500.0000	1494.	1999.8000	1929.
2499.6001	2105.	2999.3999	1908.	3499.2000	1454.

' P = 4.10 (MPA)'

1000.2000	1828.	1500.0000	2815.	1999.8000	3360.
2499.6001	3544.	2999.3999	3414.	3499.2000	2930.

' P = 5.55 (MPA)'

1000.2000	2724.	1500.0000	3804.	1999.8000	4429.
2499.6001	4663.	2999.3999	4480.	3499.2000	3854.

' P = 6.92 (MPA)'

1000.2000	3517.	1500.0000	4686.	1999.8000	5425.
2499.6001	5664.	2999.3999	5291.	3499.2000	4628.

' EXPR. DATA ' .

'EXPR DATA'

1000. 1160.	1500. 1670.	2500. 2080.	3000. 2060.	3500. 1680.
	1500. 2410.	2500. 3300.	3000. 3430.	3500. 2980.
		2500. 4490.	3000. 4640.	3500. 4380.
			3000. 5480.	3500. 5190.

END OF DATA.

CURVE 5 SCATTERED, SYMBOL TYPE RING .

SUBPLOT 25.

PAGE LAYOUT IS LRV.

GENERATE A SIMPLE PLOT .

NO BORDER. WINDOW 1.0 8.0 1.0 10.0 . WINDOW FILL.

TITLE HEIGHT=1.0, ' GPU-3 HELIUM 927K/339K ' .

Y AXIS LABEL ' INDICATED EFFICIENCY ((%))' .

Y AXIS TRANSFORM 0. 1. 0. 100.

X AXIS LABEL ' SPEED ((RPM))' .

EVERY CURVE SYMBOL COUNT 0, PARA3 .

LEGEND STYLE SIMPLEX, TEXT 'CALCULATED:' .

INPUT DATA.

' P = 2.74 (MPA)'

1000.2000	0.28960	1500.0000	0.29490	1999.8000	0.30000
2499.6001	0.27590	2999.3999	0.22250	3499.2000	0.15510

' P = 4.10 (MPA)'

1000.2000	0.34430	1500.0000	0.37430	1999.8000	0.35730
2499.6001	0.32070	2999.3999	0.27260	3499.2000	0.21250

' P = 5.55 (MPA)'

1000.2000	0.39190	1500.0000	0.39290	1999.8000	0.36590
2499.6001	0.32610	2999.3999	0.27580	3499.2000	0.21510

' P = 6.92 (MPA)'

## GRAF OUTPUT / TELLAGRAF INPUT

1000.2000	0.41420	1500.0000	0.39950	1999.8000	0.36870
2499.6001	0.32580	2999.3999	0.26940	3499.2000	0.21230
' EXPR. DATA '					
1000. 0.32	1500. 0.31	2500. 0.267	3000. 0.231	3500. 0.169	
	1500. 0.333	2500. 0.293	3000. 0.264	3500. 0.207	
		2500. 0.305	3000. 0.271	3500. 0.220	
			3000. 0.265	3500. 0.22	

END OF DATA.  
 CURVE 5 SCATTERED, SYMBOL TYPE RING .  
 SUBPLOT 26.  
 PAGE LAYOUT IS LRV.  
 GENERATE A SIMPLE PLOT .  
 NO BORDER. WINDOW 1.0 8.0 1.0 10.0 . WINDOW FILL.  
 TITLE HEIGHT=1.0, ' GPU-3 HELIUM 927K/339K '  
 Y AXIS LABEL ' INDICATED POWER ((KW))', MIN=0.0 .  
 X AXIS LABEL ' INDICATED EFFICIENCY ((%))'.  
 EVERY CURVE SYMBOL COUNT 0, PARA3 .  
 Y AXIS TRANSFORM 0. 1000000. 0. 1000.  
 X AXIS TRANSFORM 0. 1. 0. 100.  
 LEGEND STYLE SIMPLEX, TEXT 'CALCULATED:' .  
 INPUT DATA.

' P = 2.74 (MPA)'					
0.28960	1095.	0.29490	1494.	0.30000	1929.
0.27590	2105.	0.22250	1908.	0.15510	1454.
' P = 4.10 (MPA)'					
0.34430	1828.	0.37430	2815.	0.35730	3360.
0.32070	3544.	0.27260	3414.	0.21250	2930.
' P = 5.55 (MPA)'					
0.39190	2724.	0.39290	3804.	0.36590	4429.
0.32610	4663.	0.27580	4480.	0.21510	3854.
' P = 6.92 (MPA)'					
0.41420	3517.	0.39950	4686.	0.36870	5425.
0.32580	5664.	0.26940	5291.	0.21230	4628.
' EXPR. DATA '					
0.320 1160.	0.310 1670.	0.267 2080.	0.231 2060.	0.169 1680.	
	0.333 2410.	0.293 3300.	0.264 3430.	0.207 2980.	
		0.305 4490.	0.271 4640.	0.207 4380.	
			0.265 5480.	0.220 5190.	

END OF DATA.  
 CURVE 5 SCATTERED, SYMBOL TYPE RING .  
 SUBPLOT 27.  
 ROTATION=MOVIE.  
 \*\* SEND 1.  
 \*\* SEND 2.  
 \*\* SEND 3.  
 \*\* SEND 4.  
 \*\* SEND 5.  
 \*\* SEND 6.  
 SEND 7.  
 SEND 8.  
 SEND 25.  
 SEND 26.  
 SEND 27.

## REFERENCES

1. Rios, P. A., "An Analytical and Experimental Investigation of the Stirling Cycle," D. Sc. Thesis, MIT, 1969.
2. Urieli, I., "A Computer Simulation of Stirling Engine Machines," Ph.D Thesis, U. of Witwaterstrand, S. Africa, Feb. 1977.
3. Tew, R., et al., "A Stirling Engine Computer Model for Performance Calculations," NASA-TM-78884, May 1978.
4. Martini, W. R., "An Isothermal Second Order Stirling Engine Calculation Method," Proc. 13th IECEC, Paper No. 799237, pp. 1091-1097, 1978.
5. Schock, A., "Nodal Analysis of Stirling Cycle Devices," Proc. 13th IECEC, Paper No. 789191, pp. 1771-1779, 1978.
6. Gedeon, D. R., "The Optimization of Stirling Cycle Machines," Proc. 13th IECEC, Paper No. 789193, pp. 1784-1790, 1978.
7. Kirkley, D. W., "An Investigation of the Losses Occurring in Reciprocating Hot Air Engines," Ph.D. Thesis, University of Durham, Oct. 1963.
8. Glassford, A. P. M., "Adiabatic Cycle Analysis for the Valved Thermal Compressor," J. Energy 3 (5), 306-314, Sept.-Oct. 1979.
9. Rauch, J. S., "Harmonic Analysis of Stirling Engine Thermodynamics," Proc. 15th IECEC, Paper No. 809335, pp. 1696, 1980.
10. Organ, A. J., "Gas Dynamics of the Temperature Determined Stirling Cycle," J. Mech. Eng. Science 23 (4). 207-216, 1982.
11. Beans, E. W., "A Mathematical Model for the Stirling Engine Cycle," J. Eng. Power, 103, 505-510, July 1981.
12. Schmidt, G., "Theorie de Lehmann'schen Calorischen Maschine," Z.V.D.I. 15 (1) (1981).
13. Ash, J. E. and Heames, T. J., "Comparative Analysis of Computer Codes for Stirling Cycle Engines," Proc. 16th IECEC, Paper No. 819797, 1981.
14. Heames, T. J., Daley, J. G., Uherka, D. J., and Zabel, J. C., "A User Oriented Design System for Stirling Cycle Codes," Proc. 17th IECEC, Paper No. 829278, 1982.
15. "Thermophysical Properties of Matter, The TPRC Data Series, Volumes 1,3,4,6,11, Purdue University, IFI/Plenum, New York-Washington, 1970-1979.
16. "Metal Handbook," 9th Edition, Vol. 2 & 3, American Society for Metals, Metals Park, Ohio, 1980.

17. "CRC Handbook of Chemistry and Physics," 59th Edition, Weast, CRC Press Inc., 1978.
18. Iwabuchi, M., and Kanzaka, M., "Experimental Investigation into Heat Transfer under the Periodically Reversing Flow Condition in Heated Tube," Paper C24/82, I. Mech. E., pp. 125-129, 1982.
19. Ohmi, M., and Iguchi, M. "Flow Pattern and Frictional Losses in Pulsating Pipe Flow. Part 6: Frictional Losses in a Laminar Flow," Bulletin of the JSME, Vol. 24, No. 196, pp. 1756-1763. Oct. 1981.
20. Ohmi, M., and Iguchi, M., "Flow Pattern and Frictional Losses in Pulsating Pipe Flow. Part 7: Wall Shear Stress in a Turbulent Flow," Bulletin of JSME, Vol. 24, No. 196, pp. 1764-1771, Oct. 1981.
21. Baibikov, B. S., Oreshkin, O. F., and Prudovskii, A. M., "Frictional Resistance in the Case of Accelerated Flow in a Tube," Fluid Dynamics 16 (5), 749-751, Sept.-Oct. 1981, Translation Mar. 1982.
22. Patel, M. H., "An Integral Method for the Oscillating Turbulent Boundary Layer," The Aeronautical Quarterly, XXXII (4), 271-298, Nov. 1981.
23. Letelier, M. F., and Leutheusser, H. J., "Skin Function in Unsteady Laminar Pipe Flow," ASCE J. Hydraulics Div., 41-56, Jan. 1976.
24. Brown, F. T., "A Quasi Method of Characteristics with Application to Fluid Lines with Frequency Dependent Wall Shear and Heat Transfer," ASME J. Basic Eng. June 1969.
25. Kim, J. C., "Heat Transfer and Flow-Friction Characteristics in Periodically Reversing Flow for Thermal Regenerators," Proc. 5th Int. Heat Transfer Conf., Tokyo, pp. 185-189, Sept. 1974.
26. Murray, J. A., and Martin, B. W., "Performance of Thermal Regenerators Under Sinusoidal Flow Conditions, Part I," Proc. Int'l Heat Transfer Conf. (ASME), Boulder, Colo., pp. 781-788, 1961.
27. Martini, W. R., "Stirling Engine Design Manual," DOE/NASA/3152-78/1, 1978.
28. Benedict, R. P., "Fundamentals of Pipe Flow," John Wiley & Sons, 1980.
29. Ward-Smith, A. J., "Internal Fluid Flow: The Fluid Dynamics of Flow in Pipe and Ducts," Oxford University Press, New York, 1980.
30. Kays, W. M., and London, A. L., "Compact Heat Exchangers," McGraw-Hill, New York, 1955.
31. Kays, W. M., and London, A. L., "Compact Heat Exchangers," McGraw-Hill, 1964.
32. Kreith, F., "Principles of Heat Transfer," 3rd Edition, Int. Textbook Co., 1973.

33. Tong, L. S., "Heat Transfer and Friction Characteristics of Screen Matrices at High Reynolds Numbers," ONR Tech. Rep. 28, 1956.
34. General Motors Research, "A Collection of Stirling Engine Reports from General Motors," Research-1958 to-1970, Part 6, Regenerators, GMR-2690 6.004 and 6.006, 1978.
35. Hoehn, F. W., et al., "Preliminary Test Results with a Stirling Laboratory Research Engine," Proc. 14th IECEC, Paper No. 799233, 1979.
36. Chapman, A. J., "Heat Transfer," 3rd Edition, Macmillan, 1974.
37. Jakob, M., "Heat Transfer," Vol. I, John Wiley & Sons, 1949.
38. Coppage and London, "Heat Transfer and Flow Friction Characteristics of Porous Media, Chem. Eng. Prog. 52(2), 57F-63F, Feb. 1956.
39. Toscano, W. A., "Design and Development of Stirling Engines for Stationary Power Generation Applications in the 500 to 3000 Horsepower Range, Phase I, Final Report," report for Argonne National Laboratory by Foster-Miller Associates, Inc., 1980.
40. Rea, S. N., and Smith Jr., J. L., "The Influence of Pressure Cycling on Thermal Regenerators," Journal of Engineering for Industry, Aug. 1967.
41. Qvale, E. B., "An Analytical Model of Stirling-Type Engines, Ph.D. Thesis, Massachusetts Institute of Technology, Jan. 1967.
42. Qvale, E. B., and Smith Jr., J. L., "An Approximate Solution for the Thermal Performance of the Stirling Engine Regenerator," ASME Paper 68-WA-Ener-1, ASME, New York, 1968.
43. Qvale, E. B., and Smith Jr., J. L., "A Mathematical Model for Steady Operation of Stirling Type Engines," Trans. ASME, J. Eng. Power, Jan. 1968.
44. Kirkley, D. W., "A Thermodynamic Analysis of the Stirling Cycle and a Comparison with Experiment," SAE Paper 949B, Society of Automotive Engineers, New York, Jan. 1965.
45. Lance, G. N., "Numerical Methods for High Speed Computers," Iliffe, London, England, 1960.
46. Thieme, Lanny G., "Low-Power Baseline Test Results for the GPU3 Stirling Engine," DOE/NASA/1040-79/6, Apr. 1979.
47. Tew, R. C., "Initial Comparison of Single Cylinder Stirling Engine Computer Model Predictions with Test Results," DOE/NASA/1040-78/30, 1979.

## ACKNOWLEDGMENTS

We take pleasure in expressing our appreciation for the assistance of T. Lough of The Evergreen State College in editing this report and V. Stainback of Argonne in its preparation.

The analysis-development effort described in this report is supported by the Energy Conversion and Utilization Technology Division of the U.S. Department of Energy, Office of Energy Systems Research. The encouragement of Mr. Marvin Gunn, Program Manager for energy conversion technology projects, is appreciated.

Distribution for ANL-82-59Internal:

J. E. Ash	L. W. Kirsch	G. S. Rosenberg
M. J. Bernard	E. R. Koehl	K. L. Uherka
J. G. Daley (25)	J. L. Krazinski	R. S. Zeno
T. J. Heames (25)	G. A. McLennan	ANL Contract File
R. E. Holtz	P. D. Roach	ANL Libraries (3)
P. R. Huebotter	J. J. Roberts	TIS Files (6)
National Energy Software Center (10)		ANL Patent Dept.

External:

DOE-TIC, for distribution per UC-93 (149)  
 Manager, Chicago Operations Office, DOE  
 Components Technology Division Review Committee:

- A. Bishop, U. of Pittsburgh
- F. W. Buckman, Consumers Power Co.
- R. Cohen, Purdue U.
- W. M. Jacobi, Westinghouse/Power Systems
- E. E. Ungar, Bold Beranek and Newman Inc.
- J. Weisman, U. of Cincinnati
- R. A. Greenkorn, Purdue U.

Office of Energy Systems Research, USDOE:

- J. Brogan
- M. Gunn
- J. Eberhardt

Office of Building Energy Research and Development, USDOE:

- J. Ryan
- R. Fiskum

Office of Vehicle and Engine R&D, USDOE:

- R. Alpaugh
- P. Sutton
- E. Gregory

Office of Coal Utilization, USDOE:

- W. Bunker

NASA-Lewis Research Center:

- F. Cutina
- D. Beremand
- J. Slaby
- D. Alger
- B. Tomazic
- R. Tew

Oak Ridge National Laboratory:

- P. Fairchild
- C. West

US Army Mobility Equipment R&D Command, DRDME-EM, Ft. Belvoir, VA 22060

- J. Arnold
- D. Vaughn

V. VanGriethuysen, Wright-Patterson AFB, OH 45433

F. Hoehn, Jet Propulsion Laboratory, 4800 Oak Grove Dr., Pasadena, CA 91103  
 Prof. D. Uherka, U. of North Dakota, Mathematics Dept., Grand Forks, ND 58202  
 J. Zabel, 4701 Winneconne Road, Oshkosh, WI 54901  
 E. Richardson, 2232 Nevada, Davenport, IA 52804  
 T. Lough, 606 N. Quince, Olympia, WA 98506  
 Sunpower, Inc.: 6 Byard St., Athens, OH 45701  
 W. Beale  
 D. Gedeon  
 I. Urieli  
 Mechanical Technology, Inc.: 968 Albany-Shaker Road, Latham, NY 12110  
 B. Goldwater  
 G. Dochat  
 Stirling Thermal Motors, Inc.: 2841 Boardwalk, Ann Arbor, MI 48104  
 R. Meijer  
 B. Ziph  
 F. Hoehn, Jet Propulsion Laboratory, 4800 Oak Grove Dr., Pasadena, CA 91103  
 W. Chiu, General Electric Co., Systems Engineering, P.O. Box 527, King of  
 Prussia, PA 19406  
 P. Rios, General Electric R&D Center, P.O. Box 43, Schenectady, NY 12301  
 P. Pavlin, 286 Poyntz, Willowdale, Ontario, Canada  
 W. Syniuta, Advanced Mechanical Technology, Inc., 141 California St., Newton,  
 MA 02158  
 A. Harvey, Foster Miller Assoc.: 350 Second Ave., Waltham, MA 02154  
 K. Lee, Facility & Manufacturing Automation, Inc., 85 Speen St., Framingham,  
 MA 01701  
 W. Martini, Martini Engineering, 2303 Harris, Richland, WA 99352  
 Prof. J. Smith, Jr., Massachusetts Institute of Technology, Dept. of  
 Mechanical Engineering, Cambridge, MA 02139  
 R. Shoureshi, Wayne State U., Mechanical Engineering, Detroit, MI 48202  
 G. Walker, U. of Calgary, Dept. of Mechanical Engineering, 2920 24th  
 Ave., NW, Calgary, Canada T2N 1N4  
 A. Organ, Cambridge University Engineering Dept., Trumpington St.,  
 Cambridge, CB2 1PZ, England (2)  
 G. Rice, Reading University, Engineering Dept., Reading, Berkshire, U.K. (2)  
 University of Tokyo: Dept. of Mechanical Engineering, Bunkyo-Ku, Tokyo, Japan  
 Prof. M. Hirata  
 A. Azetsu  
 B. Feurer, MAN-AG, Maschinenfabrik Augsburg-Nurnberg AG, Postfach 10 00 80,  
 D-8900 Augsburg 1, West Germany  
 United Stirling: 1629 K. Street, NW, Suite 801, Washington, DC 20006  
 W. Percival  
 C. Bratt